Department of Chemical Engineering

Thiosulfate Leaching Process for Gold Extraction

Abrar Muslim

This thesis is presented for the Degree of
Doctor of Philosophy - Chemical Engineering
of
Curtin University of Technology

June 2010

Declaration

To the best of my knowledge and belief this thesis contains no material previously published by any other person except where due acknowledgment has been made.

This thesis contains no material which has been accepted for the award of any other degree or diploma in any university.

Signature: ……..

Date: 30 June 2010

BIOGRAPHY

Abrar Muslim was awarded B.Eng (ChemEng) from Syiah Kuala University in Banda Aceh, Indonesia, and he was awarded M.Eng (ChemEng) from Curtin University of Technology, Western Australia in 2007. He has been doing his PhD studies in Chemical Engineering from July 2007 at Curtin University of Technology, Western Australia under the Curtin University of Technology's sponsorship of the CIRTS and Parker Centre's sponsorship of the Top-Up scholarship.

He has focused the research for his PhD programme on Thiosulfate Leaching Process for Gold Extraction throughout the experiment and modelling work. During the PhD programme, he has worked on the gold thiosulfate leaching project for the extraction of gold at CSIRO Mineral, Western Australia.

He is originally from Syiah Kuala University. He is Associate Chemical Engineer awarded by IChemE UK in 2008, and Professional Engineer (Chemical Engineer) awarded by Engineers Australia in 2009.

For correspondence, please email him at: abr_muslim@yahoo.com.

ACKNOWLEDGMENTS

First of all, I fully thank Allah Almighty for giving me strength, ability and Allah's Will to complete this study. You are the All-Knowing the All-Wise.

I am grateful to my honourable supervisor Prof. Vishnu K. Pareek, co-supervisor Prof. Moses O Tadé from Curtin University of Technology and associate supervisor Dr. Matthew I. Jeffrey from CSIRO Minerals, for all their valuable assistance, strong support and kind advice on this project, research and preparation of this thesis.

My appreciations go to Curtin University of Technology and the Chemical Engineering Department of Curtin University of Technology for the award of CIRTS scholarship and technical support to complete this work. I am thankful Prof. H. Ming Ang, Delia Giggins, Jennie Rogers, Diana Maumill, Jann Bolton, Stephenie Blakiston, Naomi Mockford, Simret Habtemariam for their support, and the reviewers of this thesis for their valuable suggestions.

My appreciations go to Parker Cooperative Research Centre for Integrated Hydrometallurgy Solutions for the award of Top-Up scholarship, CSIRO Minerals for technical support in conducting the experimental work for this project. I wish to thank Dr. Jane Rosser, Dr. Steve Roger, Dr. Nadine Smith, Dr. Hongguang Zhang, Dr. Richardo Pascual, Dr. John Rumbal, Dr. John Farrow, Dr. David Robinson, Tony Lawton, Dr. Paul Breuer, Dr. Tian Li, Danielle Hewitt, Pauline Marosh, Heidi Pecherczyk, Milan Chovancek, Bruno Latella and Karl Bunney.

I am greatly indebted and appreciate very much my beloved wife, Cut Nurul Akmal for her encouragement and support throughout this study. To my son Diva Rayyan Rizki and my daughter Nabila Ariiqah for their own lovely ways to motivate me. To my father, mother, brothers, sister and families for their prayer.

ABSTRACT

Increasing environmental concerns over the use of cyanide for gold recovery enable researchers to determine and evaluate alternative reagents for many years. Thiosulfate leaching appears to be one of the most promising alternatives to cyanidation. Understanding gold thiosulfate leaching system plays a crucial role in order to effectively extract gold, in which the kinetics and equilibrium adsorption of thiosulfate, polythionates, gold thiosulfate and copper onto resin in resin-solution systems are taken into account. Process models associated with the adsorption of the species in resin-solution are also needed, which can be developed using experimental data, physical and chemical principles.

Experimental and modelling work for gold thiosulfate leaching system have been conducted in this study. The adsorption of thiosulfate, polythionates, gold thiosulfate and copper complexes onto strong based anion exchange resin of Purolite A500/2788 in single and multiple components resin-solution systems, has been investigated. The experimental procedures and speciation methods for the adsorption of thiosulfate, polythionates, gold thiosulfate and copper complexes on the resin in non-ammoniacal resin-solution (NARS) systems are proposed. As a result, the kinetics constants for the adsorption of thiosulfate, trithionate, tetrathionate and gold thiosulfate onto the resin in the single component NARS systems are obtained using the experimental data, the fitting of Lagergren and Ho model, and the numerical method of Levenberg-Marquardt. The resin capacity and the adsorption intensity of species on the resin are also determined using the equilibrium experiment data, Langmuir and Freundlich models and the numerical method.

The effects of thiosulfate and polythionates in solution on the adsorption isotherm of gold thiosulfate in the multiple components NARS systems are investigated. The result shows that the more thiosulfate concentration in solution at

equilibrium, the greater amount of gold thiosulfate adsorbed on the resin. Interestingly, the degradation of thiosulfate does not occur in the multiple components NARS systems. Diminishing the polythionates concentration in solution increases the gold thiosulfate loading in the multiple components NARS systems. Trithionate is likely loaded on the resin very well together with gold thiosulfate, and increasing the trithionate concentration in solution results in the greater amount of gold thiosulfate adsorbed on the resin. The loading affinity of gold thiosulfate increases with the decrease in the equilibrium concentration of tetrathionate on the resin. Overall, all the polythionates and gold thiosulfate are simultaneously adsorbed on the resin and compete with one another to occupy the available charge on the resin.

The result for the adsorption of thiosulfate and copper complexes on the resin in the multiple components resin-solution systems suggests that degassing the systems with nitrogen is needed to increase the total copper complexes adsorbed on the resin. The total copper complexes adsorbed on the resin exponentially decreases with the increase of thiosulfate concentration in solution Meanwhile, increasing ammonia in the solution results in the diminishing total copper complexes on the resin. As the solution pH of systems is maintained by the ammonia solution added in the system, the same effect of ammonia on the total copper complexes on the resin is also shown. It is highly noticed that much better adsorption of copper on the resin is determined in the systems without the addition of ammonia solution.

This study also proposed reaction mechanisms for the equilibrium adsorption phenomena of thiosulfate, polythionates, gold thiosulfate and copper complexes in multiple components resin-solution systems. As a result, equilibrium constants associated with the proposed reactions in the multiple components NARS systems for gold thiosulfate complexes are analytically solved using the experimental data. In addition to this, the competitive adsorption of thiosulfate, polythionates and gold thiosulfate adsorbed on the resin are simply emphasized. Meanwhile, the

equilibrium constants associated with the proposed reactions in the multiple components resin-solution systems for copper thiosulfate complexes are numerically solved using Newton Raphson method. As the outcome, the dynamic exponential decrease of total copper complexes adsorbed on the resin is easily described and the most dominant copper complexes species in solution and on the resin are captured.

Novel dynamic models describing the adsorption kinetics and equilibrium of thiosulfate, trithionate, tetrathionate and gold thiosulfate in non-ammoniacal resin-solution (NARS) system are mechanistically developed in this study. The models can be utilised to predict the amount of species adsorbed on the resin over time and at the equilibrium. The common Lagergren, Ho, Langmuir and Freundlich equations are taken into account to compare the developed models. Hence, the kinetics rate constants of thiosulfate, trithionate, tetrathionate and gold thiosulfate adsorbed on the resin and the parameters for the adsorption isotherm are obtained. Overall, the model-based results are in good agreement with the experimental-based results.

TABLE OF CONTENTS

LIST OF TABLES

LIST OF FIGURES

NOMENCLATURE

The following is a list of symbols used in this thesis. The other symbols which are not in the list, are directly explained following the formulas in the thesis.

Symbol	Dimension	Explanation
C_e	(mg/L), (g/L), (M), (mol/ L solution)	Equilibrium concentration of species in solution
CP_R is	(eq/L)	Capacity of resin
$c_S(e)$	(-)	Charge of counter ion (species) in solution being adsorbed on resin
$c_R(e)$	(+)	Charge of each site on resin when 1 mol of electron centre of resin being released from resin
K		Equilibrium constant of associated with the chemical exchange equilibrium relations within the resin, thiosulfate, polythionates (trithionate, tetrathionate and pentathionate), gold thiosulfate and copper complexes in resin-solution systems.
k	(/min) (/s)	Kinetic decay rate constant of species diminished from the solution, or being adsorbed on resin in resin-solution systems.
K_F	(g species/ kg dry resin)	The over-all adsorption capacity of Freundlich
K_L	(L solution/ g species)	The adsorption equilibrium constant of Langmuir
m_R	(kg), (g)	Mass of dry resin

n		The adsorption intensity of species
t	(min) (s)	Time
t_e	(min), (s)	Time required to attain an equilibrium state
$Q(t)$	(g species/ kg dry resin)	Amount of species adsorbed on resin over time
Q_e	(g species/ kg dry resin)	Amount of species adsorbed on resin at the equilibrium
Q_m	(g species/ kg dry resin)	Maximum amount of species adsorbed on resin at the equilibrium
V_S	(L), (mL)	Volume of solution
V_R	(L), (mL)	Volume of resin
WD		A sum of weighted deviation square between the experimental results and model results
$X_S(t)$	(M) (mol/ L solution)	Concentration of species in solution over time
X_Se	(M) (mol/ L solution)	Equilibrium concentration of species in solution
$X_s(\infty)$	(M) (mol/ L solution)	Equilibrium concentration of species in solution
$X_R(t)$	(M) (mol/ L resin)	Concentration of species on resin over time
X_Re	(M) (mol/ L resin)	Equilibrium concentration of species on resin

GLOSSARY OF TERMS

Adsorption	The accumulation of gases, liquids, or solutes on the surface of a solid or liquid. In this thesis, adsorption refers to the accumulation of anions (solutes of thiosulfate, polythionates, gold thiosulfate and cooper) on the surface of resin (solid), which is classified as a physical adsorption.
Adsorption Capacity	Maximum amount of adsorbate per unit mass of adsorbent.
Adsorption Intensity	The strength of adsorbate being adsorbed on the adsorbent.
Adsorption Isotherm	Given adsorption data in a curve relating the concentration of a solute on the surface of an adsorbent, to the concentration of the solute in the liquid, by which the mass of adsorbate per unit mass of adsorbent at equilibrium and at a given temperature is presented.
Analytical Method	Purely mathematical methods that do not require iteration.
Anion	Negatively charged ion.
Anion exchange resin	A resin of synthetic cross-linked polymers which have negatively charged ions attached to the side-groups of the resin. Different anions in the solution displace these attached anions from the resin as the exchange process of adsorption.
Dynamic model	Model expressing the behaviour of the system over time.
Equilibrium	A consistent ratio between a substance and a reactant.

Kinetics	The branch of chemistry concerned with measuring and studying the rates of chemical reactions. In this thesis, the main aim of kinetics study is to determine the mechanism of reactions by obtaining the rate of adsorption species on resin under the concentration of species.
Leaching	A process used in mineral processing to extract metals from ores by dissolving the metal into a solution in contact with the crushed ore. There are different types of leaching such as cyanide leaching of gold, thiosulfate leaching of gold, and bacterial or bioleaching of sulfide minerals.
Loading	A process that allows the adsorption of species onto resin in resin-solution systems.
Numerical Method	Iterative methods of solving problems on a computer
Solution	A mixture containing a liquid and a solid.
Stripping	A process that allows the desorption of species from resin in resin-solution systems

CHAPTER 1
Overview and Thesis Objectives

1.1 Background

Gold is a metallic chemical element with the symbol Au (from the Latin *aurum*), a heavy, dense, soft, shiny and the most highly ductile and malleable metal. Pure gold has a bright yellow color, traditionally considered attractive, and it has been the most precious metal in human history. It is chemically unaffected by air, moisture and most corrosive reagents. It is therefore used in the manufacture of coins, jewellery, alloys, dentistry, electronics, etc.

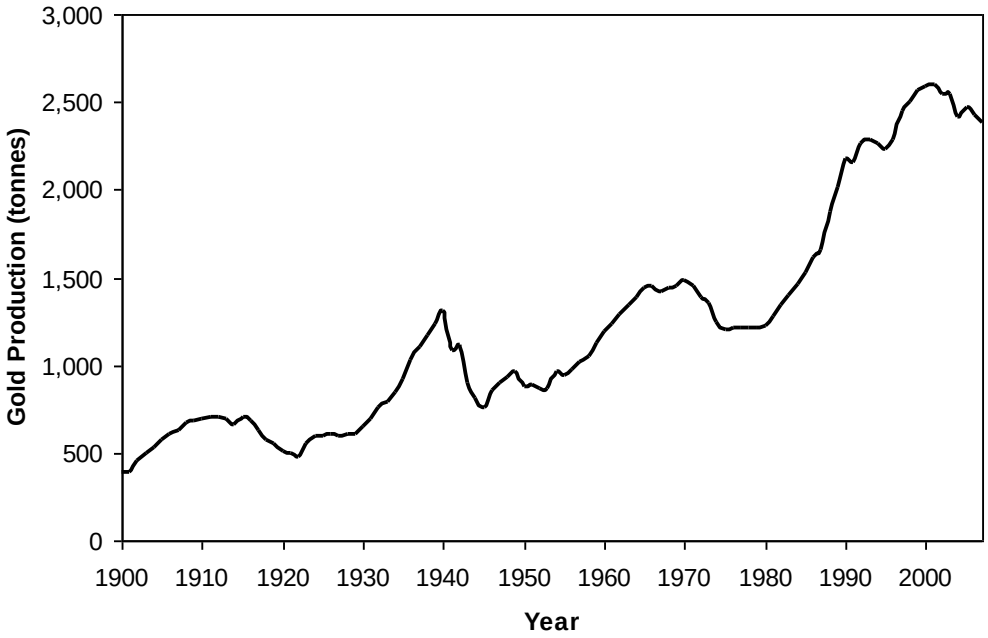

Figure 1.1 Annual world gold productions from 1990 to 2007 presented by U.S. Geological Survey (2008)

Gold production has been slightly raised since the introduction of carbon in pulp (CIP) process in the 1980's for the gold recovery using cyanide lead. World mine production of gold in 2007 fell slightly to 2,380 tonnes from 2,600 tonnes in 2001 as shown in Figure 1.1 (U.S. Geological Survey, 2008). Australian gold production was 246 tonnes in 2007 (Australian Bureau of Statistics, 2008) which is still the third largest producer of gold contribution (about 10.3% of the world's production). Meanwhile, China produced 281 tonnes, followed by South Africa with 270 tonnes.

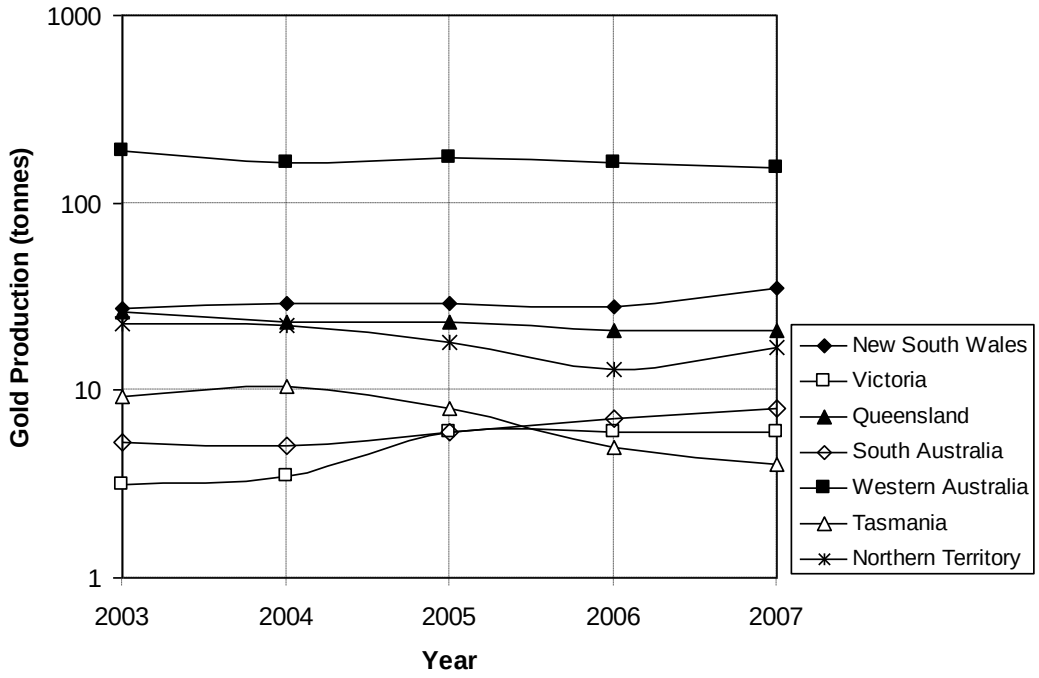

Figure 1.2 Annual gold productions in Australia from 2003 to 2007 based on Australian Bureau of Statistics (2008)

As shown in Figure 1.2, Western Australia produced about 189.1 tonnes to 155 tonnes from 2003 to 2007, respectively. These numbers are historical records for gold production worldwide, which is about 7% and 6.5% of world gold production in 2003 and 2007, respectively. It can be also forecasted that Western Australia will continuously contribute remarkable worldwide gold production by

2013-2014. Australian gold mine production is projected to be 264 by 2011-2012, and to be 248 tonnes by 2013-14 (Australian Bureau of Statistics, 2009).

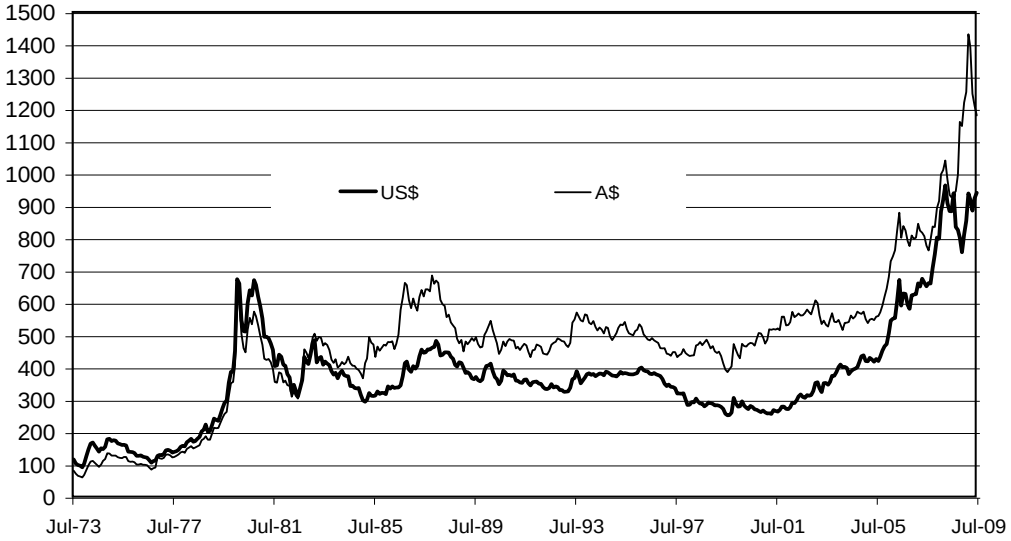

Figure 1.3 Historic gold price, US$/A$ per ounce cited in Government of Western Australia (2009)

The average gold price has increased slightly from approximately US$ 290 (A$ 550) an ounce in 2001 to approximately US$ 910 (A$ 1100) an ounce in 2009, as can be seen in Figure 1.3 (Government of Western Australia, 2009). The gold price would still increase in coming years due to strong demand for gold bars, coins and other product. Moreover, gold is commonly used as a hedge against inflation because the gold price has lower inflationary pressure in the short term (Australian Bureau of Statistics, 2009).

1.2 Motivation and Objectives of Thesis

The project of Thiosulfate Leaching Process for Gold Extraction is motivated by the need of resin-in-pulp (RIP) and resin-in-leach (RIL) processes for the extraction of gold using thiosulfate ($S_2O_3^{2-}$) as the leaching reagent. The RIP/RIL process is an environmentally-friendly alternative process compared to carbon-in-pulp (CIP) and carbon-in-leach (CIL) processes for the extraction of gold using cyanide. Understanding gold thiosulfate leaching system plays a crucial role in order to effectively develop the RIP/RIL process, in which the kinetics and equilibrium adsorption of thiosulfate, polythionates, gold thiosulfate and copper onto resin in non-ammoniacal resin-solution (NARS) systems are taken into account. Process models associated with the leaching and adsorption of the species in single component and multiple components in the NARS systems are needed. A process model can be developed based on experimental data using physical and chemical principles (Riggs, 2001).

Therefore, the overall aim of the thesis is to model the gold thiosulfate leaching process. The specific objectives of the thesis are as follows:

a. To provide the experimental procedure for the adsorption of thiosulfate, polythionates and gold thiosulfate onto strong based anion exchange resin in the single and multiple components of NARS systems.

b. To investigate the kinetics and equilibrium adsorption of thiosulfate, polythionates, gold thiosulfate and the adsorption intensity in the systems.

c. To obtain the kinetics rate constants for the adsorption of thiosulfate, polythionates, gold thiosulfate onto resin in the systems.

d. To propose the equilibrium reactions in the systems and to obtain the equilibrium constants for the adsorption reactions associated with the competing species in the systems.

e. To highlight the adsorption isotherm of gold thiosulfate on the effect of thiosulfate and polythionates in the systems.

f. To develop the experimental procedure for the adsorption of thiosulfate and copper complexes onto strong based anion exchange resin in the multiple components resin-solution systems.

g. To investigate the effects of nitrogen degas, thiosulfate and ammonia concentration in solution on the adsorption of total copper complexes on resin in the systems.

h. To propose the model for the equilibrium reactions associated with thiosulfate, polythionates and copper complexes in the systems, and validate the model using experimental data.

i. To determine the equilibrium constants for the proposed reactions in the systems and to obtain the dominant species of copper complexes in solution and on resin connected with the parameters simulation.

j. To develop dynamic models for kinetics and equilibrium adsorption of thiosulfate, polythionates, gold thiosulfate in the NARS, and to validate the models using experimental data.

k. To predict the amount of species adsorbed on resin over time and at the equilibrium in the NARS systems.

l. To obtain the kinetics constant for the adsorption of each species adsorbed on resin and to obtain the overall adsorption capacity and intensity based on the modelling in the NARS systems.

1.3 Scope and Contributions of Thesis

Leaching of gold using thiosulfate reagent relies on the fact that polythionates such as trithionate and tetrathionate are commonly generated in the system. Investigation on the kinetics of thiosulfate and polythionates in aqueous ammonia and alkaline solutions have been done in the previous studies (Byerley et al., 1973, Rolia and Chakrabarti, 1982, Zhang and Dreisinger, 2002a, Zhang and Dreisinger, 2002b). However, the kinetics of thiosulfate, polythionates and gold adsorbed on resin has not been presented in the previous studies. Meanwhile, the presence of polythionates affects the gold recovery using ion exchange resins (Nicol and O'Malley, 2002). Hence, this project highlights the kinetics studies for the adsorption of thiosulfate, polythionates and gold thiosulfate by conducting experimental and modelling work for single component resin-solution systems.

Ion-exchange resin simultaneously adsorbs thiosulfate, polythionates and gold thiosulfate with the charges on the resin's functional groups with the opposite charge (Grosse et al., 2003). Due to the limited number of charge on resin presented by the theoretical ion-exchange capacity of resin, and thiosulfate, polythionates and gold thiosulfate compete with one another, so adsorption isotherms are critical aspect to investigate. This thesis therefore emphasizes the kinetics and equilibrium studies for the adsorption of thiosulfate, polythionates and gold thiosulfate through experimental and modelling work of multiple components resin-solution systems.

Copper is generally found in the gold leaching of complex ores, which is abundant in the mineral matrix (Bhappu, 1990, Marsden and House, 1992). It reduces the efficiency of gold leaching and consumes additional reagent (Fagan et al., 1997, Huang et al., 1997). To lixiviate significant quantities of copper without consuming excessive reagent, ammoniacal thiosulfate leaching is typically much more economical than cyanidation (Aylmore, 2001). Several studies addressed the

chemistry of copper leaching in ammoniacal solution (Langhans et al., 1992, Li et al., 1995, Stupko et al., 1998, Breuer and Jeffrey, 2003, Black, 2006). Therefore, in addition to the leaching and adsorption of gold, this thesis also provides the equilibrium studies for the leaching and adsorption of copper complexes by conducting experimental and modelling work of multiple components resin-solution systems.

Therefore, the contributions of this thesis are:

- Development of experimental procedures for the kinetics and equilibrium adsorption of thiosulfate, polythionates, gold thiosulfate and copper onto resin in various resin-solution systems.
- Development of speciation method to calculate the amount of all species adsorbed on resin based on loading and stripping in the systems.
- Development of kinetics and equilibrium models for the adsorption of thiosulfate, polythionates and gold thiosulfate onto resin, and establishment of the kinetics and equilibrium constants.
- Development of equilibrium model for the leaching and adsorption of copper complexes in the resin-solution systems, and establishment of the equilibrium constants.
- Experimental-based and model-based investigations for the effects of various parameters on the kinetics and equilibrium adsorption of thiosulfate, polythionates, gold thiosulfate and copper in various resin-solution systems.

1.4 Thesis Outline

This thesis focuses on a gold thiosulfate leaching system of gold extraction process. In the unit, the adsorption of thiosulfate, polythionates, gold thiosulfate and copper take place on strong based anion exchange resin. Thiosulfate leaching process for gold extraction is done using experimental data, physical and chemical principles to show the adsorption phenomena, establish the kinetics and equilibrium constant, and optimize the gold extraction by simulating the models. Thus, the reminder of the thesis is organised as follow.

Chapter 2 contains literature review including the history of gold leaching processes from the previous ones to the recent ones.

Chapter 3 consists of the presentation of the experimental work related to the adsorption of gold thiosulfate complexes in single component resin-solution systems. The experimental procedures, speciation method, and results highlighting the adsorption of thiosulfate, polythionates and gold thiosulfate on resin in the systems, the kinetics constants and the adsorption intensity of each species adsorbed on resin in the systems.

Chapter 4 consists of the presentation of the experimental work related to multiple components resin-solution system of gold thiosulfate leaching system. The experimental procedures, speciation method, and results highlighting the adsorption of thiosulfate, polythionates and gold thiosulafate on resin in the systems, the equilibrium constants associated with gold thiosulfate complexes reactions and the competitive adsorption of all species in the systems are discussed.

Chapter 5 consists of the presentation of the experimental work related to copper complexes resin-solution systems. The experimental procedures, speciation method and results are highlighted in this chapter.

Model developments of the copper complexes resin-solution systems, proposing reaction mechanism, speciation method and the validation are presented in Chapter 6. The equilibrium constants associated with the proposed reaction mechanism are also addressed in this chapter.

Model developments of the kinetics and equilibrium models for the adsorption of single component and multiple components in resin-solution system are presented in Chapter 7. The kinetics and equilibrium constants and model simulations are addressed in this chapter.

To conclude this thesis, the conclusions and recommendations are given in Chapter 8. The appendixes contain the additional and supporting information for Chapter 3 to Chapter 7.

Figure 1.4 illustrates the link among numerous chapters of the thesis.

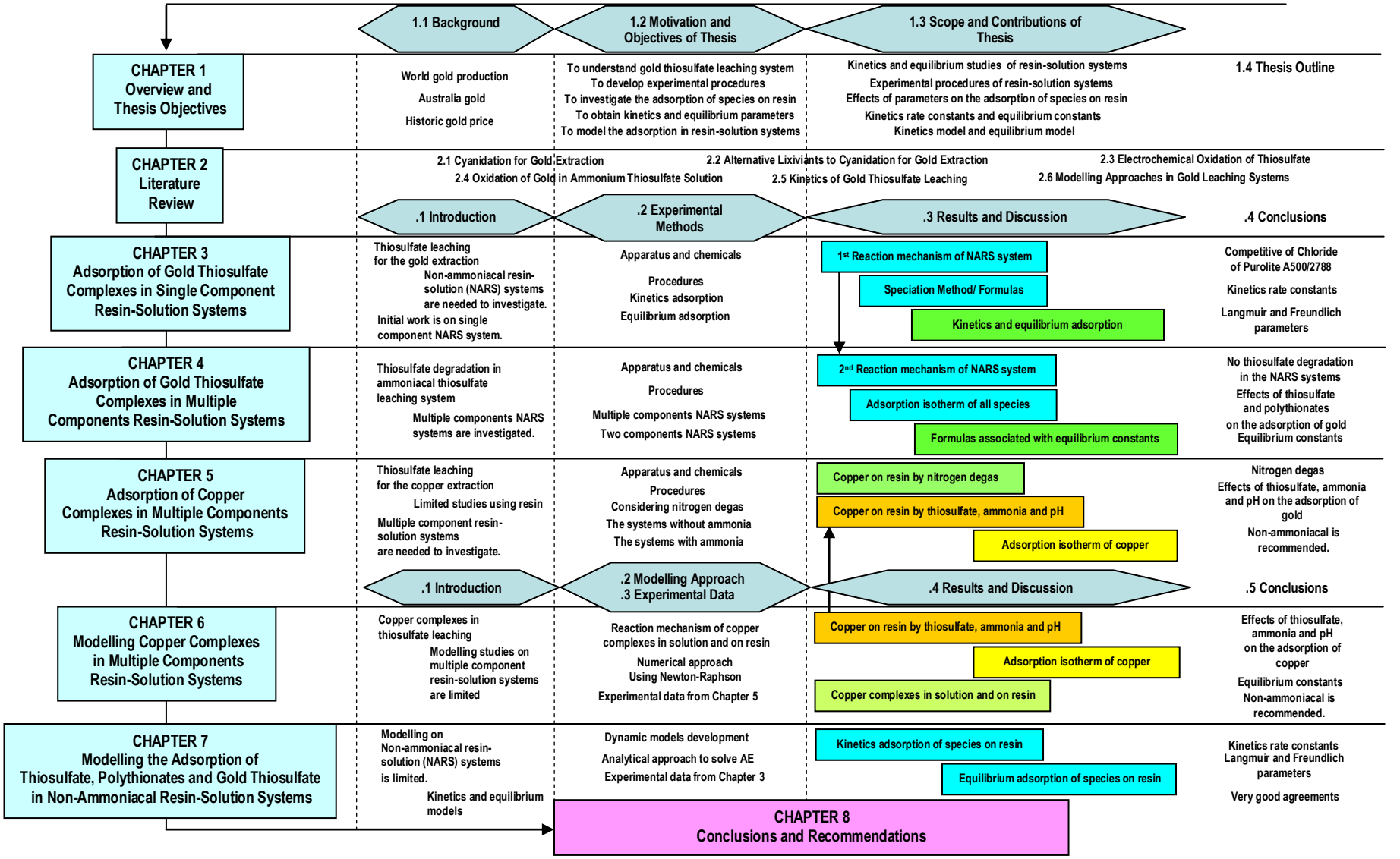

Figure 1.4 The flow chart of thesis outline

CHAPTER 2
Literature Review

2.1 Cyanidation for Gold Extraction

Cyanide has been used as a leach reagent at gold mining industries since its value as a leach reagent for gold ore treatment was firstly recognized by John Stewart MacArthur in 1880 and then patented in 1889. The cyanidation process relies on the fact that gold dissolves in aerated cyanide solution to produce the gold cyanide complex (MacArthur, 1988). It was developed into a commercial process in 1992 (Marsden and House, 1992). About 18% of total productions of manufacture sodium cyanide are used in mining operations around the world for gold recovery purposes (Logsdon et al., 1999). It has significantly been attributed as a leach reagent at gold mines due to its high efficiency and has been the most important extraction process for the extraction of gold and silver for over 100 years (Young, 2001).

Even if the cyanidation process is an effective technique, its use has become undesirable from an environmental perspective due to the acute toxicity of cyanide. In general, the dilute solutions of sodium cyanide (NaCN) are used in tank leaching and heap leaching processes at the concentration of 100–500 parts per million. Cyanide ions (CN^-) are active ingredients in the gold leaching process. The ions dissolve the gold contained in the ore by the complexion reaction (see Equation (2.1)) to form a "pregnant solution".

$$4Au + 8CN^- + O_2 + 2H_2O <=> 4Au(CN)_2^- + 4OH^- \quad (2.1)$$

The environmental impacts of cyanide as a leach reagent are wide-ranging at gold mines around the world. In the most cases, it caused severe environmental

problems due to leakage through tears and/or punctures in protective heap leach liners, or by spillage from overflowing solution ponds or tailings storage areas. Among other cases, it caused severe environmental problems along a 17-mile stretch of the Alamosa River of Colorado (USA) in 1992; it released more than 860 million gallons of cyanide-laden tailings into a major river of Guyana in 1995; and it caused severe contamination of groundwater of Montana (USA) and the substantial wildlife deaths in 1997 (Moran, 1998).

Cyanide can be poisonous to humans and to animal species in extreme quantities because it can inhibit human and animal tissues that extract oxygen from the blood after it reacts with the iron-carrying enzymes required for cells to use oxygen (Miller and Pritsos, 2001). Signs of acute poisoning to livestock, including initial muscle tremors, salivation, defecation, urination and laboured breathing, usually occur within a couple of minutes, and death can follow quickly (Korte and Coulston, 1995, CSIRO, 1998).

The cyanidation process has some disadvantage for the extraction of gold from some ore bodies. In order to improve the extraction of gold, additional treatments are applied such as pressure oxidation (Koslides and Ciminelli, 1992), ultra-fine grinding and electrolytic oxidation process (La Brooy et al., 1994), biological oxidation (Mosher and Figueroa, 1996) and roasting (Linge and Welham, 1997). In addition, since the leaching rate of gold and silver with cyanide is being controlled by the diffusion of oxygen which has limited solubility in water, the leaching kinetics is relative slow (Hartman, 1992). The leaching residence time is typically more than 1day (Han, 1994, Marsden and House, 2006).

2.2 Alternative Lixiviants to Cyanidation for Gold Extraction

A number of reagents has been used as the alternative to cyanidation for the extraction of gold, such as halide, thiourea, thiocyanate and thiosulfate. The use of halide (chlorine and bromine) systems for gold dissolution pre-dates cyanidation. Gold dissolution with chlorine is substantially faster than with cyanide but low concentrations of sulphides or other reactive components in the ore can make reagent consumption excessive and can reduce $AuCl_4^-$ back to metallic gold (La Brooy et al., 1994).

Thiourea (NH_2CSNH_2) is used in acid solution as a substitute for cyanide processing of Au ores and are becoming increasingly feasible for several reasons. The use of ferric ion in sulphuric acid is the most effective system and it improved gold extraction when it replaced the cyanide leaching reagent (Pyper and Hendrix, 1981). Thiourea has low sensitivity to base metals (Pb, Cu, Zn, As) and to residual sulphur in calcines. It has high gold recovery from pyrite and chalcopyrite concentrates, the recovery of gold from carbonaceous (refractory) is reasonable (Yannopoulos, 1991). From environmental prospective, thiourea has a lower toxicity and higher rate of gold and silver dissolution than cyanide (Lee et al., 1997, Ubaldini et al., 1998, Juarez and Dutra, 2000, Swaminathan et al., 1993). Although, thiourea is an effective reagent for gold extraction, the consumption of thiourea in gold extraction is high, the dissolution rate is low leading to an inhibiting coating of sulphur on the surface of the gold particles (Prasad et al., 1991) and it is more expensive than cyanide (La Brooy et al., 1994).

Thiocyanate is also an alternative lixiviant or leaching reagent to substitute cyanide for the extraction of gold. Correlations between thermodynamic calculations and electrochemical are able to demonstrate the participation of this reagent in the anodic dissolution of gold (Barbosa-Filho and Monhemius, 1994b). The intermediate species $(SCN)_2$ and $(SCN)_3^-$ play an important role in the

mechanism of the dissolution of gold by thiocyanate and it offers the advantage of much greater stability against oxidative decomposition (Barbosa-Filho and Monhemius, 1994c, Barbosa-Filho and Monhemius, 1994a). Using iodide-catalysed thiocyanate solutions to leach gold ores from the Dominican Republic, the thiocyanate system gave comparable results to the cyanide system, and exhibited considerably greater effectiveness than thiourea (Monhemius and Ball, 1995). More than 95% gold with the degree of 99.2-99.8% is recovered in weak acidic solutions (pH=2-5) at KSCN concentration of 0.4 mol/L and the desorption of gold from ion exchangers can be done by thiocarbamide solutions in H_2SO_4 at room temperature, and from carbon adsorbents by basic thiocarbamide solutions at ~150^{o}C (Kholmogorov et al., 2002).

Thiosulfate ($S_2O_3^{2-}$) which is commercially generated by boiling aqueous solution of sulfite with an excess of elemental sulphur (Bailar et al., 1973), is widely used in photography, paper industry, pharmaceutical applications, nuclear industry and medical research (Dhawale, 1993). It has a low toxicity with a LD_{50} (dose need to kill 50% of a population) of 7.5 ± 0.752 g/ kg for mice. Ammonium thiosulfate has also been used as a fertilizer for soils low in sulfur for many decades (Aylmore and Muir, 2001). Thiosulfate is relatively cheap and regarded as environmentally friendly reagent (Muir and Aylmore, 2004).

2.3 Electrochemical Oxidation of Thiosulfate

The electrochemical oxidation of thiosulfate has been investigated since 1932. A research on the anodic oxidation of thiosulfate to tetrathionate and sulfate concluded that tetrathionate can be obtained in highest yield at platinum electrode in neutral solution (pH = 5-7) at high density (0.2 A cm^2), and thiosulfate is oxidized by H_2O_2 produced at the anode (Glasstone and Hickling, 1932). It was reported that thiosulfate is oxidized on gold in neutral solutions in the double layer region where the gold is free of oxide layers. The authors have found that thiosulfate ions decompose when in contact with gold at open circuit, creating a layer of sulphur during the anodic oxidation of thiosulfate, which eventually blocks the surface of the gold electrode (Pedraza et al., 1988).

The electrochemical oxidation of gold was firstly conducted (White, 1905) using a direct oxidative dissolution of gold metal in an alkaline and near neutral solution of thiosulfate. Gold, as well as copper, is recovered from copper bearing sulphidic material containing gold (Berezowsky et al., 1978). Gold and silver are recovered from difficult-to-treat ores, particularly those containing manganese, by lixiviating using an ammonium thiosulfate leach solution containing copper, sufficient ammonia to maintain a pH of at least 7.5, and at least 0.05% sulfite ion (Kerley, 1983). The oxidation of gold in thiosulfate solution is believed to occur according to Equation (2.2), and the dissolved oxygen (E^0 = 0.4 V in alkaline solutions) should oxidise gold to gold thiosulfate (Antelman and Harris, 1982).

$$Au + 2S_2O_3^{2-} \rightarrow Au(S_2O_3)_2^{3-} + e^- \qquad (2.2)$$

The steady-state anodic polarization curve for gold in thiosulfate solution at 20 ^oC was presented in terms of the dissolution of gold and the anodic oxidation of thiosulfate ion (Jiang et al., 1993). The dissolution of Au in aqueous thiosulfate solution and the effect of the presence of ammonia in the solution were

investigated using voltammetry and electrochemical impedance spectra (EIS) methods. As a result, the anodic voltammetric curves of the Au electrode in thiosulfate solutions do not indicate the features of Au dissolution. But, the passivation of Au is completely eliminated by addition of ammonia into the system (Zhu et al., 1994). A rotating electrochemical quartz crystal microbalance (REQCM) allows the measurement of mass changes in situ, and thus, the leaching rate can be readily obtained for a wide range of solution concentrations (Jeffrey, 2001). A study using a combination of standard electrochemical techniques and the REQCM concluded that copper(II) readily affects the gold oxidation half reaction. To achieve appreciable gold oxidation rates, copper(II) concentrations that is greater than 2 mM are recommended (Breuer and Jeffrey, 2002). Moreover, recent electrochemical results reported that the gold oxidation from a rotating disc in a non-ammoniacal solution of potassium thiosulfate was faster than that in sodium thiosulfate at the same salt concentration of 0.2 M and at an applied potential of 0.25 V, under argon (Chandra and Jeffrey, 2004).

2.4 Oxidation of Gold in Ammonium Thiosulfate Solution

Studies on the kinetics and mechanism of oxidation of thiosulfate ion in aqueous ammonia solution have been carried out, and established that the rate of oxidation and uptake of oxygen is dependent upon the concentration thiosulfate. The rate of oxidation and uptake of oxygen is also inversely proportional to ammonia concentration (Byerley et al., 1973). The use of ammonium thiosulfate and oxygen under pressure to recover gold was proposed to improve the leaching of gold (Berezowsky et al., 1978). However, other studies concluded that the use of excessive oxygen increases the oxidative degradation of thiosulfate (Hemmati et al., 1989, Langhans et al., 1992).

Copper which is generally found in the gold leaching of complex ores (Bhappu, 1990, Marsden and House, 1992), reduces the efficiency of gold leaching and consumes additional reagent (Fagan et al., 1997, Huang et al., 1997). A patented process using copper ions and sulfides was developed (Kerley, 1983) to improve the leaching of gold. Because copper ions can be catalysts for the oxidation of thiosulfate by oxygen or other oxidant, there should only be sufficient copper present to maximize the leaching of gold and minimize thiosulfate consumption, and this only improves the initial rate of gold extraction (Zipperian et al., 1988, Abbruzzese et al., 1995).

Interestingly, the leaching of gold linearly increases with the Cu(II) concentration at low concentration (less than 5 mM) while the higher Cu(II) concentration almost does not affect the gold leaching rate. The reaction is dependent on the relative concentrations of thiosulfate, ammonia and copper with the recommended optimum condition (for standard gold leaching circuits) of 0.4 M thiosulfate, 0.6 M ammonia and 10 mM copper (Jeffrey et al., 2001). Recent concurrent thermodynamic and kinetic analysis of the literature data on gold oxidation by ammoniacal Cu(II) solutions has shown the importance of considering the

adsorption of thiosulfate ion onto the gold surface by a sequence of equations presented (Senanayake, 2004). Ammoniacal thiosulfate leaching is typically much more economical than cyanidation to lixiviate significant quantities of copper without consuming excessive reagent (Aylmore, 2001).

2.5 Kinetics of Gold Thiosulfate Leaching

A study on the kinetics and mechanism of oxidation of thiosulfate ion in aqueous ammonia solution also shows that trithionate is the main oxidation product. This result has practical relevance because of the need to limit the concentration of these species when recovering gold using resins (Byerley et al., 1975). Fundamental studies on the kinetics of decomposition of tetrathionate, trithionate and thiosulfate in alkaline solution have shown that at the same time as tetrathionate is decomposed by raising the pH to 11, trithionate is more stable and requires unacceptably higher pH or temperature to affect decomposition (Rolia and Chakrabarti, 1982).

The kinetics of tetrathionate decomposition in strong alkaline solutions deaerated with nitrogen has been investigated by means of ion chromatography. The results show that the reaction is first order with respect to both tetrathionate and hydroxide, and the activation energy of the reaction in the temperature range of 22-40^{o}C is 98.5 kJ mol^{-1} (Zhang and Dreisinger, 2002b). Tetrathionate, as the product of thiosulfate oxidation, strongly poisoned the resins in the recovery of gold and copper from ammonium thiosulfate (ATS) solutions using anion-exchange resins (Zhang and Dreisinger, 2002a). The presence of polythionates affects the gold recovery using ion exchange resins (Nicol and O'Malley, 2002).

In the latest publication, analytical procedures based on ion chromatography utilising an anion exchange column and UV detection are described for the quantification of thiosulfate, polythionates and gold thiosulfate both in leach solutions and adsorbed on anion exchange resins. One of the results shows that tetrathionate and pentathionate are the dominant reaction products from thiosulfate oxidation at pH 8.5 and 9, whilst trithionate and sulfate are formed at pH 10.4 (Jeffrey and Brunt, 2007).

Therefore, the thiosulfate consumption and polyhionates decomposition (which results from the oxidation of ammonia in the system) would be the limitation of the ammoniacal resin-solution system of the kinetics of gold thiosulfate leaching in the previous studies. This limitation will be addressed in this thesis. The kinetics of gold thiosulfate leaching and the isotherm adsorption for thiosulfate, polythionates and gold thiosulfate in non-ammoniacal resin-solution systems will also be obtained.

2.6 Modelling Approaches in Gold Leaching Systems

A number of modelling approaches using different mathematical formulations have been published in the literature that model gold leaching systems. A variable activation energy model was developed using the activation energy equation and the Arrhenius expression for chloridization of oxide copper ore and cyanidation of gold ore (Brittan, 1975). Mathematical models of leaching reactors using the population balance were presented for the pressure leaching of sphalerite and zinc (Crundwell and Bryson, 1992, Crundwell, 1995). A mathematical model of leaching of gold in cyanide solution was derived using the shrinking-particle model where the reaction mechanism is described by the electrochemical model (Crundwell and Godorr, 1997). To simulate the transient evolution of the dissolved chemical species in the heap and column isothermal leaching processes, a model was developed. It can be used to predict the general features of the process time evolution despite some bias due to the model simplification (de Andrade Lima, 2004).

A number of researchers have attempted to model a carbon-in-pulp (CIP) and carbon-in-leach (CIL) processes for the treatment of lower gold grade and problematic ore, and for the investigation of operational variables and design. A simple empirical model for adsorption, the *kn* model of Equation (2.3) was proposed by Fleming et al. (1980) during the first development of CIP process;

$$y - y_o = kC_{ss}t^n \tag{2.3}$$

where y_o is the initial concentration of gold on the carbon and y is the concentration of gold on the carbon after an adsorption period, t, C_{ss} is the equilibrium gold concentration in solution, and k and n are the model parameters. Then, Nicol et al. (1984) developed the first CIP/CIL process model, assuming that the flow of pulp and carbon are in continuous counter-current mode, and the

model presented steady state condition of constant gold concentration at each tank.

A dynamic model of CIP/CIL process using population-balance methods was presented (Woollacott et al., 1990). A linear kinetic adsorption rate (Dixon et al., 1978) was used in the Stange CIP model (Stange et al., 1990), and the model results were in quite good agreement with actual CIP plant data. The linear kinetics adsorption rate is expressed as:

$$R = k_1 \ C(y_1^+ - y_1) - Ky_1 \tag{2.4}$$

where k_1 is the rate constant, y_1^+ is the loading capacity of carbon, y_1 is the carbon loading, C is the species concentration in solution, and K is the model parameter. Film and intra-particle diffusions, simultaneous leaching and loading of multi components species were incorporated in a CIP model (Liebenberg and van Deventer, 1998). A mixer-integer nonlinear programming of mathematical models, approach was taken into account to construct and optimize CIP processes of gold recovery plants (Kiranoudis et al., 1998). The linear kinetics adsorption by Dixon et al. was adopted in the mathematical models.

The most resent dynamic models of CIL process were proposed by van Deventer et al. (2004) and de Andrade Lima (2007). Semi-empirical regression network kinetic model was developed by van Deventer et al. for the dynamic modelling of the carbon-in-leach (CIL) process for gold recovery. A phenomenological model for the CIL kinetics with three intrinsic reactions of adsorption, leaching and preg-robbing (Equations (2.5), (2.6) and (2.7), respectively) were proposed in the modelling approach:

$$F_{1,ij} = \frac{6kf_j W_i}{\rho_c d_c}(C_{ij} - C_{ij,s,c}) \tag{2.5}$$

$$F_{2,ij} = kl_j M_j (G_{ij} - G_j^{\infty}) \tag{2.6}$$

$$F_{3,ij} = \frac{6kp_j M_i}{\rho_o d_o}(C_{ij} - C_{ij,s,o}) \tag{2.7}$$

where kf_j, kl_j and kp_j represent the adsorptive, leaching and preg-robbing coefficients for an adsorbate *j*; W_i and M_i are the masses of carbon and ore of stage *i*, respectively; $C_{ij,s,c}$ and $C_{ij,s,o}$ are the concentration of component *j* at the activated carbon and ore surface of stage *i*, respectively; d_c and d_o are the diameter of carbon and ore particles of stage *i*, respectively; and G_j^{∞} is the refractory, unleachable grade of the ore.

A dynamic model of CIL process was numerically solved using a least square method such unconstrained optimization method to fit the plant data for calibration of the model parameters (de Andrade Lima, 2007). The adsorption kinetic used in the dynamic model is typically the same as Dixon et al. model of Equation (2.4).

All the kinetics and dynamic models for the adsorption of gold need the equilibrium parameters such as the equilibrium concentration of gold in solution and the loading capacity of carbon to calculate the concentration of gold on carbon. Therefore, development of dynamic models for the adsorption of gold on adsorbent in which the model can be used to predict the concentration of gold on adsorbent over time before reaching the equilibrium stage is a novel contribution of this thesis.

CHAPTER 3
Adsorption of Gold Thiosulfate Complexes in Single Component Resin-Solution Systems

3.1 Introduction

The cyanidation process relies on the fact that gold dissolves in aerated cyanide solution to produce the gold cyanide complex (MacArthur, 1988). Due to its high efficiency, it has been the most important extraction process of gold and silver for over 100 years (MacArthur, 1988, Marsden and House, 1992, Logsdon et al., 1999, Young, 2001). However, its use in certain environments has been restricted owing to the acute toxicity of cyanide (Korte and Coulston, 1995, Moran, 1998, Miller and Pritsos, 2001). In order to improve the process, additional treatments can be adapted when processing refractory ores such as pressure oxidation, ultra-fine grinding, roasting and biological oxidation (Koslides and Ciminelli, 1992, La Brooy et al., 1994, Mosher and Figueroa, 1996, Linge and Welham, 1997). Among the alternatives to cyanide (Hilson and Monhemius, 2006), thiosulfate is the most promising one because it is environmentally friendly and it is a relatively cheap reagent (Muir and Aylmore, 2004).

There have been a number of extensive studies on the leaching of gold with thiosulfate ($S_2O_3^{2-}$). Trithionate and tetrathionate are commonly generated in the gold leaching system using thiosulfate reagent. Trithionate is the main oxidation product of thiosulfate oxidation in aqueous ammonia solution (Byerley et al., 1975). Higher pH and temperature of alkaline solution affect the decomposition of tetrathionate, trithionate and thiosulfate (Rolia and Chakrabarti, 1982). Zhang and Dreisinger (2002a) reported that tetrathionate is the product of thiosulfate oxidation in the system with ammonium thiosulfate solutions and anion-exchange resins. In addition, the latest research shows that tetrathionate and pentathionate

are the dominant reaction products from thiosulfate oxidation at pH 8.5 and 9, whilst trithionate and sulfate are formed at pH 10.4 (Jeffrey and Brunt, 2007).

The advantages and problems associated with gold leaching and recovery in ammoniacal thiosulfate system with copper(II) were reviewed (Ritchie et al., 2001, Muir and Aylmore, 2003). The importance of kinetic studies in non-ammoniacal thiosulfate systems increased the application for recovery of gold (Ji et al., 2003). Most research has focused on the rate expressions, various equilibriums to interpret the gold oxidation kinetics in which thiosulfate ion of $S_2O_3^{2-}$ present in various salts (Sillen and Martell, 1964, Wang, 1992, Zhang and Nicol, 2003, Chandra and Jeffrey, 2004, Senanayake, 2004). However, there is still limited study on the kinetics and equilibrium adsorption of thiosulfate, polythionates and gold thiosulfate onto resin in single component resin-solution of non-ammoniacal systems. Meanwhile, the presence of polythionates affects the gold recovery using ion exchange resins (Nicol and O'Malley, 2002).

Therefore, the work in this chapter is mainly aimed to investigate the adsorption of thiosulfate, polythionates and gold thiosulfate on strong based anion exchange resin in the single component of non-ammoniacal resin-solution systems. The specific objectives of the work are:

a. To provide the experimental procedure and speciation method for the adsorption of thiosulfate, polythionates and gold thiosulfate adsorptions on strong based anion exchange resin in single component resin-solution non-ammoniacal systems.

b. To obtain the kinetics constant for the adsorption of each species adsorbed on resin in the systems.

c. To highlight the adsorption intensity of each species adsorbed on resin in the systems.

3.2 Experimental Methods

All the experimental work for the adsorption of thiosulfate, polythionates and gold thiosulfate on strong based anion exchange resin in single component resin-solution non-ammoniacal systems had been done in the Thiosulfate Laboratory at Australian Mineral Research Centre, CSIRO Mineral in Western Australia.

3.2.1 Apparatus and Chemicals

A Waters 2695 HPLC separation module was used to analyze the concentrations of thiosulfate and polythionates. The separation was achieved using a Dionex IonPac AS16 ion exchange column equipped with an IonPac AG16 guard column. The mobile phase was a solution of sodium perchlorate (0.075 – 0.2 M). The species detection was via a Waters 2996 Photodiode Array Detector (UV). Empower software was used for the calculation of peak area (Waters, 2002). Details about the mobile solution and the wavelengths of UV adsorption and peak retention times of the involved species have been described in the literature (Jeffrey and Brunt, 2007). Gold was analysed by inductively coupled plasma optical emission spectrometry (ICP-OES). All the thiosulfate and polythionates analysis have been done by the PhD candidate of this thesis in the HPLC Laboratory at the Australian Mineral Research Centre (see Figure A.3 in Appendix A), and all the gold thiosulfate analysis have been done by the staff of Analytical Chemistry Unit at the Australian Mineral Research Centre.

All solutions were prepared from either analytical grade or synthesized reagents with deionized water. Sodium thiosulfate ($Na_2S_2O_3$) and sodium tetrathionate ($Na_2S_4O_6.2H_2O$), 99% pure was obtained from Aldrich. Sodium trithionate ($Na_2S_3O_6$) was prepared using the methods described by Kelly and Wood (Kelly

and Wood, 1994). Trisodium gold thiosulfate salt ($Na_3Au(S_2O_3)_2.2H_2O$) was prepared and recrystallised using the procedure described by Ruben et al. (2002).

The resin used was Purolite A500/2788 in the chloride form with a macrospore structure. This resin has been selected for previous work (Jeffrey and Brunt, 2007, Zhang and Dreisinger, 2002a) and was found to be highly efficient for the recovery of gold from thiosulfate solutions. The wet form of the resin contained 53-58 % moisture, the resin capacity is 1.15 meq/mL, and the specific gravity is 1.08 g/mL (PUROLITE, 2008).

3.2.2 Procedures

All the experiments of the adsorption of thiosulfate, polythionates and gold thiosulfate on strong based anion exchange resin in single component resin-solution non-ammoniacal system were conducted at the neutral pH and the ambient temperature (~23 °C). The concentration on the resin for a particular species was calculated from the change in its solution concentration in the system.

A. The Experiments on Kinetics Adsorption

Initially, the kinetics experiment was conducted to generate kinetics data for the adsorption of thiosulfate on resin in the system. The steps of the experiments are described as follows;

1) Prepare 200 mL of 3 mM $Na_2S_2O_3.5H_2O$ (sodium thiosulfate) solution in 200 mL volumetric flask.

2) Take 1 mL sample of the solution for HPLC analysis as the loading sample at t = 0 minute.

3) Prepare 0.333 g resin, and place it in a conical flask.

4) Place the 199 mL solution in the conical flask to present a resin-solution system for the adsorption of thiosulfate onto resin.

5) Stir it at 155 rpm with IKA overhead stirrers, and start timer for loading.

6) Take 1 mL samples of the solution for HPLC analysis the loading samples at t = 30, 60, 90, 120, 180, and 300 minutes.

7) After 5 hours loading, decant and wash the resin 4 times with DI water into a large vial. Suck the remaining H_2O using pipette.

8) Add 50 mL $NaClO_4$ (0.5M) into the vial for the dilution of thiosulfate from the resin, shake it at 150 U/minute and start the timer for 30 minutes of the 1st stripping.

9) Take 1 mL sample of the solution for HPLC analysis as the 1st stripping sample.

10) Decant and wash the resin 4 times with DI water in the vial. Suck the remaining H_2O using pipette.

11) Re-add 50 mL $NaClO_4$ (0.5M) into the vial for the dilution of thiosulfate from the resin, shake it at 150 U/minute on a Jubalo SW-20C shaker and start the timer for 30 minutes of the 2nd stripping.

12) Take 1 mL sample of the solution for HPLC analysis as the 2nd stripping sample.

13) Decant and wash the resin 4 times with DI water in the vial. Before placing the resin in a small glass vial, measure the empty vial mass.

14) Place the resin in a small glass vial, and suck the remaining H_2O using pipette.

15) Dry the resin at 60 ^{o}C in an oven for about 16 hours.

16) Measure the mass of vial with resin to obtain the dried resin mass; the dried resin mass = the mass of vial with resin – the empty vial mass.

The 1st to 16th steps were repeated to generate kinetics data for the adsorption of trithionate and tetrathionate on resin in the systems with the initial concentrations of species being 3 mM. The same procedures were also repeated to generate kinetics data for the adsorption of gold thiosulfate on resin in the system with the initial gold concentrations of 100 mg/L, but the HPLC analysis was replaced with the ICP-OES analysis for gold. Instead of 1 mL samples, 10 mL samples were taken for the ICP-OES analysis. The flowchart presenting the procedure of kinetics experiment is summarized by Figure A.1 in Appendix A.

B. The Experiments on Equilibrium Adsorption

The equilibrium experiments were run for 5 hours based on the kinetics measurements, to make sure equilibrium was achieved. The same procedures of kinetics experiments were also done for the equilibrium experiments with various initial concentrations of species. The samples for the HPLC analysis and ICP-OES analysis for the particular species were taken before loading (t = 0 hour) and after loading (t = 5 hours), before stripping and after stripping. The agreements between the loading and stripping experiments in terms of the quantities of various species loaded on the resin were investigated to highlight the mass balance of species adsorbed on resin and diluted from resin. The flowchart presenting the equilibrium experimental procedure is summarized by Figure A.2 in Appendix A.

3.3 Results and Discussion

3.3.1 Speciation on Adsorption of Single Component

All the species such as thiosulfate, trithionate, tetrathionate and pentathionate in the HPLC analysis were quantified at the peak retention time as shown in Figure 3.1 and at the wavelength of peak UV adsorption of 214 nm except trithionate which was quantified at 192 nm. The wavelength of peak UV adsorption for thiosulfate (as an example) is shown in Figure 3.2.

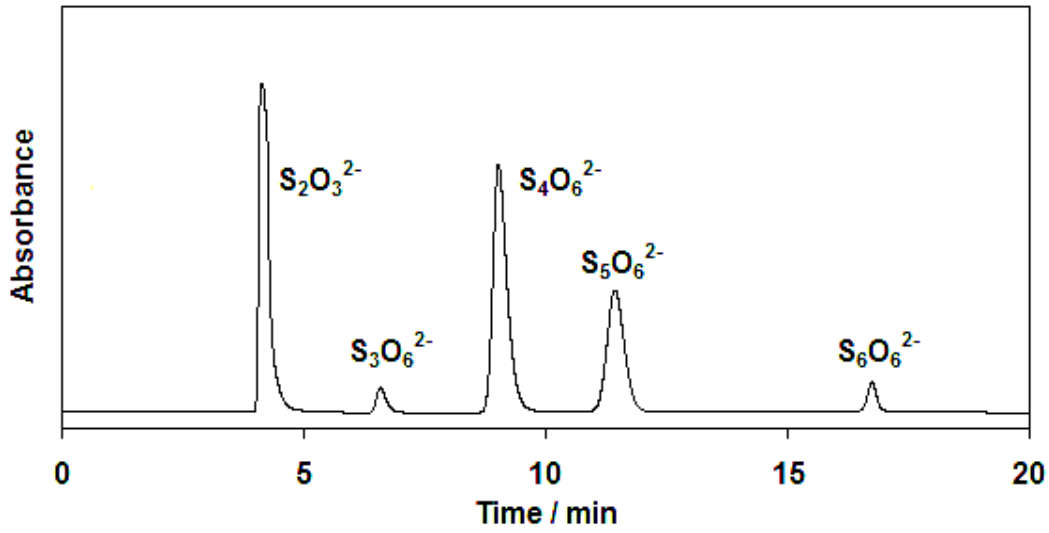

Figure 3.1 The UV detector-based HPLC chromatograms for the peak retention time of thiosulfate, trithionate, tetrathionate and pentathionate

There are a number of commercially available strong base ion exchange resins and the strong based anion exchange resin of Purolite A500/2788 has been used in this project, which has macroporous polystyrene crosslinked with divinylbenzene and the trimetyl ammonium or quaternary ammonium, $R4N^+$ as the functional group. The resin can be used for the adsorption of gold from thiosulfate leaching

of gold ores (PUROLITE, 2008). The exchange centre of the resin is the chloride electron as shown in Figure 3.3.

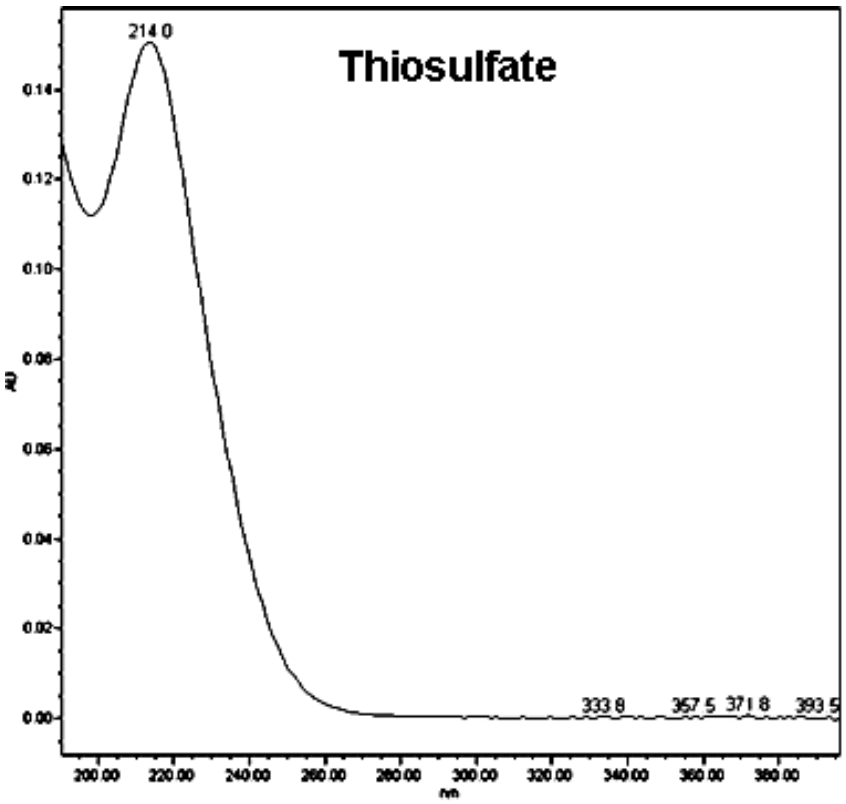

Figure 3.2 The UV detector-based HPLC chromatogram for the thiosulfate wavelength of peak UV adsorption

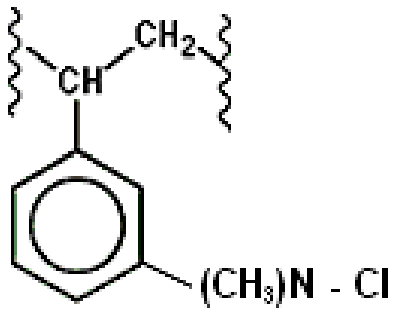

Figure 3.3 The illustration of Purolite A500/2788 structure

In single component of non-ammoniacal resin-solution system, the chemical exchange equilibrium relations within the resin and thiosulfate, polythionates (trithionate, tetrathionate and pentathionate) or gold thiosulfate can be theoretically specified by Equations (3.1), (3.2), (3.3), (3.4), and (3.5), respectively:

$$2R\text{-}Cl_{(s)} + S_2O_3^{2-}{}_{(aq)} \Leftrightarrow R_2S_2O_{3(s)} + 2Cl^-_{(aq)} \quad (3.1)$$

$$2R\text{-}Cl_{(s)} + S_3O_6^{2-}{}_{(aq)} \Leftrightarrow R_2S_3O_{6(s)} + 2Cl^-_{(aq)} \quad (3.2)$$

$$2R\text{-}Cl_{(s)} + S_4O_6^{2-}{}_{(aq)} \Leftrightarrow R_2S_4O_{6(s)} + 2Cl^-_{(aq)} \quad (3.3)$$

$$2R\text{-}Cl_{(s)} + S_5O_6^{2-}{}_{(aq)} \Leftrightarrow R_2S_5O_{6(s)} + 2Cl^-_{(aq)} \quad (3.4)$$

$$3R\text{-}Cl_{(s)} + Au(S_2O_3)_2^{3-}{}_{(aq)} \Leftrightarrow R_3Au(S_2O_3)_{2\,(s)} + 2Cl^-_{(aq)} \quad (3.5)$$

where R represents the resin functional group. According to Equation (3.1) as an example, the equilibrium constant, $K_{3.1}$ for the reaction can be represented by:

$$K_{3.1} = \frac{R_2S_2O_3}{\left[S_2O_3^{2-}\right]} \times \frac{\left[Cl^-\right]^2}{RCl^{\,2}} \quad (3.6)$$

where all the species concentration presented in equilibrium condition; $\left[S_2O_3^{2-}\right]$ is the thiosulfate concentration in solution (M = mol/ L solution), obtained based on the HPLC reading, $R_2S_2O_3$ represents the thiosulfate concentration on resin (M = mol/ L resin), $\left[Cl^-\right]$ is the chloride concentration in solution (M), and RCl is the chloride concentration on resin (M). The additional expressions for Equation (3.6) are as follows:

$$R_2S_2O_3 = \left[S_2O_3^{2-}\right]_0 - \left[S_2O_3^{2-}\right] \frac{V_S}{V_R} \tag{3.7}$$

$$\left[Cl^-\right] = \left[S_2O_3^{2-}\right]_0 - \left[S_2O_3^{2-}\right] \frac{c_S(e)}{c_R(e)} \tag{3.8}$$

$$RCl = -\frac{CP_R}{c_R(e)} - \left[Cl^-\right]\frac{V_S}{V_R} \tag{3.9}$$

where $\left[S_2O_3^{2-}\right]_0$ is denoted as the initial thiosulfate concentration (M), $c_R(e)$ is the charge of each site on resin (+1) when 1 mol chloride being released from resin, and $c_S(e)$ corresponds to the charge of 1 mol thiosulfate (-2), CP_R is the resin capacity (eq/L), V_S and V_R are the solution volume and the resin volume, respectively. Similarly, Equations (3.6) to (3.9) can be derived for Equations (3.2) to (3.5).

If thiosulfate competes with the resin exchange centre chloride in the single component resin-solution system, the value of equilibrium constant $K_{3.1}$ should not change with the change of the equilibrium thiosulfate concentration. However, the experimental result shows that the $K_{3.1}$ value changes with the change of the equilibrium thiosulfate concentration, as can be seen in Figure 3.4. This clearly indicates that there is no competition between thiosulfate and chloride in the system. In other words, chloride is a very weak anion compared to thiosulfate, so chloride does not re-occupy the site of resin to keep constant of the $K_{3.1}$ value. In addition, there is also no competition between tetrathionate and chloride in the single component of tetrathionate in resin-solution system, the equilibrium constant for Equation (3.3), $K_{3.3}$ decreases with the increase in the equilibrium concentration of tetrathionate, as clearly shown in Figure 3.5.

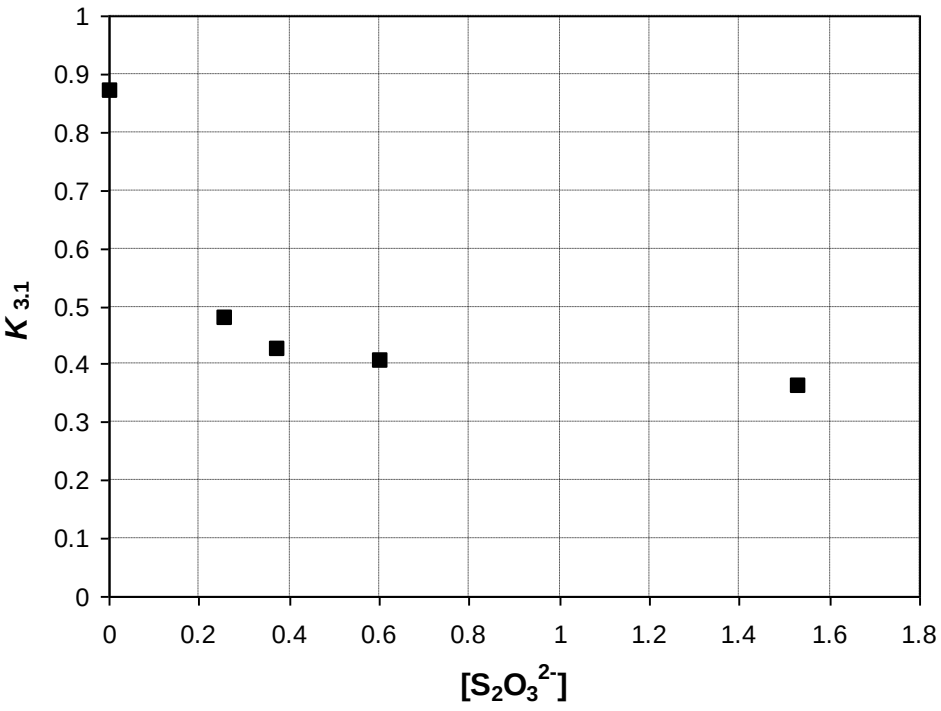

Figure 3.4 $K_{3.1}$ over equilibrium thiosulfate concentration

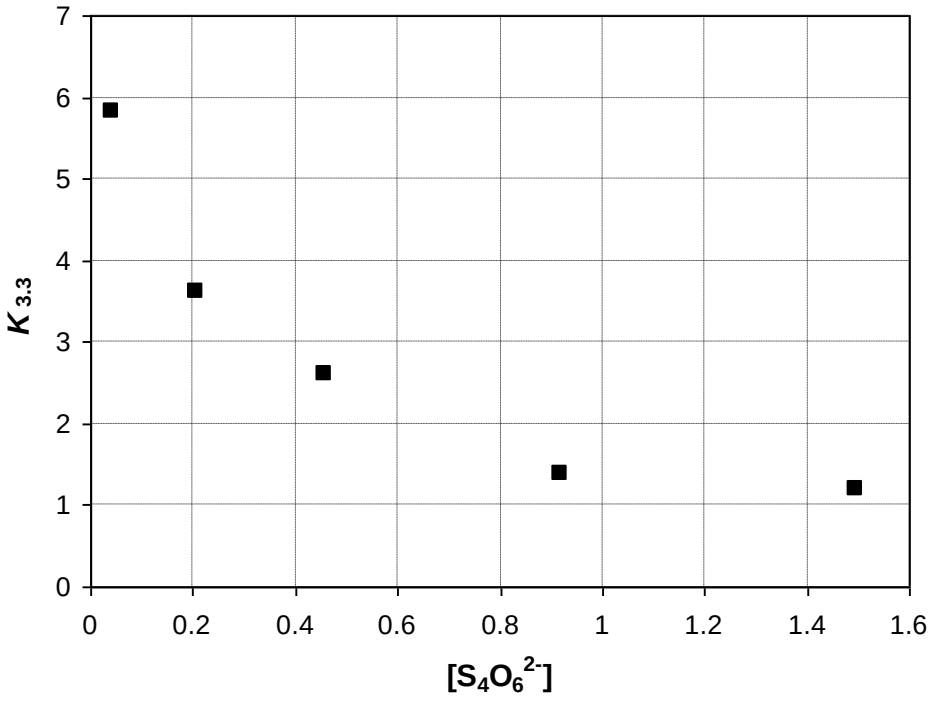

Figure 3.5 $K_{3.3}$ over equilibrium tetrathionate concentration

Investigation on the equilibrium constants associated with Equations (3.2), (3.4) and (3.5) also results in the same profile as the previous ones. It can finally be concluded that chloride is a very weak anion compared to thiosulfate, polythionates and gold thiosulfate, and there is no competition loading between chloride and the species in the single component resin-solution system.

3.3.2 Kinetics Adsorption of Single Component

Since the adsorption of thiosulfate, polythionates and gold thiosulfate onto the ion exchange resin is a heterogeneous process, with the rate of adsorption being limited by the mass transfer of the anionic species from the solution to the ion exchange sites of resin, and the resin exchange centre of chloride is very weak compared to the species, Equations (3.1) to (3.5) can therefore be advanced to:

$$\left[S_2O_3^{2-}\right]_{X_S(t)} \xrightarrow{k_2} \left[S_2O_3^{2-}\right]_{X_Se} \xleftrightarrow{K_2} \left[S_2O_3^{2-}\right]_{X_Re} \xrightarrow{k_2} \left[S_2O_3^{2-}\right]_{X_R(t)} \quad (3.10)$$

$$\left[S_3O_6^{2-}\right]_{X_S(t)} \xrightarrow{k_3} \left[S_3O_6^{2-}\right]_{X_Se} \xleftrightarrow{K_3} \left[S_3O_6^{2-}\right]_{X_Re} \xrightarrow{k_3} \left[S_3O_6^{2-}\right]_{X_R(t)} \quad (3.11)$$

$$\left[S_4O_6^{2-}\right]_{X_S(t)} \xrightarrow{k_4} \left[S_4O_6^{2-}\right]_{X_Se} \xleftrightarrow{K_4} \left[S_4O_6^{2-}\right]_{S_Re} \xrightarrow{k_4} \left[S_4O_6^{2-}\right]_{X_R(t)} \quad (3.12)$$

$$\left[S_5O_6^{2-}\right]_{X_S(t)} \xrightarrow{k_5} \left[S_5O_6^{2-}\right]_{X_Se} \xleftrightarrow{K_5} \left[S_5O_6^{2-}\right]_{X_Re} \xrightarrow{k_5} \left[S_5O_6^{2-}\right]_{X_R(t)} \quad (3.13)$$

$$\left[Au\ S_2O_3{}_2^{3-}\right]_{X_S(t)} \xrightarrow{k_{Au}} \left[Au\ S_2O_3{}_2^{3-}\right]_{X_Se} \xleftrightarrow{K_{Au}}$$
$$\left[Au\ S_2O_3{}_2^{3-}\right]_{X_Re} \xrightarrow{k_{Au}} \left[Au\ S_2O_3{}_2^{3-}\right]_{X_R(t)} \quad (3.14)$$

where $X_S(t)$ (M = mol/ L solution) refers to the concentration of species in solution over time t (s); X_Se (M) is the equilibrium concentration of species in solution;

$X_R(t)$ (M = mol/ L resin) refers to the concentration of species on resin over time *t*; X_Re (M) is the equilibrium concentration of species on resin; K_2, K_3, K_4, K_5 and K_{Au} are the equilibrium constants for the adsorption of thiosulfate, trithionate, tetrathionate, pentathionate and gold thiosulfate, respectively in the systems between the species concentration in solution and on resin. The species concentrations in solution, $X_S(t)$ and X_Se are determined from HPLC reading calibrated with standard solution. The species concentration on resin, $X_R(t)$ and X_Re are calculated using Equation (3.7). The loading of species on resin over time, $Q(t)$ and at the equilibrium Q_e are determined from $X_R(t)\ V_R/\ m_R$ and $X_Re\ V_R/\ m_R$, respectively where V_R is the resin volume (L) and m_R is the dry resin mass (kg). The kinetics and equilibrium constants can be determined from experimental data using the models in the available literature.

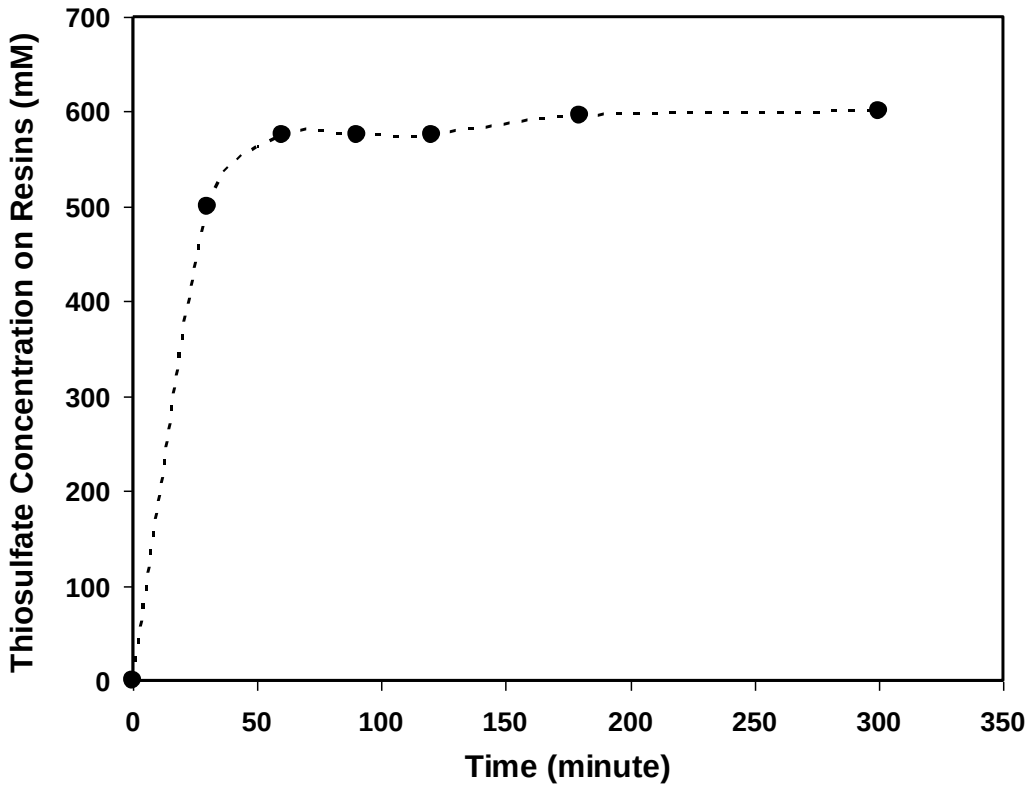

Figure 3.6 The thiosulfate concentration versus time for the kinetics adsorption onto the anion exchange resin (mM = mmol/ L resin)

Figure 3.6 shows the thiosulfate concentration on resin over time based on the experimental data of loading for the kinetics adsorption of thiosulfate onto the anion exchange resin in the resin-solution system with the initial thiosulfate concentration of 3 mM and 0.333 g resin. As can be seen in Figure 3.6, thiosulfate concentration on resin sharply increases in the first 30 minutes loading, from 0 mM to about 500.486 mM. Then, it gradually increases to 575.828 mM at 30 minutes of loading time. From the kinetics test, the equilibrium concentration of thiosulfate on resin is approximately 601.131 mM that results in the equilibrium thiosulfate loading of 168.316 g thiosulfate/ kg dry resin at 300 minutes of loading time, as can be seen in Figure 3.7.

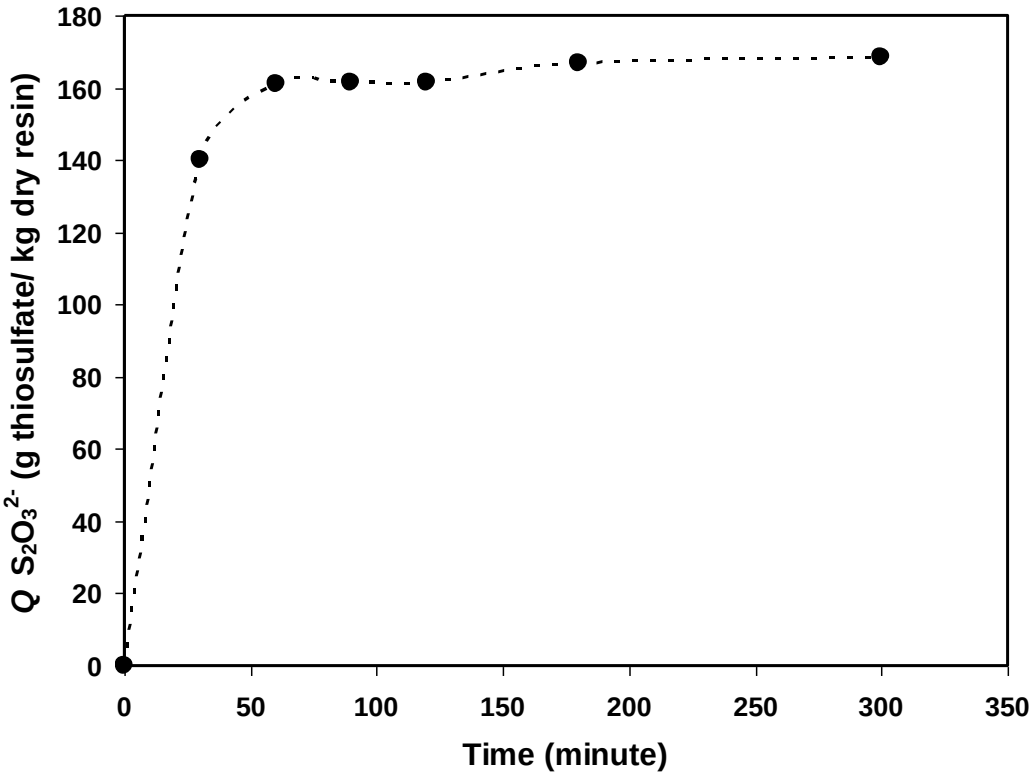

Figure 3.7 The thiosulfate loading versus time for the kinetics adsorption onto the anion exchange resin

Trithionate and tetrathionate loading over time in the resin-solution system with the initial concentration trithionate and tetrathionate in each system being 3 mM and 0.333 g resin are presented by both graphs shown in Figure 3.8. Interestingly, trithionate loading is almost the same as tetrathionate loading for the first 90 minutes. Then, tetrathionate loading still gradually increases until reaching the equilibrium loading of about 307.649 g tetrathionate/ kg dry resin. Meanwhile, trithionate loading is not very much increased compared to tetrathionate loading, and the equilibrium loading is about 257.951 g trithionate/ kg dry resin at 300 minutes of loading time.

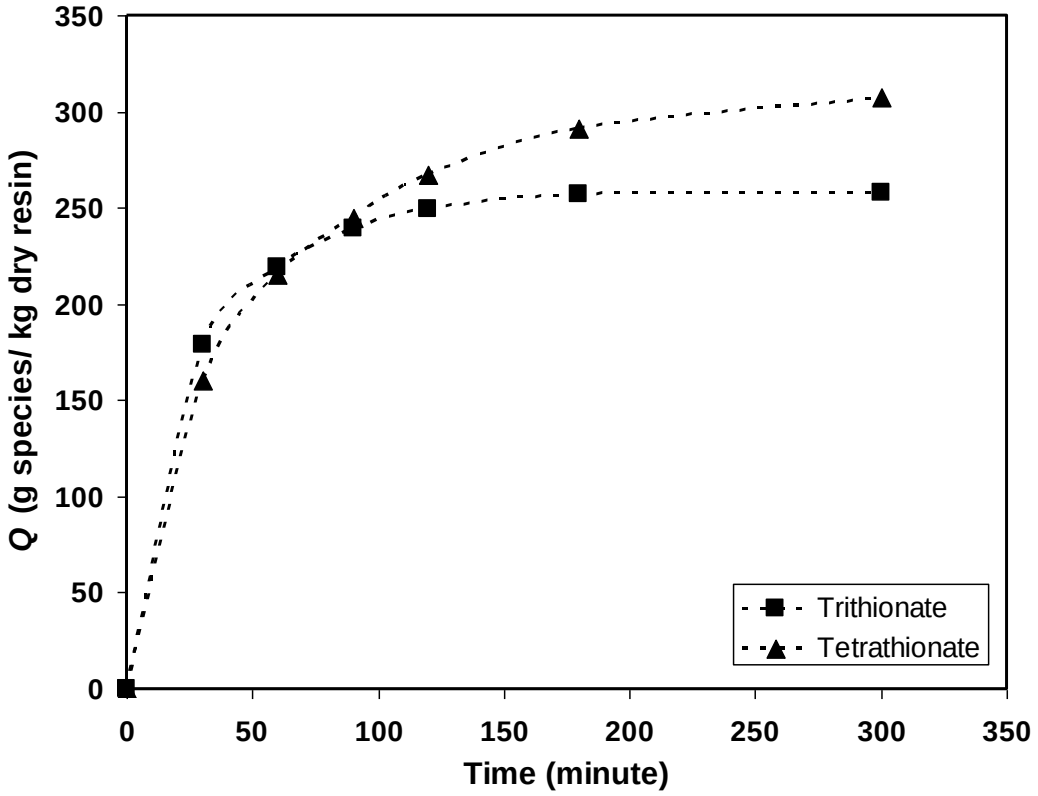

Figure 3.8 The loading of trithionate and tetrathionate versus time for the kinetics adsorption onto the anion exchange resin

The loading of gold thiosulfate for the kinetics adsorption of gold thiosulfate onto the anion exchange resin in the resin-solution system with the initial thiosulfate concentration of 100 mg/L solution and 0.333 g resin, is shown in Figure 3.9. As can be seen in Figure 3.9, gold thiosulfate loading increases moderately for the first 90 minutes loading from 0 to 57.146 g gold thiosulfate/ kg dry resin. Then, it gradually increases to reach the equilibrium loading of 66.447 g gold thiosulfate/ kg dry resin at 180 minutes of loading time, which is approximately 120 faster than thiosulfate and polythionates.

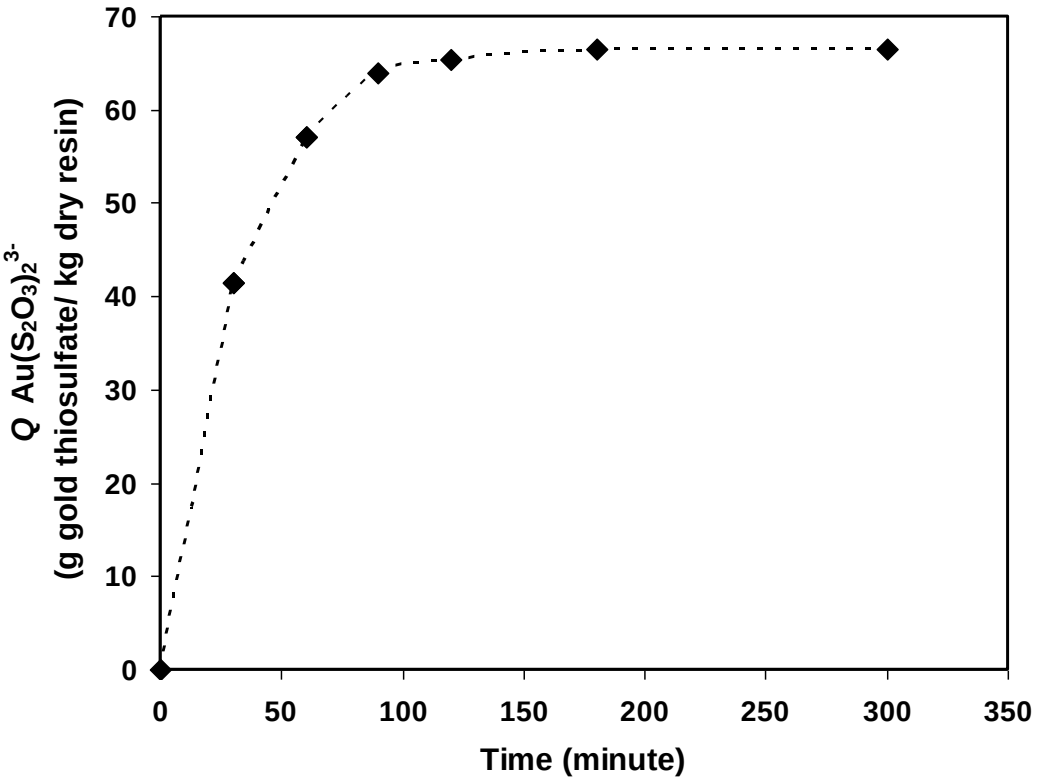

Figure 3.9 The loading of gold thiosulfate versus time for the kinetics adsorption onto the anion exchange resin

The experimental work for the kinetics adsorption of pentathionate onto the anion exchange resin in the resin-solution system could not be done because pentathionate cannot be purchased in pure form.

In order to obtain the kinetics constant for the adsorption of each species adsorbed on resin in the system, the Lagergren equation (Lagergren, 1989, Vázquez et al., 2007) representing the pseudo-first-order model shown by Equation (3.15) and Ho equation (Ho et al., 1996) as the pseudo-second-order model shown by Equation (3.16) are adopted, and the equations can be represented as:

$$\frac{d}{dt}Q_L(t) = k_L \left(Q_e - Q_L(t) \right) \tag{3.15}$$

$$\frac{d}{dt}Q_H(t) = k_H \left(Q_e - Q_H(t) \right)^2 \tag{3.16}$$

where k_L (min^{-1}) and k_H (kg g^{-1} min^{-1}) are the rate constants of adsorption based on Lagergren and Ho, respectively; $Q_L(t)$ and $Q_H(t)$ (g species/ kg dry resin) are the species loading at time t (min) based on Lagergren and Ho model, respectively; Q_e is denoted as the adsorption of species on resin at the equilibrium time (g species/ kg dry resin). Levenberg-Marquardt method (Williams et al., 2002) are used to minimize the sum of weighted deviation square between the experimental and model results. The functions can be expressed as Equations (3.17) and (3.18):

$$WD_L = \sum_{t=0}^{300} \left[Q_{Exp.t} - Q_L(k_L, t) \right]^2 \tag{3.17}$$

$$WD_H = \sum_{t=0}^{300} \left[Q_{Exp.t} - Q_H(k_H, t) \right]^2 \tag{3.18}$$

where WD_L and WD_H are the sum of weighted deviation square between the experimental results and model results associated with Lagergren and Ho equations, respectively, and WD_L and WD_H are minimized, so that $WD_L \geq 0$

and $WD_H \geq 0$ subject to the constants of $k_L > 0$ and $k_H > 0$, respectively; and $Q_{Exp.t}$ (g species/ kg dry resin) is the species loading at the loading time *t* based on the experimental data.

Table 3.1 shows the thiosulfate loading over time based on the experiment for kinetics adsorption with the equilibrium concentration of thiosulfate on resin being 168.317 g thiosulfate/ kg dry resin. Using the experiment-based thiosulfate concentration on resin including the equilibrium concentration, the time and the Levenberg-Marquardt method, the kinetics constants k_L and k_H were worked out which are approximately 0.0528 and 0.0012 min^{-1}, respectively with the correlation coefficient R^2 being 0.995 and 0.997, respectively. The thiosulfate loading over time based on the reference models are shown in the 3rd and 4th columns of Table 3.1.

Table 3.1 Thiosulfate loading based on experiment and reference models

Time	Thiosulfate Loading		
t (minute)	$Q_{Exp.t}$ (g species/ kg dry resin)	$Q_L(t)$ (g species/ kg dry resin)	$Q_H(t)$ (g species/ kg dry resin)
0	0.000	0.000	0.000
30	140.136	138.758	144.825
60	161.232	163.128	155.689
90	161.341	167.408	159.683
120	161.262	168.160	161.757
180	166.778	168.315	163.886
300	168.317	168.320	165.630

Similarly, trithionate loading over time based on the experiment and reference models are listed in Table 3.2. The kinetics constant for the adsorption of trithionate on resin based on the reference models, k_L and k_H are approximately 0.0304 and 0.0007 min^{-1}, respectively with the correlation coefficient R^2 being

0.996 and 0.968, respectively. Meanwhile, tetrathionate loading over time based on the experiment and reference models are shown in Table 3.3, and the kinetics constant for the adsorption of tetrathionate on resin based on the reference models, k_L and k_H are approximately 0.0205 and 0.0001 min^{-1}, respectively with the correlation coefficient R^2 being 0.991 and 0.988, respectively.

Table 3.2 Trithionate loading based on experiment and reference models

Time	Trithionate Loading		
t (minute)	$Q_{Exp.t}$ (g species/ kg dry resin)	$Q_L(t)$ (g species/ kg dry resin)	$Q_H(t)$ (g species/ kg dry resin)
0	0.000	0.000	0.000
30	179.150	154.326	218.698
60	219.050	216.322	236.708
90	238.950	241.227	243.389
120	249.550	251.232	246.873
180	257.100	256.866	250.458
300	257.950	257.946	253.402

Table 3.3 Tetrathionate loading based on experiment and reference models

Time	Tetrathionate Loading		
t (minute)	$Q_{Exp.t}$ (g species/ kg dry resin)	$Q_L(t)$ (g species/ kg dry resin)	$Q_H(t)$ (g species/ kg dry resin)
0	0.000	0.000	0.000
30	160.143	141.321	173.491
60	215.183	217.725	221.866
90	244.785	259.032	244.600
120	266.778	281.365	257.809
180	291.382	299.966	272.525
300	307.649	306.992	285.566

Finally, Table 3.4 shows the gold thiosulfate loading over time based on the experiment and reference models. Surprisingly, the loadings of gold thiosulfate

over time based on the experiment are almost the same as the ones by experiment. The first-order model of Lagergren-based result shown in the 3rd column in Table 3.4 is much better compared to the second-order model of Ho-based results shown the 4th column in Table 3.4. The rate constants of gold thiosulfate based on Lagergren and Ho models, k_L and k_H are approximately 0.0333 and 0.002 min^{-1}, respectively with the correlation coefficient R^2 being 0.999 and 0.913.

Table 3.4 Gold thiosulfate loading based on experiment and reference models

Time	Gold Thiosulfate Loading		
t (minute)	$Q_{Exp.t}$ (g species/ kg dry resin)	$Q_L(t)$ (g species/ kg dry resin)	$Q_H(t)$ (g species/ kg dry resin)
0	0.000	0.000	0.000
30	41.394	41.973	44.964
60	57.146	57.433	53.635
90	63.921	63.127	57.319
120	65.407	65.224	59.357
180	66.447	66.281	61.546
300	66.447	66.444	63.417

3.3.3 Equilibrium Adsorption of Single Component

In general, contact time is an important variable in adsorption as well as the adsorption of thiosulfate, polythionates and gold thiosulfate onto the ion exchange resin. The adsorption capacity of resin practically increases with time, and at some point in time, it reaches a constant value where no more species can be adsorbed on resin. At this point, the amount of species being adsorbed onto resin is in a state of dynamic equilibrium with the amount of species in solution, and the concentration of species in solution is also in a state of dynamic equilibrium with the concentration of species on resin presented as X_Se and X_Re, respectively as shown by Equations (3.10)-(3.14). Accordingly, the time required to attain the

equilibrium state is termed as an equilibrium time (t_e) and the amount of species adsorbed at the time t_e is defined as an equilibrium adsorption capacity.

It would be essential to have a satisfactory description of the equilibrium state between the species in solution (aqueous phase) and the species on resin (solid phase) of the adsorption systems in order to successfully represent the dynamic adsorptive behavior of species from the fluid phase to the solid phase. Therefore, the Langmuir and Freundlich isotherms which are the two most well-known isotherms are adopted to describe the equilibrium of adsorption systems.

The saturated monolayer isotherm which has been the most commonly used adsorption isotherm of a solute from a liquid solution (Langmuir, 1961) can be represented as:

$$Q_e = \frac{Q_m K_L C_e}{1 + K_L C_e} \tag{3.19}$$

where C_e (g species/ L solution) is the equilibrium concentration of species in solution; Q_e (g species/ kg dry resin) is the amount of species adsorbed on resin at the equilibrium; Q_m (g species/ kg dry resin) is the maximum amount of species adsorbed on resin at the equilibrium; and K_L (L solution/ g species) is the adsorption equilibrium constant. A plot of C_e / Q_e versus C_e should give a straight line with a slope of $1/Q_m$ and an intercept of $1/K_L Q_m$.

Meanwhile, the Freundlich isotherm (Weber, 1972) can be rewritten as:

$$Q_e = K_F C_e^{1/n} \tag{3.20}$$

where K_F (g species/ kg dry resin) is the Freundlich over-all adsorption capacity; and *n* indicates the adsorption intensity.

Equilibrium adsorption data as shown in Table 3.5 were collected from the equilibrium experiments with various initial concentrations of thiosulfate, trithionate and tetrathionate in the range of 0-3 mM. The loading of species over the equilibrium concentration of species in solution is plotted in Figure 3.10.

Table 3.5 Equilibrium adsorption of thiosulfate, trithionate and tetrathionate

Thiosulfate		Trithionate		Tetrathionate	
C_e (mg/L)	Q_e (mg/g)	C_e (mg/L)	Q_e (mg/g)	C_e (mg/L)	Q_e (mg/g)
0.470	101.761	2.165	163.088	1.568	191.270
28.784	155.828	4.050	240.385	7.582	277.275
67.858	162.263	80.850	248.375	87.471	295.186
171.604	168.140	238.450	257.875	287.093	298.163

As clearly shown in Figure 3.10, overall the loading of all species versus the equilibrium concentration of species in solution follows first order trend. The loading of trithionate is higher than the loading of thiosulfate at the same equilibrium concentration of both species in solution. The highest loading at the same equilibrium concentration in solution is for tetrathionate. The loadings of trithionate and tetrathionate seem to reach the maximum loading faster than thiosulfate, and the order of maximum loading of species is likely to be tetrathionate > trithionate > thiosulfate. Furthermore, the strength order of species adsorbed on resin at the maximum loading species seems to be trithionate > tetrathionate > thiosulfate. Therefore, Langmuir and Freundlich isotherms are taken into account.

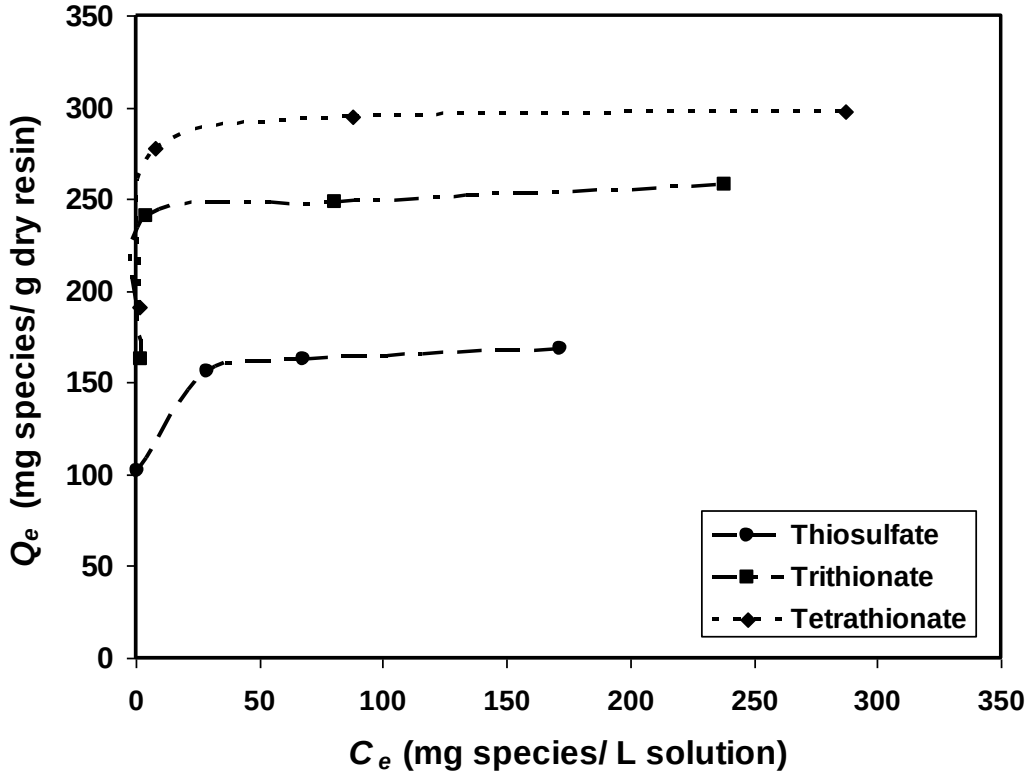

Figure 3.10 The loading of thiosulfate, trithionate and tetrathionate over the equilibrium concentration of the species in solution

As the results of Langmuir isotherm, the Langmuir isotherms of thiosulfate, trithionate and tetrathionate are fitted very well to the experimental data with the correlation coefficient R^2 being 0.999, 0.999 and 1.000, respectively as shown in Figure 3.11, and the adsorption is favourable. Linear relationships of C_e / Q_e over C_e are undoubtedly shown by the thiosulfate, trithionate and tetrathionate of Langmuir fits.

From the slope of Langmuir fit for thiosulfate (the top line in Figure 3.11), the maximum amount of thiosulfate adsorbed on resin is approximately 169.492 g thiosulfate/ kg dry resin. The adsorption equilibrium constant for thiosulfate is

approximately 0.590 L solution/ g thiosulfate, which is calculated from the slope and intercept of the Langmuir fit.

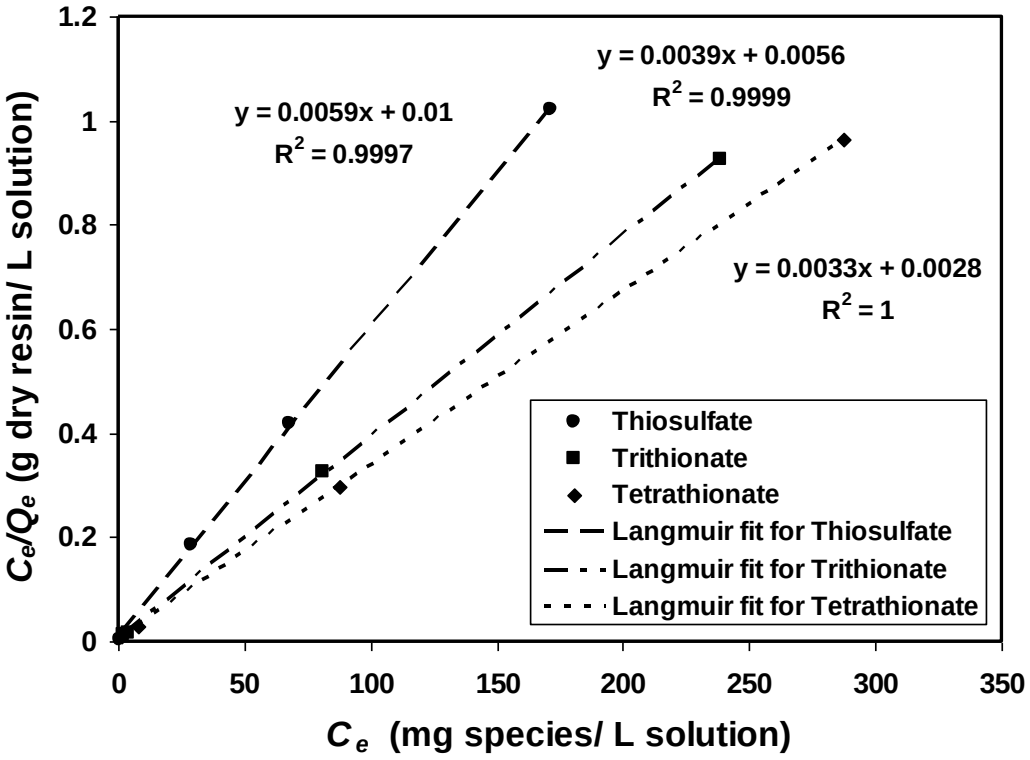

Figure 3.11 Langmuir fit for the adsorption of thiosulfate, trithionate and tetrathionate onto the anion exchange resin

As expected in the previous discussion, the maximum amount of trithionate adsorbed on resin is approximately 256.410 g trithionate/ kg dry resin calculated from the slop of the middle fit in Figure 3.11. The trithionate's adsorption equilibrium constant is approximately 0.696 L solution/ g trithionate, which is higher than the thiosulfate's one. Meanwhile, the maximum amount of tetrathionate adsorbed on resin is approximately 312.500 g tetrathionate/ kg dry resin, and the adsorption equilibrium constant for tetrathionate is approximately 1.143 L solution/ g tetrathionate, obtained from the slope and the intercept of the

bottom fit in Figure 3.11. It should be noted that even if the maximum loading of trithionate is less than the maximum loading of tetrathionate, the adsorption equilibrium constant for trithionate is higher than that for the tetrathionate. This implies that more trithionate is adsorbed than tetrathionate and thiosulfate based on experimental data and the Langmuir isotherm.

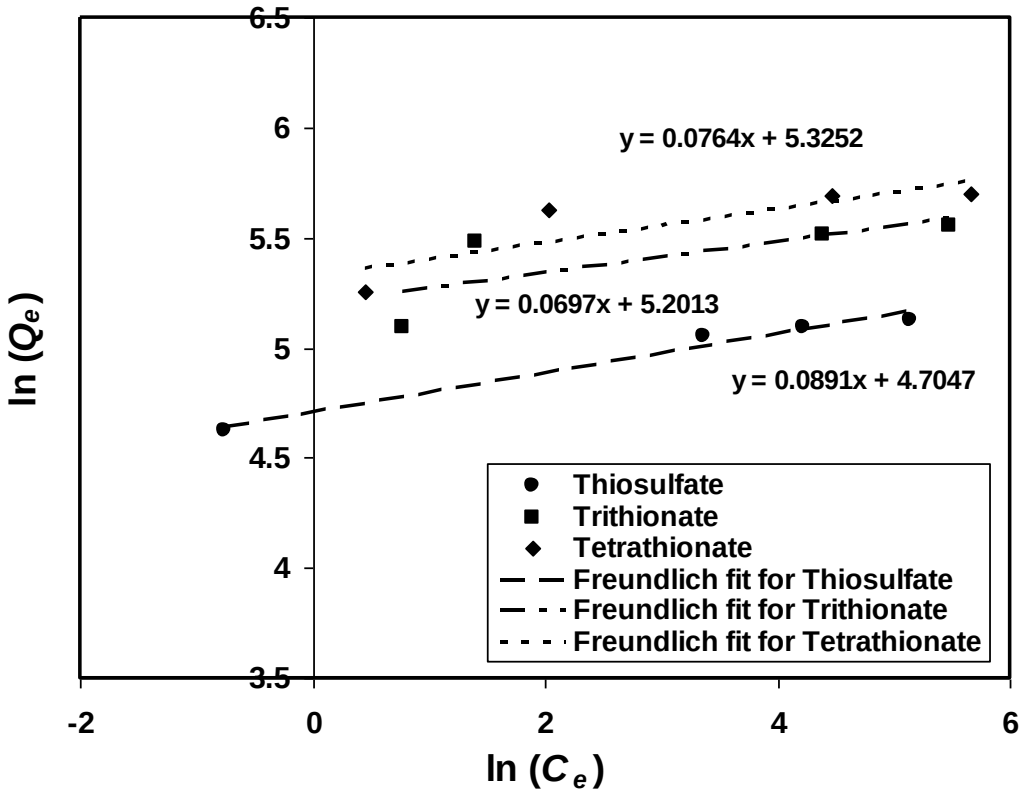

Figure 3.12 Freundlich fit for the adsorption of thiosulfate, trithionate and tetrathionate onto the anion exchange resin

As shown by the bottom line in Figure 3.12, Freundlich isotherm for thiosulfate is fitted well to the experimental data with the R^2 being approximately 0.977. From the intercept and slope, the Freundlich over-all adsorption capacity, K_F and the adsorption intensity, n are approximately 110.465 g thiosulfate/ kg dry resin and 11.223, respectively. The K_F and n are approximately 181.508 g trithionate/ kg

dry resin and 14.347, respectively for the Freundlich isotherm of trithionate which are higher than the ones for tetrathionate, 205.449 g tetrathionate/ kg dry resin and 13.351, respectively (calculated from the intercept and slope of the middle and top lines in Figure 3.12). From the *n* values, it is clearly shown that more trithionate is adsorbed on resin compared to the other species based on the experimental data and Freundlich isotherm.

3.4 Conclusions

The experimental procedures and speciation method provided can be used to investigate the adsorption of thiosulfate, polythionates and gold thiosulfate adsorptions on strong based anion exchange resin in single component resin-solution non-ammoniacal (NARS) systems. The speciation result shows that chloride is a very weak anion compared to thiosulfate, polythionates and gold thiosulfate, and there is no competitive loading between chloride and the species in the single component resin-solution system.

The kinetics constants for the adsorption of thiosulfate, trithionate, tetrathionate and gold thiosulfate onto the anion exchange resin of Purolite A500/2788 are obtained using the experimental data, the fitting of Lagergren and Ho models, and the numerical method of Levenberg-Marquardt, which are listed in Table 3.6. From the average R^2 values, the best fit model for the adsorption kinetics is the fitting of Lagergren model.

Table 3.6 The kinetics rate constants based on Lagergren and Ho

	Lagergren Fitting		**Ho Fitting**	
Species	**Rate Constant k_L (min^{-1})**	**R^2**	**Rate Constant k_H (min^{-1})**	**R^2**
Thiosulfate	0.0528	0.995	0.0012	0.997
Trithionate	0.0304	0.996	0.0007	0.968
Tetrathionate	0.0205	0.991	0.0001	0.988
Gold thiosulfate	0.0333	0.999	0.002	0.913

Note: All the experiments were conducted at the ambient temperature (~23 °C).

The resin capacity and the adsorption intensity of thiosulfate, trithionate and tetrathionate adsorbed on resin were determined using the equilibrium experiment data, Langmuir and Freundlich models and the numerical method of Levenberg-Marquardt, which are shown in Table 3.7. From the values of Langmuir equilibrium constant and Freundlich adsorption, it is clearly shown that more trithionate is adsorbed on the resin compared to thiosulfate and tetrathionate. The best fit model for the equilibrium adsorption of thiosulfate and polythionates is shown by the Langmuir model based on the average R^2 values. In addition, the Langmuir and Freundlich isotherms for the adsorption of gold thiosulfate are not described in Chapter 3 because of the unavailable experimental data for gold thiosulfate. The data needed for the Langmuir and Freundlich isotherms are worked out using the model proposed in Chapter 7.

Table 3.7 The equilibrium adsorption based Langmuir and Freundlich

	Langmuir Fitting			**Freundlich Fitting**		
Species	**Resin capacity, Q_m (g/kg)**	**Equilibrium constant, K_L (L/g)**	**R^2**	**Resin capacity, K_F (g/kg)**	**Adsorption intensity, n**	**R^2**
Thiosulfate	169.492	0.590	0.999	110.465	11.223	0.977
Trithionate	256.410	0.696	0.999	181.465	14.347	0.956
Tetrathionate	312.500	0.179	1	205.449	13.351	0.997

Note: All the experiments were conducted at the ambient temperature (~23 °C).

CHAPTER 4
Adsorption of Gold Thiosulfate Complexes in Multiple Components Resin-Solution Systems

4.1 Introduction

Alternative reagents have been evaluated in recent studies since there are increasing environmental concerns over the use of cyanide as reagent in the gold recovery. Possibly, thiosulfate leaching appears to be one of the most promising alternatives to cyanidation. And not surprisingly many studies on thiosulfate leaching using different oxidants have been published in the last decade. The use of ammonium thiosulfate and oxygen under pressure to recover gold was proposed to improve the leaching of gold (Berezowsky et al., 1978). However, other studies concluded that the use of excessive oxygen increases the oxidative degradation of thiosulfate (Hemmati et al., 1989, Langhans et al., 1992).

On one hand, in the system of ammonium thiosulfate (ATS) solutions using anion-exchange resin, tetrathionate, as the product of thiosulfate oxidation, strongly poisoned the resin in the recovery of gold and copper from Zhang and Dreisinger (2002). The presence of polythionates affects the gold recovery using ion exchange resin (Nicol and O'Malley, 2002). Interestingly, analytical procedures based on ion chromatography utilising an anion exchange column and UV detection are described for the quantification of thiosulfate, polythionates and gold thiosulfate both in leach solutions and adsorbed on anion exchange resin. One of the results shows that tetrathionate and pentathionate are the dominant reaction products from thiosulfate oxidation at pH 8.5 and 9, whilst trithionate and sulfate are formed at pH 10.4 (Jeffrey and Brunt, 2007). On the other hand, electrochemical results reported that the gold oxidation from a rotating disc in a non-ammoniacal solution of potassium thiosulfate was faster than that in sodium

thiosulfate at the same salt concentration of 0.2 M and at an applied potential of 0.25 V, under argon (Chandra and Jeffrey, 2004). Therefore, further research on the system of non-ammoniacal sodium thiosulfate using resin would be worthy to take into account.

In general, ion-exchange resin simultaneously adsorbs thiosulfate, polythionates and gold thiosulfate with the charges on the resin's functional groups with the opposite charge. Due to the limited number of charge on resin presented by the theoretical ion-exchange capacity of resin, and thiosulfate, polythionates and gold thiosulfate competes one another, so equilibrium adsorption are critical aspect to investigate. Therefore, the work in this chapter is mainly aimed at investigating the adsorption of thiosulfate, polythionates and gold thiosulfate on strong based anion exchange resin in the multiple components of non-ammoniacal resin-solution (NARS) systems. The specific objectives of the work are:

a. To provide the experimental procedure for the adsorption of thiosulfate, polythionates and gold thiosulfate on strong based anion exchange resin in the multiple components NARS systems.

b. To investigate the adsorption of thiosulfate, polythionates and gold thiosulfate in the multiple components NARS systems.

c. To obtain the equilibrium constants associated with the adsorption reactions in the multiple components NARS systems.

4.2 Experimental Methods

All the experimental work for the adsorption of thiosulfate, polythionates and gold thiosulfate on strong based anion exchange resin in the multiple components NARS systems had been done in the Thiosulfate Laboratory at Australian Mineral Research Centre, CSIRO Mineral in Western Australia.

4.2.1 Apparatus and Chemicals

The same HPLC separation module described in Chapter 3 was used to analyze the concentrations of thiosulfate and polythionates in the experiments of multiple components resin-solution non-ammoniacal systems. The separation was achieved using a Dionex IonPac AS16 ion exchange column equipped with an IonPac AG16 guard column. The mobile phase was a solution of sodium perchlorate (0.075 – 0.2 M). The species detection was via a Waters 2996 Photodiode Array Detector (UV). Empower software was used for the calculation of peak area (Waters, 2002). Details about the mobile solution and the wavelengths of UV adsorption and peak retention times of the involved species have been described in the literature (Jeffrey and Brunt, 2007). Gold was also analysed by inductively coupled plasma optical emission spectrometry (ICP-OES). All the thiosulfate and polythionates analysis have been done by the PhD candidate of this thesis in the HPLC Laboratory at the Australian Mineral Research Centre, and all the gold thiosulfate analysis have been done by the staff of Analytical Chemistry Unit at the Australian Mineral Research Centre.

Pentathionate cannot be purchased in pure form, a synthetic polythionates mixture was prepared by mixing 25 mM sodium thiosulfate ($Na_2S_2O_3$) with 50 mM sodium tetrathionate ($Na_2S_4O_6.2H_2O$ and 10 mM sulfite in solution allowing rearrangement to occur for a few weeks (Steudel and Holdt, 1986). The resulting

solution contained a mixture of thiosulfate, trithionate, tetrathionate and pentathionate whose concentrations were determined by HPLC immediately before being used as a source for pentathionate. Meanwhile, sodium thiosulfate ($Na_2S_2O_3$) and sodium tetrathionate ($Na_2S_4O_6.2H_2O$), 99% pure was obtained from Aldrich. Sodium trithionate ($Na_2S_3O_6$) was prepared using the methods described by Kelly and Wood (Kelly and Wood, 1994). Trisodium gold thiosulfate salt ($Na_3Au(S_2O_3)_2.2H_2O$) was prepared and recrystallised using the procedure described by Ruben et al. (2002).

Purolite A500/2788 in the chloride form with a macrospore structure was also used. The wet form of the resin contained 53-58 % moisture, the resin capacity is 1.15 meq/mL, and the specific gravity is 1.08 g/mL (PUROLITE, 2008).

4.2.2 Procedures

All the experiments of the adsorption of thiosulfate, polythionates and gold thiosulfate on strong based anion exchange resin in multiple components resin-solution non-ammoniacal systems were conducted at the neutral pH and the ambient temperature (~23 °C). The concentration on the resin for a particular species was calculated from the change in its solution concentration in the system.

A. The experiments on equilibrium adsorption for thiosulfate and polythionates

The equilibrium experiment was initially conducted to investigate the competition between species for the adsorption on resin. The steps of experiments with two components are described as follows;

1) Prepare 200 mL of loading solution consisting of 1 mM sodium trithionate ($Na_2S_3O_6$) and 1 mM sodium tetrathionate ($Na_2S_4O_6.2H_2O$) in a 200 mL volumetric flask.

2) Take 1 mL sample of the solution for HPLC analysis as the loading sample at t = 0 minute.

3) Prepare 0.333 g resin, and place it in a conical flask.

4) Place the 199 mL solution in the conical flask to present a resin-solution system for the adsorption of thiosulfate onto resin.

5) Stir it at 155 rpm with IKA overhead stirrers, and start the timer for loading.

6) Take 1 mL sample of the solution for HPLC analysis at just after 5 hours loading.

7) After 5 hours loading, decant and wash the resin 4 times with DI water into a large vial. Suck the remaining H_2O using pipette.

8) Add 50 mL $NaClO_4$ (0.5M) into the vial for the dilution of thiosulfate from resin, shake it at 150 U/minute and start the timer for 30 minutes of the 1st stripping.

9) Take 1 mL sample of the solution for HPLC analysis as the 1st stripping sample.

10) Decant and wash the resin 4 times with DI water in the vial. Suck the remaining H_2O using pipette.

11) Re-add 50 mL $NaClO_4$ (0.5M) into the vial for the dilution of thiosulfate from resin, shake it at 150 U/minute on a Jubalo SW-20C shaker and start the timer for 30 minutes of the 2nd stripping.

12) Take 1 mL sample of the solution for HPLC analysis as the 2nd stripping sample.

13) Decant and wash the resin 4 times with DI water in the vial. Before placing the resin in a small glass vial, measure the empty vial mass.

14) Place the resin in a small glass vial, and suck the remaining H_2O using pipette.

15) Dry the resin at 60 ^oC in an oven for about 16 hours.

16) Measure the mass of vial with resin to obtain the dried resin mass; the dried resin mass = the mass of vial with resin – the empty vial mass.

The 1st to 16th steps were repeated for the other 8 batches with the initial trithionate and tetrathionate concentrations in the range 1-3 mM.

To generate a set of equilibrium data for the equilibrium constant of thiosulfate and trithionate reaction on resin in the multiple components NARS systems, the 1st to 16th steps were repeated for the 8 batches with the initial trithionate concentration in the range 1.5-5 mM and the constant initial thiosulfate concentration of 50 mM thiosulfate. The large initial concentration of thiosulfate was taken into account to ensure the competition loading between thiosulfate and trithionate take place since thiosulfate has much less intensity compared to trithionate as mentioned in Chapter 3.

The 1st to 16th steps with the initial trithionate concentration at the range 1-3 mM and the initial thiosulfate concentration at the range of 1-3 mM to generate a set of equilibrium data for the equilibrium constant of trithioante and tetrathionate reaction on resin in the multiple components NARS systems. The synthetic polythionates mixture was diluted with DI water to prepare loading solution consisting of about 1.5 mM thiosulfate, 1.3 mM trithionate, 2.5 mM tetrathionate

and 0.9 mM pentathionate. Then, the diluted mixture was used in the experiments to generate a set of equilibrium data for the equilibrium constant of tetrathionate and pentathionate reaction on resin in the multiple components NARS systems.

B. The experiments on equilibrium adsorption for polythionates and gold thiosulfate

The equilibrium experiment of gold loading in the multiple components NARS systems was accomplished by mixing sodium gold thiosulfate with sodium thiosulfate and sodium trithionate. The steps of experiments are described as follow;

1) Prepare 210 mL of loading solution consisting of 0.2 mg/L trisodium gold thiosulfate salt ($Na_3Au(S_2O_3)_2.2H_2O$), 5 mM $Na_2S_2O_3.5H_2O$ (sodium thiosulfate) and 5 mM sodium trithionate ($Na_2S_3O_6$) and in a 200 mL volumetric flask. To make the 210 mL loading solution, all the chemicals were diluted with DI water until it reached the 200 mL level. Additional 10 mL DI water is then added into the solution using a single-channel pipette to make up 210 mL solution.

2) Then, take 1 mL sample of the solution for HPLC analysis and ICP-OES analysis as the loading sample at t = 0 minute.

3) Prepare 0.5 g resin, and place it in a conical flask.

4) Place the 199 mL solution in the conical flask to present a resin-solution system for the adsorption of thiosulfate onto resin.

5) Stir it at 155 rpm with IKA overhead stirrers, and start the timer for loading.

6) Take 1 mL sample of the solution for HPLC analysis at just after 5 hours loading.

7) After 5 hours loading, decant and wash the resin 4 times with DI water into a large vial. Suck the remaining H_2O using pipette.

8) Add 50 mL $NaClO_4$ (0.5M) into the vial for the dilution of thiosulfate from resin, shake it at 150 U/minute and start the timer for 30 minutes of the 1st stripping.

9) Take 1 mL sample of the solution for HPLC analysis as the 1st stripping sample.

10) Decant and wash the resin 4 times with DI water in the vial. Suck the remaining H_2O using pipette.

11) Re-add 50 mL $NaClO_4$ (0.5M) into the vial for the dilution of thiosulfate from resin, shake it at 150 U/minute on a Jubalo SW-20C shaker and start the timer for 30 minutes of the 2nd stripping.

12) Take 1 mL sample of the solution for HPLC analysis as the 2nd stripping sample.

13) Decant and wash the resin 4 times with DI water in the vial. Before placing the resin in a small glass vial, measure the empty vial mass.

14) Place the resin in a small glass vial, and suck the remaining H_2O using pipette.

15) Dry the resin at 60 ^oC in an oven for about 16 hours.

16) Measure the mass of vial with resin to obtain the dried resin mass; the dried resin mass = the mass of vial with resin – the empty vial mass.

The 1st to 16th steps were repeated for the 6 batches with the initial concentration of gold thiosulfate at the range 0.2-10 mg/L and the constant initial thiosulfate and trithionate concentration of 5 mM to investigate the adsorption of thiosulfate,

polythionates and gold thiosulfate and the effect of polythionates on gold loading in the multiple components NARS systems.

Then, the 1st to 16th steps were also repeated for the 2 sets of 6 batches with the initial concentration of gold thiosulfate in the range 0.2-10 mg/L and the constant initial thiosulfate of 100 mM, and the synthetic polythionates mixture solution. Finally, the 1st to 16th steps were repeated for the 8 batches with the constant initial concentration of gold thiosulfate of 10 mg/L, the constant initial thiosulfate concentration of 5 and 100 mM, and the initial trithionate concentration in the range of 2.5-15 mM to obtain the equilibrium constant associated with gold thiosulfate reaction in the multiple components NARS systems.

4.3 Results and Discussion

4.3.1 Equilibrium Adsorption of Thiosulfate and Polythionates in Two Components NARS systems

In order to investigate the competitive adsorption of all the species on resin in the multiple components NARS systems, experiments with two components were firstly conducted. Figure 4.1 shows the equilibrium adsorption of trithionate based on loading solution containing trithionate and tetrathionate with the initial concentration of both species in the range of 1-3 mM.

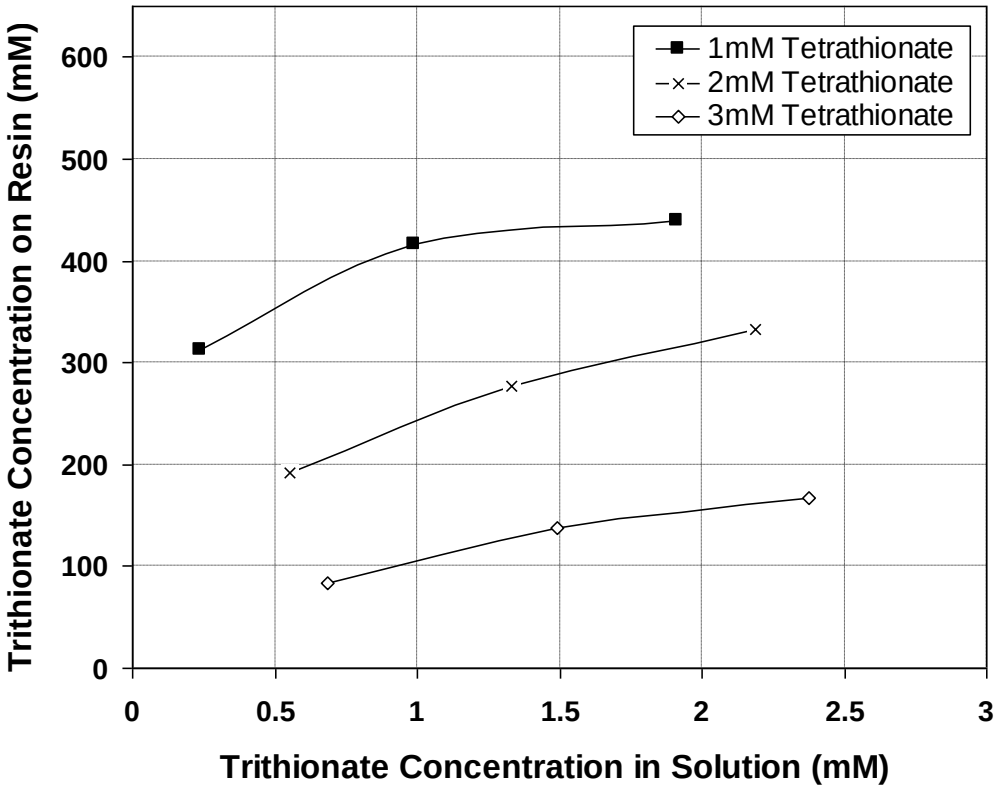

Figure 4.1 The equilibrium loading of trithionate plotted as an isotherm for three initial concentrations of tetrathionate in solution

As a result, the equilibrium trithionate concentration on the resin decreases with the increase in tetrathionate concentration in solution. This is reasonable because the more trithionate added in the tetrathionate solution, the more trithionate is adsorbed on resin, occupying the available charge on resin. Similarly, the equilibrium tetrathionate concentration on the resin increases with the increase in trithionate concentration in solution as shown in Figure 4.2. This implies that the more tetrathionate is added to the trithionate solution, the more tetrathionate is adsorbed on resin, occupying the available charge on resin. However, increasing the concentration of both species at certain level results in the constant equilibrium concentration of both species on resin since the resin has a constant capacity.

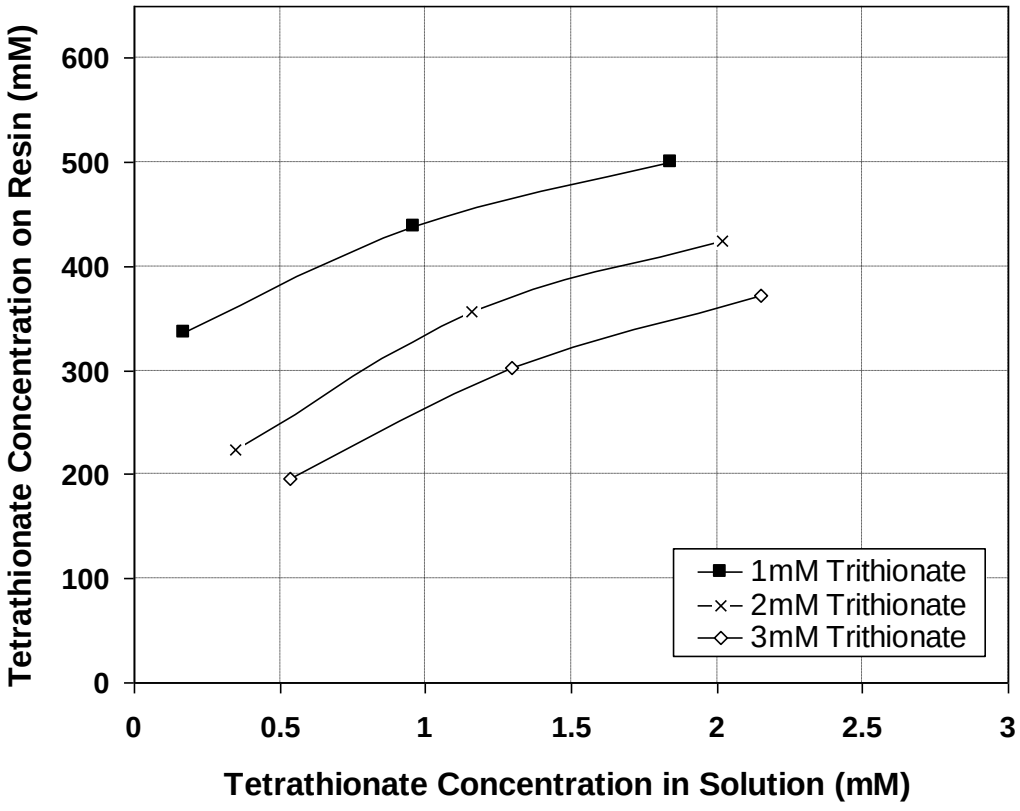

Figure 4.2 The equilibrium loading of tetrathionate plotted as an isotherm for three initial concentrations of trithionate in solution

4.3.2 Equilibrium Constants for Thiosulfate and Polythionates in Multiple Components NARS systems

During the competitive adsorption of thiosulfate and polythionates, the chloride initially present on the resin is almost completely desorbed, since it is weakly adsorbed compared to thiosulfate and polythionates as discussed in Chapter 3. Thus, the equilibrium reactions in the absence of high concentrations of chloride in the multiple components NARS systems can be represented by the following equilibrium equations:

$$R_2S_2O_{3(s)} + S_3O_6^{2-}{}_{(aq)} <=> R_2S_3O_{6(s)} + S_2O_3^{2-}{}_{(aq)} \qquad K_{3/2} \quad (4.1)$$

$$R_2S_3O_{6(s)} + S_4O_6^{2-}{}_{(aq)} <=> R_2S_4O_{6(s)} + S_3O_6^{2-}{}_{(aq)} \qquad K_{4/3} \quad (4.2)$$

$$R_2S_4O_{6(s)} + S_5O_6^{2-}{}_{(aq)} <=> R_2S_5O_{6(s)} + S_4O_6^{2-}{}_{(aq)} \qquad K_{5/4} \quad (4.3)$$

$$R_2S_5O_{6(s)} + S_6O_6^{2-}{}_{(aq)} <=> R_2S_6O_{6(s)} + S_5O_6^{2-}{}_{(aq)} \qquad K_{6/5} \quad (4.4)$$

where $K_{3/2}$ represents the equilibrium constant for replacing thiosulfate with trithionate on the resin, $K_{3/2} = R_2S_3O_6 \left[S_2O_3^{2-}\right] / \; R_2S_2O_3 \left[S_3O_6^{2-}\right]$; $K_{4/3}$ represents the equilibrium constant for replacing trithionate with tetrathionate on the resin, $K_{4/3} = R_2S_4O_6 \left[S_3O_6^{2-}\right] / \; R_2S_3O_6 \left[S_4O_6^{2-}\right]$; $K_{5/4}$ represents the equilibrium constant for replacing tetrathionate with pentathionate on the resin, $K_{5/4} = R_2S_5O_6 \left[S_4O_6^{2-}\right] / \; R_2S_4O_6 \left[S_5O_6^{2-}\right]$; and $K_{6/5}$ represents the equilibrium constant for replacing pentathionate with hexathionate on the resin, $K_{6/5} = R_2S_6O_6 \left[S_5O_6^{2-}\right] / \; R_2S_5O_6 \left[S_6O_6^{2-}\right]$.

Therefore in the case of the system containing thiosulfate and trithionate, a plot of $R_2S_3O_6 \ / \left[S_3O_6^{2-} \right]$ vs. $R_2S_2O_3 \ / \left[S_2O_3^{2-} \right]$, should yield a straight line with the slope being the equilibrium constant, $K_{3/2}$.

Figure 4.3 shows the loading affinity of trithionate over the loading affinity of thiosulfate based on the concentration of both species in loading and stripping. As can be seen in Figure 4.3, the slope of straight line is approximately 95.104 representing $K_{3/2}$, and it concludes that the trithionate is much more strongly adsorbed on resin than thiosulfate.

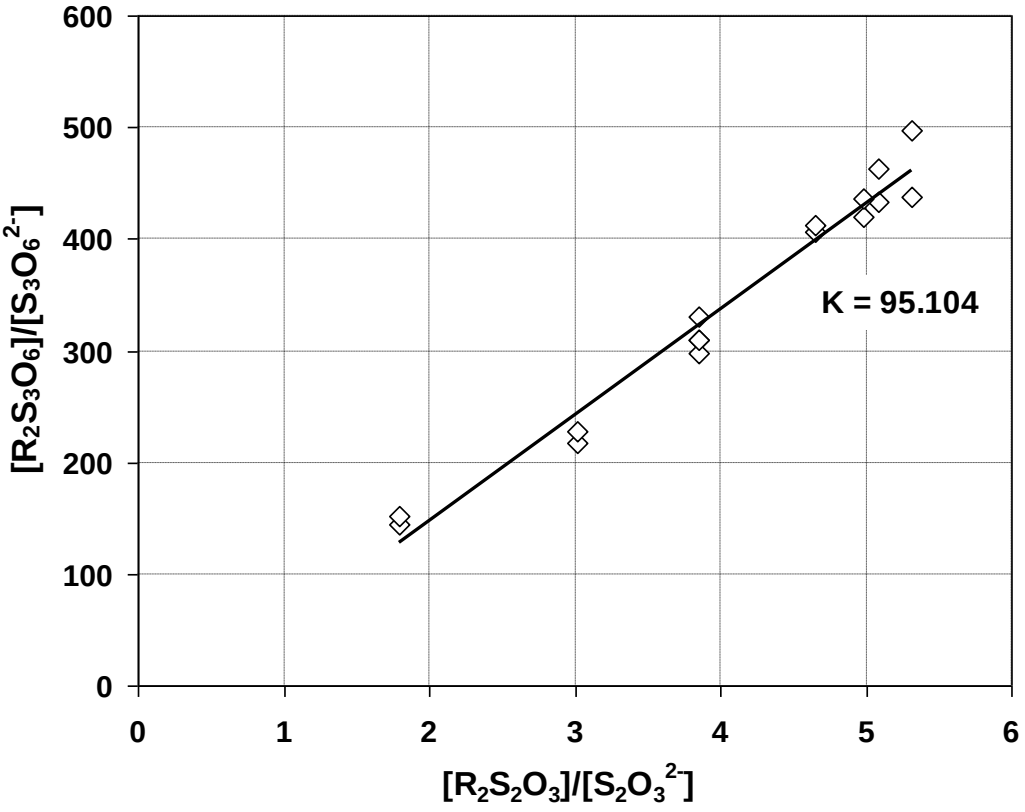

Figure 4.3 The graphical representation of the equilibrium constant for trithionate loading over thiosulfate

Similarly, Figure 4.4 shows the loading affinity of tetrathionate over the loading affinity of trithionate. As can be seen in Figure 4.4, the slope of straight line is obtained and $K_{4/3}$ is determined to be 1.446. Since this value is above 1, the adsorption of tetrathionate is stronger that the adsorption of trithionate.

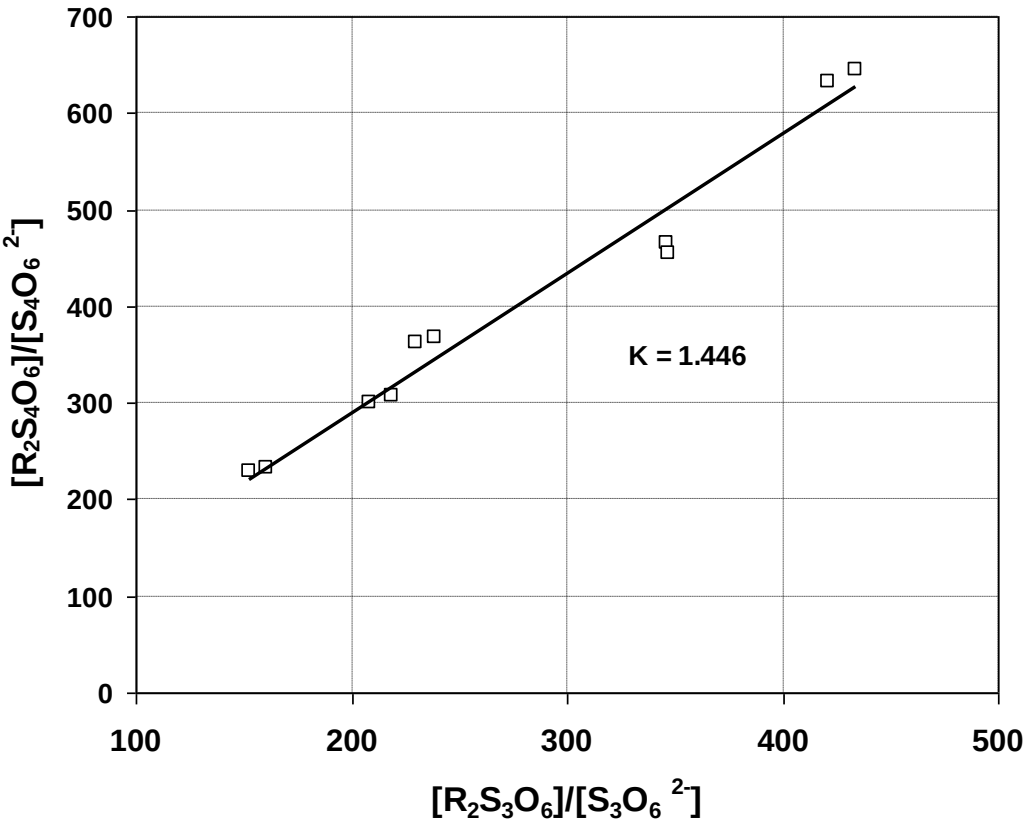

Figure 4.4 The graphical representation of the equilibrium constant for tetrathionate loading over trithionate

The equilibrium experiments using a synthetic polythionates mixture gave the equilibrium constant of tetrathionate and pentathionate reaction, Equation (4.3) in the multiple components of non-ammoniacal resin-solution systems. The result for the equilibrium loading of all the species on resin with the solution containing

thiosulfate, trithionate, tetrathionate and pentathionate are listed in Table B.1 of Appendix B.

As shown in Figure 4.5, the result of 5 batches test gave the equilibrium constant, and $K_{5/4}$ was determined to be 1.569, 1.580, 1.597, 1.578 and 1.580 for the 1st batch to the 5th batch, respectively which is really consistent. The equilibrium constant $K_{5/4}$ is approximately 1.580 on the average, and from this result, it is worthy to note that pentathionate has higher competitive strength of adsorption than tetrathionate.

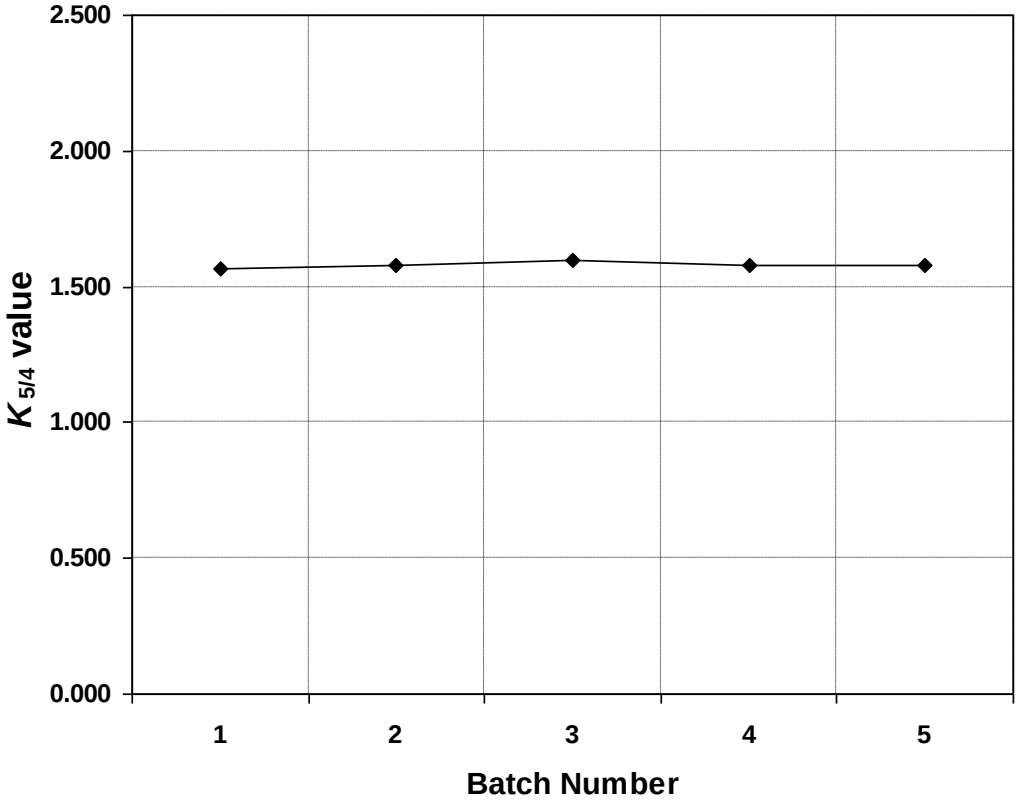

Figure 4.5 The equilibrium constant of tetrathionate and pentathionate reaction in the multiple components NARS systems

Small amounts of hexathionate were detected in loading and tripping solutions but the concentrations were not high enough for the equilibrium constant of pentathionate and exathionate reaction ($K_{6/5}$) to be made.

4.3.3 Equilibrium Adsorption of Thiosulfate, Polythionate and Gold Thiosulfate in Multiple Components NARS systems

In general, the adsorption of gold onto ion exchange resin is affected by the concentration of polythionates in ammoniacal thiosulfate solution. To investigate the effect of polythionates in the multiple components NARS systems, synthetic polythionates mixture solution of loading solutions is required with various initial gold concentrations. The results on the equilibrium experiment of gold thiosulfate complexes for the investigation of the adsorption of thiosulfate, polythionates and gold thiosulfate and the effect of polythionates on gold loading in the multiple components NARS systems are shown in Tables 4.1-4.4 wherein all the result of gold thiosulfate concentration by ICP-OES are listed in Table B.2 of Appendix B.

Table 4.1 shows the initial concentrations of thiosulfate, trithionate, tetrathionate and gold thiosulfate based on measurement. As set in the experiment, the concentration of thiosulfate, trithionate and tetrathionate are fairly consistent, and gold concentration is varied from 0.262 mg/L to 10.476 mg/L. The concentration change of all species in the multiple components NARS systems after 5 h loading can be calculated using the related concentration of species and gold shown in Tables 4.1 and 4.2. The average concentration change of thiosulfate, trithionate, tetrathionate and gold thiosulfate are approximately 1.8 %, 45.3 %, 56.9 % and 86.4 %, respectively. The loading percentages of thiosulfate, trithionate and tetrathionate are reasonable because it is in line with the competitive loading of the species on resin as highlighted in the previous discussion on the equilibrium constants of associated reactions in regard to the species. The high loading

percentage of gold thiosulfate is the fact that gold thiosulfate has higher competitive strength of adsorption than thiosulfate and the polythionates. Therefore, the equilibrium constants of associated reaction for gold thiosulfate are interesting to be obtained which are addressed in the further discussion.

Table 4.1 The initial concentrations of all species in loading solutions

Batch Num.	Initial Concentrations			
	Gold (mg/L)	$S_2O_3^{2-}$ (mM)	$S_3O_6^{2-}$ (mM)	$S_4O_6^{2-}$ (mM)
1	0.262	5.322	5.153	0.018
2	0.480	5.300	5.156	0.015
3	0.713	5.268	5.168	0.018
4	2.025	5.127	4.911	0.020
5	5.109	5.164	4.960	0.015
6	10.476	5.172	4.913	0.016

Table 4.2 The equilibrium concentrations of all species in loading solution

Batch Num.	Equilibrium Concentrations			
	Gold (mg/L)	$S_2O_3^{2-}$ (mM)	$S_3O_6^{2-}$ (mM)	$S_4O_6^{2-}$ (mM)
1	0.044	5.269	2.751	0.006
2	0.064	5.227	2.774	0.008
3	0.093	5.188	2.712	0.006
4	0.258	4.981	2.732	0.008
5	0.645	5.068	2.805	0.008
6	1.362	5.044	2.768	0.007

The equilibrium concentrations of thiosulfate, the polythionates and gold thiosulfate on resin the multiple components NARS systems based on loading and stripping measurement are listed in Table 4.3 and Table 4.4, respectively. From these presentations, the amount of thiosulfate adsorbed on the resin is very small compared to the trithionate concentration, which is at the concentration in the range of 20.754-25.144 mM based on loading (see Table 4.3) and 14.317-39.284 mM based on stripping (see Table 4.4). Meanwhile, the concentration of

thiosulfate adsorbed on the resin is in the range of approximately 606.276-629.452 mM based on loading (see Table 4.3) and 586.519-665.122 mM based on stripping (see Table 4.4). As expected, the change of tetrathionate concentration on resin (17.868 and 42.484 %) is much larger than the trithioante ones (3.682 and 11.818 %) based on both loading and striping, respectively. However, with the very small initial concentration of tetrathionate, the amount of tetrathionate adsorbed on the resin is also very small which is varied at the concentration in the range of 1.899-3.301 mM based on stripping. Meanwhile, the trithionate concentration is in the range of 586.519-665.122 mM based on stripping.

Table 4.3 The equilibrium concentration of species on resin based on loading

Batch Num.	Concentrations on Resin			
	Gold (mg/L)	$S_2O_3^{2-}$ (mM)	$S_3O_6^{2-}$ (mM)	$S_4O_6^{2-}$ (mM)
1	58.701	22.251	629.452	6.097
2	113.292	21.893	617.020	5.485
3	168.127	20.754	619.235	6.015
4	478.317	20.804	615.535	5.798
5	1214.824	24.171	606.851	5.083
6	2494.185	25.144	606.276	5.007

Table 4.4 The equilibrium concentration of species on resin based on stripping

Batch Num.	Concentrations on Resin			
	Gold (mg/L)	$S_2O_3^{2-}$ (mM)	$S_3O_6^{2-}$ (mM)	$S_4O_6^{2-}$ (mM)
1	51.891	14.317	644.596	3.226
2	102.839	19.762	649.759	1.934
3	160.928	21.638	665.122	3.213
4	483.680	39.284	589.815	3.301
5	1153.464	25.923	586.519	1.899
6	2401.638	34.921	586.932	2.452

4.3.4 The Effect of Thiosulfate and Polythionates on the Adsorption of Gold Thiosulfate on resin

It is also important to note that thiosulfate degradation in the previous studies (Jeffrey and Brunt, 2007, Wan, 1997, Nicol and O'Malley, 2002) with tetrathionate as the one of the principle product in ammoniacal thiosulfate solution, does not occur in the multiple components NARS systems, since there is very small decrease in thiosulfate concentration during 5 h loading. It could be, because the adsorption of thiosulfate on the resin is not due to its degradation to form tetrathionate. In addition, there is no significant decrease in the stripping-based thiosulfate concentration compared to the loading-based concentration.

Trithionate will likely load on the resin very well together with gold thiosulfate. It could be true because the amount of trithionate adsorbed on resin is almost constant; 619.235, 615.535, 606.851 and 606.276 mM (loading-based in Table 4.3); and 665.122, 589.815, 586.519 and 586.932 mM (stripping-based in Table 4.4), for the increased gold concentration in solution of 0.621, 1.767, 4.463 and 9.115 mg/L, and for the increased gold concentration in resin of 237.688, 714.625, 1695.136 and 3510.550 mg/L, respectively.

Figure 4.6.a represents the adsorption isotherm of gold thiosulfate onto resin in the multiple component NARS system containing the equilibrium concentration of thiosulfate, trithionate and tetrahionate being 5.129, 2.757 and 0.007 mM, respectively on average (see Table 4.2). The loading of gold thiosulfate is illustrated as the mass of gold thiosulfate (mg) per the mass of dry resin (kg), which is also the most commonly used unit in gold industries. As can be seen in Figure 4.6.a, the mass of gold thiosulfate per kg resin linearly increase with the increase in the gold thiosulfate concentration in the solution with the correlation coefficient, R^2 = 0.999. Both the stripping-based experimental data and the

loading-based experimental data are considered to plot the gold thiosulfate loading to clearly show how close both results are.

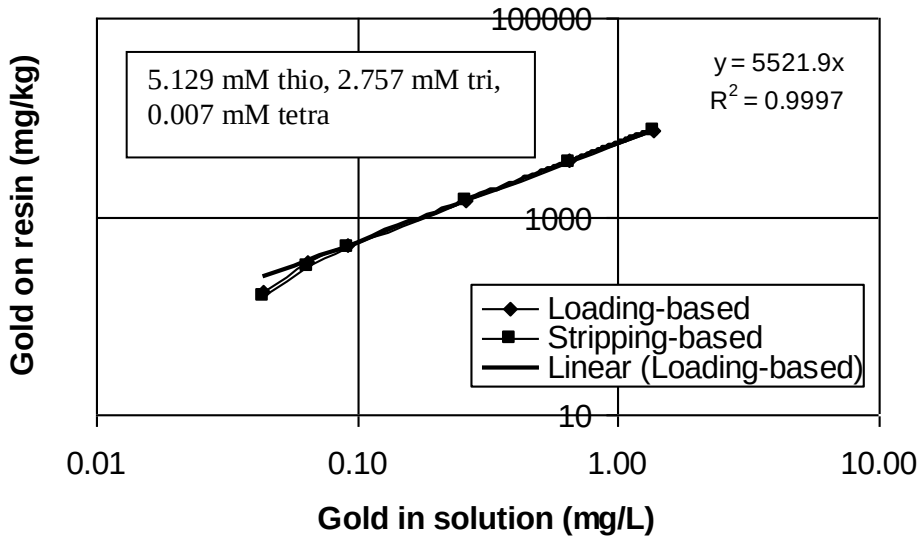

(a)

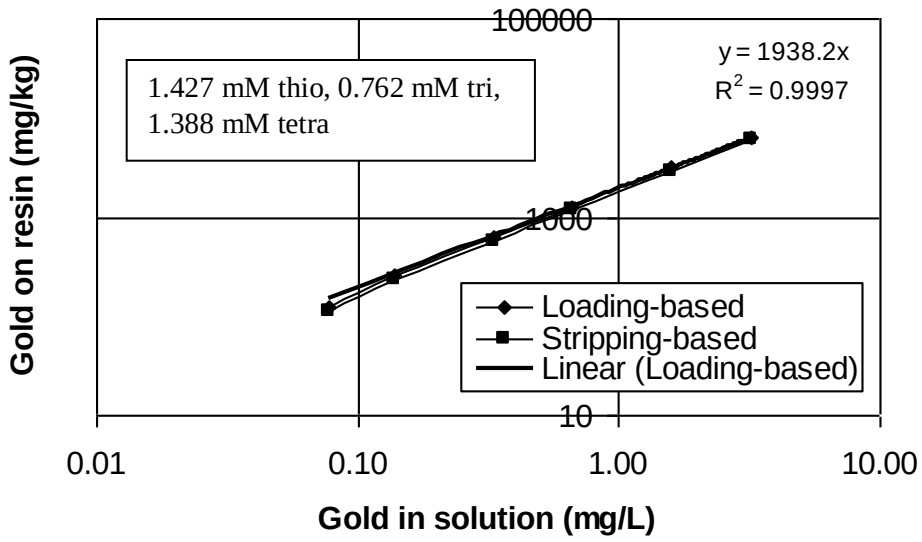

(b)

Figure 4.6 The adsorption isotherm of gold thiosulfate in the multiple components NARS systems with the synthetic polythionates mixture solution with 5 g resin

The slope of the gold thiosulfate isotherm is approximately 5521.9 (stripping-based) meaning that the gold thiosulfate adsorbed on every 1 kg resin is approximately 5521.9 mg for 1 mg/L gold thiosulfate in the solution. Thus, when the gold thiosulfate concentration in the solution is 2.5 mg/L, the gold adsorbed on resin of 13804.75 mg/kg resin will be obtained. The intercept is zero, and it is reasonable because when the gold concentration in solution is zero, no gold can be adsorbed on resin. In addition, the loading of gold thiosulfate on resin calculated from the strip solution is in excellent agreement with the loadings calculated from the loading solution. The change in both loading and stripping-based gold thiosulfate concentrations is only 5.8% on average indicating the mass balance of gold thiosulfate on loading and tripping works very well.

Figure 4.6.b shows the result on the adsorption isotherm of gold thiosulfate onto resin in the multiple component NARS system with the equilibrium concentration of polythionates being 0.762 mM trithionate and 1.388 mM tetrationate and the equilibrium thiosulfate concentration of 1.427 mM. The speciation of thiosulfate, polythionates and gold thiosulfate for the multiple components NARS system with the synthetic polythionates mixture solution and all the result of gold thiosulfate concentration by ICP-OES are listed in Table B.3 and Table B.4 of Appendix B.

As can be seen in Figure 4.6.b, the slope of the gold thiosulfate adsorption isotherm is decreased to be 1938 from 5521 shown in Figure 4.6.a, but the intercept remains at zero. In other words, thiosulfate concentration at equilibrium affects the loading of gold thiosulfate on the resin in the multiple components NARS system where the more thiosulfate concentration at equilibrium, the greater the amount of gold thiosulfate loaded on resin per kg of resin. This is also supported by the result shown in Figure 4.7 in which the increase in the thiosulfate concentration at equilibrium from 1.427 mM (Figure 4.6.b) to 97.967 mM (Figure 4.7) lifts the adsorption isotherm curve up with the slope being almost 15 times higher than the one by the smaller thiosulfate concentration

(1.427 mM). The speciation of thiosulfate, polythionates and gold thiosulfate for the multiple components NARS system with the initial thiosulfate of 100 mM (Figure 4.7) and all the result of gold thiosulfate concentration by ICP-OES are listed in Table B.5 and Table B.6 of Appendix B.

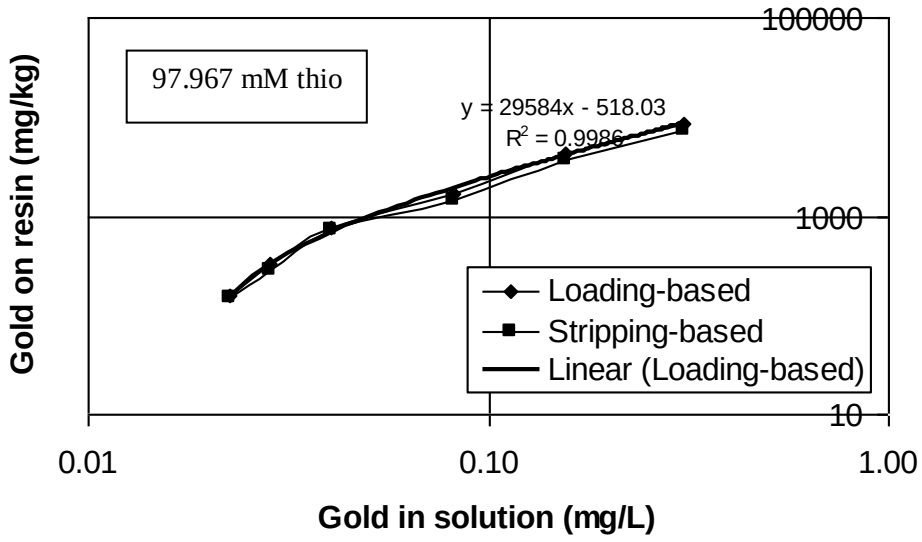

Figure 4.7 The gold thiosulfate loading in the multiple components NARS systems with 100 mM thiosulfate and 0.5 g resin

Surprisingly, the change in the polythionates concentration affects the intercept of the linear plot where diminishing the polythionates concentration in solution increases the gold thiosulfate loading in the multiple components NARS systems. From both Figure 4.6.b and Figure 4.7, it could be concluded that decreasing the polythionates concentration from 2.15 mM to 0 mM significantly decrease the intercept from 0 to -518.03. This is a contradictory phenomenon compared to the result of multiple components ammoniacal resin solution system in the previous research (Jeffrey and Brunt, 2007) where the authors stated that the intercept of the adsorption isotherm curve significantly decreases with the increase in the

polythionates concentration from 2.35 mM to 7.7 mM. Those different performances of adsorption of gold thiosulfate on resin may be due to the absence and presence of ammonia. It is also worthy to show the diversity efforts in dealing with the polythionates formed at the equilibrium in the thiosulfate resin-solution systems.

Overall, trithionate is loaded on the resin very well together with gold thiosulfate in the multiple components NARS system. This is likely because the amount of trithionate loaded on resin is in certain proportion to the amount of gold thiosulfate. The amount of trithionate adsorbed on resin is almost constant; 619.235, 615.535, 606.851 and 606.276 mM (loading-based on Table 4.3); and 665.122, 589.815, 586.519 and 586.932 mM (stripping-based on Table 4.4), for the increased gold concentration in solution of 0.621, 1.767, 4.463 and 9.115 mg/L (loading-based on Table 4.3, and for the increased gold concentration in resin of 237.688, 714.625, 1695.136 and 3510.550 mg/L (stripping-based on Table 4.4). The equilibrium between gold thiosulfate complex and trithionate can then be easily obtained.

It is important to note that the equilibrium concentration of tetrathionate on resin also affects gold thiosulfate loading in the multiple components NARS system. Using the synthetic polythionates mixture solution with about 1.5 mM thiosulfate, 1.3 mM trithionate, 2.5 mM tetrahionate and 1 mM pentathionate, and the initial concentration of gold thiosulfate in the range of 2-10 mg/L with 0.5 g resin, the effect of tetrahionate on gold thiosulfate loading in the multiple components NARS system is highlighted in Figure 4.7. As revealed in Figure 4.7, the loading affinity of gold thiosulfate for each batch increases with the decrease in the equilibrium concentration of tetrathionate on resin. In contrast, the loading affinity of gold thiosulfate is almost stable when the equilibrium concentration of tetrathionate adsorbed on resin being approximately 303.614 and 5.581 mM. As expected, the loading affinity of gold thiosulfate is also controlled by the initial concentration of gold on resin when there is no tetrathionate on resin at the

equilibrium condition. Since tetrathionate is an attractive species in the adsorption of gold thiosulfate on resin, the equilibrium constant of the reactions related to tetrathionate and gold thiosulfate is needed to obtain for the multiple components NARS system.

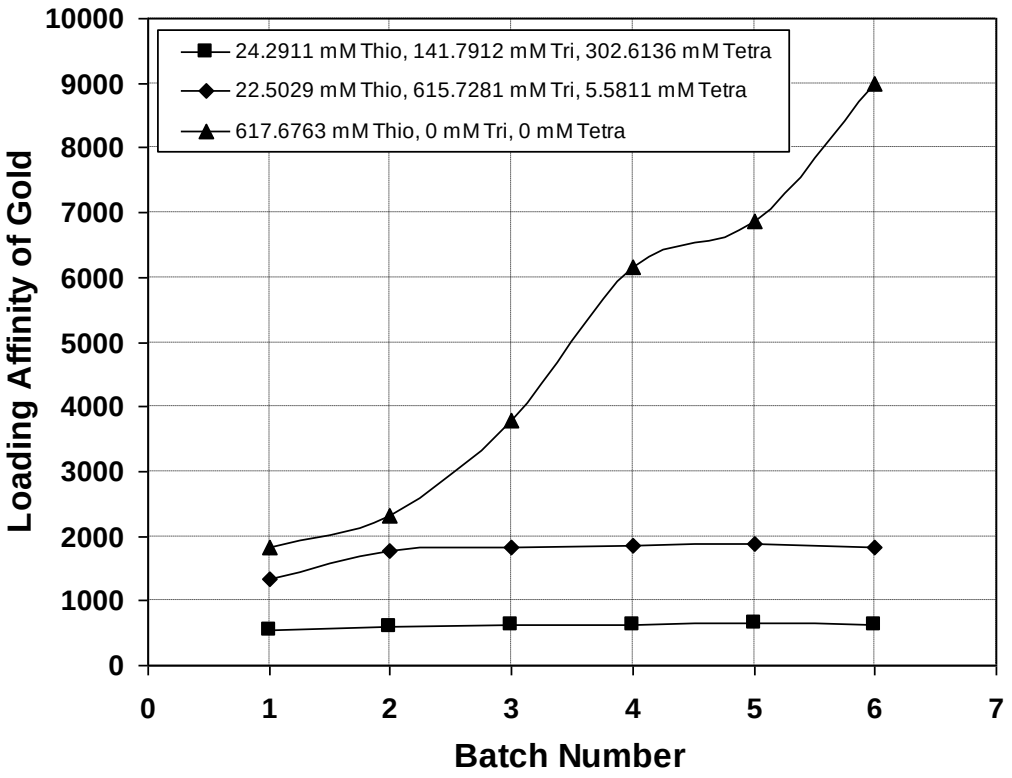

Figure 4.8 Gold thiosulfate loading in the multiple components NARS system with 1.5 mM thiosulfate, 1.3 mM trithionate, 2.5 mM tetrahionate, 1 mM pentathionate, 0.2-10 mg/L gold thiosulfate and 0.5 g resin

4.3.5 Equilibrium Constants for Polythionates and Gold Thiosulfate in Multiple Components NARS systems

From the previous discussion, the equilibrium constants associated with the reactions of polythionates and gold thiosulfate complex are needed to clearly highlight the competitive strength within all the species in the multiple components NARS systems. The reactions of trithionate, tetrathionate, pentathionate or exathionate with gold thiosulfate complex in the multiple components NARS systems can be expressed as the following equations:

$$3R_2S_3O_{6(s)} + 2Au(S_2O_3)_2^{3-}{}_{(aq)} \;<=>\; 2R_3Au(S_2O_3)_{2\,(s)} + 3S_3O_6^{2-}{}_{(aq)} \quad K_{Au/3} \qquad (4.5)$$

$$3R_2S_4O_{6(s)} + 2Au(S_2O_3)_2^{3-}{}_{(aq)} \;<=>\; 2R_3Au(S_2O_3)_{2\,(s)} + 3S_4O_6^{2-}{}_{(aq)} \quad K_{Au/4} \qquad (4.6)$$

$$3R_2S_5O_{6(s)} + 2Au(S_2O_3)_2^{3-}{}_{(aq)} \;<=>\; 2R_3Au(S_2O_3)_{2\,(s)} + 3S_5O_6^{2-}{}_{(aq)} \quad K_{Au/5} \qquad (4.7)$$

$$3R_2S_6O_{6(s)} + 2Au(S_2O_3)_2^{3-}{}_{(aq)} \;<=>\; 2R_3Au(S_2O_3)_{2\,(s)} + 3S_6O_6^{2-}{}_{(aq)} \quad K_{Au/6} \qquad (4.8)$$

Thus, the equilibrium constant for Equation (4.5) can be written as:

$$K_{Au/3} = \left(\frac{R_3Au(S_2O_3)_2}{\left[Au(S_2O_3)_2^{3-} \right]} \right)^2 \times \left(\frac{\left[S_3O_6^{2-} \right]}{R_2S_3O_6} \right)^3 \qquad (4.9)$$

By taking logarithm the equation becomes:

$$\log K_{Au/3} + 3\log\left(\frac{R_2S_3O_6}{\left[S_3O_6^{2-} \right]} \right) = 2\log\left(\frac{R_3Au(S_2O_3)_2}{\left[Au(S_2O_3)_2^{3-} \right]} \right) \qquad (4.10)$$

It should thus be clear that if the adsorption isotherm follows this model, a plot of log ($[R_3Au(S_2O_3)_2]/[Au(S_2O_3)_2^{3-}]$) vs. log ($[R_2S_3O_6]/[S_3O_6^{2-}]$) yields a straight line

with the slope and intercept. The results by ICP-OES and HPLC for the equilibrium experiment of the multiple components NARS systems with the initial concentration of gold thiosulfate being about 10 mg/L, 5 and 100 mM initial thiosulfate and the initial trithionate concentration in the range of 2.5-15 mM, are shown in Table B.7 and Table B.8 in Appendix B. Meanwhile the plot of adsorption isotherm using both loading and stripping data in Table B.8 of Appendix B for the equilibrium constant associated with Equation (10) is shown in Figure 4.9. From the intercept of 0.5 log $K_{Au/3}$, the equilibrium constant $K_{Au/3}$ is determined to be 0.399.

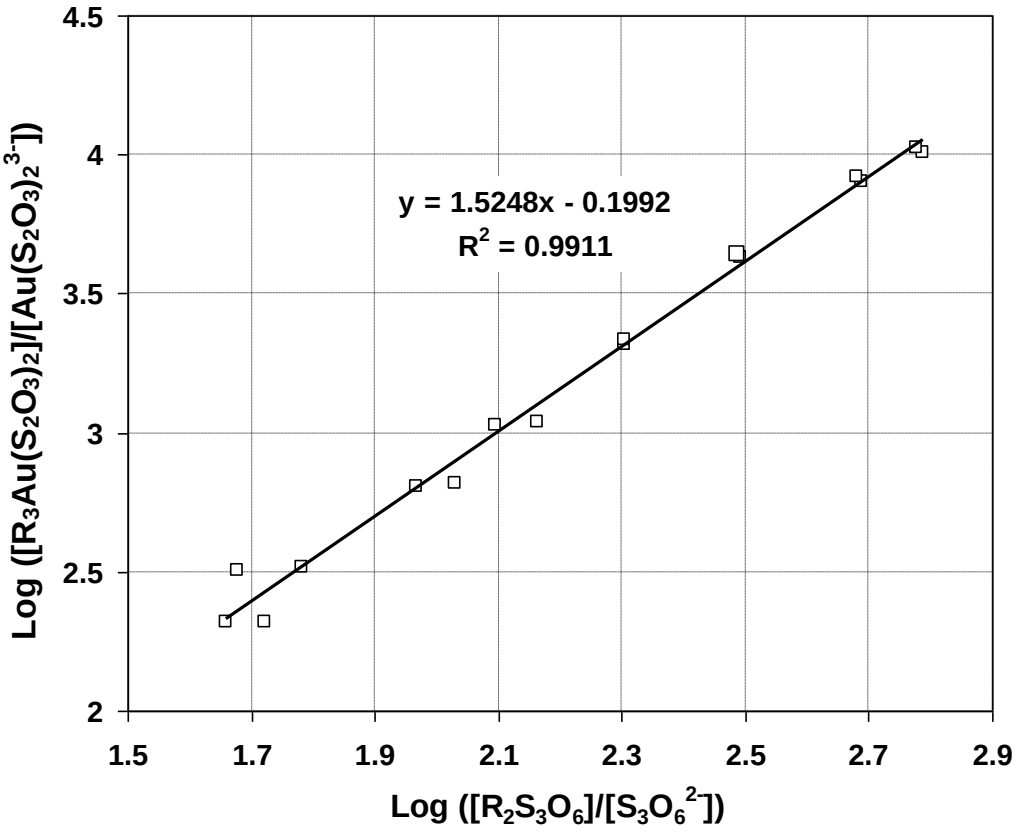

Figure 4.9 The graphical representation of the equilibrium constant for gold thiosulfate loading over trithionate. The slope of the plot is the order, and the intercept is 0.5 log $K_{Au/3}$

As highlighted in the previous discussion, tetrathionate is an attractive species in the adsorption of gold thiosulfate on resin in the multiple components NARS system. The equilibrium constant of the reactions related to tetrathionate and gold thiosulfate could be worked out using reaction mechanism. As shown in Figure 4.4, the equilibrium constant for the reaction of trithionate and tetrathionate in the multiple components NARS system, $K_{4/3}$ is 1.446. Meanwhile, the equilibrium constant for the reaction of trithionate and gold thiosulfate in the multiple components NARS system, $K_{Au/3}$ is 0.399, obtained from Figure 4.9. Therefore, the equilibrium constant for the reaction of tetrathionate and gold thiosulfate in the multiple components NARS system, denoted as $K_{Au/4}$ can be obtained as follow;

$3R_2S_4O_{6(s)} + 3S_3O_6^{2-}{}_{(aq)} \quad <=> 3R_2S_3O_{6(s)} + 3S_4O_6^{2-}{}_{(aq)}$ ……..(a) $1/K_{4/3}$

$3R_2S_3O_{6(s)} + 2Au(S_2O_3)_2^{3-}{}_{(aq)} <=> 2R_3Au(S_2O_3)_{2(s)} + 3S_3O_6^{2-}{}_{(aq)}$ ….(b) $K_{Au/3}$

_____ +

$3R_2S_4O_{6(s)} + 2Au(S_2O_3)_2^{3-}{}_{(aq)} <=> 2R_3Au(S_2O_3)_{2(s)} + 3S_4O_6^{2-}{}_{(aq)}$ ….(c) $K_{Au/4}$

The equilibrium constant for Equation (a) equals $1/K_{4/3}$ which is not equal to $1/(K_{4/3})^3$. This is a special case because of the entire coefficient in the original reaction being one, and this case is described on some specific examples in the available literature (Clark, 2002). The $K_{4/3}$ value is shown in Figure 4.4. $K_{Au/4}$ is calculated to be approximately 0.276. This is a reasonable number because the $K_{Au/4}$ value is supposed to be less than 1, and it should be less than the $K_{Au/3}$ value since tetrathionate is more competitive to adsorb on resin than trithionate as highlighted in the discussion of Figure 4.4.

Similarly, the equilibrium constant for the reaction of pentathionate and gold thiosulfate in the multiple components NARS system, $K_{Au/5}$ could be obtained. The ways to obtain it could be illustrated as follow;

The first way;

$3R_2S_5O_{6(s)} + 3S_4O_6^{2-}{}_{(aq)} <=> 3R_2S_4O_{6(s)} + 3S_5O_6^{2-}{}_{(aq)}$ ……..(d) $1/K_{5/4}$

$3R_2S_4O_{6(s)} + 2Au(S_2O_3)_2^{3-}{}_{(aq)} <=> 2R_3Au(S_2O_3)_{2(s)} + 3S_4O_6^{2-}{}_{(aq)}$ ….(c') $K_{Au/4}$

_____ +

$3R_2S_5O_{6(s)} + 2Au(S_2O_3)_2^{3-}{}_{(aq)} <=> 2R_3Au(S_2O_3)_{2(s)} + 3S_5O_6^{2-}{}_{(aq)}$ ….(e) $K_{Au/5}$

The second way;

$3R_2S_4O_{6(s)} + 3S_3O_6^{2-}{}_{(aq)} <=> 3R_2S_3O_{6(s)} + 3S_4O_6^{2-}{}_{(aq)}$ ……...(a') $1/K_{4/3}$

$3R_2S_5O_{6(s)} + 3S_4O_6^{2-}{}_{(aq)} <=> 3R_2S_4O_{6(s)} + 3S_5O_6^{2-}{}_{(aq)}$ …...……..(d') $1/K_{5/4}$

$3R_2S_3O_{6(s)} + 2Au(S_2O_3)_2^{3-}{}_{(aq)} <=> 2R_3Au(S_2O_3)_{2(s)} + 3S_3O_6^{2-}{}_{(aq)}$ ….(b') $K_{Au/3}$

_____ +

$3R_2S_5O_{6(s)} + 2Au(S_2O_3)_2^{3-}{}_{(aq)} <=> 2R_3Au(S_2O_3)_{2(s)} + 3S_5O_6^{2-}{}_{(aq)}$ ….(e') $K_{Au/5}$

Figure 4.10 shows the equilibrium constant for the reaction of pentathionate and gold thiosulfate based on the first reaction mechanism using the equilibrium constant $K_{5/4}$ shown in Figure 4.5 and the equilibrium constant $K_{Au/4}$ addressed in the previous discussion. $K_{Au/5}$ is determined to be approximately 0.1759, 0.1747, 0.1729, 0.1749 and 0.1747 for the 1st batch to the 5th batch based on the first reaction mechanism. Meanwhile, it is approximately 0.1759, 0.1747, 0.1728, 0.1749 and 0.1746, respectively based on the second reaction mechanism. Overall, all the numbers are consistent, and $K_{Au/5}$ is approximately 0.175. This is

acceptable because $K_{Au/5}$ is supposed to be less than $K_{Au/4}$ since pentahionate is more competitive to adsorb on the resin than tetrahionate.

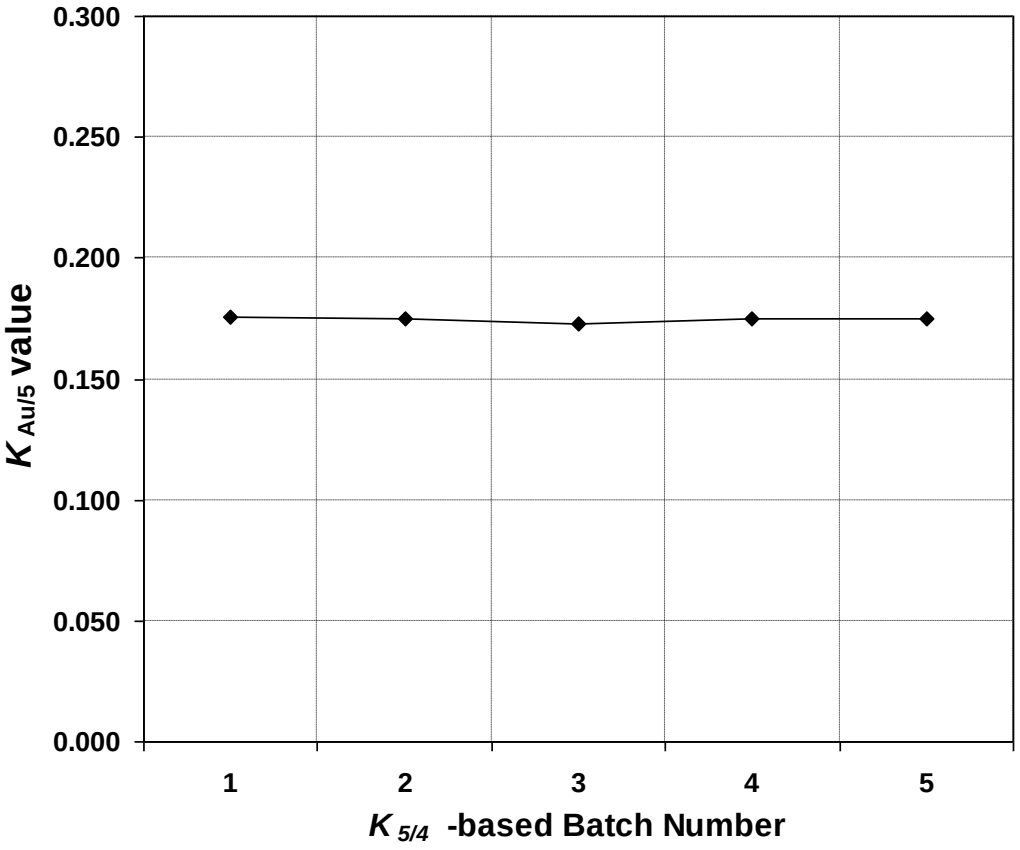

Figure 4.10 The equilibrium constant of pentathionate and gold thiosulfate reaction in the multiple components NARS systems

Similarly, the equilibrium constant of thiosulfate and gold thiosulfate reaction could be obtained to be 37.947. Since equilibrium constant of pentathionate and exathionate reaction ($K_{6/5}$) cannot be determined in the previous discussion, equilibrium constant of exathionate and gold thiosulfate reaction ($K_{Au/6}$) cannot be determined in this work using the reaction mechanism of related species.

4.4 Conclusions

The experimental procedures can be used to investigate the adsorption of thiosulfate, polythionates and gold thiosulfate adsorptions on strong based anion exchange resin in the multiple components non-ammoniacal resin-solution (NARS) systems. Unlike the system with ammonia in the previous literature, the degradation of thiosulfate does not occur in the multiple components NARS systems since there is no significant decrease of thiosulfate concentration between the loading and stripping results. The more thiosulfate concentration in solution at equilibrium, the greater amount of gold thiosulfate adsorbed on the resin. The mass of gold thiosulfate per kg resin linearly increase with the increase in the gold thiosulfate concentration in the solution wherein the polythionates concentration affects the adsorption isotherm of gold thiosulfate.

The polythionates concentration affects the adsorption isotherm of gold thiosulfate intercept of the linear plot where diminishing the polythionates concentration in solution increase the gold thiosulfate loading in the multiple components NARS systems. Trithionate is to be loaded on the resin very well together with gold thiosulfate, and increasing the trithionate concentration in solution results in the greater amount of gold thiosulfate adsorbed on the resin. The loading affinity of gold thiosulfate increases with the decrease in the equilibrium concentration of tetrathionate on the resin. Overall, all the polythionates and gold thiosulfate compete with one another to occupy the available charge on the resin, and all the species are simultaneously adsorbed on the resin.

Equilibrium constants associated with the proposed reactions in the multiple components NARS systems are used to also investigate the competitive adsorption of thiosulfate, polythionates and gold thiosulfate on resin. The equilibrium constants are summarised in Table 4.5:

Table 4.5 The proposed equilibrium reactions and the equilibrium constants in the multiple components NARS systems

Equilibrium Reactions	Equilibrium Constants
$R_2S_2O_{3(s)} + S_3O_6^{2-}{}_{(aq)} <=> R_2S_3O_{6(s)} + S_2O_3^{2-}{}_{(aq)}$	95.104
$R_2S_3O_{6(s)} + S_4O_6^{2-}{}_{(aq)} <=> R_2S_4O_{6(s)} + S_3O_6^{2-}{}_{(aq)}$	1.446
$R_2S_4O_{6(s)} + S_5O_6^{2-}{}_{(aq)} <=> R_2S_5O_{6(s)} + S_4O_6^{2-}{}_{(aq)}$	1.580
$3R_2S_2O_{3(s)} + 2Au(S_2O_3)_2^{3-}{}_{(aq)} <=> 2R_3Au(S_2O_3)_{2\,(s)} + 3S_2O_3^{2-}{}_{(aq)}$	37.947
$3R_2S_3O_{6(s)} + 2Au(S_2O_3)_2^{3-}{}_{(aq)} <=> 2R_3Au(S_2O_3)_{2\,(s)} + 3S_3O_6^{2-}{}_{(aq)}$	0.399
$3R_2S_4O_{6(s)} + 2Au(S_2O_3)_2^{3-}{}_{(aq)} <=> 2R_3Au(S_2O_3)_{2\,(s)} + 3S_4O_6^{2-}{}_{(aq)}$	0.276
$3R_2S_5O_{6(s)} + 2Au(S_2O_3)_2^{3-}{}_{(aq)} <=> 2R_3Au(S_2O_3)_{2\,(s)} + 3S_5O_6^{2-}{}_{(aq)}$	0.175

Therefore, the order of competitive adsorption of thiosulfate, polythionates and gold thiosulfate on the resin is $S_2O_3^{2-} < Au(S_2O_3)_2^{3-} < S_3O_6^{2-} < S_4O_6^{2-} < S_5O_6^{2-}$.

CHAPTER 5
Adsorption of Copper Complexes in Multiple Components Resin-Solution Systems

5.1 Introduction

In general, copper is found in the gold leaching of complex ores (Bhappu, 1990), Marsden and House, 1992). The present of copper reduces the efficiency of gold leaching and consumes additional reagent (Fagan et al., 1997, Huang et al., 1997). To improve the recovery of gold, ammonium thiosulfate and oxygen under pressure was used (Berezowsky et al., 1978). Because copper ions can be catalysts for the oxidation of thiosulfate by oxygen or other oxidant, there should only be sufficient copper present to maximize leaching of gold and minimize thiosulfate consumption, and it only improves the initial rate of gold extraction (Zipperian et al., 1988, Abbruzzese et al., 1995).

The chemistry of gold leaching involving thiosulfate, ammonium and copper ions are complex due to the oxidation by dissolved oxygen (Langhans et al., 1992, Tozawa et al., 1981, Li et al., 1995). Using ammoniacal thiosulfate in the gold leaching is typically much more economical than cyanidation to lixiviate significant quantities of copper without consuming excessive reagent (Aylmore, 2001). The leaching of gold linearly increases with the Cu(II) concentration at low concentration (less than 5 mM) while the higher Cu(II) concentration almost does not affect the gold leaching rate (Jeffrey et al., 2001). The oxidation of thiosulfate in the presence of copper(II) and oxygen is very complex wherein oxygen increases the rate of copper(II) reduction to copper(I) by thiosulfate (Breuer and Jeffrey, 2003). Therefore, limiting the presence of oxygen and ammonia in the leach solution would be worthy to investigate copper complexes in the copper leaching systems.

Anion exchange resin had been intensively used in the quantification of thiosulfate and polythionates in gold leach solution on the resins (Jeffrey and Brunt, 2007). However, there are still limited studies on the adsorption of copper complexes onto resin at the equilibrium stage.

Therefore, the main objective of this work is to investigate the adsorption of thiosulfate, polythionates and copper complexes on strong based anion exchange resin in multiple components resin-solution systems. The specific objectives of the work are:

a. To provide the experimental procedure for the adsorption of thiosulfate and copper complexes adsorptions on strong based anion exchange resin in the multiple components resin-solution systems.

b. To investigate the equilibrium adsorption of thiosulfate and copper by limiting oxygen in multiple components resin-solution systems.

c. To investigate the effect of thiosulfate and ammonia concentration and the solution pH in multiple components resin-solution systems on the equilibrium adsorption of total copper complexes on resin.

d. To highlight the adsorption isotherm of total copper complexes in multiple components resin-solution systems.

5.2 Experimental Methods

All the experimental work for the adsorption of thiosulfate, polythionates and copper complexes on strong based anion exchange resin in the multiple components resin-solution systems were done in the Thiosulfate Laboratory at Australian Mineral Research Centre, CSIRO Mineral in Western Australia.

5.2.1 Apparatus and Chemicals

The concentrations of thiosulfate, polythionates and the total copper complexes in the experiments of multiple components resin-solution systems was also analysed using the Waters 2695 HPLC separation module. For HPLC analysis, the copper must be masked with ethylenediamine (Aksu and Doyle, 2002), as copper thiosulfate peak interferes with the analysis of thiosulfate and polythionates. The HPLC separation was achieved using a Dionex IonPac AS16 ion exchange column equipped with an IonPac AG16 guard column. The mobile phase was a solution of sodium perchlorate (0.075 – 0.2 M). The species detection was via a Waters 2996 Photodiode Array Detector (UV). Empower software was used for the calculation of peak area (Waters, 2002). Details about the mobile solution and the wavelengths of UV adsorption and peak retention times of the involved species have been described in the literature (Jeffrey and Brunt, 2007).All the thiosulfate and polythionates analysis have been done by the PhD candidate of this thesis in the HPLC Laboratory at the Australian Mineral Research Centre. For the ICP analysis of total copper complexes, the samples were treated with NaCN (0.0167 M), and the analysis of samples has been done by the staff of Analytical Chemistry Unit at the Australian Mineral Research Centre.

Copper was introduced as cupric sulphate ($CuSO_4.5H_2O$). Ammonia-containing solutions were prepared using a 2 M NH_3 stock solution standardised by acid-base

titration (Karen, 2009). Purolite A500/2788 in the chloride form with a macrospore structure was also used. The wet form of the resin contained 53-58 % moisture, the resin capacity is 1.15 meq/mL, and the specific gravity is 1.08 g/mL (PUROLITE, 2008).

5.2.2 Procedures

All the experiments of the adsorption of thiosulfate, polythionates and copper on strong based anion exchange resin in multiple components resin-solution systems were conducted at the ambient temperature (~23 °C) and variable pH. The concentration on the resin for a particular species was calculated from the change in its solution concentration in the system. The effect of limiting oxygen presence in the system was taken into account by non-degassing and degassing of the solution with nitrogen.

A. The experiments on equilibrium adsorption for thiosulfate, polythionates and copper without nitrogen degas

The equilibrium experiment was initially conducted to investigate the effect of oxygen presence on the multiple components resin-solution systems. The steps for the experiments with multiple components are described as follow;

1) Prepare 200 ml of loading solution consisting of 25 mM $(NH_4)S_2O_3$ (ammonium thiosulfate), 5 mM sodium trithionate ($Na_2S_3O_6$), 2 mM cupric sulphate ($CuSO_4.5H_2O$) and 50 mM ammonia in a 200ml volumetric flask. In dealing with ammonia loss, the ammonia solution is quickly added last before rapidly putting DI water into the flask to reach the 200 ml level. Then, quickly closing the flask with the cap.

2) Prepare 0.5 g resin, and place it in a conical flask, and place it in a 130 ml sealed plastic bottle.

3) Quickly place the 200 mL solution in the bottle until it is full (130 mL total volume), and tightly sealed.

4) Place it on a roller at 35 rpm and start the loading.

5) Take 1 mL sample of the solution for HPLC analysis at just after 2 hours loading, and then measure the solution pH using pH probe.

6) After 2 hours loading, decant and wash the resin 4 times with DI water into a large vial. Suck the remaining H_2O using pipette.

7) Add 50 mL $NaClO_4$ (0.5M) into the vial for the dilution of thiosulfate from resin, shake it at 150 U/minute and start the timer for 30 minutes of the 1^{st} stripping.

8) Take 1 mL sample of the solution for HPLC analysis as the 1^{st} stripping sample.

9) Decant and wash the resin 4 times with DI water in the vial. Suck the remaining H_2O.

10) Re-add 50 mL $NaClO_4$ (0.5M) into the vial for the dilution of thiosulfate from resin, shake it at 150 U/minute on a Jubalo SW-20C shaker and start the timer for 30 minutes of the 2^{nd} stripping.

11) Take 1 mL sample of the solution for HPLC analysis as the 2^{nd} stripping sample.

12) Decant and wash the resin 4 times with DI water in the vial. Before placing the resin in a small glass vial, measure the empty vial mass.

13) Place the resin in a small glass vial, and suck the remaining H_2O.

14) Dry the resin at 60 ^{o}C in an oven for about 16 hours.

15) Measure the mass of vial with resin to obtain the dried resin mass; the dried resin mass = the mass of vial with resin – the empty vial mass.

The 1st to 15th steps were repeated for the systems with the initial sodium thiosulfate in the range of 25-100 mM $(NH_4)S_2O_3$ (ammonium thiosulfate), 5 mM sodium trithionate ($Na_2S_3O_6$), 2 mM cupric sulphate ($CuSO_4.5H_2O$) and the initial ammonia concentration in the range of 0-400 mM.

B. The experiments on equilibrium adsorption for thiosulfate, polythionates and copper with nitrogen degas

All the 12 batches in the previous experimental procedure were repeated for the equilibrium adsorption for thiosulfate, polythionates and copper with nitrogen degas. For the loading solution with the addition of ammonia, the solution was degassed with N_2 at the flow rate of 200 mL/min for 30 mins before adding ammonia. Then, the solution was quickly added with ammonia solution and DI water, re-degassed with N_2 for 3 mins and the volumetric flask was closed with the cap. The identical bottle was degassed with N_2 at the same flow rate for 2 mins. Following that, 0.5 g resin was put in the bottle and the bottle quickly closed with the cap. The solution was placed in the bottle until full (130 mL total volume), and the bottles were tightly sealed and placed on a roller at 35 rpm for 5 hours loading. After loading, the stripping was carried out as the previous experiments. The samples for HPLC and ICP-OES, and the resin were also analyzed as the same approaches, and the pH of 5 hours loading solution was measured using pH probe.

For the ICP analysis of total copper complexes, instead of using 1 mL NaCN (0.0167 M) as applied gold thiosulfate samples (see Chapter 4 and Appendix B),

2 mL NaCN (0.0167 M) was added to each sample to stabilize the copper complexes in the sample. See Figures C.1.a and C.1.b in Appendix C where there is very small amount of salt as the precipitation result of copper complexes in the samples were treated with 2 mL NaCN (0.0167 M) after 5 days. Meanwhile, the samples with 2 mL NaCN (0.0167 M) has more salt on the bottom as the precipitation result of copper complexes in the samples after 5 days.

5.3 Results and Discussions

5.3.1 Equilibrium Adsorption of Thiosulfate and Copper by Limiting Oxygen

The experimental results for the equilibrium adsorption in multiple components resin-solution systems to investigate the effect of limiting oxygen on thiosulfate and copper are shown in Figures 5.1 and 5.2. Figure 5.1.a shows the result of multiple components resin-solution system with the initial concentration of species in solution such as 25 mM, 5 mM sodium trithionate, 1 mM copper(II) and ammonia concentration in the range of 0-200 mM.

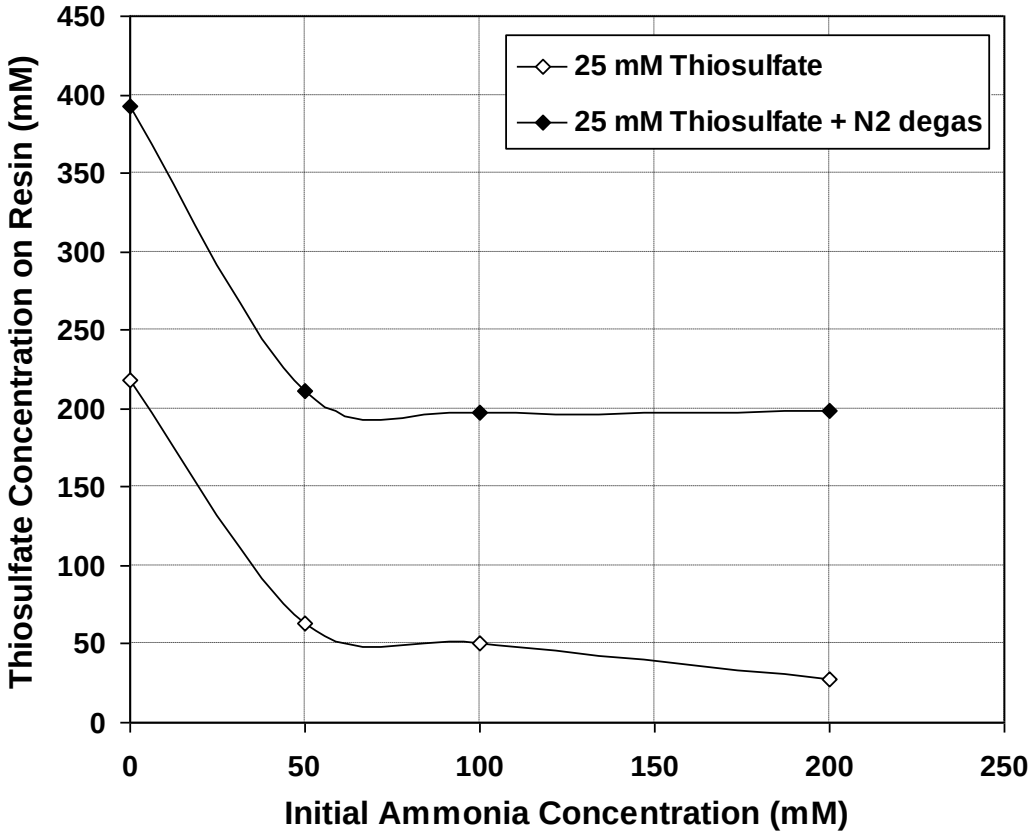

(a)

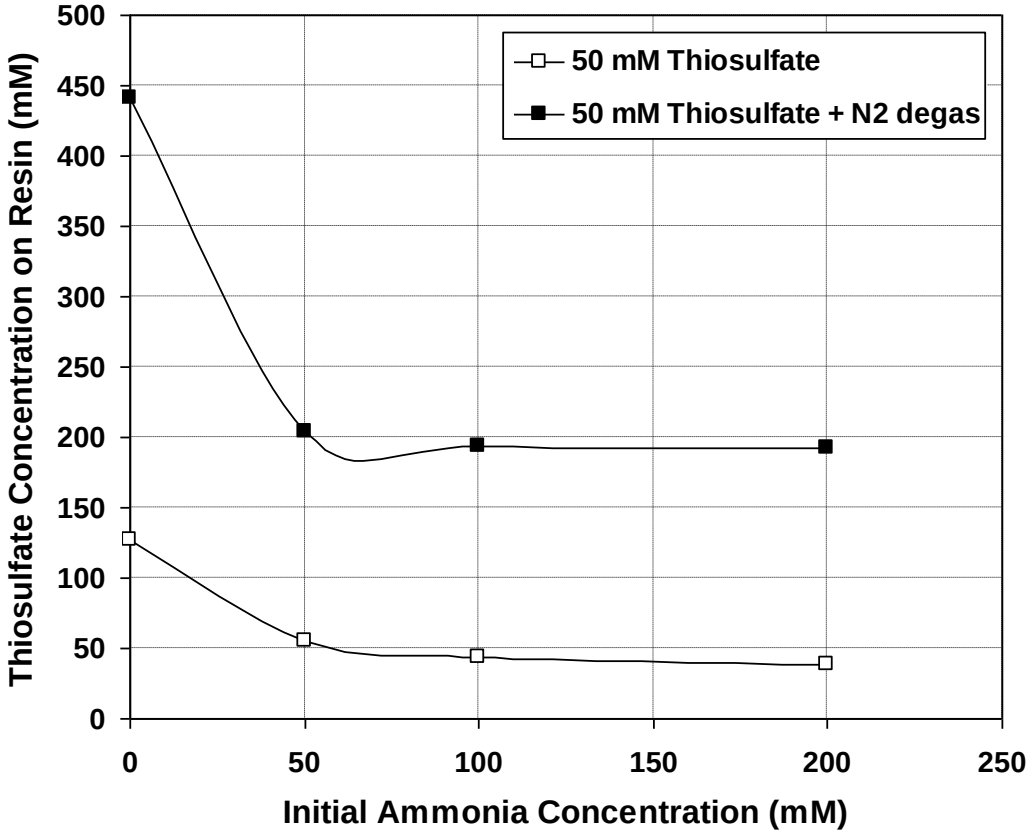

(b)

Figure 5.1 The measured thiosulfate concentration on resin over the initial ammonia in solution of multiple components resin-solution systems by N_2 degas with (a) 25 mM thiosulfate (b) 50 mM thiosulfate

As shown in Figure 5.1.a, limiting oxygen presence in the system by degassing nitrogen, the thiosulfate concentration on resin is lifted from approximately 217.727, 62.998, 50.381 and 27.706 mM to 392.957, 211.786, 197.715 and 199.001 mM for the initial ammonia concentration in solution of 0, 50, 100 and 200 mM, respectively. Moreover, in the system with 50 mM thiosulfate as can be seen in Figure 5.1.b, degassing nitrogen also results in the increase of the thiosulfate concentration on resin to be approximately 440.422, 204.084, 194.220, 192.912 mM from approximately 127.157, 54.845, 43.799, and 38.186 mM for

the initial ammonia concentration in solution of 0, 50, 100 and 200 mM, respectively.

More importantly, the concentration of copper on resin based on the stripping samples of HPLC analysis is increased by approximately 59.8, 97.6, 116.8 and 224.9 % for the initial ammonia concentration in solution of 0, 50, 100 and 200 mM, respectively by nitrogen degas in the system with 25 mM thiosulfate as revealed in Figure 5.2.a. The percentages are much more for the system with 50 mM thiosulfate, which are 203.4, 196.5, 205.6 and 328.6 %, respectively from approximately 38.355, 15.869, 12.254 and 7.333 mM to approximately 116.364, 47.37.444 and 31.433 mM, respectively as can be worked out from Figure 5.2.b. for the same the initial ammonia concentration in solution.

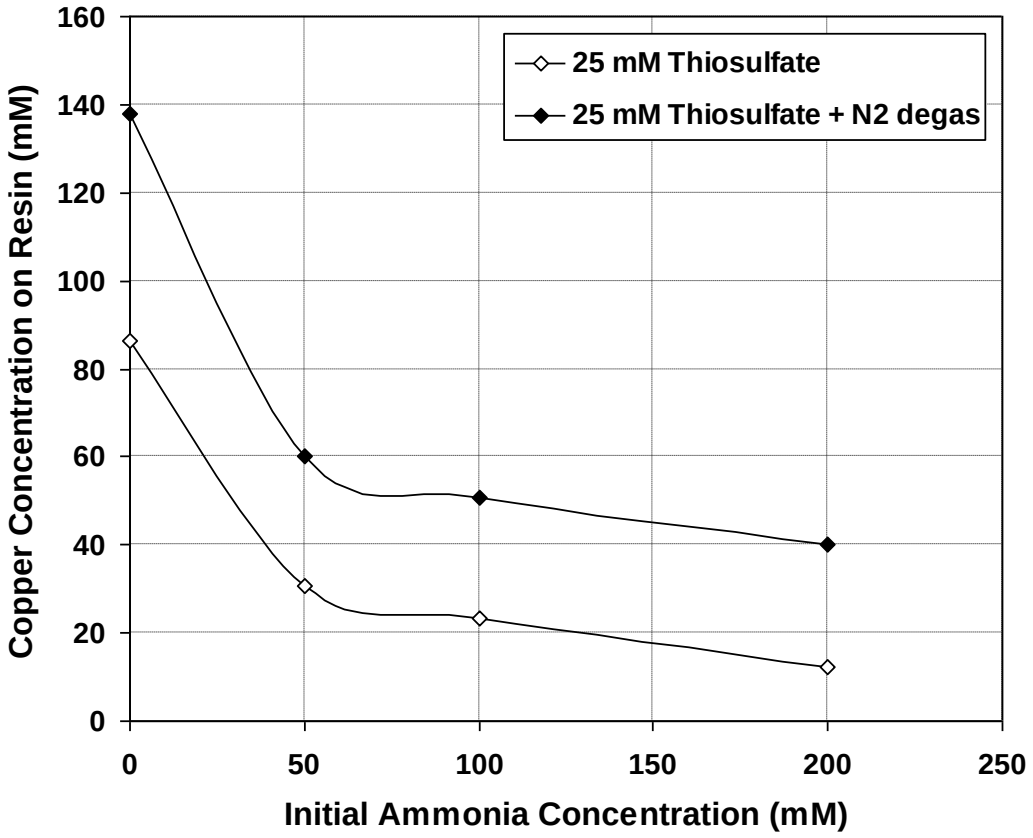

(a)

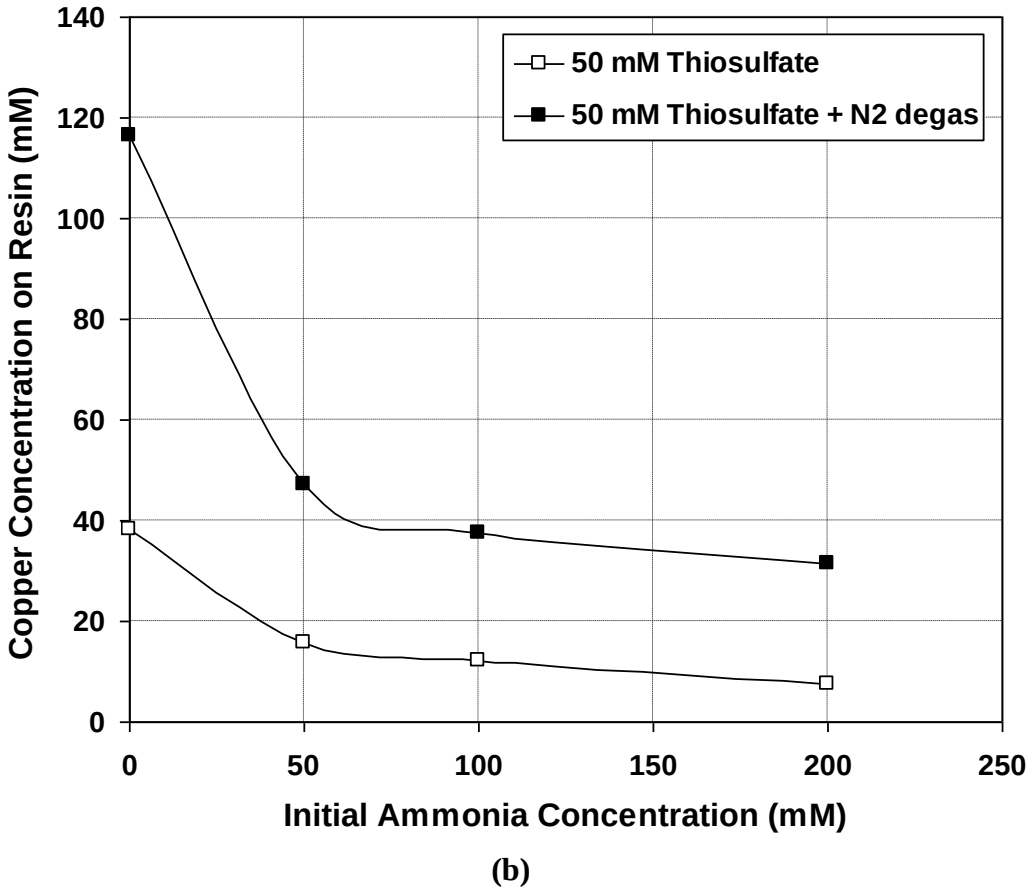

Figure 5.2 The measured copper concentration on resin over the initial ammonia in solution in the systems with 50 mM thiosulfate and (a) without N_2 degas (b) with N_2 degas

Therefore, limiting oxygen in the multiple components resin-solution systems by degassing nitrogen is recommended for increasing copper adsorbed on resin. This was done for the rest of the experiments addressed in this chapter. In addition, since the same trends of thiosulfate and copper concentrations on anion exchange resin are highlighted in Figures 5.1 and 5.2, there is a considerable correlation between thiosulfate and copper in forming the copper complexes which could be adsorbed on the resin. This need requires further explanation on copper complexes by means of experimental and modelling work as discussed in Chapter 5 and Chapter 6.

5.3.2 Equilibrium Adsorption of Copper on Resin by Thiosulfate Concentration in Solution

It is clearly shown in Figure 5.3 plotted from the data based on measurement in the multiple components resin-solution system that increasing the initial concentration of thiosulfate in solution results in the linear increase of equilibrium concentration of thiosulfate in solution. Due to the amount of thiosulfate adsorbed on resin is in proportion to the amount of thiosulfate lost in solution, the concentration of thiosulfate on resin increases linearly with the increase in the equilibrium concentration of thiosulfate in solution for the condition shown in Figure 5.3.

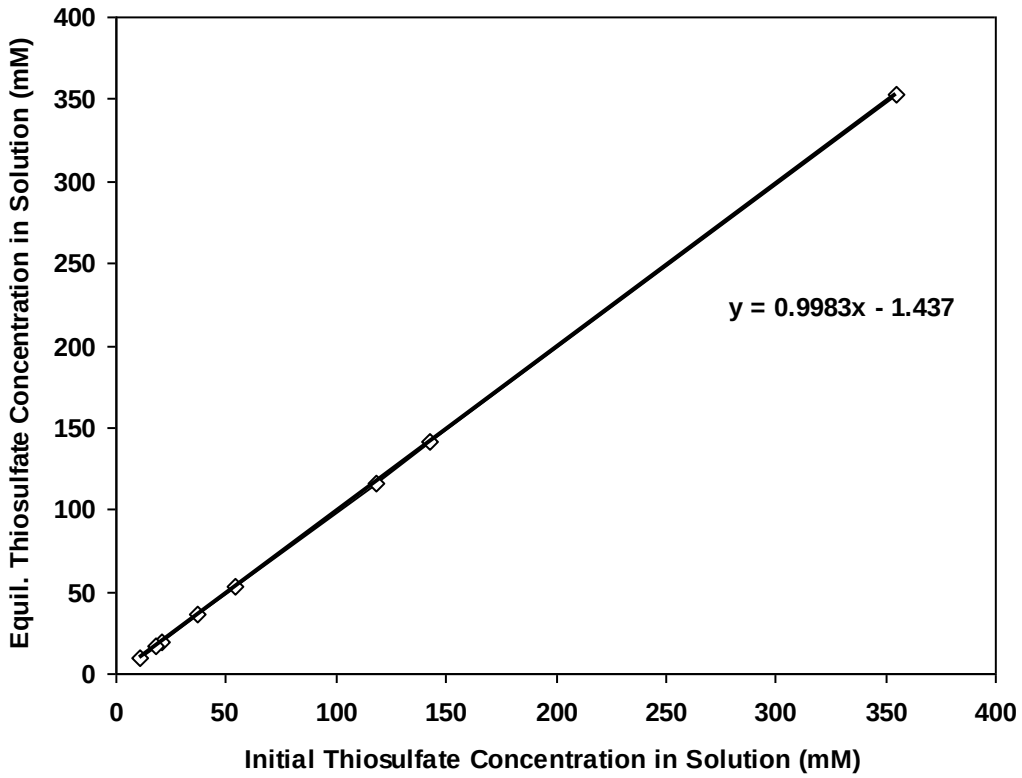

Figure 5.3 The initial thiosulfate concentration in solution versus the equilibrium thiosulfate concentration in solution

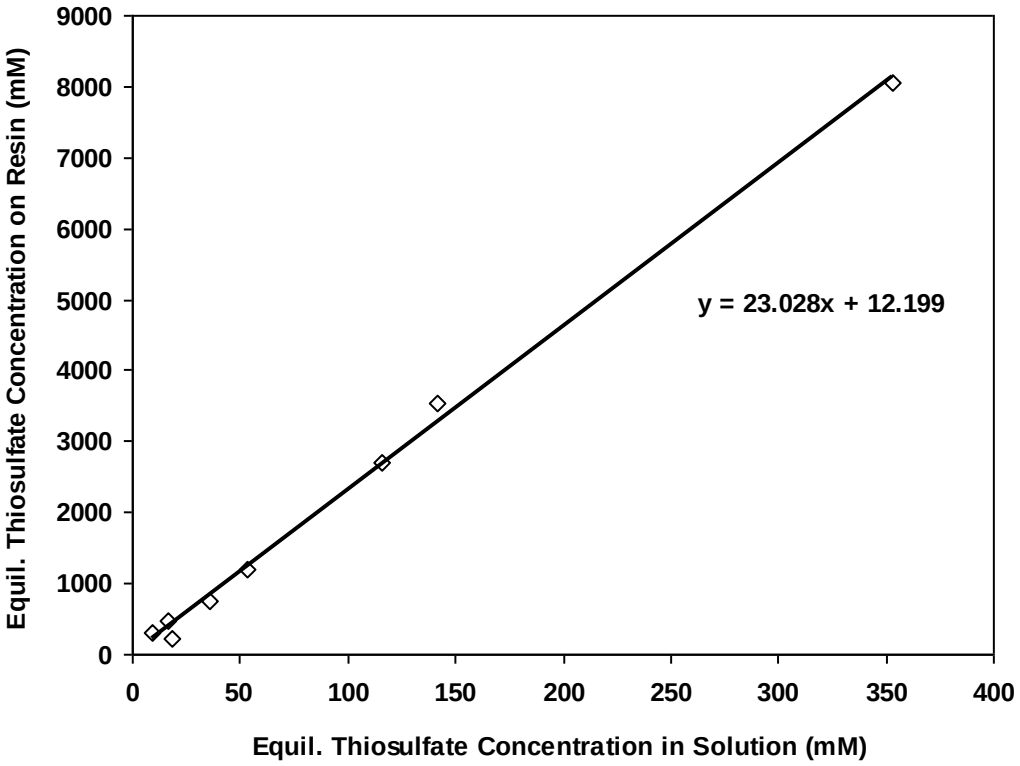

Figure 5.4 The equilibrium thiosulfate concentration in solution versus the equilibrium thiosulfate concentration on resin

This is also evidently demonstrated by plotting the experimental data, as can be seen in Figure 5.4. The slope in Figure 5.4 is larger than the slope in Figure 5.3 because the solution volume is larger than the resin volume.

The total copper complexes adsorbed on resin can be calculated based on the measurement of the copper lost in solution of multiple components resin-solution system. The relationship between the thiosulfate concentration in solution and the copper on resin in multiple components resin-solution system with the absence of ammonia is shown in Figure 5.5, and the result of ICP-OES analysis on the total copper complexes are addressed in Table C.1 of Appendix C where in samples at loading time 0 (t = 0) and 2 hours (t = 2), the 1st and 2nd stripping are listed. The

total copper complexes plotted in Figure 5.5 are taken from the change concentration of copper in stripping solution.

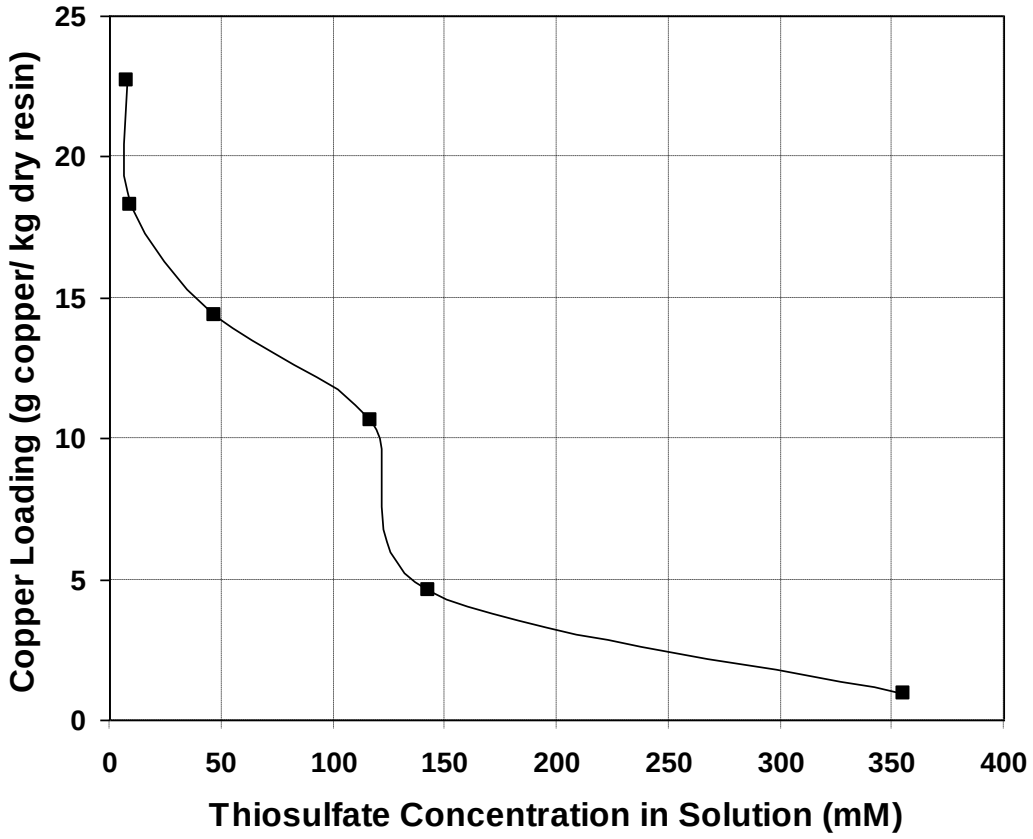

Figure 5.5 The measured copper on resin over the thiosulfate concentration in solution without ammonia. The initial concentration of thiosulfate in solution applied is in the range of 0-400 mM

As clearly shown in Figure 5.5, the copper adsorbed on resin seems to be dynamic exponentially decreased with the increase of thiosulfate concentration in solution. Firstly, it sharply drops from about 22.683 to 18.314 g copper/ kg dry resin for the increase of thiosulfate concentration in solution from about 7.607 to 9.514 mM, and then it gradually decreases to about 10.646 mM at the thiosulfate

concentration of 116.577 mM. Secondly, it suddenly drops to be 4.589 mM at the thiosulfate concentration of 143.073 mM, and then it gradually decreases with the increase of thiosulfate concentration in solution. From this trend, it is important to investigate the transition of copper complexes species in solution and on resin in the loading system. In addition, it follows a single exponential trend, the fitting equation is $y = 22.294e^{-0.009x}$ with the correlation coefficient R^2 being 0.972.

5.3.3 The effect of Ammonia Concentration and Solution pH on Equilibrium Adsorption of Copper on Resin

The effect of ammonia concentration in solution on total copper complexes adsorbed on resin in the multiple components resin-solution system with the various initial concentration of thiosulfate in solution is viewed in Figure 5.6, and the result of ICP-OES analysis on the total copper complexes are listed in Table C.2 of Appendix C where in samples at loading time 0 (t = 0) and 2 hours (t = 2), and the 1st and 2nd stripping are also listed. As can be clearly seen in Figure 5.6, the total copper complexes adsorbed on resin sharply decreases from approximately 22.322 g copper/kg dry resin when no ammonia is applied in solution to approximately 10.7122 g copper/kg dry resin when 50 mM ammonia being applied in solution with the initial concentration of thiosulfate being 20 mM. Then, as the ammonia concentration in solution increases to 200 and 400 mM, the total copper complexes adsorbed on resin gradually decreases to 7.688 and 6.552 mM, respectively.

Compared to the total copper complexes adsorbed on resin in the multiple components resin-solution system with the initial concentration of thiosulfate being 20 mM, the profile of the total copper complexes adsorbed on resin with the initial concentration of thiosulfate being 100 mM is decreased moderately from approximately 10.646 g copper/kg dry resin when no ammonia being applied in

solution to approximately 7.881 g copper/kg dry resin when 50 mM ammonia being applied in solution (see the bottom graph in Figure 5.6). The same shape of graph is also shown between the one with 20 mM thiosulfate and 100 mM thiosulfate. But for the one with 100 mM thiosulfate, the total copper complexes adsorbed on resin is lower proportionally, which is 6.079 and 5.097 g copper/kg dry resin for the ammonia concentration in solution of 200 and 400 mM, respectively as shown by the bottom graph in Figure 5.6. Thus, the dominant species of copper complexes on the resin control most amount of total copper complexes adsorbed on the resin (see the further discussion in Chapter 6).

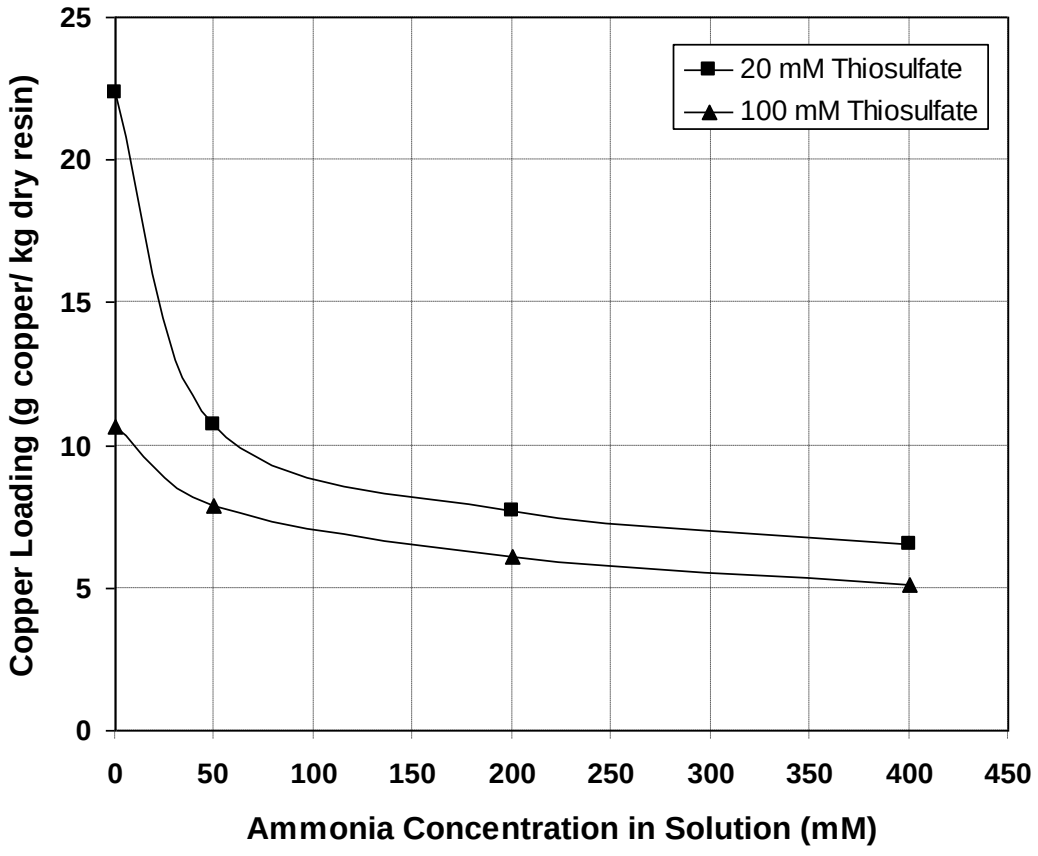

Figure 5.6 The measured copper concentration on resin over initial concentration of ammonia in solution with various thiosulfate concentrations

Meanwhile, the relationship between the total copper complexes adsorbed on resin and the solution pH is sighted in Figure 5.7. Because the pH solution is normally generated by the concentration of ammonia in the solution, it is not surprising that the profile of the total copper complexes adsorbed on resin over the solution pH is almost the same as Figure 5.6. The more solution pH, the less total copper complexes adsorbed on resin is obtained.

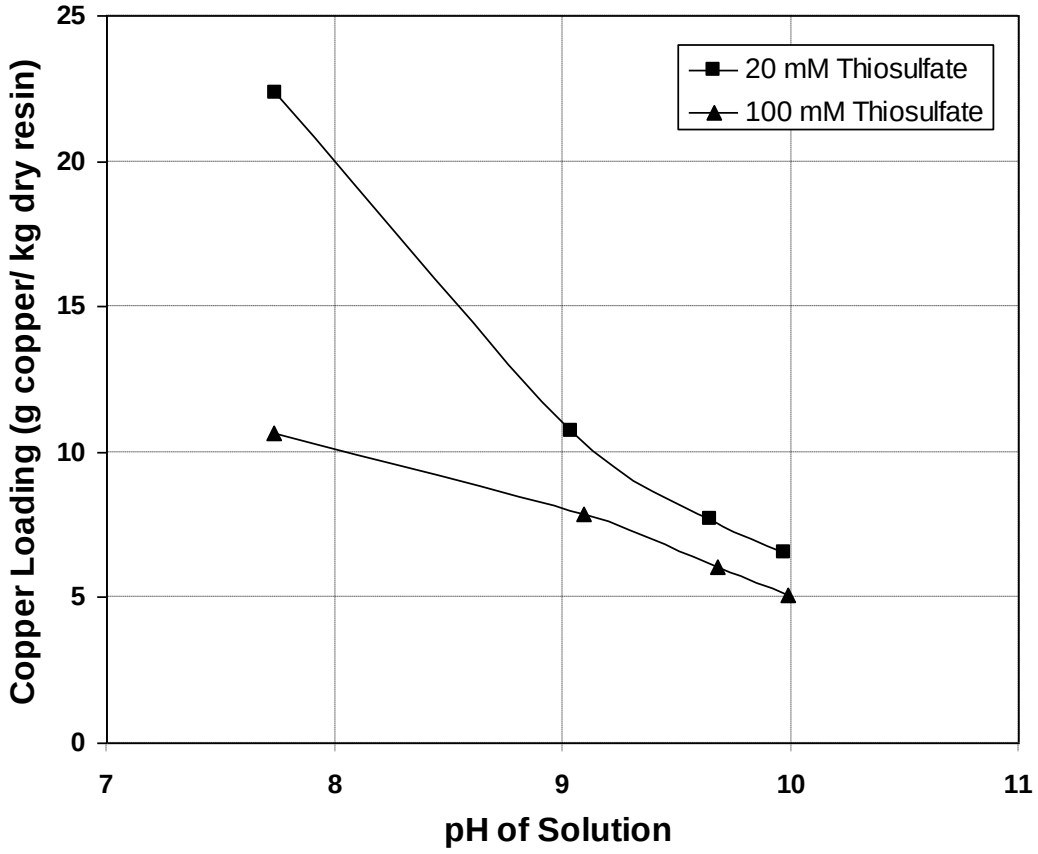

Figure 5.7 The measured copper concentrations on resin over solution pH with various thiosulfate concentrations

5.3.4 Adsorption Isotherm of Copper in Multiple Components Resin-Solution Systems

The adsorption isotherm of total copper complexes in the multiple components resin-solution system is clearly shown in Figure 5.8. The ammonia concentration applied in the system for the adsorption isotherm of total copper on resin shown by the bottom plots of the equation Yc = -674.15x + 81630 is in the range of 50-400 with the equilibrium concentration of thiosulfate in solution being in the range of 6.932-85.841 mM. Meanwhile, when there is no ammonia applied, the system for the adsorption isotherm of total copper on resin are shown by the top plots of the equation Ya = -494.84x + 66491, and the equilibrium concentration of thiosulfate in solution is in the range of 9.016-143.073 mM.

It should be noted that unlike the adsorption isotherm which linearly increase with the increase in the gold thiosulfate concentration in the solution presented in Figure 4.5 of Chapter 4, the adsorption isotherm of total copper complexes decrease with the increase in the total copper complexes in solution with and without ammonia applied in the system, as shown in Figure 5.8. As can be seen in Figure 5.8, increasing ammonia concentration in the system results in the lower total copper complexes adsorbed on resin. Overall, although the slope of the bottom linear fitting line is less than the top linear fitting line, the adsorption of total copper complexes with the addition of ammonia in the system may not be lifted up to the one without the addition of ammonia because the total copper adsorbed on the top plot (see the G plot in Figure 5.8) of the bottom line consists 50 mM ammonia.

Therefore, non-ammoniacal resin-solution (NARS) systems give much better adsorption isotherm of copper on the resin as clearly highlighted in the previous results and discussions.

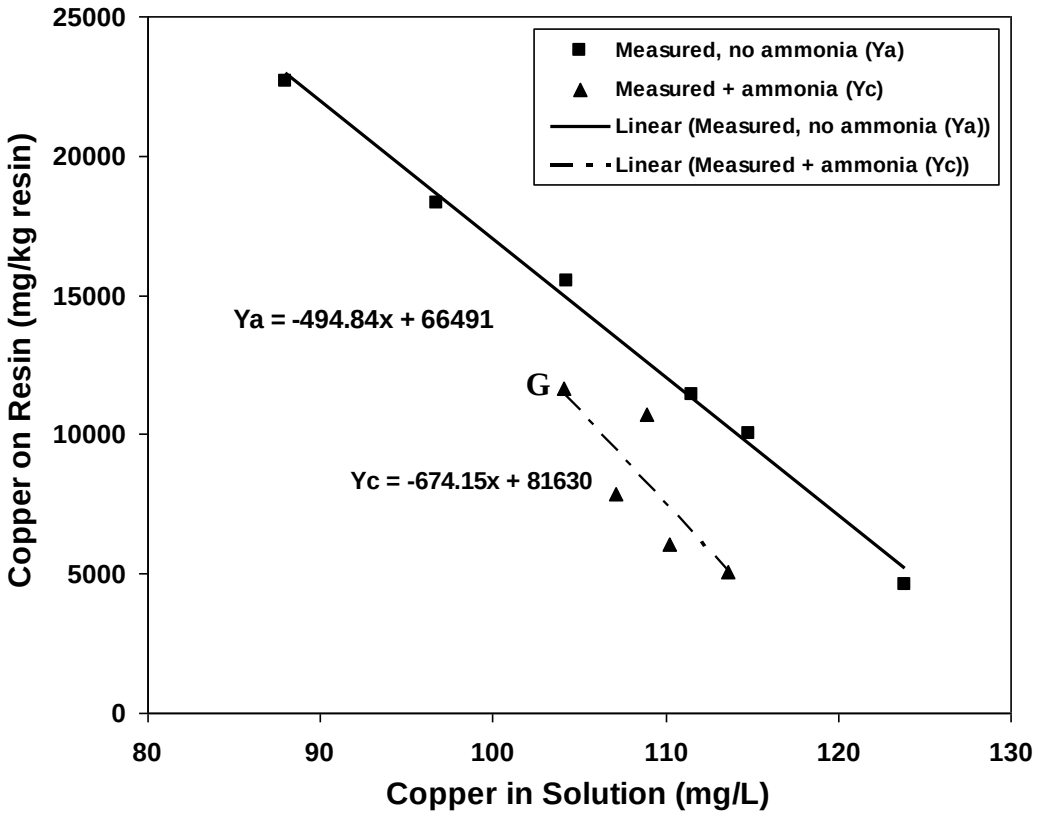

Figure 5.8 Adsorption isotherm of copper onto resin based on measurement in the system with and without the addition of ammonia

5.4 Conclusions

This chapter provides the experimental procedures for the adsorption of thiosulfate and copper complexes on strong based anion exchange resin in the multiple components resin-solution systems. To increase the total copper complexes adsorbed on resin in multiple components resin-solution systems with various thiosulfate and ammonia concentrations in solution, degassing nitrogen is recommended in the experimental procedure to limit the presence of oxygen in the systems.

A result shows that the concentration of thiosulfate in solution and adsorbed on resin is a linear increase with the increase in the initial concentration of thiosulfate in solution in multiple components resin-solution systems. The total copper complexes adsorbed on resin dynamic exponentially decreases with the increase of thiosulfate concentration in solution. Meanwhile, increasing ammonia in the solution results in the diminishing total copper complexes on the resin. As the solution pH of systems is maintained by the ammonia solution added in the system, the same effect of ammonia on the total copper complexes on resin is also shown. These profiles require further investigation (as discussed in Chapter 6) for the copper complexes species in solution and on resin in the systems.

Overall, non-ammoniacal resin-solution systems give much better adsorption isotherm of copper on resin as clearly demonstrated in this chapter.

CHAPTER 6
Modelling Copper Complexes in Multiple Components Resin-Solution Systems

6.1 Introduction

The leaching of copper using thiosulfate reagent has been investigated since it is almost presented in gold thiosulfate leaching, and it is mainly found that the concentration of copper is higher than the concentration of gold. It was recommended that the concentration of copper added as catalyst should be less than 5 mM to get the leaching of gold being linearly increases with the Cu(II) (Jeffrey et al., 2001). Limiting the presence of oxygen leach solution was proposed to decrease the oxidation of thiosulfate and reduction rate of copper(II) to copper(I) by thiosulfate (Breuer and Jeffrey, 2003).

The fundamental thermodynamic data associated with copper (I) and copper (II) had been addressed (Stupko et al., 1998, Black, 2006). It was found in the recent study that the copper complex of $CuNH_3(S_2O_3)_2^{3-}$ and $CuNH_3S_2O_3^-$ is the more stable species than the other species in solution with high concentrations of ammonia and/or thiosulfate. The equilibrium constants for the reactions associated with copper(I)-thiosulfate and copper(I)-ammonia in solution of systems were also determined in various media. In the media of ammonium thiosulfate solutions with strong base exchange resin, tetrathionate must be completely removed because it reduces the adsorption of copper (Zhang and Dreisinger, 2002). Anion exchange resin had been intensively used in the quantification of thiosulfate and polythionates in gold leach solution on the resins (Jeffrey and Brunt, 2007). However, there are still limited studies on the adsorption of copper complexes onto the resin at the equilibrium stage, and the equilibrium constants for the

reactions associated with thiosulfate, polythionates, ammonia and copper complexes on resin have not yet been determined in previous studies.

Numerical method of Newton-Raphson was efficiently applied to model the multiple component in aqueous system (Robinson et al., 2000). The method was also used to specify the metals of Cu, Ca and Mg and the ligands of organics, carbonates and bicarbonates and to predict the concentration of various copper species (Jagadeesh et al., 2006). The method has been applied in mineral and hydrometallurgy (Reuter and Sudhölter, 1996, Mansur et al., 2002, Himmi et al., 2008, Casas et al., 2005). Interestingly, a mechanistic model had been developed to calculate equilibrium between the various copper cyanide complexes in both the aqueous and carbon phases by using Newton-Raphson method (Dai et al., 2009). Yet, a model of reaction mechanism and the application of Newton-Raphson method for the speciation of copper complexes in multiple components resin-solution systems with ammonium thiosulfate solution have not been proposed in the previous studies.

Therefore, the main objective of this work is to investigate the adsorption of thiosulfate, polythionates and copper complexes on resin at the equilibrium in multiple components resin-solution systems with ammonium thiosulfate solution. The specific objectives of the work are:

a. To model the reaction mechanism associated with thiosulfate, polythionates and copper complexes in the multiple components resin-solution systems.

b. To investigate the effect of thiosulfate and ammonia concentration in solution of systems on the adsorption of total copper complexes on the resin and the dominant species connected with the parameters.

c. To determine the equilibrium constants for the proposed reactions in the systems.

6.2 Modelling Approach

The leaching and adsorption of copper in a multiple components resin-solution system is expected to be a simultaneous complex process. Copper (I) in solution reacts with thiosulfate as the leaching reagent in excessive amount to form copper thiosulfate complexes in solution. In the same time, copper (I) in solution also reacts with ammonia being added to form copper amine complexes. Due to the competitive adsorption of thiosulfate and trithionate, the copper thiosulfate complexes and the copper amine complexes are expected to also react with trithionate on resin. Then, all the species in the multiple components resin-solution system compete largely with one another to adsorb on anion exchange resin. Therefore, the equilibrium reaction mechanism associated with thiosulfate, trithionate, ammonia and copper complexes in the multiple components resin-solution system could be expressed by the following equations:

$$Cu^{+}_{(aq)} + S_2O_3^{2-}{}_{(aq)} <=> CuS_2O_3^{-}{}_{(aq)} \qquad log\,\beta_1 = 9.29 \qquad (6.1)$$

$$Cu^{+}_{(aq)} + 2S_2O_3^{2-}{}_{(aq)} <=> Cu(S_2O_3)_2^{3-}{}_{(aq)} \qquad log\,\beta_2 = 12.17 \qquad (6.2)$$

$$Cu^{+}_{(aq)} + 3S_2O_3^{2-}{}_{(aq)} <=> Cu(S_2O_3)_3^{5-}{}_{(aq)} \qquad log\,\beta_3 = 14.48 \qquad (6.3)$$

$$Cu^{+}_{(aq)} + NH_{3(aq)} <=> CuNH_3^{+}{}_{(aq)} \qquad log\,\beta_4 = 5.8 \qquad (6.4)$$

$$Cu^{+}_{(aq)} + 2NH_{3(aq)} <=> Cu(NH_3)_2^{+}{}_{(aq)} \qquad log\,\beta_5 = 10.37 \qquad (6.5)$$

$$Cu^{+}_{(aq)} + 3NH_{3(aq)} <=> Cu(NH_3)_3^{+}{}_{(aq)} \qquad log\,\beta_6 = 9.93 \qquad (6.6)$$

$$Cu^{+}_{(aq)} + NH_{3(aq)} + S_2O_3^{2-}{}_{(aq)} <=> CuNH_3S_2O_3^{-}{}_{(aq)} \qquad log\,\beta_7 = 12.67 \qquad (6.7)$$

$$Cu^{+}_{(aq)} + NH_{3(aq)} + 2S_2O_3^{2-}{}_{(aq)} <=> CuNH_3(S_2O_3)_2^{3-}{}_{(aq)} \qquad log\,\beta_8 = 14.02 \qquad (6.8)$$

$$CuS_2O_3^{-}{}_{(aq)} + 1/2R_2S_3O_{6(s)} <=> RCuS_2O_{3(s)} + 1/2S_3O_6^{2-}{}_{(aq)} \qquad log\,K_1 \qquad (6.9)$$

$$Cu(S_2O_3)_2^{3-}{}_{(aq)} + 3/2R_2S_3O_{6(s)} <=> R_3Cu(S_2O_3)_{2(s)} + 3/2S_3O_6^{2-}{}_{(aq)} \qquad log\,K_2 \qquad (6.10)$$

$$Cu(S_2O_3)_3^{5-}{}_{(aq)} + 5/2R_2S_3O_{6(s)} <=> R_5Cu(S_2O_3)_{3(s)} + 5/2S_3O_6^{2-}{}_{(aq)} \qquad log\,K_3 \qquad (6.11)$$

$$CuNH_3S_2O_3^{-}{}_{(aq)} + 1/2R_2S_3O_{6(s)} <=> RCuNH_3S_2O_{3(s)} + 1/2S_3O_6^{2-}{}_{(aq)} \qquad log\,K_4 \qquad (6.12)$$

$$CuNH_3(S_2O_3)_2^{3-}{}_{(aq)} + 3/2R_2S_3O_{6(s)} <=> R_3CuNH_3(S_2O_3)_{2(s)} + 3/2S_3O_6^{2-}{}_{(aq)} \quad log\ K_5 \quad (6.13)$$

$$R_2S_2O_{3(s)} + S_3O_6^{2-}{}_{(aq)} <=> R_2S_3O_{6(s)} + S_2O_3^{2-}{}_{(aq)} \quad log\ K_6 \quad (6.14)$$

where $log\ \beta_1$ - $log\ \beta_8$ are taken from the available literature (Stupko et al., 1998, Black, 2006) and $log\ K_6$ is taken from the result shown in Figure 4.3 of Chapter 4, and the equilibrium constants K_1–K_5 are then obtained in this modelling approach.

From Equations (6.1)-(6.14), there are 19 unknowns established with regards to the concentration of each species in solution ([…]) and on resin ([…]-R) which are namely; $[Cu^+]$, $[CuS_2O_3^-]$, $[Cu(S_2O_3)_2^{3-}]$, $[Cu(S_2O_3)_3^{5-}]$, $[CuNH_3]$, $[Cu(NH_3)_2^+]$, $[Cu(NH_3)_3^+]$, $[CuNH_3S_2O_3^-]$, $[CuNH_3(S_2O_3)_2^{3-}]$, $[NH_3]$, $[S_2O_3^{2-}]$, $[CuS_2O_3^-]$-R, $[Cu(S_2O_3)_2^{3-}]$-R, $[Cu(S_2O_3)_3^{5-}]$-R, $[CuNH_3S_2O_3^-]$-R, $[CuNH_3(S_2O_3)_2^{3-}]$-R, $[S_2O_3^{2-}]$-R, $[S_3O_6^{2-}]$-R and $[S_3O_6^{2-}]$. In order to be able to solve the 19 unknowns, at least 5 other equations are required. The required 5 equations can be the 4 mass balance equations for each species (Equations (6.15)-(6.18)), and a charge balance equation on resin (Equation (6.19)):

$$\begin{aligned} Vs * [Cu\ (I)]_{total} = Vs * ([Cu^+] + [CuS_2O_3^-] + [Cu(S_2O_3)_2^{3-}] + [Cu(S_2O_3)_3^{5-}] \\ + [CuNH_3] + [Cu(NH_3)_2^+] + [Cu(NH_3)_3^+] + [CuNH_3S_2O_3^-] \\ + [CuNH_3(S_2O_3)_2^{3-}]\ ) + Vr * ([CuS_2O_3^-]\text{-}R + [Cu(S_2O_3)_2^{3-}]\text{-}R \\ + [Cu(S_2O_3)_3^{5-}]\text{-}R + [CuNH_3S_2O_3^-]\text{-}R + [CuNH_3(S_2O_3)_2^{3-}]\text{-}R) \end{aligned} \quad (6.15)$$

$$\begin{aligned} Vs * [S_2O_3^{2-}]_{total} = Vs * ([CuS_2O_3^-] + 2[Cu(S_2O_3)_2^{3-}] + 3[Cu(S_2O_3)_3^{5-}] \\ + [CuNH_3S_2O_3^-] + 2[CuNH_3(S_2O_3)_2^{3-}] + [S_2O_3^{2-}]) \\ + Vr * ([CuS_2O_3^-]\text{-}R + 2[Cu(S_2O_3)_2^{3-}]\text{-}R + 3[Cu(S_2O_3)_3^{5-}]\text{-}R \\ + [CuNH_3S_2O_3^-]\text{-}R + 2[CuNH_3(S_2O_3)_2^{3-}]\text{-}R + [\ S_2O_3^{2-}]\text{-}R\ ) \end{aligned} \quad (6.16)$$

$$Vs * [NH_3]_{total} = Vs* ([CuNH_3] + 2[Cu(NH_3)_2^{+}] + 3[Cu(NH_3)_3^{+}] + [CuNH_3S_2O_3^{-}] + [CuNH_3(S_2O_3)_2^{3-}] + [NH_3]) + Vr * ([CuNH_3S_2O_3^{-}]\text{-}R + [CuNH_3(S_2O_3)_2^{3-}]\text{-}R) \quad (6.17)$$

$$Vs * [S_3O_6^{2-}]_{total} = Vs * [S_3O_6^{2-}] + Vr * [S_3O_6^{2-}]\text{-}R \quad (6.18)$$

$$1300 = -1 * [CuS_2O_3^{-}]\text{-}R + -3 * [Cu(S_2O_3)_2^{3-}]\text{-}R + -5 * [Cu(S_2O_3)_3^{5-}]\text{-}R + -1 * [CuNH_3S_2O_3^{-}]\text{-}R + -3 * [CuNH_3(S_2O_3)_2^{3-}]\text{-}R + -2 * [S_2O_3^{2-}]\text{-}R + -2 * [S_3O_6^{2-}] \quad (6.19)$$

where Vs and Vr are the solution and resin volume, respectively, and the number of 1300 indicates the total available charge on resin. A numerical method utilising the multi-dimensional Newton-Raphson (Norman, 2001) approach in Excel software has been adopted. The Taylor Series $\underline{f}\ \underline{x}+\underline{h}$ of 19 functions associated to Equations [6.1] to (6.19) with 19 unknowns, the column vector $\underline{f}(\underline{x})$ of the 19 unknowns and Jocobian matrix $J(x)$ could be expressed as Equations (6.20), (6.21) and (6.22), respectively where the iteration function can be represented as Equation (A.23):

$$\underline{f}\ \underline{x}+\underline{h} = \underline{f}\ \underline{x} + \underline{f}'\ \underline{x}\ \underline{h}+..., \underline{f} \in R^{19x1}; \underline{x}, \underline{h} \in R^{19x1} \quad (6.20)$$

$$\underline{f}(\underline{x}) = \begin{bmatrix} f_1(\underline{x}) \\ f_2(\underline{x}) \\ \vdots \\ f_{19}(\underline{x}) \end{bmatrix} \quad (6.21)$$

$$J(x) = \begin{bmatrix} \frac{\partial f_1(\underline{x})}{\partial x_1} & \frac{\partial f_1(\underline{x})}{\partial x_2} & \cdots & \frac{\partial f_1(\underline{x})}{\partial x_{19}} \\ \frac{\partial f_2(\underline{x})}{\partial x_1} & \cdots & \cdots & \cdots \\ \vdots & \vdots & \ddots & \vdots \\ \frac{\partial f_{19}(\underline{x})}{\partial x_1} & \cdots & \cdots & \frac{\partial f_{19}(\underline{x})}{\partial x_{19}} \end{bmatrix} \tag{6.22}$$

$$\underline{x}_{k+1} = \underline{x}_k - J^{-1}\,\underline{f}\ \ \underline{x}_k \tag{6.23}$$

6.3 Experimental Data

In order to obtain the equilibrium constants K_1–K_5, the proposed model is simulated with a wide range of parameters such as the concentrations of thiosulfate and ammonia. A set of experimental data with a wide range of parameters such the concentrations of thiosulfate and ammonia is also needed. Therefore, the experimental results of equilibrium adsorption in the multiple components resin-solution systems with nitrogen degas from Chapter 5 were taken into account. To minimize the sum of weighted deviation square between the modelling results and experimental result, Levenberg-Marquardt method (Williams et al., 2002) was applied.

6.4 Results and Discussion

Taking natural logs of all the equations (6.1)-(6.19) for the multi-dimensional Newton-Raphson methods results:

$$f_1 = \ln \beta_1 + \ln\left[Cu^+\right] + \ln\left[S_2O_3^{2-}\right] - \ln\left[CuS_2O_3^-\right]$$

$$f_2 = \ln \beta_2 + \ln\left[Cu^+\right] + 2\ln\left[S_2O_3^{2-}\right] - \ln\left[Cu(S_2O_3)_2^{3-}\right]$$

$$f_3 = \ln \beta_3 + \ln\left[Cu^+\right] + 3\ln\left[S_2O_3^{2-}\right] - \ln\left[Cu(S_2O_3)_3^{5-}\right]$$

$$f_4 = \ln \beta_4 + \ln\left[Cu^+\right] + \ln\ NH_3\ - \ln\left[CuNH_3^+\right]$$

$$f_5 = \ln \beta_5 + \ln\left[Cu^+\right] + 2\ln\ NH_3\ - \ln\left[Cu(NH_3)_2^+\right]$$

$$f_6 = \ln \beta_6 + \ln\left[Cu^+\right] + 3\ln\ NH_3\ - \ln\left[Cu(NH_3)_3^+\right]$$

$$f_7 = \ln \beta_7 + \ln\left[Cu^+\right] + \ln\left[NH_3^+\right] + \ln\left[S_2O_3^{2-}\right] - \ln\left[CuNH_3S_2O_3^-\right]$$

$$f_8 = \ln \beta_8 + \ln\left[Cu^+\right] + \ln\left[NH_3^+\right] + 2\ln\left[S_2O_3^{2-}\right] - \ln\left[CuNH_3(S_2O_3)_2^{3-}\right]$$

$$f_9 = Vs * \ e^{\ln\left[Cu^+\right]} + e^{\ln\left[CuS_2O_3^-\right]} + e^{\ln\left[Cu(S_2O_3)_2^{3-}\right]} + e^{\ln\left[Cu(S_2O_3)_3^{5-}\right]}$$
$$+ e^{\ln\ CuNH_3} + e^{\ln\left[Cu(NH_3)_2^+\right]} + e^{\ln\left[Cu(NH_3)_3^+\right]} + e^{\ln\left[CuNH_3S_2O_3^-\right]}$$
$$+ e^{\ln\left[CuNH_3(S_2O_3)_2^{3-}\right]} - \ Cu(I)\ _{total} + Vr * \ e^{\ln\left[CuS_2O_3^-\right]-R}$$
$$+ e^{\ln\left[Cu(S_2O_3)_2^{3-}\right]-R} + e^{\ln\left[Cu(S_2O_3)_3^{5-}\right]-R} + e^{\ln\left[CuNH_3S_2O_3^-\right]-R}$$
$$+ e^{\ln\left[CuNH_3(S_2O_3)_2^{3-}\right]-R}$$

$$f_{10} = Vs * \ e^{\ln\left[CuS_2O_3^-\right]} + 2e^{\ln\left[Cu(S_2O_3)_2^{3-}\right]} + 3e^{\ln\left[Cu(S_2O_3)_3^{5-}\right]}$$
$$+ e^{\ln\left[CuNH_3S_2O_3^-\right]} + 2e^{\ln\left[CuNH_3(S_2O_3)_2^{3-}\right]} + e^{\ln\left[S_2O_3^{2-}\right]} - \left[S_2O_3^{2-}\right]_{total}$$

$$+Vr*\ e^{\ln\left[CuS_2O_3^-\right]-R}+2e^{\ln\left[Cu(S_2O_3)_2^{3-}\right]-R}+3e^{\ln\left[Cu(S_2O_3)_3^{5-}\right]-R}$$

$$+e^{\ln\left[CuNH_3S_2O_3^-\right]-R}+2e^{\ln\left[CuNH_3(S_2O_3)_2^{3-}\right]-R}+e^{\ln\left[S_2O_3^{2-}\right]-R}$$

$$f_{11}=Vs*\ e^{\ln\ CuNH_3}+2e^{\ln\left[Cu(NH_3)_2^+\right]}+3e^{\ln\left[Cu(NH_3)_3^+\right]}$$

$$+e^{\ln\left[CuNH_3S_2O_3^-\right]}+2e^{\ln\left[CuNH_3(S_2O_3)_2^{3-}\right]}+e^{\ln\ NH_3}\ -\ NH_{3\ total}$$

$$+Vr*\ e^{\ln\left[CuNH_3S_2O_3^-\right]-R}+2e^{\ln\left[CuNH_3(S_2O_3)_2^{3-}\right]-R}+e^{\ln\ NH_3}$$

$$f_{12}=\ln K_1+\ln\left[CuS_2O_3^-\right]+\frac{1}{2}\ln\ \left[S_3O_6^{2-}\right]-R\ -\ln\ \left[CuS_2O_3^-\right]-R$$
$$-\frac{1}{2}\ln\left[S_3O_6^{2-}\right]$$

$$f_{13}=\ln K_2+\ln\left[Cu\ \ S_2O_{3\ 2}^{3-}\right]+\frac{3}{2}\ln\ \left[S_3O_6^{2-}\right]-R\ -\ln\ \left[Cu\ \ S_2O_{3\ 2}^{3-}\right]-R$$
$$-\frac{3}{2}\ln\left[S_3O_6^{2-}\right]$$

$$f_{14}=\ln K_3+\ln\left[Cu\ \ S_2O_{3\ 3}^{5-}\right]+\frac{5}{2}\ln\ \left[S_3O_6^{2-}\right]-R\ -\ln\ \left[Cu\ \ S_2O_{3\ 3}^{5-}\right]-R$$
$$-\frac{5}{2}\ln\left[S_3O_6^{2-}\right]$$

$$f_{15}=\ln K_4+\ln\left[CuNH_3S_2O_3^-\right]+\frac{1}{2}\ln\ \left[S_3O_6^{2-}\right]-R\ -\ln\ \left[CuNH_3S_2O_3^-\right]-R$$
$$-\frac{1}{2}\ln\left[S_3O_6^{2-}\right]$$

$$f_{16}=\ln K_5+\ln\left[CuNH_3\ \ S_2O_{3\ 2}^{3-}\right]+\frac{3}{2}\ln\ \left[S_3O_6^{2-}\right]-R$$
$$-\ln\ \left[CuNH_3\ \ S_2O_{3\ 2}^{3-}\right]-R\ -\frac{3}{2}\ln\left[S_3O_6^{2-}\right]$$

$$f_{17}=\ln K_6+\ln\ \left[S_2O_3^{2-}\right]-R\ +\ln\left[S_3O_6^{2-}\right]-\ln\ \left[S_3O_6^{2-}\right]-R\ -\ln\left[S_2O_3^{2-}\right]$$

$$f_{18} = Vs * \ e^{\ln\left[S_3O_6^{2-}\right]} - \left[S_3O_6^{2-}\right]_{total} + Vr * e^{\ln\left[S_3O_6^{2-}\right]-R}$$

$$f_{19} = e^{\ln\left[CuS_2O_3^{-}\right]-R} + e^{3\ln\left[Cu\ S_2O_3{}_2^{3-}\right]-R} + 5e^{\ln\left[Cu\ S_2O_3{}_3^{5-}\right]-R}$$
$$+e^{\ln\left[CuNH_3S_2O_3^{-}\right]-R} + 3e^{\ln\left[CuNH_3\ S_2O_3{}_2^{3-}\right]-R}$$
$$+2e^{\ln\left[S_2O_3^{2-}\right]-R} + 2e^{\ln\left[S_3O_6^{2-}\right]-R} - 1300$$

Then, a column vector x of the unknowns is obtained as follow:

$$x = \begin{bmatrix} \ln\left[Cu^{+}\right] \\ \ln\left[CuS_2O_3^{-}\right] \\ \ln\left[Cu(S_2O_3)_2^{3-}\right] \\ \ln\left[Cu(S_2O_3)_3^{5-}\right] \\ \ln\left[CuNH_3^{+}\right] \\ \ln\left[Cu(NH_3)_2^{+}\right] \\ \ln\left[Cu(NH_3)_3^{+}\right] \\ \ln\left[CuNH_3S_2O_3^{-}\right] \\ \ln\left[CuNH_3(S_2O_3)_2^{3-}\right] \\ \ln\ NH_3 \\ \ln\left[S_2O_3^{2-}\right] \\ \ln\left[CuS_2O_3^{-}\right]-R \\ \ln\left[(CuS_2O_3)_2^{3-}\right]-R \\ \ln\left[(CuS_2O_3)_3^{5-}\right]-R \\ \ln\left[CuNH_3S_2O_3^{-}\right]-R \\ \ln\left[CuNH_3(S_2O_3)_2^{3-}\right]-R \\ \ln\left[S_2O_3^{2-}\right]-R \\ \ln\left[S_3O_6^{2-}\right]-R \\ \ln\left[S_3O_6^{2-}\right] \end{bmatrix}$$

The column vector of the nineteen *f* functions to solve and the Jacobian matrix are listed in Equation D.1 and Table D.1 in Appendix D, respectively.

6.4.1 Model-based Equilibrium Adsorption of Copper on Resin by Thiosulfate Concentration in Solution

Figure 6.1 shows the model-based total copper complexes adsorbed on resin, and an example of the multi-dimensional Newton-Raphson method application to obtain the model-based total copper complexes adsorbed on resin for the D.2 plot in Figure 6.1 is listed in Tables D.2 of Appendix D.

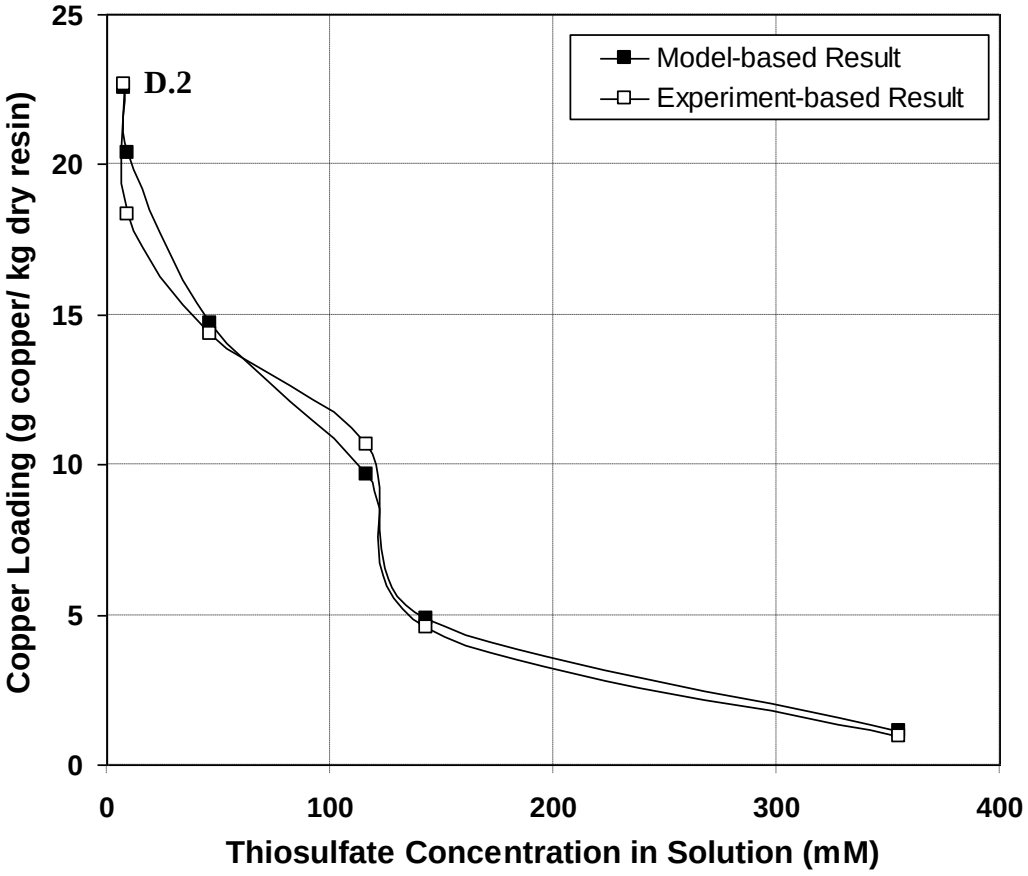

Figure 6.1 The model-based total copper complexes on resin over the thiosulfate concentration in solution without ammonia with 0-400 mM initial concentration of thiosulfate in solution

Interestingly, the model-based profile of total copper complexes adsorbed on resin is typically the same as the one based on experiment as revealed in Figure 6.1. The total copper complexes adsorbed on resin is approximately 22.561, 14.703, 4.842 and 1.227 mM for approximately 7.607, 46.728, 143.073 and 355.150 mM thiosulfate concentrations in solution, respectively, which is also the same as the one based on the experiment. It is approximately 20.348 mM for the 9.514 mM thiosulfate concentrations in solution, which is much lower than the experiment-based one. It is a bit higher than the one for the experiment with 116.577 mM thiosulfate concentrations in solution, which is 9.662 mM. Assuming it also follows a single exponential trend as discussed in Chapter 5, the model-based fitting equation is $y = 22.231e^{-0.0086x}$ with the correlation coefficient R^2 being 0.981. As obtained by Figure 6.2, the model-based results is in a good agreement with the ones by the experiment with the correlation coefficient R^2 being 0.987.

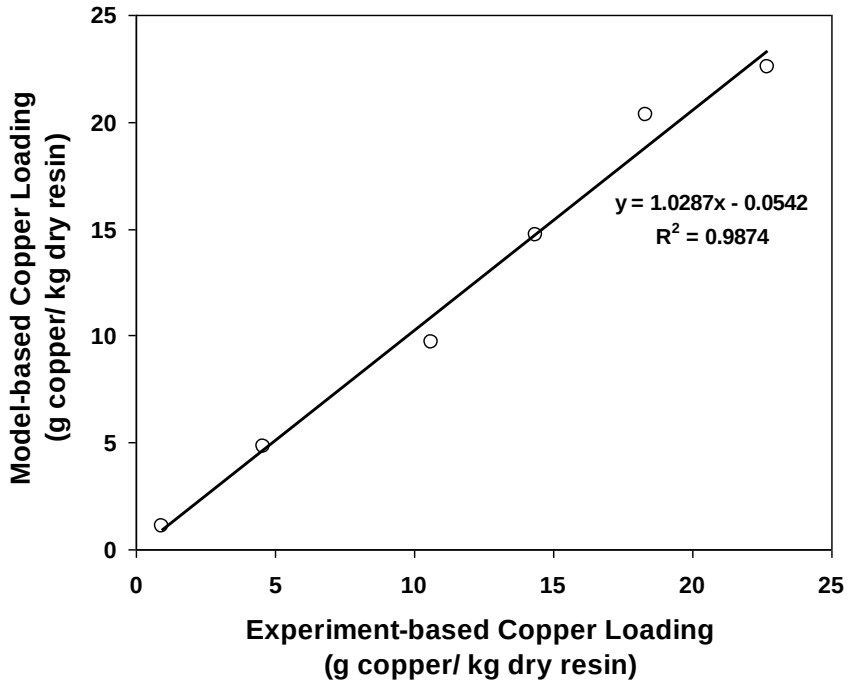

Figure 6.2 The relationship between the experiment-based and model-based total copper complexes on resin in the system without ammonia with 0-400 mM initial concentration of thiosulfate in solution

6.4.2 Model-based Equilibrium Adsorption of Copper on Resin by Ammonia Concentration and Solution pH

Re-producing Figure 5.6 in Chapter 5 using the data of model-based result, gives the total copper complexes adsorbed on resin for the initial thiosulfate concentrations of 20 and 100 mM with the various concentration of ammonia in solution as can be seen in Figure 6.3. The effects of ammonia concentration at the various initial thiosulfate concentrations are obviously shown on the results which are the same effect as shown by the experimental results discussed in Chapter 5.

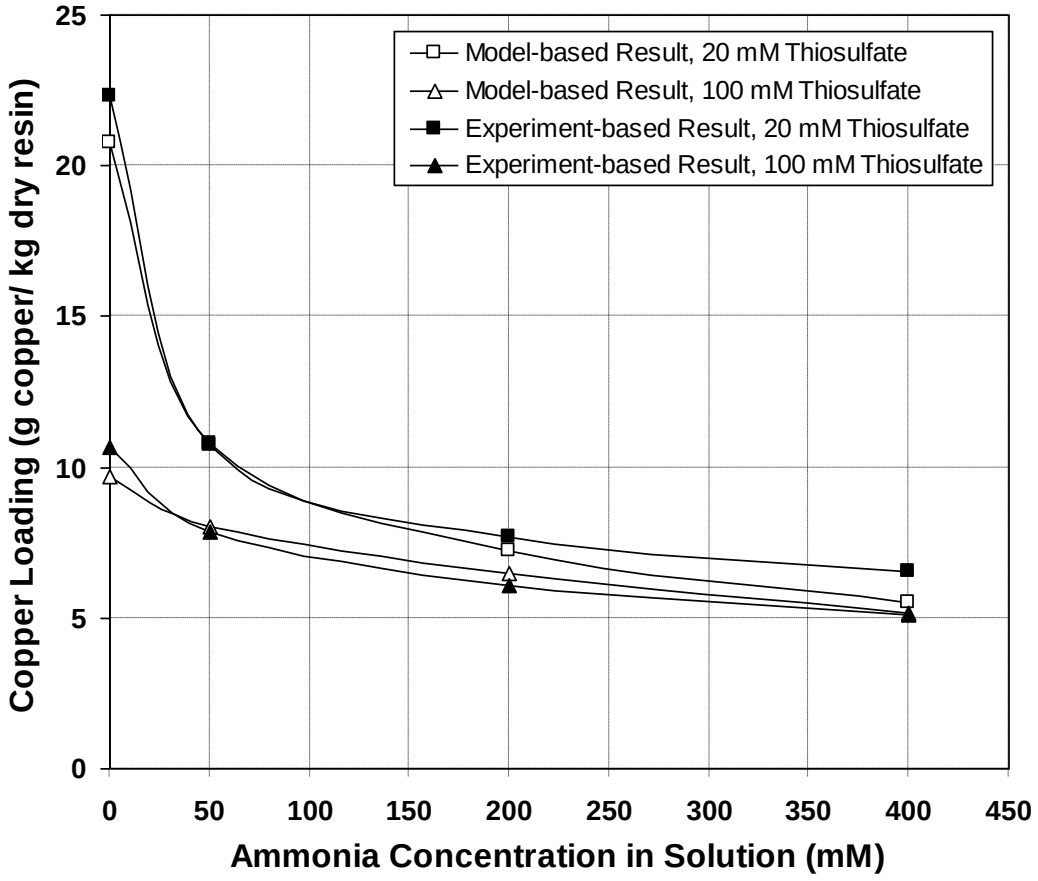

Figure 6.3 Model-based copper concentrations on resin over initial concentration of ammonia in solution with various thiosulfate concentrations

The profile of total copper complexes adsorbed on resin over the solution pH is shown in Figure 6.4. The total copper complexes adsorbed on resin with the initial concentration of thiosulfate being 100 mM is typically the same as the one by experiment, especially at the solution pH of 9.04, 9.65 and 9.97. It is a bit different at the solution pH of 7.74, which is approximately 9.661 g copper/kg dry resin being 9.244 % less than the one by experiment. Meanwhile, it is approximately 20.783 g copper/kg dry resin for the initial concentration of thiosulfate of 20 mM which is a bit less than the measured value of 22.322 g copper/kg dry resin. It is approximately 5.521 and 6.552 g copper/kg dry resin at the solution pH of 9.97.

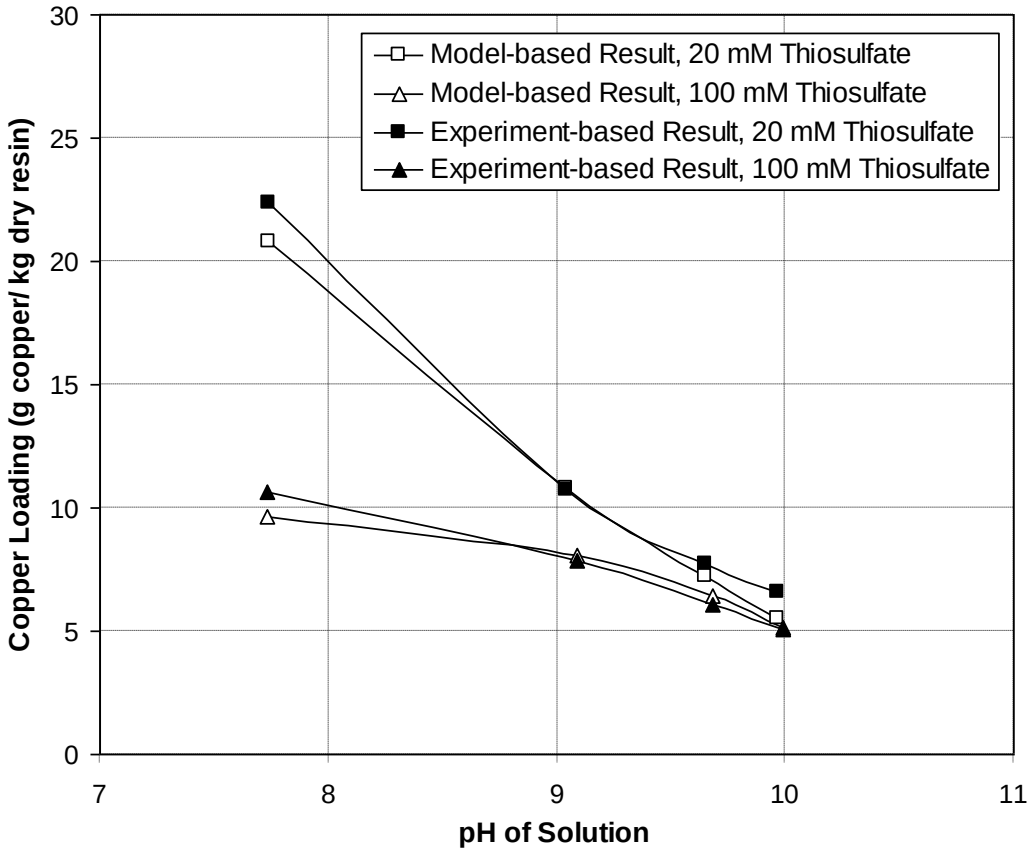

Figure 6.4 Model-based copper concentrations on resin over solution pH with various thiosulfate concentrations

Overall, model-based adsorption of total copper complexes is therefore in good agreement with the ones based on measurement where the correlation coefficient, R^2 between the model-based result and the experimental-based result is approximately 0.998.

6.4.3 Model-based Adsorption Isotherm of Copper in Multiple Components Resin-Solution Systems

Re-producing Figure 5.8 using the modelling data, gives the model-based adsorption isotherm of total copper complexes in the multiple components resin-solution system as can be seen in Figure 6.5. The same conditions are applied in the modelling result with linear fitting of Yd = -694.9x + 84084, such as the ammonia concentration being in the range of 50-400 mM and the thiosulfate concentration being in the range of 6.932-85.841 mM. The correlation coefficient, R^2 between model and experiment-based results in the system with the addition of ammonia is approximately 0.966. Meanwhile when there is no ammonia applied the system for the adsorption isotherm of total copper complexes on resin shown by the top plots of the equation Yb = -493.89x + 67810, the equilibrium concentration of thiosulfate in solution is also in the range of 9.016-143.073 mM. It gives the better correlation coefficient, R^2 between model and experiment-based results which is approximately 0.998. As expected, non-ammoniacal resin-solution (NARS) system also gives much better adsorption isotherm of copper on resin as clearly shown in Figure 6.5.

The equilibrium constants associated with Equations (6.9)-(6.13); K_1, K_2, K_3 K_4 and K_5 are obtained which is approximately 1.00E+02, 1.06E+00, 1.00E-08, 1.51E+00, 4.57E-05 and 9.50E+01, respectively.

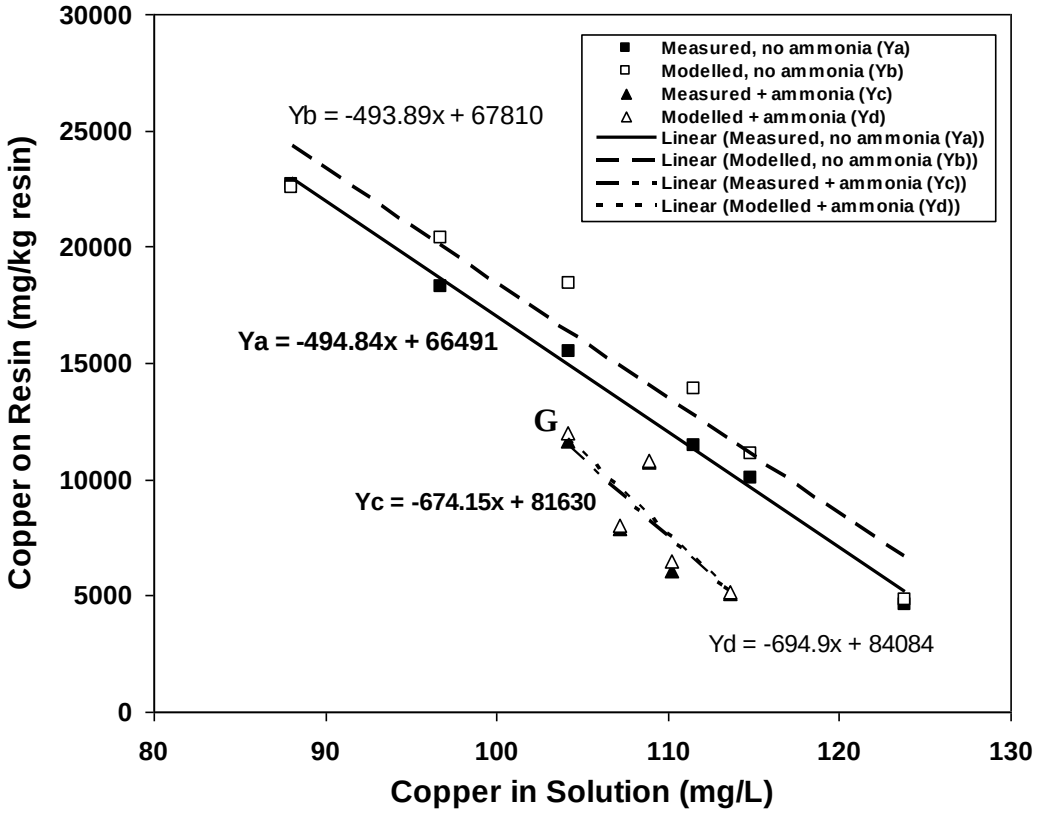

Figure 6.5 Adsorption isotherm of copper onto resin based on measurement and model in the system with and without the addition of ammonia solution

6.4.4 Model-based Copper Complexes Species in Multiple Components Resin-Solution Systems

The other remarkable outcome of modelling approach is the speciation of copper complexes in the multiple components resin-solution systems. Firstly, the speciation of copper complexes in the system without ammonia is shown in Figure 6.6 with the initial conditions applied were 0-400 mM thiosulfate, 5 mM sodium trithionate and 2 mM cupper(II) sulphate. The dynamic exponential trends

by both experiment-based and model-based results which are shown in Figure 6.1 could be explained by the presentation of copper complexes species on resin shown Figure 6.6 and copper complexes species in solution shown Figure 6.7. The concentration (% M) of all the species in the system without ammonia is listed in Table D.3 of Appendix D.

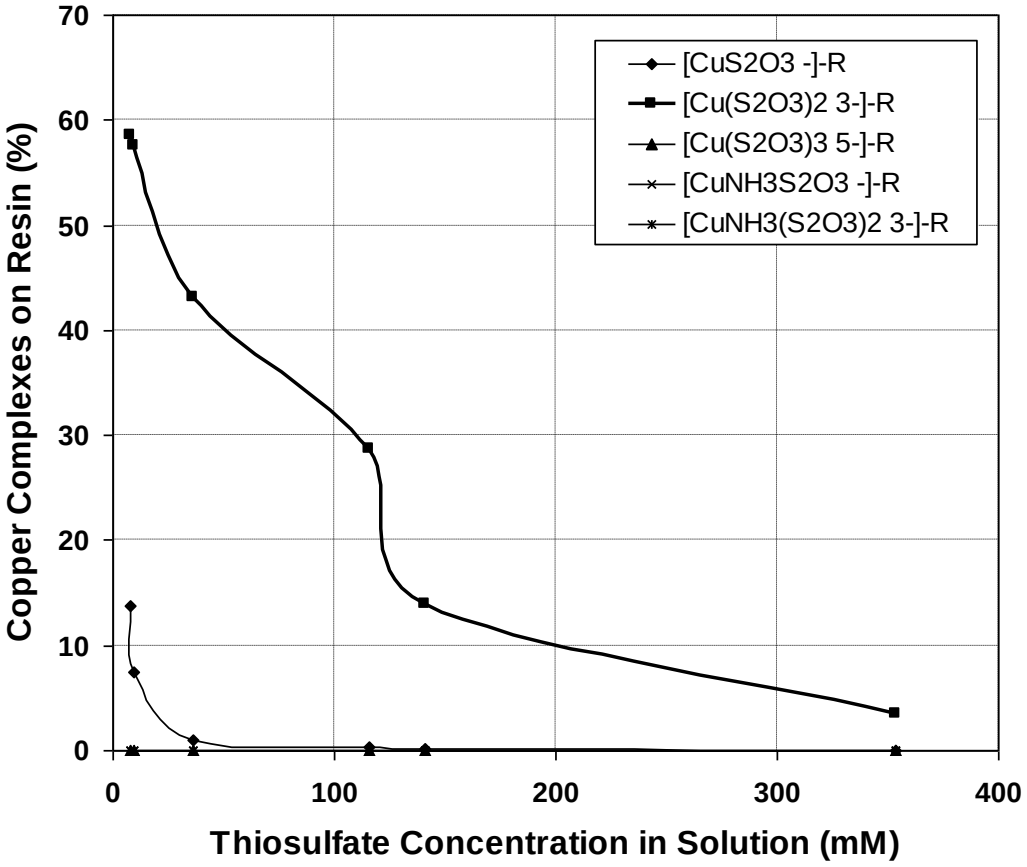

Figure 6.6 The graphical representation of model-based equilibrium concentration of copper complexes species on resin over the equilibrium concentration of thiosulfate in solution without ammonia

The result in Figure 6.6 obviously shows that $Cu(S_2O_3)_2^{3-}$ is the most dominant species of copper complexes on resin in the multiple components resin-solution system without ammonia. The trend of this species adsorbed on resin over the

equilibrium thiosulfate concentration in solution is typically the same as the model-based and measured total copper complexes adsorbed on resin shown in Figure 6.1. As viewed in Figure 6.7 and listed in Table D.3 of Appendix D, it could be noticed that the percentage of copper complex species of $Cu(S_2O_3)_2^{3-}$ in solution is in a considerable range which is approximately 11.194-3.596 % from the increase in the equilibrium thiosulfate concentration in solution at the range of approximately 7.607-116.115 mM.

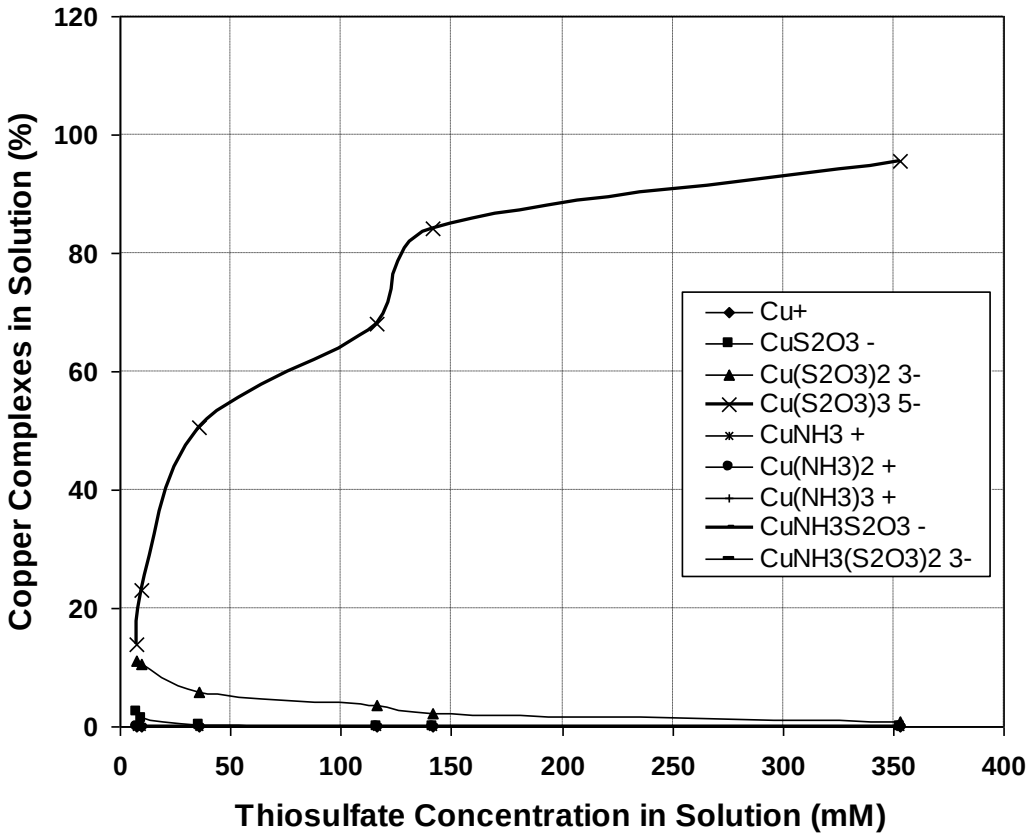

Figure 6.7 The graphical representation of model-based equilibrium concentration of copper complexes species in solution over the equilibrium concentration of thiosulfate in solution without ammonia

Increasing the equilibrium thiosulfate concentration in solution from approximately 116.114 mM to 141.300 mM results in an increase of the

concentration of copper complex species $Cu(S_2O_3)_3^{5-}$ in solution (see Figure 6.7 and Table D.3 of Appendix) which is the reactant of the equilibrium reaction of Equation (6.11). As the consequence, copper complexes species $Cu(S_2O_3)_2^{3-}$ on resin (see Figure 6.6) proportionally decreases from 28.719 % to 13.931 % with the increasing thiosulfate concentration in solution from approximately 116.114 mM to 141.300 mM, respectively.

Not surprisingly, the equilibrium concentration of copper complexes in solution at equilibrium can be specified. As a result shown in Figure 6.8 and Table D.4 of Appendix wherein the initial condition was applied; 20 mM thiosulfate, 5 mM sodium trithionate and 2 mM cupper(II) sulphate, 0-400 mM ammonia, the most dominant species of copper complexes species in solution is $CuNH_3S_2O_3^-$. The copper complex species $CuNH_3S_2O_3^-$ in solution sharply increases from approximately 2.851 % to 34.499 % for the increase of ammonia concentration in solution from 0 mM to 50 mM, respectively. Then, it gradually increase from approximately 34.499 % to 51.697 % for the same increase of ammonia concentration in solution from 50 mM to 400 mM, respectively. The second dominant copper complex species in solution is $CuNH_3(S_2O_3)_2^{3-}$, the species also gradually increase from approximately 12.707 % to 19.901 %, respectively.

Interestingly, the contradictory trends occur in the copper complexes species $Cu(S_2O_3)_3^{5-}$ and $Cu(S_2O_3)_2^{3-}$ in solution where the species in the solution decrease gradually from approximately 12.378 % to 2.481 % and from about 3.685 % to 0.707 %, respectively for the increase ammonia concentration in solution from 50 mM to 400 mM, respectively (see Figure 6.8 and Table D.4 of Appendix). These indicate that introducing ammonia in the multiple components resin-solution system promotes the reaction of both species $Cu(S_2O_3)_2^{3-}$ and $Cu(S_2O_3)_3^{5-}$ with ammonia to form mixed complexes $CuNH_3S_2O_3^-$ and $CuNH_3(S_2O_3)_2^{3-}$, respectively. Moreover, increasing ammonia concentration in the solution result in increased percentages of $CuNH_3S_2O_3^-$ and $CuNH_3(S_2O_3)_2^{3-}$, and decreased percentages of $Cu(S_2O_3)_2^{3-}$ and $Cu(S_2O_3)_3^{5-}$, as revealed in Figure 6.8.

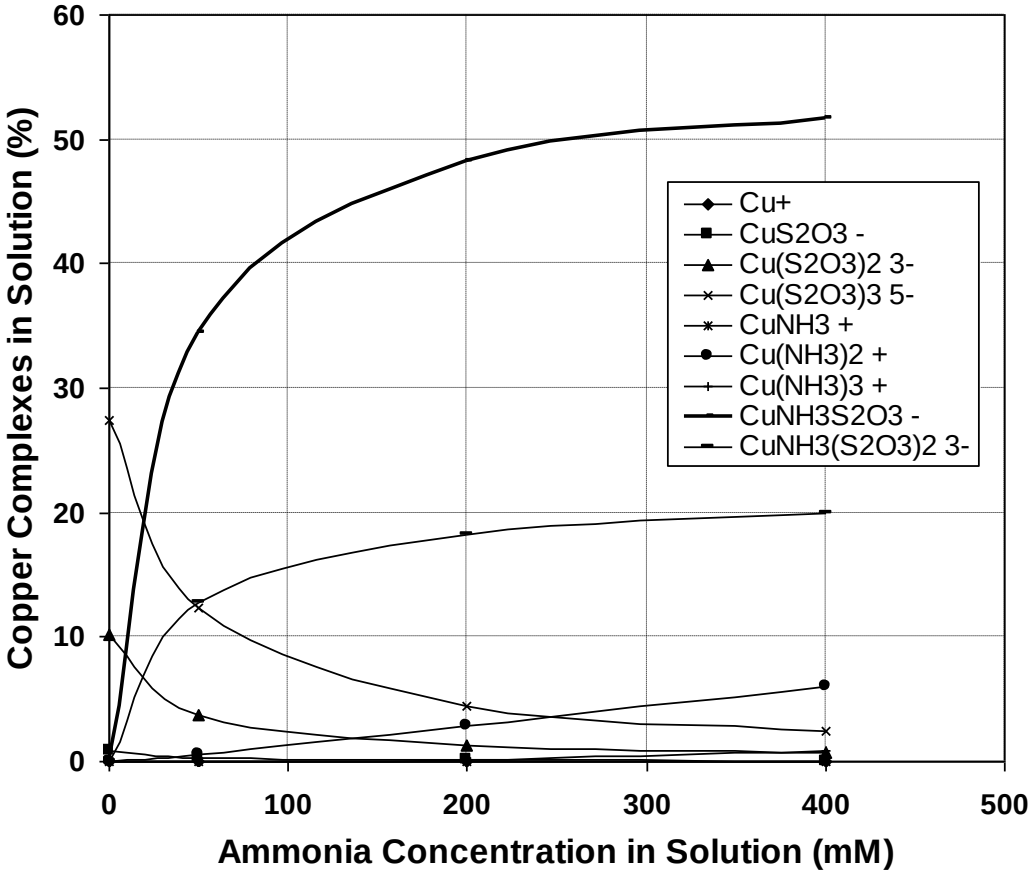

Figure 6.8 The graphical representation of model-based equilibrium concentration of copper complexes species in solution over ammonia concentration in solution

Meanwhile, the equilibrium concentration of copper complexes on resin over the ammonia concentration in solution is shown in Figure 6.9 and Table D.4 of Appendix. The most dominant species of copper complex species on resin is $Cu(S_2O_3)_2^{3-}$. The species $Cu(S_2O_3)_2^{3-}$ sharply decreases from approximately 56.573 % to 29.878 % for the increase of ammonia in solution from 0 mM to 50 mM. Then, it gradually decreases from approximately 29.9 % to 11.2 % for an increase in ammonia concentration in solution from 50 mM to 400 mM, respectively. The second dominant copper complex on resin is $CuNH_3S_2O_3^-$, and the species gradually increase from approximately 3.39 % to 6.34 %, respectively

(see Figure 6.9). Interestingly, the total percentage of copper complexes adsorbed on resin for the concentration ammonia being 0 mM, 50 mM, 200 mM, and 400 mM in the system is approximately 61.559 %, 35.191 %, 23.799 % and 17.945 %, respectively, and the total percentage of copper complexes in the solution for the concentration ammonia being 0 mM, 50 mM, 200 mM, and 400 mM is approximately 38.402 %, 64.087 %, 75.404 % and 81.699 %, respectively. These percentages give the sum of related species in the system of 99.962 %, 99.278 %, 99.203 % and 99.644 %, respectively which demonstrate that there is almost no copper lost during the leaching and adsorption processes.

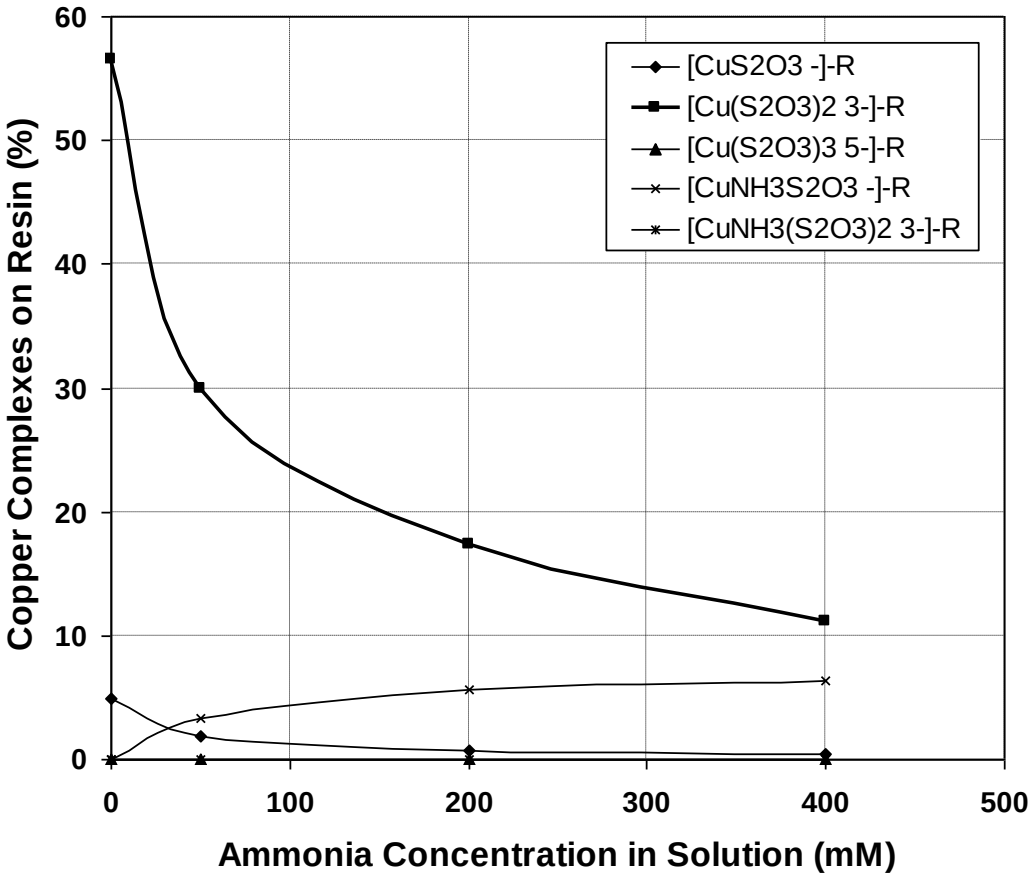

Figure 6.9 The graphical representation of model-based equilibrium concentration of copper complexes species on resin over ammonia concentration in solution

6.5 Conclusions

To model the copper complexes in multiple components resin-solution systems, a numerical method of multi-dimensional Newton-Raphson was utilised. Dynamic exponentially decrease of model-based total copper complexes adsorbed on resin with the increase of thiosulfate concentration in solution was highlighted, which is supporting the results by experiments discussed in Chapter 5. These profiles are answered by the presentation of modelling results addressed in Chapter 6.

The total copper complexes on resin decrease with the increase ammonia in solution and the solution pH. The modelling results show that copper complex species $Cu(S_2O_3)_2^{3-}$ is the most dominant species on resin, and copper complex species $Cu(S_2O_3)_3^{5}$ is the most dominant species in solution in the system without ammonia.

In the system with ammonia, copper complex species $Cu(S_2O_3)_2^{3-}$ is also the most dominant species on resin, and copper complex species $CuNH_3S_2O_3^{-}$ is the most dominant species in solution. Overall, the proposed reaction mechanism could be used to present the copper complexes in the systems.

All the model-based results are in good agreements with the ones by experiments with the average correlation coefficient, R^2 being 0.993. The equilibrium constants are summarised in Table 6.1:

Table 6.1 The proposed equilibrium reactions and the equilibrium constants in the multiple components resin-solution system of copper complexes

Equilibrium Reactions	Equilibrium Constants
$CuS_2O_3^-{}_{(aq)} + 1/2R_2S_3O_{6(s)} <=> RCuS_2O_{3(s)} + 1/2S_3O_6^{2-}{}_{(aq)}$	1.00E+02
$Cu(S_2O_3)_2^{3-}{}_{(aq)} + 3/2R_2S_3O_{6(s)} <=> R_3Cu(S_2O_3)_{2(s)} + 3/2S_3O_6^{2-}{}_{(aq)}$	1.06E+00
$Cu(S_2O_3)_3^{5-}{}_{(aq)} + 5/2R_2S_3O_{6(s)} <=> R_5Cu(S_2O_3)_{3(s)} + 5/2S_3O_6^{2-}{}_{(aq)}$	1.00E-08
$CuNH_3S_2O_3^-{}_{(aq)} + 1/2R_2S_3O_{6(s)} <=> RCuNH_3S_2O_{3(s)} + 1/2S_3O_6^{2-}{}_{(aq)}$	1.51E+00
$CuNH_3(S_2O_3)_2^{3-}{}_{(aq)} + 3/2R_2S_3O_{6(s)} <=> R_3CuNH_3(S_2O_3)_{2(s)} + 3/2S_3O_6^{2-}{}_{(aq)}$	4.57E-05

CHAPTER 7

Modelling Adsorption of Thiosulfate, Polythionates and Gold Thiosulfate in Non-Ammoniacal Resin-Solution Systems

7.1 Introduction

Cyanide has been used as a leach reagent at gold mining industries since its value as a leach reagent for gold ore treatment was firstly recognized by John Stewart MacArthur in 1880 and then patented in 1888. The cyanidation process relies on the fact that gold dissolves in aerated cyanide solution to produce the gold cyanide complex. It has been the most important extraction process for gold and silver for over 100 years (MacArthur, 1988, Marsden and House, 1992, Logsdon et al., 1999, Young, 2001).

In fact, the affinity of gold thiosulfate complex for carbon is less than the affinity of gold cyanide ion for carbon (Kononova et al., 2001), which would contribute to the poor capacity of carbon adsorbents for gold thiosulfate. Ion-exchange resins have abundant functional groups of like charge which concentrate the thiosulfate complex of opposite charge (counter-ions) and activated carbon adsorbs the aurocyanide ions between optimally spaced uncharged graphitic layers of the matrix (Grosse et al., 2003). Commercial anion exchange resins for the recovery of gold from thiosulfate leach liquors and pulps was evaluated, the result showed that anion exchange resins are more effective than carbon for the recovery of gold thiosulfate complex (Nicol and O'Malley, 2002).

Lagergren model (Lagergren, 1989, Vázquez et al., 2007) and Ho model (Ho et al., 1996) are commonly employed to present adsorption kinetics and to obtain the rate constant based on experimental data. Freundlich model is normally used to present the over-all adsorption capacity and intensity (Faust and Aly, 1998) based

on experimental data. Moreover, the equilibrium concentration of sorbent in the models is obtained from experiment.

There is still limited study on dynamic models for kinetics and equilibrium adsorption of thiosulfate, polythionates and gold in the leaching of gold using thiosulfate reagent particularly in non-ammoniacal resin-solution (NARS) systems. Therefore, the main objective of this study is to model the adsorption of thiosulfate, polythionates and gold thiosulfate in multiple components NARS systems. The specific objectives of the work are:

a. To develop dynamic models for kinetics and equilibrium adsorption of thiosulfate, polythionates, gold thiosulfate in the NARS systems.

b. To predict the amount of species adsorbed on resin over time and at the equilibrium in the NARS systems.

c. To obtain the kinetics constant for the adsorption of each species adsorbed on resin and to obtain the overall adsorption capacity and intensity based on the modelling in the NARS systems.

7.2 Modelling Approach

The adsorption kinetics of an ion exchange reaction could be similar with homogeneous chemical reaction with the assumption that all the available exchange sites are in contact with the solution over time. Therefore the rate of thiosulfate, polythionates and gold adsorbed on resin in the batch NARS system is proportional to thiosulfate, polythionates and gold lost in the solution, and it can be expressed as:

$$\frac{d}{dt} X_R(t) = k \frac{X_S(t) - X_S(\infty)\ V_S}{V_R} \tag{7.1}$$

where,

k = the rate constant of species adsorbed on resin (s^{-1})

t = the adsorption time (s)

V_R = the resin volume (L)

V_S = the solution volume (L)

$X_R(t)$ = the species concentration on resins at time t (M)

$X_S(t)$ = the species concentration in solution at time t (M)

$X_S(\infty)$ = the species concentration in solution at the equilibrium condition (M)

Meanwhile the overall mass balance of species is:

$$V_R X_R(t) + V_S X_S(t) = V_S X_S(0) \tag{7.2}$$

Substituting Equation (7.2) into Equation (7.1), factoring k, and simplifying give the equations below:

$$\frac{d}{dt}X_R(t) = k\ -X_R(t) + \delta \tag{7.3}$$

where

$$\delta = \left(\frac{X_S(0)}{V_R} - \frac{X_S(\infty)}{V_R} \right) V_S \tag{7.3a}$$

Integrating Equation (7.3) results:

$$X_R(t) = \delta - Ce^{-kt} \tag{7.4}$$

where C is an integration constant. When $t = 0$, $C = \delta$, then the concentration of species adsorbed over time could be predicted using Equation (7.5):

$$X_R(t) = \delta\ \ 1 - e^{-kt} \tag{7.5}$$

The adsorption of species on resin at time t, $Q(t)$ (g/kg) can be expressed as Equation (7.6):

$$Q(t) = \frac{X_S(0) - X_S(\infty)}{\dfrac{m_R}{V_S MW\ \ 1 - e^{-kt}}} \tag{7.6}$$

where m_R represents the mass of dry resin (g) and MW is the molecular weight of species (g mol^{-1}). Since Equations (7.5) and (7.6) consist of the equilibrium constant of species, $X_S(\infty)$ is needed to derive a model, so that the concentration of species adsorbed on resin could be predicted at any time before reaching the equilibrium condition. Because $X_S(\infty)$ also represents the concentration of

species in the solution, the species concentration on resins at any time *t*, $X_S(t)$ is required. Substituting Equation (7.5) into Equation (7.2) for $X_R(t)$, gives:

$$X_s(t) = X_S(0) - X_S(\infty)\ e^{-kt} + X_S(\infty) \tag{7.7}$$

While the species concentration at the time *t* such as the adsorption equilibrium condition is being reached, $X_s(t)$ value is equal to $X_S(\infty)$ value. In modelling the equilibrium concentration of species, the deviation between $X_s(0)$ and $X_S(\infty)$ values denoted as AE is consequently applied and give the mathematical expression as below:

$$X_S(\infty) = \frac{\left| X_S(0)e^{-kt_e} - AEe^{-kt_e} \right|}{e^{-kt_e}} \tag{7.8}$$

where t_e (s) is the time when the adsorption equilibrium condition is being reached, which can be obtained from the batch test. The AE value is obtained from the experimental and simulated results of batch experiments. The absolute value is needed to take into account in Equation (7.8) because AE can be represented as $X_s(0) - X_s(\infty)$ or $X_s(\infty) - X_s(0)$, and there will be a deviation between experimental-based $X_s(\infty)$ and model-based $X_s(\infty)$. Substituting Equation (7.8) into Equation (7.6) results:

$$Q(t) = \frac{\left(X_S(0) - \dfrac{\left| X_S(0)e^{-kt_e} - AEe^{-kt_e} \right|}{e^{-kt_e}} \right)}{\dfrac{m_R}{V_S MW\ \ 1 - e^{-kt}}} \tag{7.9}$$

Then, the equilibrium exchange relationship between the liquid and solid phases can be represented by:

$$Q_e = \frac{\left(X_S(0) - \frac{\left| X_S(0)e^{-kt_e} - AEe^{-kt_e} \right|}{e^{-kt_e}} \right)}{\frac{m_R}{V_S MW \ \ 1-e^{-kt_e}}} \tag{7.10}$$

where Q_e is denoted as the adsorption of species on resin at the equilibrium time (g species/ kg dry resin). It is also worthy to model the adsorption kinetics based on the initial concentration of liquid phase, so the equilibrium concentration of species in liquid and on solid phase can be predicted before the equilibrium condition reached. In addition, manipulating the initial concentration of liquid phase is also needed when optimization and control approach are required. Hence, Equations (7.9) and (7.10) would be modified to expand the AE as a function of initial concentration of species in solution. Because resin capacity, CP_R (eq/L) is fixed in batch NARS system, the total of available charge surface sites on resin, S_R (eq) is also constant. The constant value is dependent on the resin volume, V_R (L); $S_R = CP_R V_R$. As the consequence, the AE value attains a maxima when S_R is filled by charge species, S_S (eq), and the AE trend will be:

$$AE \ \ X_S(0) \ = AE_{\max}\left(1 - e^{-\frac{X_S(0)}{C_A}}\right) \tag{7.11}$$

where C_A is denotes a correction factor, which can be obtained from experimental and model simulation; and $AE_{\max}$ is maximum AE where the value can be determined using experimental data at the maximum initial concentration of species by which it is assumed that all species in solution filled

all the available charge surface sites on resin. Instead of using $AE_{\max}$ term, M term is presented to adopt the step response of a first-order process (Seborg, Edgar et al. 2004), Equation (7.11) can be expressed as:

$$AE\ \ X_S(0)\ = M\left(1-e^{-\frac{X_S(0)}{C_A}}\right),\ X_S(0)\subseteq X_{R-S\max}(0) \qquad (7.12)$$

where M is the magnitude of the response; $M = S_S = S_R c_R /(V_S c_S)$, and $X_{R-S\max}(0)$ is the maximum concentration of species in solution based on resin calculation; $X_{R-S\max}(0) = S_S c_S / c_R$. The $c_R(e)$ is the charge on each site on resin when 1 mol of resin exchange centre being released from resin, and $c_S(e)$ corresponds to the charge of 1 mol species. When $X_S(0)$ > $X_{R-S\max}(0)$, Equation (7.12) becomes:

$$AE\ \ X_S(0)\ = M\left(1-e^{-\frac{X_{R-S\max}(0)}{C_A}}\right) \qquad (7.13)$$

To compare the modelling result on the adsorption kinetics studies using resin and species adsorbed on resin, the Lagergren equation (Lagergren 1989; Vázquez, Rodríguez-Iglesias et al. 2007) representing the pseudo-first-order model shown by Equation (3.15) and Ho equation (Ho, Wase et al. 1996) as the pseudo-second-order model shown by Equation (3.16) shown in Chapter 3 are taken into account. The Langmuir equation (Langmuir, 1916) and Freundlich equation (Weber, 1972) are also taken into account to address the adsorption capacity of resin and the adsorption intensity of species based on modelling. The modelling results are compared to the experimental result worked out using Equations (3.19) and (3.20) shown in Chapter 3.

7.3 Experimental Data

In order to obtain the kinetics rate constants for the adsorption of thiosulfate, trithonate, tetrathionate and gold thiosulfate adsorbed on resin in the NARS system, the proposed models are simulated with a wide range of the concentration of species. A set of experimental data with a wide range of the concentration of species are also used. Therefore, the experimental results for the kinetics and equilibrium isotherm adsorption of thiosulfate, trithionate, tetrathionate and gold thiosulfate presented in Chapter 3 were taken into account. To minimize the sum of weighted deviation square between the modelling results and experimental result, Levenberg-Marquardt method (Williams et al., 2002) was applied.

7.4 Results and Discussions

The commercial strong based anion exchange resin of Purolite A500/2788 is used in the experimental work and modelling (PUROLITE, 2008). The exchange centre of the resin is the chloride electron. The resin (0.333 g wet) used in the experiments and modelling has parameters as listed in Table 7.1. As can be seen in Table 7.1, m_R value based on experiment is varied but it is still acceptable and much closed to the model-based value. For instance, experiment-based m_R are approximately 0.2004, 0.2003, 0.1993, 0.2006 and 0.1998 g for the 5 batches.

Table 7.1 Resin parameters for experiments and modelling

Parameter	Experiments	Modelling
CP_R (eq/L)	1.3	1.3
$c_R(e)$	-1	-1
m_R (g)	~ 0.2	0.2
V_R (L)	~ 0.0005	0.0005
S_R (eq)	~ 0.65	0.65

In order to obtain the kinetics rate constant for the adsorption of each species adsorbed on resin in the NARS system, the proposed models of Equations (7.9) and (7.12) with C_A being 1 are simulated. Unlike the Lagergren and Ho equations, the equilibrium concentration of species on resin is not required in obtaining the kinetics rate constant using the proposed model. To minimize the sum of weighted deviation square between the experimental results and model

results Levenberg-Marquardt method (Williams et al. 2002) was applied, and the function can be written as Equation (7.14):

$$WD_M = \sum_{t=0}^{300} \left[Q_{Exp.t} - Q_M (k_M, t) \right]^2 \tag{7.14}$$

where WD_M are the sum of weighted deviation square between the experimental results and model results associated with the proposed (Muslim) model; WD_M is minimized, so that $WD_M \geq 0$ is subjected to the Muslim model-based kinetic rate constant of $k_M > 0$; and $Q_{Exp.t}$ (g species/ kg dry resin) is the species loading at the loading time *t* (minute) based on the experimental data.

7.4.1 Model-based Kinetics Adsorption of Thiosulfate, Polythionates and Gold Thiosulfate

Figure 7.1 shows the results plotted based on the experiment, Lagergren, Ho and Muslim on the kinetics adsorption of thiosulfate in the NARS system with the initial concentration of thiosulfate in solution being 3 mM and 0.333 g resin. As can be seen by the dot plot in Figure 7.1, thiosulfate concentration on resin sharply increases from 0 to 140.136 g thiosulfate/ kg dry resin for the first 30 minutes of loading time. It is approximately 138,739 133.785 and 144.825 g thiosulfate/ kg dry resin based on Muslim, Lagergren and Ho models at 30 minutes of loading time. Then, it slowly increases with time following first-order model until reaching the equilibrium which is approximately 168.317, 168.297, and 168.317 and 165.629 g thiosulfate/ kg dry resin based on the experiment, Muslim, Lagergren and Ho models, respectively at 300 minutes of loading time.

The Muslim model-based rate constants of thiosulfate adsorption, k_M is approximately 0.0579 minute^{-1} which is almost the same as the one by Lagergren (see the k_L value highlighted in Chapter 3). There is a very good agreement between the experimental result and Muslim model-based result with the correlation coefficients, R^2 of approximately 0.998.

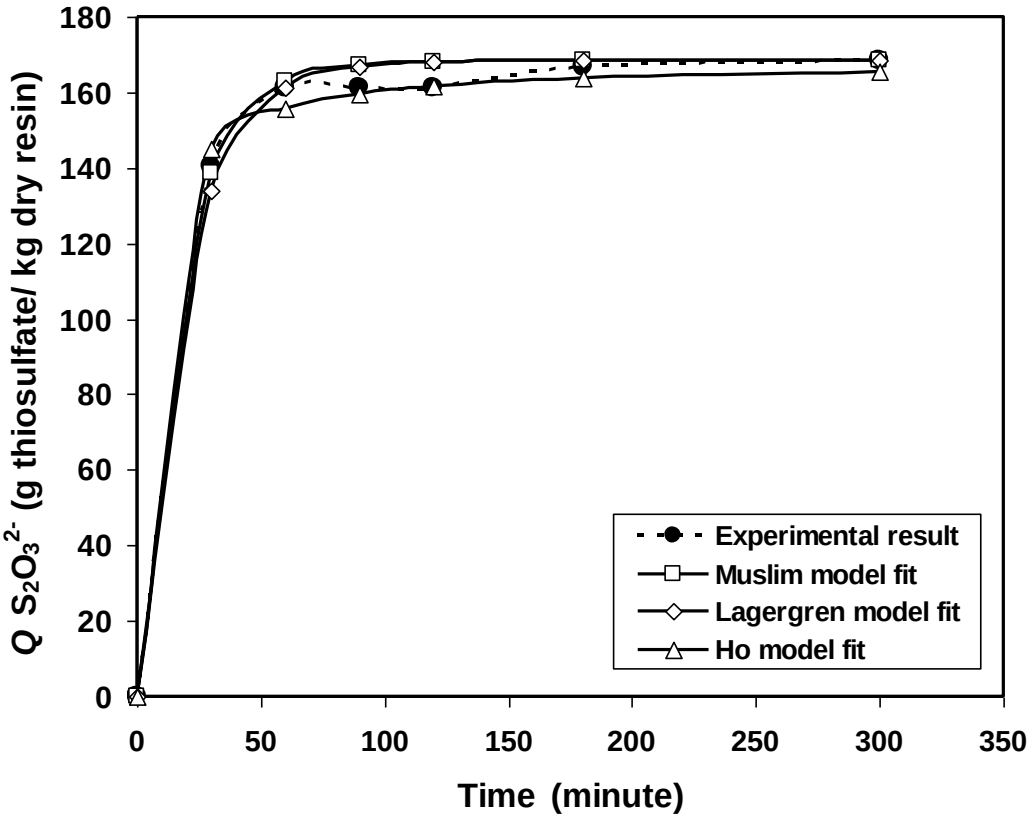

Figure 7.1 Kinetics adsorption of thiosulfate based on experiment, Lagergrne, Ho and Muslim models

The profile of trithionate adsorbed on resin versus the loading time in the NARS system with the initial concentration of trithionate in solution being 3 mM and 0.333 g resin, is shown in Figure 7.2. The Muslim model-based rate constant of trithionate adsorption, k_M is approximately 0.0359 minute^{-1}, and it is

approximately 0.0304 and 0.0007 minute^{-1} based on Lagregren and Ho models (the value of k_L and k_H written in Chapter 3). As revealed in Figure 7.2, Muslim model-based result still has the same trend with the one by experiment, Lagergren and Ho models. The equilibrium of trithionate adsorbed on resin based on Muslim model is approximately 248.078 g trithionate/ kg dry resin which lower than the others (257.950, 257.921 and 253.402 g trithionate/ kg dry resin based on experiment, Lagergren and Ho models). Muslim model-based results on trithionate adsorbed on resin has a very good agreement with the experiment-based result with the R^2 being approximately 0.996.

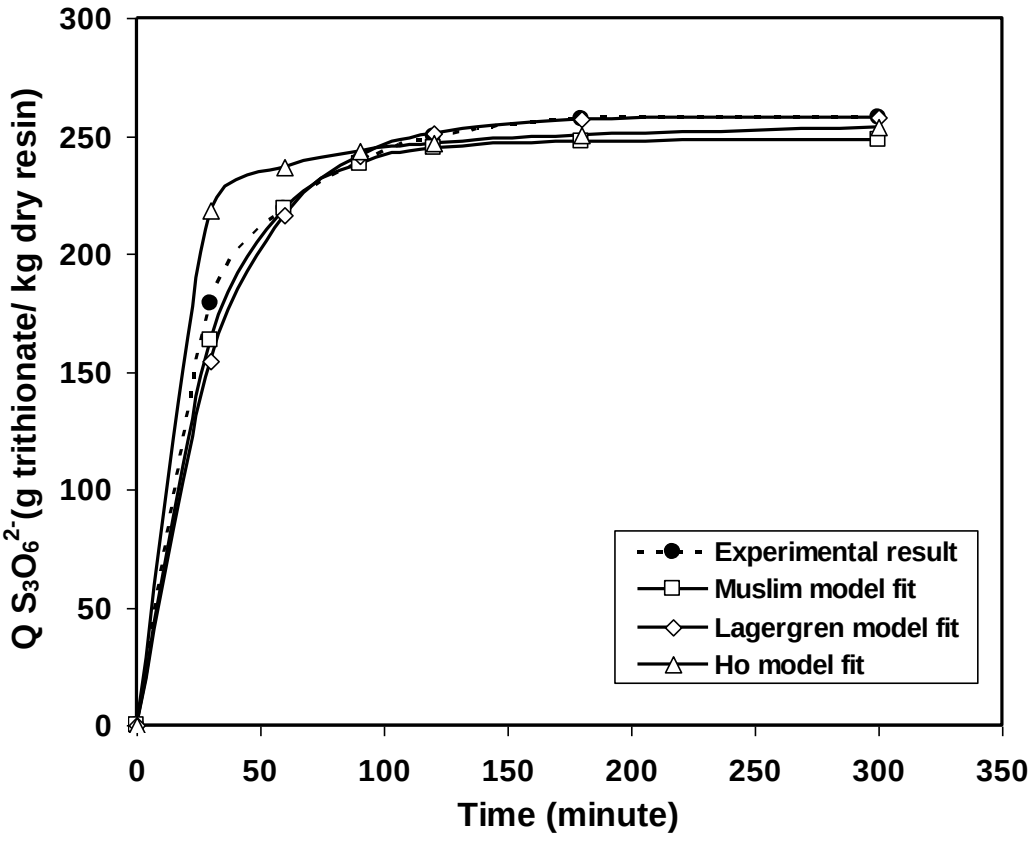

Figure 7.2 Kinetics adsorption of trithionate based on experiment, Lagergren, Ho and Muslim models

Similarly, Muslim model-based result on tetrathionate fits well with the experiment-based result as revealed in Figure 7.3, with the R^2 being approximately 0.991 which is the same value with the R^2 of Lagergren model-based result. The rate constant of tetrathionate adsorption based on Muslim, k_M is approximately 0.0199 minute^{-1} which is close to the one by Lagergren model of approximately 0.0205 minute^{-1}.

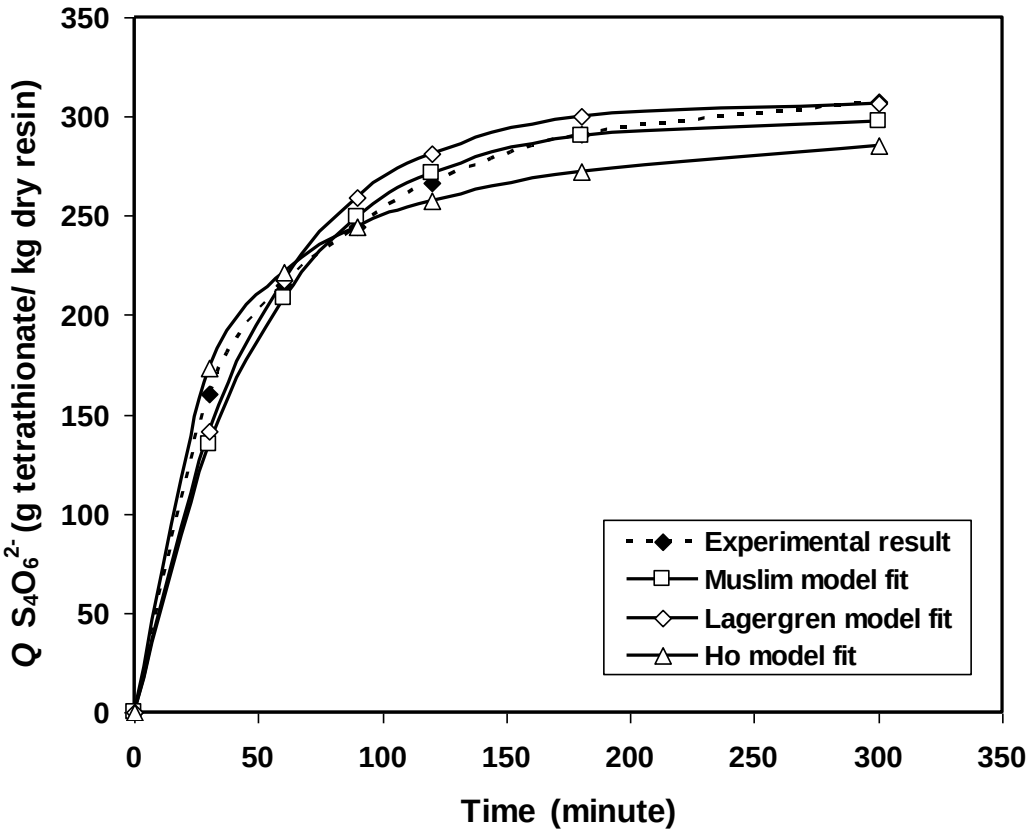

Figure 7.3 Kinetics adsorption of trithionate based on experiment, Lagergren, Ho and Muslim models

Figure 7.4 shows a very interesting profile on the NARS systems with the initial concentration of gold thiosulfate in solution being 100 mg/L and 0.333 g resin. The concentration of gold thiosulfate in solution over time based on ICP-OES

analysis is listed in Table E.1 of Appendix E. As clearly shown in Figure 7.4, both Muslim and Lagergren models results fit very well with the experiment-based result with the R^2 being approximately 0.999. As expected, the rate constant of gold thiosulfate based on Muslim model, k_M being approximately 0.0331 minute^{-1} is typically the same as the one by Lagergren model, k_L being approximately 0.0333 minute^{-1}. Meanwhile, Ho model-based result yields the R^2 being approximately 0.913 with the k_H being approximately 0.002 minute^{-1}.

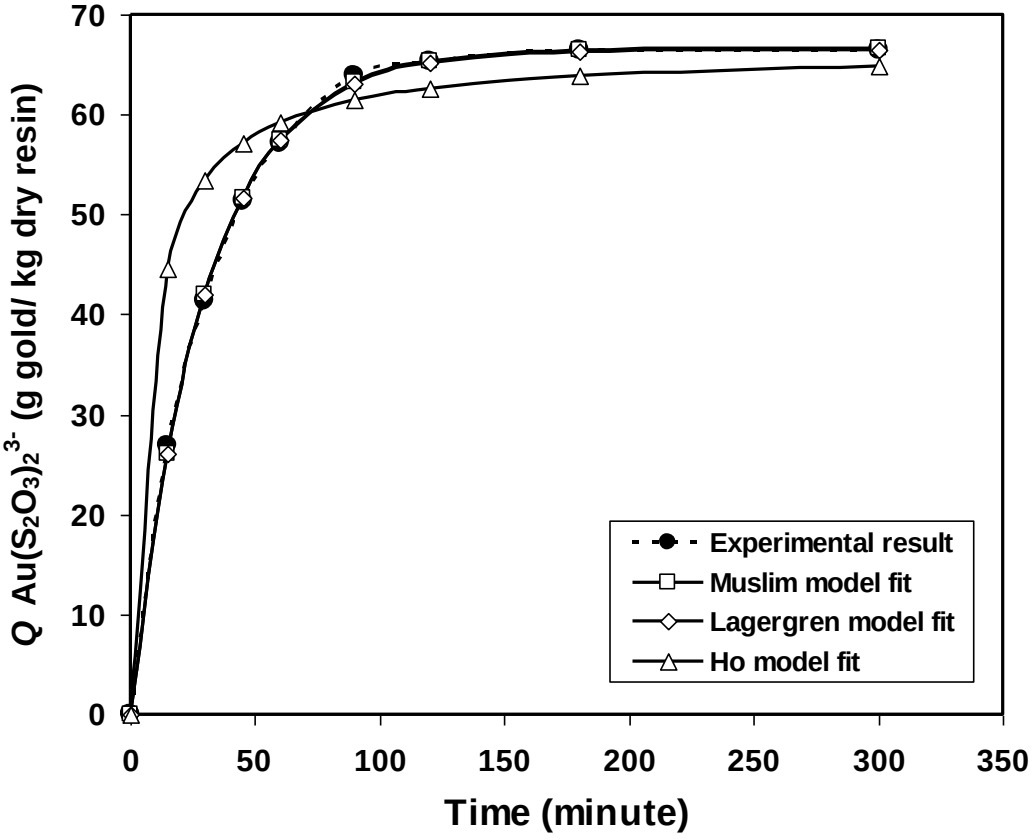

Figure 7.4 Kinetics adsorption of gold thiosulfate based on experiment, Lagergren, Ho and Muslim models

From the results and discussion on the kinetics adsorption of each species adsorbed on resin in the NARS systems, the pseudo-first-order models of Lagergren and Muslim dynamic model of kinetics adsorption is a much acceptable method to present the loading of species especially gold thiosulfate onto the strong based anion exchange resin of Purolite A500/2788.

7.4.2 Model-based Equilibrium Adsorption Isotherm for Freundlich Parameters

The initial concentrations of thiosulfate, trithionate and tetrathionate in range of 0-3 mM were applied in the experiment and modelling works of equilibrium adsorption. The equilibrium concentration of species in solution, C_e and the equilibrium concentration of species on resin, Q_e based on the experiments are shown in Table 3.5 of Chapter 3. Levenberg-Marquardt method (Williams et al. 2002) was also used to minimize the sum of weighted deviation square between the experiment-based AE and Muslim model-based AE. The function is expressed as Equation (7.15):

$$WD_{AE} = \sum_{X_S=0}^{3} \left[AE_{Exp.X_S} - AE_M(X_S, C_A) \right]^2 \tag{7.15}$$

where WD_{AE} is the sum of weighted deviation square between the experimental results and model results associated with the AE value; WD_{AE} is minimized, so that $WD_{AE} \geq 0$ subjected to the constants of $C_A > 0$; $AE_{Exp.X_S}$ and $AE_M(X_S, C_A)$ are the AE values based on experiment and Muslim model, respectively. Using the rate constant of each species in the previous results and the

Levenberg-Marquardt-based optimised C_A value for thiosulfate, trithionate and tetrathionate being 1.0081, 1.3007 and 1.2500 respectively, Freundlich isotherm of the species was worked out using Muslim models of Equations (7.8), (7.10), (7.12) and (7.13). The results are compared with the ones by experiment. Figure 7.5 shows one of the results wherein the graph slopes and intercepts presenting $1/n$ and $\ln(K_F)$, respectively associated with the Freundlich isotherm, Equation (3.20) in Chapter 3.

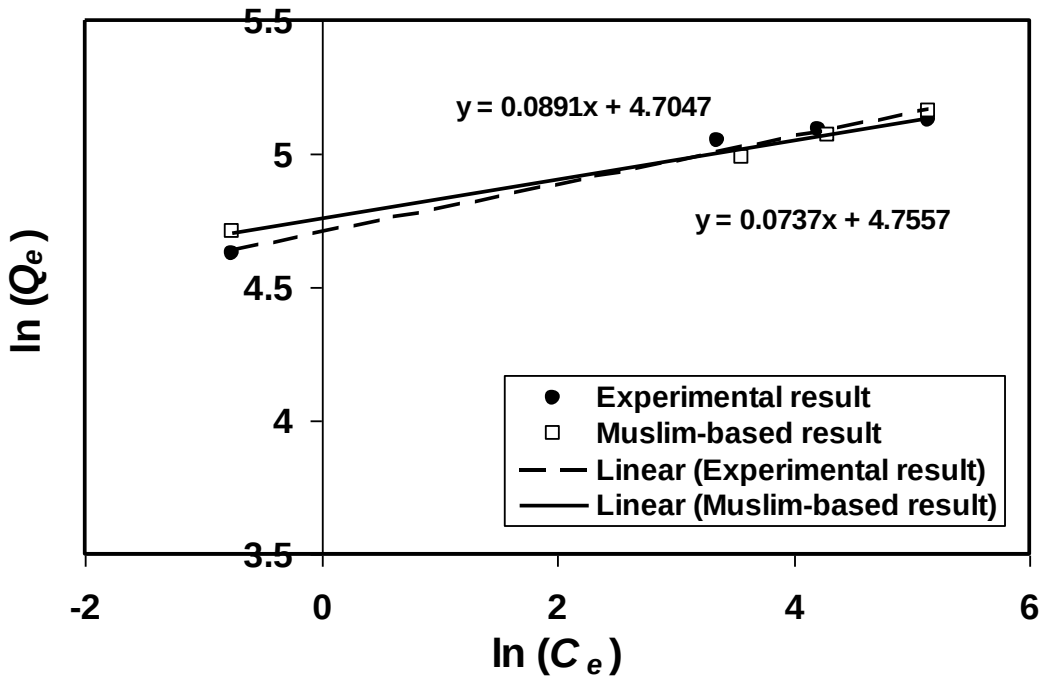

Figure 7.5 Freundlich isotherm of thiosulfate based on the experiment and Muslim model

As shown by the fitting equations in Figure 7.5 with R^2 being approximately 0.977 (experimental result) and 0.986 (Muslim model-based result), Muslim model gives a more reasonable adsorption isotherm profile compared to the one by experiment. The Freundlich over-all adsorption capacity, K_F is approximately

116.245 g thiosulfate/ kg dry resin based on Muslim model, and it is about 110.465 g thiosulfate/ kg dry resin based on the experiment. The adsorption intensity, *n* is approximately 13.568 based on Muslim model, and it is about 11.223 based on the experiment.

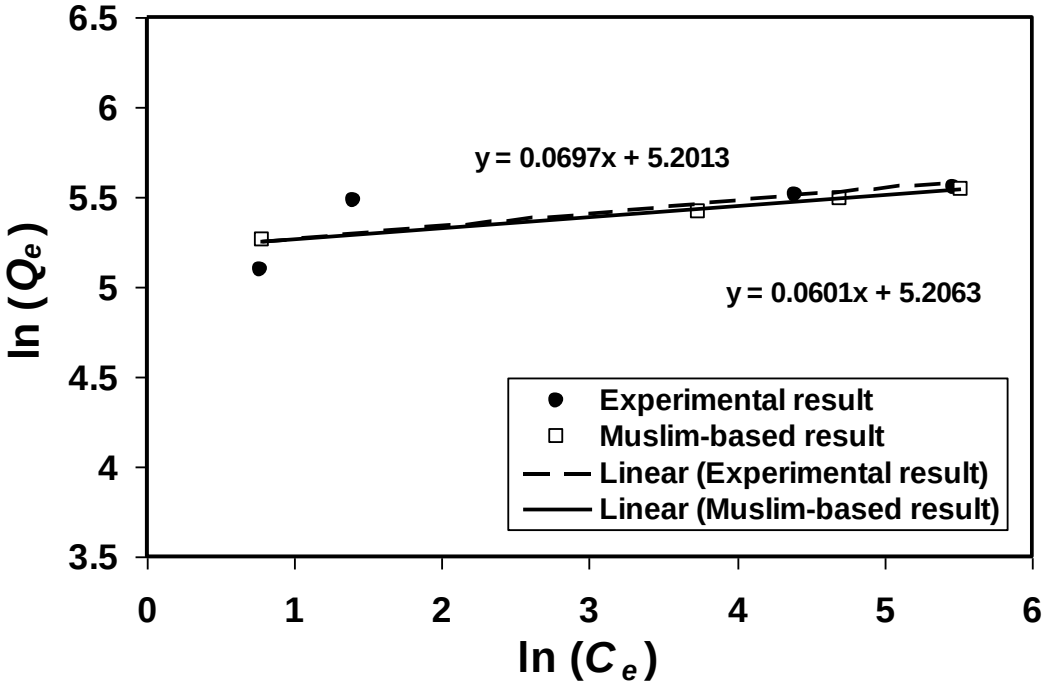

Figure 7.6 Freundlich isotherm of trithionate based on experiment and Muslim model

The K_F values for trithionate and tetrathionate which are obtained from the intercept in Figures 7.6 and 7.7, are approximately 182.418 and 204.384 g species/ kg dry resin, respectively based on Muslim model. These numbers are higher than the thiosulfate K_F. Meanwhile, the experiment-based K_F values are 181.508 and 205.449 g species/ kg dry resin, respectively which are typically the same as the ones by Muslim model. The *n* values based on Muslim model for trithionate and tetrathionate which are obtained from the slopes in Figures 7.6 and 7.7, are approximately 16.639 and 14.347, respectively.

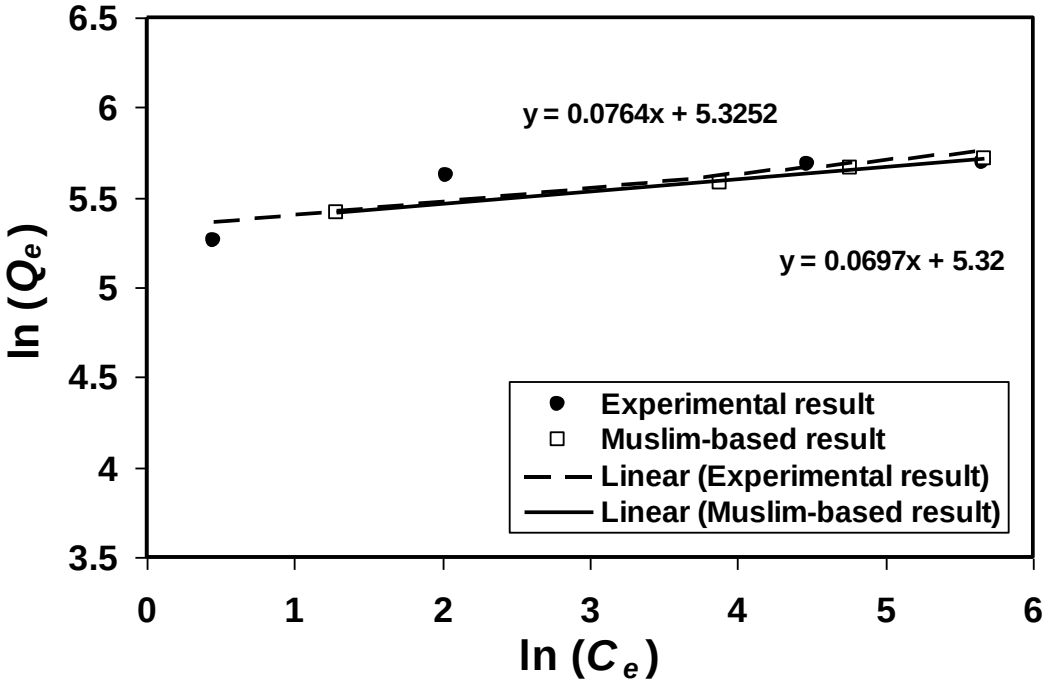

Figure 7.7 Freundlich isotherm of tetrathionate based on experiment and Muslim model

From the *n* values, it is clearly shown that trithionate is adsorbed more on the resin compared to the other species.

7.4.3 Model-based Equilibrium Adsorption Isotherm for Langmuir Parameters

As can be obtained from the slope of Langmuir fit y = 0.0057x + 0.012, the maximum amount of thiosulfate adsorbed on the resin (Q_m written in Equation (3.19)) is approximately 172.418 g thiosulfate/ kg dry resin which is 1.724 % higher than the one by the experiment of 169.492 g thiosulfate/ kg dry resin. The Muslim model-based Langmuir adsorption equilibrium constant K_L for thiosulfate

is approximately 0.483 L solution/ g thiosulfate, which is calculated from the intercept of the Langmuir fit.

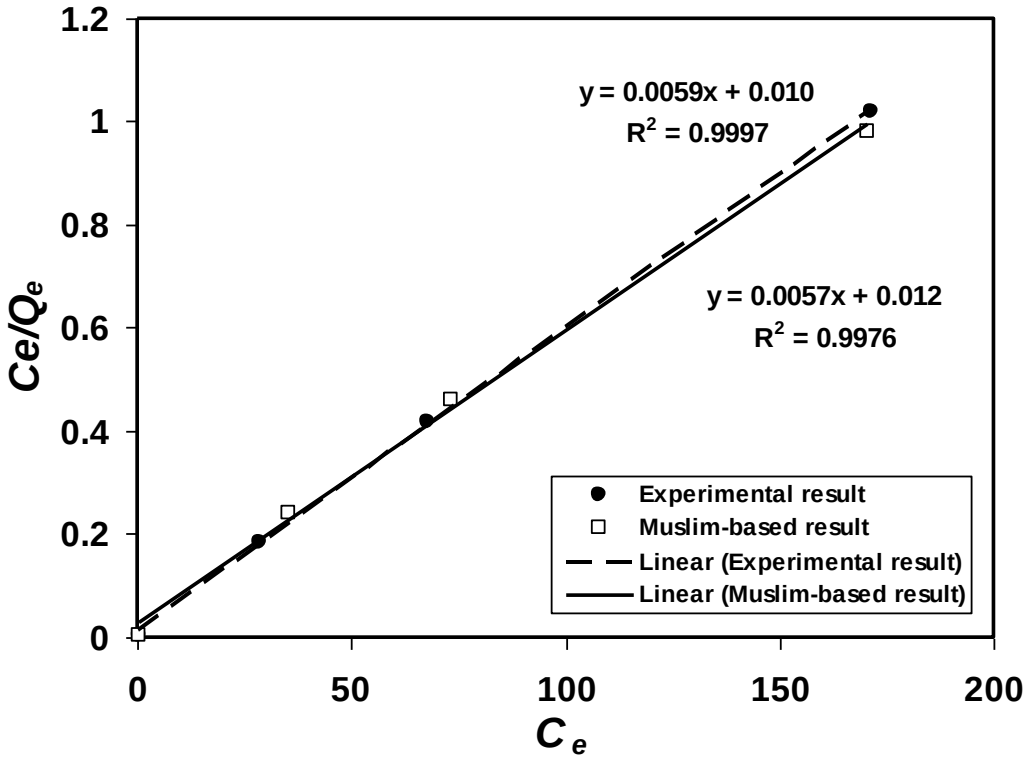

Figure 7.8 Langmuir isotherm of thiosulfate based on experiment and Muslim model

Interestingly, the slopes of Langmuir fit based on Muslim model and the experiment are the same as shown in Figure 7.9, and this results in the same maximum amount of trithionate adsorbed on resin which is approximately 256.410 g trithionate/ kg dry resin. The Muslim model-based adsorption equilibrium constant trithionate's adsorption equilibrium constant is approximately 0.619 L solution/ g trithionate, which is 11.111 % lower than the one by the experiment.

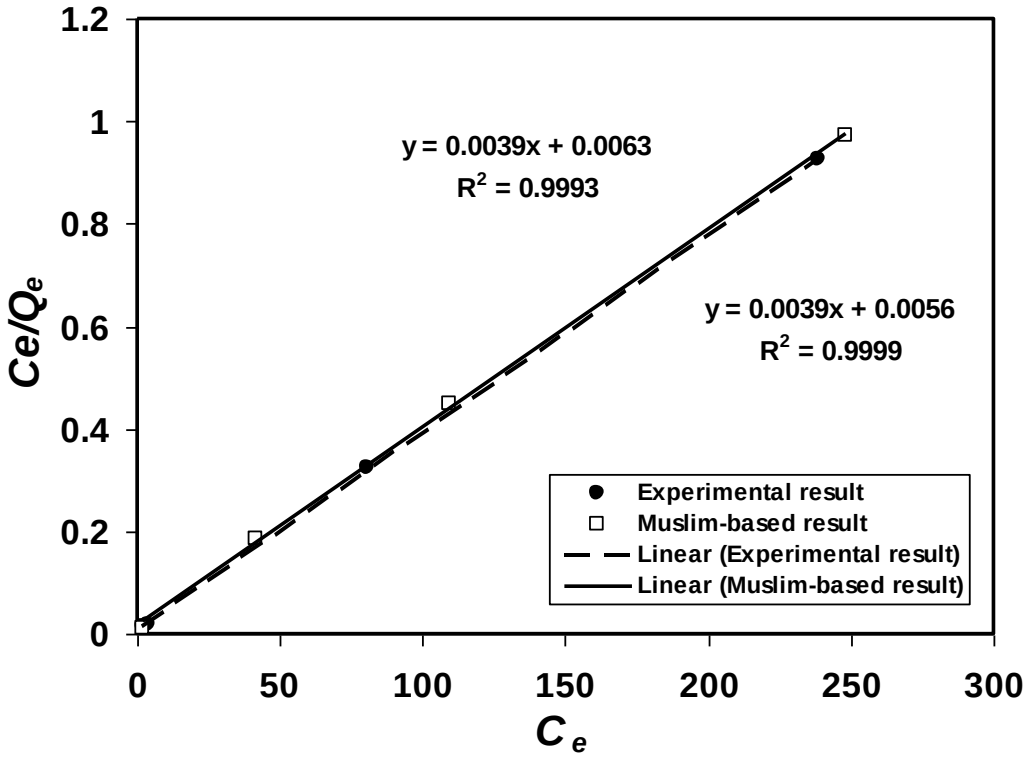

Figure 7.9 Langmuir isotherm of trithionate based on experiment and Muslim model

The Muslim model-based maximum amount of tetrathionate adsorbed on resin is approximately 303.031 g tetrathionate/ kg dry resin which 3.030 % lower than the one by experiment of 312.500 g tetrathionate/ kg dry resin. Meanwhile, the adsorption equilibrium constant for tetrathionate based on Muslim model is approximately 0.943 L solution/ g tetrathionate, obtained from the intercept of the Langmuir fit, y = 0.0032x + 0.0035 shown in Figure 7.10. As expected, the adsorption equilibrium constant for trithionate is higher than the tetrathionate's value meaning that more trithionate is adsorbed than tetrathionate and thiosulfate.

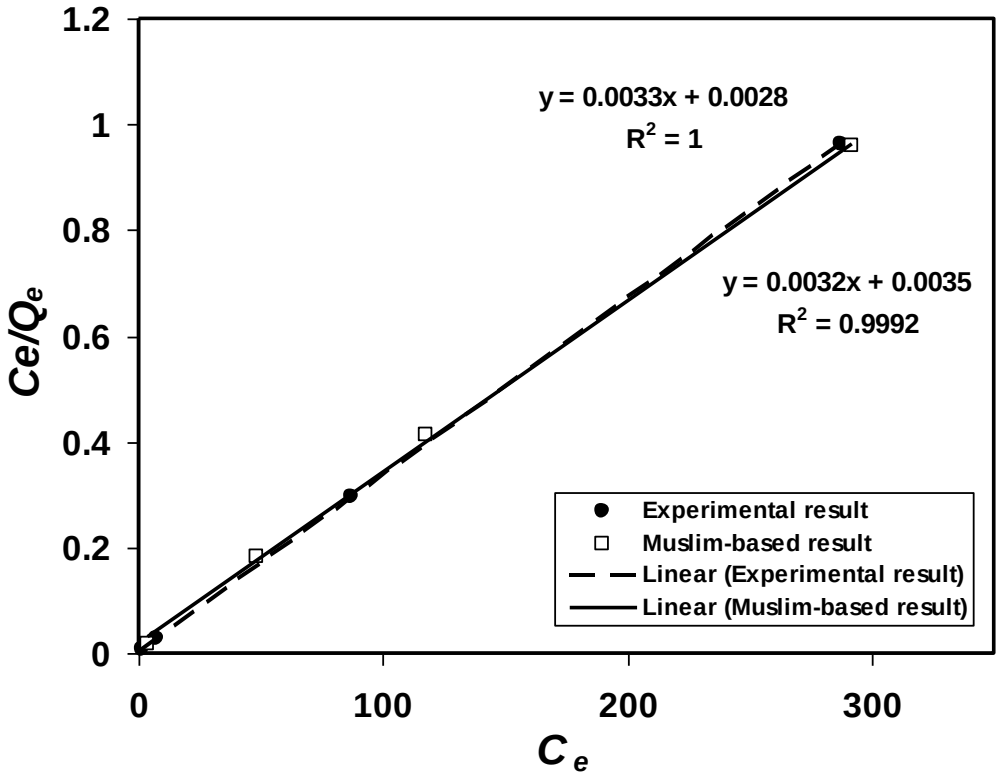

Figure 7.10 Langmuir isotherm of tetrathionate based on experiment and Muslim model

The modelling results on Freundlich and Langmuir isotherms show the reliable Muslim model to obtain the equilibrium adsorption isotherm parameters in the previous discussion. Therefore, the equilibrium isotherm adsorption parameters of Freundlich and Langmuir using Muslim model is reliable. The initial concentration of gold thiosulfate applied is in the range of 150-1000 mg/L with the Levenberg-Marquardt-based optimised C_A value being 1.3007. From the model simulation on Freundlich isotherm, the K_F value for gold thiosulfate is approximately 249.935 g gold thiosulfate/ kg dry resin with the *n* values being 13.793. Meanwhile, for the parameters of Langmuir isotherm, Q_m is approximately 322.581 g gold thiosulfate/ kg dry resin with the K_L value being 0.579 L solution/ g gold thiosulfate.

7.5 Conclusions

Dynamic models representing the adsorption kinetics and equilibrium of thiosulfate, trithionate, tetrathionate and gold thiosulfate in non-ammoniacal resin-solution (NARS) system are mechanistically developed. A set of data from the NARS experiment with commercial strong based anion exchange resin of Purolite A500/2788 are taken into account.

As a result on the proposed kinetics model, the rate constants are obtained which are 0.0579, 0.0359, 0.0199 and 0.0331 minutes^{-1} for thiosulfate, trithionate, tetrathionate and gold thiosulfate, respectively the correlation coefficient, R^2 is approximately 0.998, 0.996, 0.991 and 0.999, respectively. The results also show that Muslim dynamic model of kinetics adsorption is an acceptable method to present the loading of species especially gold thiosulfate onto the strong based anion exchange resin.

Using the rate constants and the proposed equilibrium model, parameters in the Langmuir and Freundlich equilibrium isotherms for the adsorption of thiosulfate, trithionate, tetrathionate and gold thiosulfate on resin were obtained and listed in Table 7.2.

Table 7.2. Equilibrium adsorption isotherm parameters of Langmuir and Freundlich obtained by Muslim model simulation

Species	Langmuir Fitting		Freundlich Fitting	
	Resin capacity, Q_m (g/kg)	**Equilibrium constant, K_L (L/g)**	**Resin capacity, K_F (g/kg)**	**Adsorption intensity, n**
Thiosulfate	172.418	0.483	116.245	13.568
Trithionate	256.410	0.619	182.418	16.638
Tetrathionate	303.031	0.943	204.384	14.347
Gold Thiosulfate	322.581	0.579	249.935	13.793

CHAPTER 8
Conclusions and Recommendations

8.1 Conclusions

Experimental and modelling work for gold thiosulfate leaching system have been conducted. The adsorption of thiosulfate, polythionates, gold thiosulfate and copper complexes in gold thiosulfate leaching has been investigated. The experimental procedures, speciation method, and the results highlighting the adsorption of thiosulfate, polythionates, gold thiosulfate and copper complexes on strong based anion exchange resin of Purolite A500/2788 in the resin-solution systems were systematically described with the results concisely discussed.

The reaction mechanisms describing the kinetics and equilibrium adsorption phenomena of thiosulfate, polythionates, gold thiosulfate and copper complexes are proposed with the parameters in single component and multiple components of resin-solution systems. The results for the multiple components of non-ammoniacal resin-solution (NARS) systems show that the more thiosulfate concentration in solution at equilibrium, the greater the amount of gold thiosulfate adsorbed on the resin, and the degradation of thiosulfate does not occur in the systems. Gold thiosulfate loading increases by diminishing the polythionates concentration in the solution. Increasing the trithionate concentration in solution results in the greater amount of gold thiosulfate adsorbed on the resin. Thiosulfate, polythionates and gold thiosulfate are simultaneously adsorbed on the resin and compete with one another to occupy the available charge on the resin with the proposed equilibrium constants for the gold extraction of thiosulfate leaching.

To increase the total copper complexes adsorbed on the resin in the multiple components resin-solution systems suggests, degassing the systems with nitrogen

is needed. The total copper complexes adsorbed on the resin decreases exponentially with the increase of thiosulfate concentration in solution. Increasing ammonia and the solution pH in the solution results in the decreasing of total copper complexes on the resin. The same profiles are also shown in modelling work wherein the model-based results are in good agreement with the experimental-based results. In addition, the equilibrium constants associated with the proposed reactions in the systems for copper thiosulfate complexes are also established with the most dominant copper complexes species in solution and on the resin. It is noticed that much better adsorption isotherm of copper on the resin is determined by the experimental and modelling work for the systems without the addition of ammonia solution.

The kinetics and equilibrium models are mechanistically developed in line with the reaction mechanisms, and the models are solved analytically and numerically. The common kinetics and equilibrium adsorption of Lagergren, Ho, Langmuir and Freundlich equations are also taken into account for comparison with the developed models. Consequently, the kinetics and equilibrium constants and the adsorption intensity for the gold extraction of thiosulfate leaching are established. Overall, the model based results are in good agreement with experimental and the Lagergren, Ho, Langmuir and Freundlich equations.

Finally, the investigations on the adsorption of thiosulfate, polythionates, gold thiosulfate and copper complexes in gold thiosulfate leaching highlights the prospect of non-ammoniacal resin-solution (NARS) systems in gold extraction using thiosulfate reagent for application.

8.2 Recommendations

In this thesis, the experimental and modelling work for the adsorption of thiosulfate, polythionates, gold thiosulfate and copper complexes in gold thiosulfate leaching have been done in batch systems. Small scale of volumetric flasks and vials/bottles for the loading and stripping were also used for the experiment. Therefore, it would be worthwhile to conduct the experimental work in future projects of gold thiosulfate leaching for continuous process with larger scale of typical flasks and vials/bottles to practically present continuous stirred tank reactors (CSTRs) in pilot scale.

Multiple CSTRs in series and pilot scale to be used in the experiment and modelling work of gold thiosulfate leaching are also strongly recommended for future projects to accommodate the need of Resin-in-Pulp (RIP) and Resin-in Leach (RIL) in gold extraction using thiosulfate reagent.

REFERENCES

ABBRUZZESE, C., FORNARI, P., MASSIDDA, R., VEGLIO, F. & UBALDINI, S. (1995) Thiosulphate leaching for gold hydrometallurgy. *Hydrometallurgy,* 39**,** 265-276.

AKSU, S. & DOYLE, F. M. (2002) Electrochemistry of Copper in Aqueous Ethylenediamine Solutions. *Journal of The Electrochemical Society,* 149**,** B340-B347.

ANTELMAN, M. S. & HARRIS, F. J. (1982) The Encyclopedia of Chemical Electrode Potentials. Plenum, New York.

AUSTRALIAN BUREUAU of STATISTICS (2008) Australian Mineral Statistic December Quarter 2007. Available: http://www.abare.gov.au/interactive/08ams_mar/.

AUSTRALIAN BUREUAU of STATISTICS (2009) Australian Commodities March Quarter; Volume 16 Number 1. Available: http://www.abare.gov.au/interactive/09ac_mar/htm/gold.htm.

AYLMORE, M. G. (2001) Treatment of a refractory gold–copper sulfide concentrate by copper ammoniacal thiosulfate leaching. *Miner. Eng.* 14(6)**,** 615–637.

AYLMORE, M. G. & MUIR, D. M. (2001) Thiosulfate leaching of gold--A review. *Minerals Engineering,* 14**,** 135-174.

BAILAR, J. C., EMELEUS, H. J., NYHOLM, R. & TROTMAN-DICKENSON, A. F. (1973) *Comprehensive Inorganic Chemistry,* Oxford, England.

BARBOSA-FILHO, O. & MONHEMIUS, A. J. (1994a) Leaching of gold in thiocyanate solutions - part 3: rates and mechanism of gold dissolution. *Transactions of the Institution of Mining and Metallurgy,* 103**,** C117-C125.

BARBOSA-FILHO, O. & MONHEMIUS, A. J. (1994b) Leaching of gold in thiocyanate solutions – part 1: chemistry and thermodynamics. *Transactions of the Institution of Mining and Metallurgy,* 103**,** C105-C110.

BEREZOWSKY, R. M., SEFTON, V. B. & GORMELY, L. S. (1978) Recovery of precious metals from metal sulfides. *US Patent 4070182*. Sherritt Gordon Mines Limited.

BHAPPU, R. B. (1990) Hydrometallurgical processing of precious metal ores. In: Arbiter, N. and Han, K.N., Editors. *Gold: Advances in Precious Metal Recovery,* Gordon and Breach Science Publishers, New York, 66-80.

BLACK, S. B. (2006) The thermodynamic chemistry of the aqueous copper-ammonia thiosulfate system. *Chemistry*. Perth, Murdoch University.

BREUER, P. L. & JEFFREY, M. I. (2002) An electrochemical study of gold leaching in thiosulfate solutions containing copper and ammonia. *Hydrometallurgy,* 65**,** 145-157.

BREUER, P. L. & JEFFREY, M. I. (2003) Copper catalysed oxidation of thiosulfate by oxygen in gold leach solutions. *Minerals Engineering,* 16**,** 21-30.

BRITTAN, M. I. (1975) Variable activation energy model for leaching kinetics. *International Journal of Mineral Processing,* 2**,** 321-331.

BYERLEY, J. J., FOUDA, S. A. & REMPEL, G. L. (1973) Kinetics and Mechanism of the Oxidation of Thiosulfate Ions by Copper(II) Ions in Aqueous Ammonia Solution. *J. Chem. Soc., Dalton Trans.*, 889-893.

BYERLEY, J. J., FOUDA, S. A. & REMPEL, G. L. (1975) Activation of copper(II) ammine complexes by molecular oxygen for the oxidation of thiosulfate ions. *Journal of the Chemical Society, Dalton Transactions*, 1329-1338.

CASAS, J. M., CRISÓSTOMO, G. & CIFUENTES, L. (2005) Speciation of the Fe(II)-Fe(III)-H2SO4-H2O system at 25 and 50 °C. *Hydrometallurgy*, 80, 254-264.

CHANDRA, I. & JEFFREY, M. I. (2004) An electrochemical study of the effect of additives and electrolyte on the dissolution of gold in thiosulfate solutions. *Hydrometallurgy*, 73, 305-312.

CLARK, J. (2002) EQUILIBRIUM CONSTANTS: Kc. Available: http://www.chemguide.co.uk/physical/equilibria/kc.html.

CRUNDWELL, F. K. (1995) Progress in the mathematical modelling of leaching reactors. *Hydrometallurgy*, 39, 321-335.

CRUNDWELL, F. K. & BRYSON, A. W. (1992) The modelling of particulate leaching reactors-- the population balance approach. *Hydrometallurgy*, 29, 275-295.

CRUNDWELL, F. K. & GODORR, S. A. (1997) A mathematical model of the leaching of gold in cyanide solutions. *Hydrometallurgy*, 44, 147-162.

CSIRO (2007) KEY ACHIEVEMENTS. Available: http://www.minerals.csiro.au/gold/key_ achievements.html.

CSIRO (1998) Best practice environmental management in mining: cyanide management. Commenwealth of Australia. Available: http://www.nml.csiro.au/assets/documents/itrinternet/Cyanide_Management20051117155355.pdf.

DAI, X., JEFFREY, M. I. & BREUER, P. L. (2009) A mechanistic model of the equilibrium adsorption of copper cyanide species onto activated carbon. *Hydrometallurgy,* 101**,** 99-107.

DE ANDRADE LIMA, L. R. P. (2004) A mathematical model for isothermal heap and column leaching. *Braz. J. Chem. Eng.,* 21**,** 435-447.

DE ANDRADE LIMA, L. R. P. (2007) Dynamic simulation of the carbon-in-pulp and carbon-in-leach processes. *Braz. J. Chem. Eng.,* 24(4)**,** 623-635.

DHAWALE, S. W. (1993) Thiosulfate: An interesting sulfur oxoanion that is useful in both medicine and industry--but is implicated in corrosion. *Journal of Chemical Education* 70**,** 12-14.

DIXON, S., CHO, E. H. & PITT, C. H. (1978) The interaction between gold cyanide, silver cyanide and high surface area charcoal. *AICHE Symp. Ser.* 74(173), 75-83.

FAGAN, P.A., PAULL, B., HADDAD, P.R., DUNNE, R. & KAMAR, H. (1997) Ion chromatographic analysis of cyanide in gold processing samples containing large concentrations of copper(I) and other metallo-cyanide complexes. *J. Chromatogr.* 770**,** 175-183.

FLEMING, C. A. (1989) Recovery of gold by resin-in-pulp at the Golden Jubilee Mine. In: *Precious Metals'89, The Minerals, Metals and Materials Society*, Warrendale, Pennsylvania, 105-119.

FLEMING, C. A. (1993) CIP and RIP – where the next? In: *Hydrometallurgy: Fundamental, Technology and Innovations – Proceeding of the Milton E. Wadsworth IV International Symposium on Hydrometallurgy, Society for Mining, Metallurgy and Exploration*, Littleton, Colorado, 379-393.

FLEMING, C. A., MCMULLEN, J., THOMAS, K. G. & WELLS, J. A. (2003) Recent advances in the development of an alternative to the cyanidation process: thiosulfate leaching and resin in pulp. *Minerals and Metallurgical Processing,* 20**,** 1-9.

GLASSTONE, S. & HICKLING, A. (1932) Studies in electrolytic oxidation. Part I. The electrolytic oxidation of sodium thiosulphate at a platinum anode. *J. Chem. Soc.***,** 2345 - 2356.

GREEN, B. R., KOTZE, M. H. & WYETHE, J. P. (2002) Developments in ion exchange – Mintek's contribution. *JOM, October*, 37-43.

HAN, K. N. (1994) Ammonia extraction of gold and silver from ores and other materials.

HARTMAN, H. L. (1992) *S.M.E. Mining Engineering Handbook,* New York, Society of Mining Engineers, American Institute of Mining, Metallurgical, and Petroleum Engineers.

HEMMATI, M., HENDRIX, J. L., NELSON, J. H. & MILOSAVLJEVIC, E. B. (1989) Study of the thiosulphate leaching of gold from carbonaceous ore and the quantitative determination of thiosulphate in the leached solution. London, UK, The Institution of Mining and Metallurgy.

HIMMI, B., MESSNAOUI, B., KITANE, S., EDDAIF, A., ALAOUI, A., BOUKLOUZ, A. & SOUFIAOUI, M. (2008) Study of Zn (II) extraction by 5-azidomethyl-8-hydroxyquinoline: Experiment and modelling. Hydrometallurgy, 93**,** 39-44.

HO, Y. S., WASE, D. A. J. & FORSTER, C. F. (1996) Kinetic studies of competitive heavy metal adsorption by sphagnum moss peat. *Environmental Technology,* 17**,** 71-77.

HUANG, Q., PAULL, B. & HADDAD, P. R. (1997) Optimisation of selectivity in the separation of metallo-cyanide complexes by ion-interaction liquid chromatography. *J. Chromatogr.* 770**,** 3-11.

JAGADEESH, E. P., AZEEZ, P. A. & BANERJEE, D. K. (2006) Modeling chemical speciation of copper in River Yamuna at Delhi, India. *Chemical Speciation and Bioavailability,* 18**,** 61-69.

JEFFREY, M. I. (2001) Kinetic aspects of gold and silver leaching in ammonia-thiosulfate solutions. *Hydrometallurgy,* 60**,** 7-16.

JEFFREY, M. I., BREUER, R. L. & CHOO, W. L. (2001) A kinetic study that compares the leaching of gold in the cyanide, thiosulfate, and chloride systems. *Metallurgical and Materials Transactions B,* 32B**,** 979-986B.

JEFFREY, M. I. & BRUNT, S. D. (2007) The quantification of thiosulfate and polythionates in gold leach solutions and on anion exchange resins. *Hydrometallurgy,* 89**,** 52-60.

JI, J., FLEMING, C., WEST-SELLS, P. G. & HACKL, R.P. (2003) A novel thiosulfate system for leaching gold without the use of copper and ammonia In: C.A. Young, A.M. Alfantazy, C.G. Anderson, D.B. Dreisinger, B. Harris and A. James, Editors, *Hydrometallurgy-2003*, TMS, Warrendale (2003), 227–244.

JIANG, T., CHEN, J., XU, S., HISKEY, J. B. & WARREN, G. W. (1993) A Kinetic Study of Gold Leaching with Thiosulphate. IN HISKEY, J. B. & WARREN, G. W. (Eds.) *Hydrometallurgy: Fundamentals, Technology and Innovations, Proc. 4th Milton E. Wadsworth Intl. Symp.* Littleton, CO, USA, AIME.

JUAREZ, C. M. & DUTRA, A. J. B. (2000) Gold electrowinning from thiourea solutions. *Minerals Engineering,* 13**,** 1083-1096.

KAREN, C. T. (2009) *Chemistry: an introduction to general, organic and biological chemistry,* Upper Saddle River, NJ, Pearson Prentice Hall.

KELLY, D. P. & WOOD, A. P. (1994) Synthesis and Determination of Thiosulphate and Polythionates. *Methods in Enzymology,* 243**,** 475-501.

KERLEY, B. J. J. (1983) Recovery of precious metals from difficult ores. *US Patent 4269622.*

KHOLMOGOROV, A. G., KONONOVA, O. N., PASHKOV, G. L. & KONONOV, Y. S. (2002) Thiocyanate solutions in gold technology. *Hydrometallurgy,* 64**,** 43-48.

KIRANOUDIS, C. T., MAROULIS, Z. B., PAPASSIOPI, N. & PASPALIARIS, I. (1998) Modelling and optimization of carbon-in-pulp gold recovery processes. *IMA Journal of Mathematics Applied in Business & Industry,* 9**,** 35-54.

KIRANOUDIS, C. T., VOROS, N. G., KRITIKOS, T., MAROULIS, Z. B., MARINOSKOURIS, D., PAPASSIOPI, N., DIMITROPOULOU, O., PASPALIARIS, I. & KONTOPOULOS, A. (1997) Object-oriented simulation of hydrometallurgical processes: Part I. Requirements and implementation. *Metallurgical and Materials Transactions B,* 28**,** 777-784.

KORTE, F. & COULSTON, F. (1995) From Single-Substance Evaluation to Ecological Process Concept: The Dilemma of Processing Gold with Cyanide. *Ecotoxicology and Environmental Safety,* 32**,** 96-101.

KOSLIDES, T. & CIMINELLI, V. S. T. (1992) Pressure oxidation of arsenopyrite and pyrite in alkaline solutions. *Hydrometallurgy,* 30**,** 87-106.

LA BROOY, S. R., LINGE, H. G. & WALKER, G. S. (1994) Review of gold extraction from ores. *Minerals Engineering,* 7**,** 1213-1241.

LAGERGREN, S. (1989) About the theory of so-called adsorption of soluble substances. *Kungliga Svenska Vetenskapsakademies Handlingar,* 24**,** 1-39.

LANGHANS, J. W., JR., LEI, K. P. V. & CARNAHAN, T. G. (1992) Copper-catalyzed thiosulfate leaching of low-grade gold ores. *Hydrometallurgy,* 29**,** 191-203.

LANGMUIR, I. (1961) The Constitution and Fundamental Properties of Solids and Liquids, *J. Am. Chem. Soc.,* 38**,** 2221–2295.

LEE, H. Y., KIM, S. G. & OH, J. K. (1997) Cementation behavior of gold and silver onto Zn, Al, and Fe powders from acid thiourea solutions. *Canadian Metallurgical Quarterly,* 36**,** 149-155.

LEWIS, G. V. (2000) "The Penjom Process" An innovative approach to extracting gold from carbonaceous ore. In: *Gold Processing in the 21st Century: An International Forum, AJ Parker Cooperative Research Centre for Hydrometallurgy,* Perth, Australia.

LIEBENBERG, S. P. & VAN DEVENTER, J. S. J. (1998) The quantification of shifting adsorption equilibria of gold and base metal in CIP plants. *Mineral Engineering,* 11(6)**,** 551-562.

LI, J., MILLER, J. D., WAN, R. Y. & LE VIER, K. M. (1995) *The ammoniacal Thiosulphate System for Precious Metal Recovery.* Littleton, Co, Soc. for Min., Metall. and Explor.

LINGE, H. G. & WELHAM, N. J. (1997) Gold Recovery From a Refractory Arsenopyrite (Feass) Concentrate by in-Situ Slurry Oxidation. *Minerals Engineering,* 10**,** 557-566.

LOGSDON, M. J., HAGELSTEIN, K. & MUDDER, T. I. (1999) The management of cyanide in gold extraction. *ICME Publications.* Ontario, Canada.

MACARTHUR, J. S., FORREST, R. W. & FORREST, W. (1988) Improvement in obtaining gold and silver from ores and other compounds. *British Patent 14174.*

MANSUR, M. B., SLATER, M. J. & BISCAIA, E. C. (2002) Kinetic analysis of the reactive liquid-liquid test system ZnSO4/D2EHPA/n-heptane. *Hydrometallurgy,* 63**,** 107-116.

MARSDEN, J. & HOUSE, I. (1992) *The Chemistry of Gold Extraction,* London, UK, Ellis Horwood Ltd.

MARSDEN, J. & HOUSE, I. (2006) *The Chemistry of Gold Extraction*, The Society for Mining, Metallurgy, and Exploration, Inc. (SME).

MCQUISTON, F. W. & SHOEMAKER, R. S. (1981) *Gold and Silver Cyanidation Plant Practice*, vol. 2, American Institute of Mining, Metallurgical, and Petroleum Engineers, Inc., New York.

MILLER, G. C. & PRITSOS, C. A. (2001) Unresolved problems with the use of cyanide in open pit precious metals mining, Cyanide: social, industrial and economic aspects. *TMS Annual Meeting.* New Orleans, USA.

MONHEMIUS, A. J. & BALL, S. P. (1995) Leaching of Dominican gold ores in iodide-catalysed thiocyanate solutions. *Transactions of the Institution of Mining and Metallurgy*, 104**,** C117-C124.

MORAN, R. (1998) Cyanide uncertainties: observations on the chemistry, toxicity, and analysis of cyanide in mining-related waters. *MPC issue paper no. 1.* Washington, Mineral Policy Center.

MOSHER, J. B. & FIGUEROA, L. (1996) Biological oxidation of cyanide: A viable treatment option for the minerals processing industry? *Minerals Engineering,* 9**,** 573-581.

MUIR, D. M. & AYLMORE, M. G. (2004) Thiosulphate as an alternative to cyanide for gold-processing issues and impediments. *Mineral Processing and Extractive Metallurgy,* 113**,** 2-12.

NICOL, M. J., FLEMING, C. A. & CROMBERGE, G. (1984) The absorption of gold cyanide onto activated carbon. I. The kinetics of absorption from pulp. *J.S. Afr. Inst. Min. Metall.*, 84(2)**,** 50-54.

NICOL, M. J. & O'MALLEY, G. (2002) Recovering gold from thiosulfate leach pulps via ion exchange. *JOM,* 54**,** 44-46.

NORMAN, W. L. (2001) *Applied mathematics methods for chemical engineers,* Boca Raton, Florida, CRC Press LLC.

PEDRAZA, A. M., VILLEGAS, I., FREUND, P. L. & CHORNIK, B. (1988) Electro-oxidation of thiosulphate ion on gold : Study by means of cyclic voltammetry and auger electron spectroscopy. *Journal of Electroanalytical Chemistry,* 250**,** 443-449.

PRASAD, M. S., MENSAH-BINEY, R. & PIZARRO, R. S. (1991) Modern trends in gold processing -- overview. *Minerals Engineering,* 4**,** 1257-1277.

PUROLITE (2008) Purolite® A500/2788 http://www.purolite.com/ProductID/210/FolderID/60/PageVars/Library/Products/ProductDetails.htm.

PYPER, R. A. & HENDRIX, J. L. (1981) Extraction of Gold From Finely Disseminated Gold Ores by Use of Acidic Thiourea Solution *Extraction Metallurgy* 81**,** 57-75.

REUTER, M. A. & SUDHÖLTER, S. C. (1996) Use of simulated annealing and neural nets for the eco-techno-economic synthesis of mineral and metallurgical flowsheets. *Minerals Engineering,* 9**,** 283-299.

RIGGS, J. B. (2001) *Chemical Process Control,* 2nd Ed., Ferret Publishing, Texas, USA.

RITCHIE, I. M., NICOL, M. J. & STAUNTON, W. P. (2001) Are there realistic alternatives to cyanide as a lixiviant for gold at the present time? In: E.D. Young, L.G. Twidwell and C.G. Anderson, Editors, *Cyanide: Social, Industrial and Economic Aspects*, TMS, Warrendale, 427–440.

ROBINSON, B. A., VISWANATHAN, H. S. & VALOCCHI, A. J. (2000) Efficient numerical techniques for modeling multicomponent ground-water transport based upon simultaneous solution of strongly coupled subsets of chemical components. *Advances in Water Resources,* 23**,** 307-324.

ROLIA, E. & CHAKRABARTI, C. L. (1982) Kinetics of decomposition of tetrathionate, trithionate and thiosulphate in alkaline media. *Environmental Science and Technology,* 16**,** 852-857.

RUBEN, H., ZALKIN, A., FALTENS, M. O. & TEMPLETON, D. H. (2002) Crystal structure of sodium gold(I) thiosulfate dihydrate, Na3Au(S2O3)2.2H2O. *Inorganic Chemistry,* 13**,** 1836-1839.

SENANAYAKE, G. (2004) Analysis of reaction kinetics, speciation and mechanism of gold leaching and thiosulfate oxidation by ammoniacal copper(II) solutions. *Hydrometallurgy,* 75**,** 55-75.

SILLEN, L. G. & MARTELL, E. (1964) Stability Constants of Metal-ion Complexes, *Special Publication Nos. 17 and 26*, Chemical Society, London.

STANGE, W., KING, R. P. & WOOLLACOTT, L. C. (1990) Towards more effective simulation of CIP and CIL processes. 2. A population-balance-based simulation approach. *J.S. Afr. Inst. Min. Metall.*, 90(11)**,** 307-314.

STEUDEL, R. & HOLDT, G. (1986) Ion-pair chromatographic separation of polythionates SnO62- with up to thirteen sulphur atoms. *Journal of Chromatography A,* 361**,** 379-384.

STUPKO, T. V., MINOROV, V. E. & PASHKOV, G. L. (1998) Temperature effect on equilibrium formations of metal ion complexes with ammonia in aqueous ammonium sulfate solution. *Zhurnal Prikladnoi Khimii,* 71**,** 1087-1090.

SWAMINATHAN, C., PYKE, P. & JOHNSTON, R. F. (1993) Reagent trends in the gold extraction industry. *Minerals Engineering,* 6**,** 1-16.

TOZAWA, K., INUI, Y. & UMETSU, Y. (1981) Dissolution of gold in ammoniacal thiosulfate solution. *Metallurgical Society AIME, pp. 12, 1981*.

UBALDINI, S., FORNARI, P., MASSIDDA, R. & ABBRUZZESE, C. (1998) An innovative thiourea gold leaching process. *Hydrometallurgy,* 48**,** 113-124.

U.S. GEOLOGICAL SURVEY (2008) Mineral Commodity Gold Statistics, in Kelly, T.D., and Matos, G.R., comps., Historical statistics for mineral and material commodities in the United States: U.S. Geological Survey Data Series 140. Available: http://minerals.usgs.gov/ds/2005/140/.

VAN DEVENTER, J. S. J., KAM, K. M. & VAN DER WALT, T. J. (2004) Dynamic modelling of a carbon-in-leach process with the regression network. *Chemical Engineering Science* 59**,** 4575-4589.

VÁZQUEZ, I., RODRÍGUEZ-IGLESIAS, J., MARAÑÓN, E., CASTRILLÓN, L. & ÁLVAREZ, M. (2007) Removal of residual phenols from coke wastewater by adsorption. *Journal of Hazardous Materials,* 147**,** 395-400.

WAN, R. Y. (1997) *Importance of solution chemistry for thiosulphate leaching of gold*. Carlton, Vic, The Australasian Institute of Mining and Metallurgy.

WANG, X. H. (1992) Thermodynamic equilibrium calculations on gold silver lixiviant systems relevant to gold extraction from complex ores, *Electrochemistry in Minerals and Metals Processing vol. III*, The Electrochemical Society, Pennington, NJ, 452–477.

WATERS (2002) Empower Software. Workgroup UPGRADE ed. Milford, USA, Waters Corporation.

WEBER, W. J. Jr. (1972). *Physicochemical Processes for Water Quality Control*, John Wiley & Sons., New York, U.S.A.

WHITE, H. A. (1905) The solubility of gold in thiosulphate and thiocyanates. *Chemical, Metallurgical and Mining Society,* 5**,** 109-111.

WILLIAMS, H. P., T., S. A., WILLIAMS, T. V. & BRIAN, P. F. (2002) *Numerical Recipes in C++*, Cambridge, United Kingdom, Cambridge University Press.

WOOLLACOTT, L. C., STANGE, W. & KING, R. P. (1990) Towards more effective simulation of CIP and CIL processes. 1. The modelling of adsoprption and leaching. *J.S. Afr. Inst. Min. Metall*., 90(10)**,** 275-282.

YANNOPOULOS, J. C. (1991) *The extractive metallurgy of gold,* USA, Springer-Verlag.

YOUNG, C. A. (2001) *Cyanide: social, industrial and economic aspects,* New Orleans, Minerals and Materials Society.

ZHANG, H. & DREISINGER, D. B. (2002a) The adsorption of gold and copper onto ion-exchange resins from ammoniacal thiosulfate solutions. *Hydrometallurgy,* 66**,** 67-76.

ZHANG, H. & DREISINGER, D. B. (2002b) The kinetics for the decomposition of tetrathionate in alkaline solutions. *Hydrometallurgy,* 66**,** 59-65.

ZHANG, Z. & NICOL, M. J. (2003) An electrochemical study of the dissolution of gold in thiosulfate solutions: Part I. Alkaline solutions, *J. Appl. Electrochem.* 33 (2003)**,** 767–775.

ZHU, G., FANG, Z. H. & CHEN, J. Y. (1994) Electrochemical studies on the mechanism of gold dissolution in thiosulfate solutions. *Trans. Nonferrous Met. Soc. China,* 4**,** 50-53.

ZIPPERIAN, D., RAGHAVAN, S. & WILSON, J. P. (1988) Gold and silver extraction by ammoniacal thiosulfate leaching from a rhyolite ore. *Hydrometallurgy,* 19**,** 361-375.

APPENDIX A

Appendix A contains additional information for the single component resin-solution systems (Chapter 3).

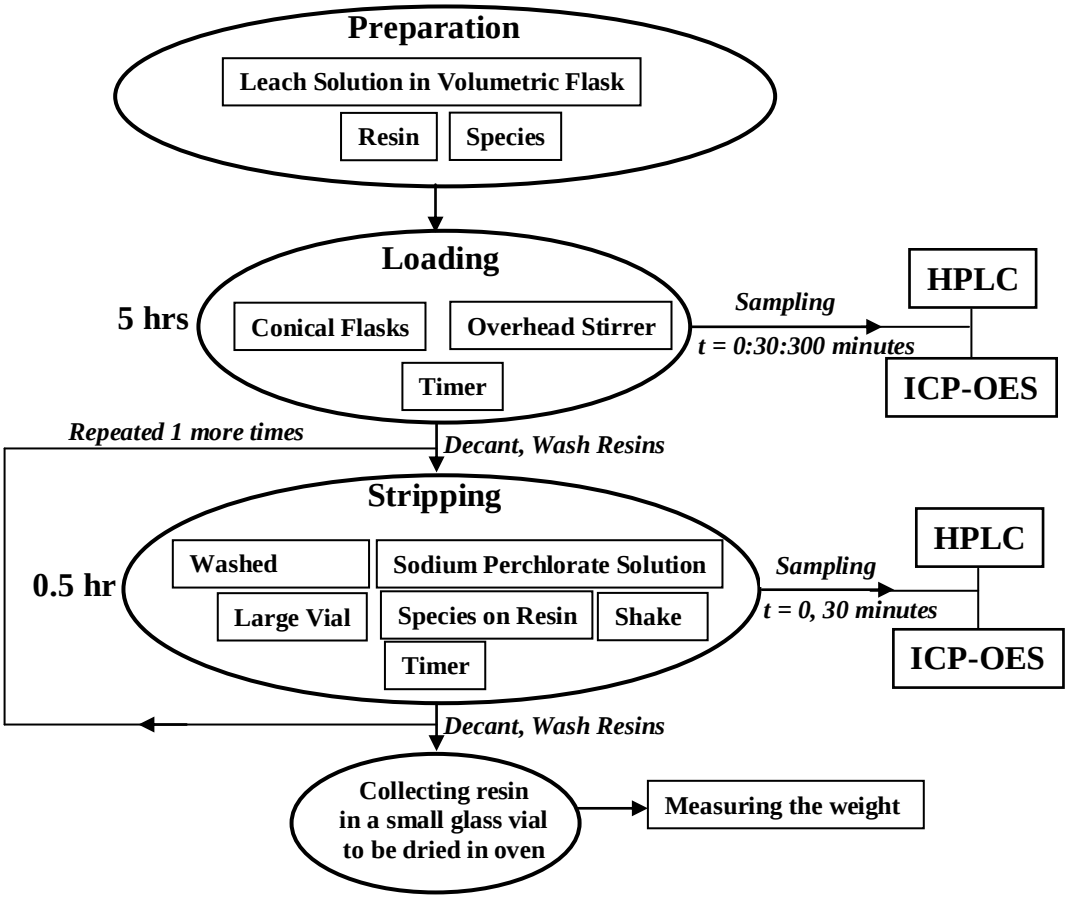

Figure A.1 Flowchart of kinetics experiment for the adsorption

Note:

All the experiments were conducted at the neutral pH and the ambient temperature (~23 °C). The HPLC was used for the analysis of thiosulfate and polythionates, the ICP-OES was used for the analysis of gold thiosulfate.

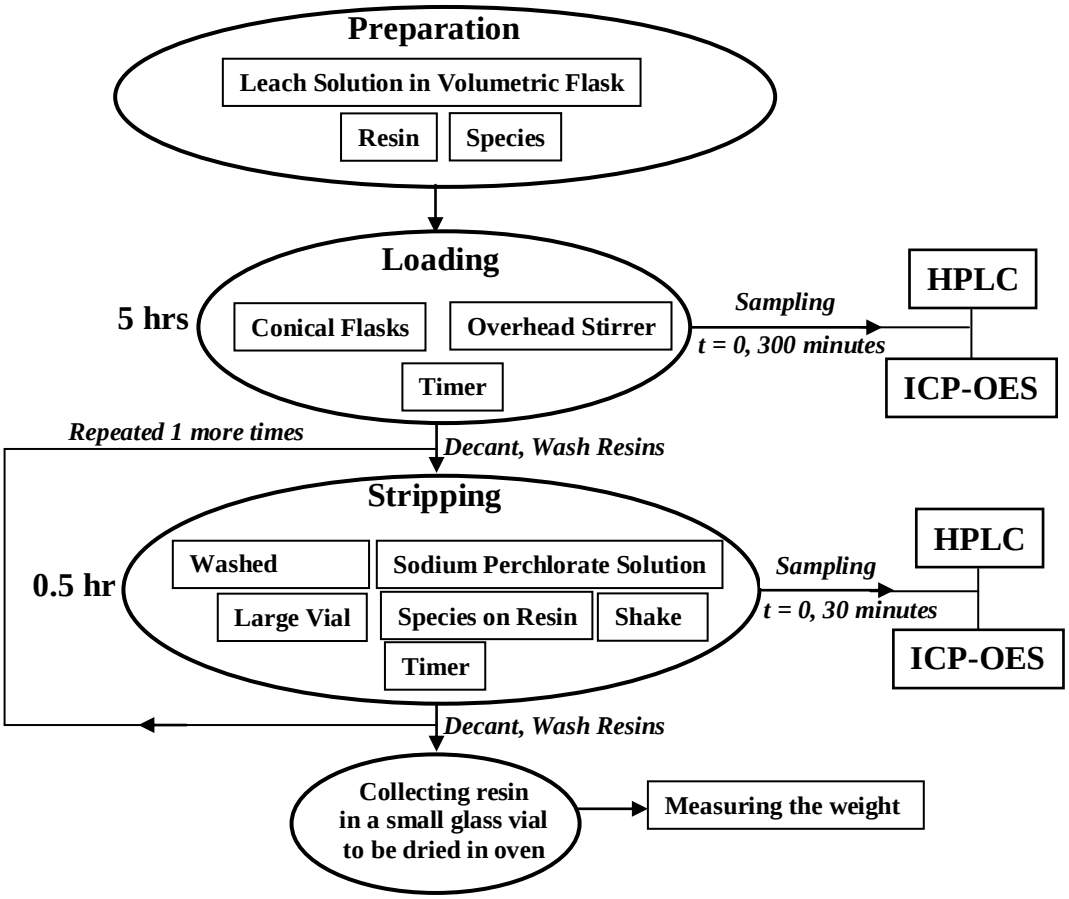

Figure A.2 Flowchart of equilibrium experiment for the adsorption

Note:

All the experiments were conducted at the neutral pH and the ambient temperature (~23 °C). The HPLC was used for the analysis of thiosulfate and polythionates, the ICP-OES was used for the analysis of gold thiosulfate.

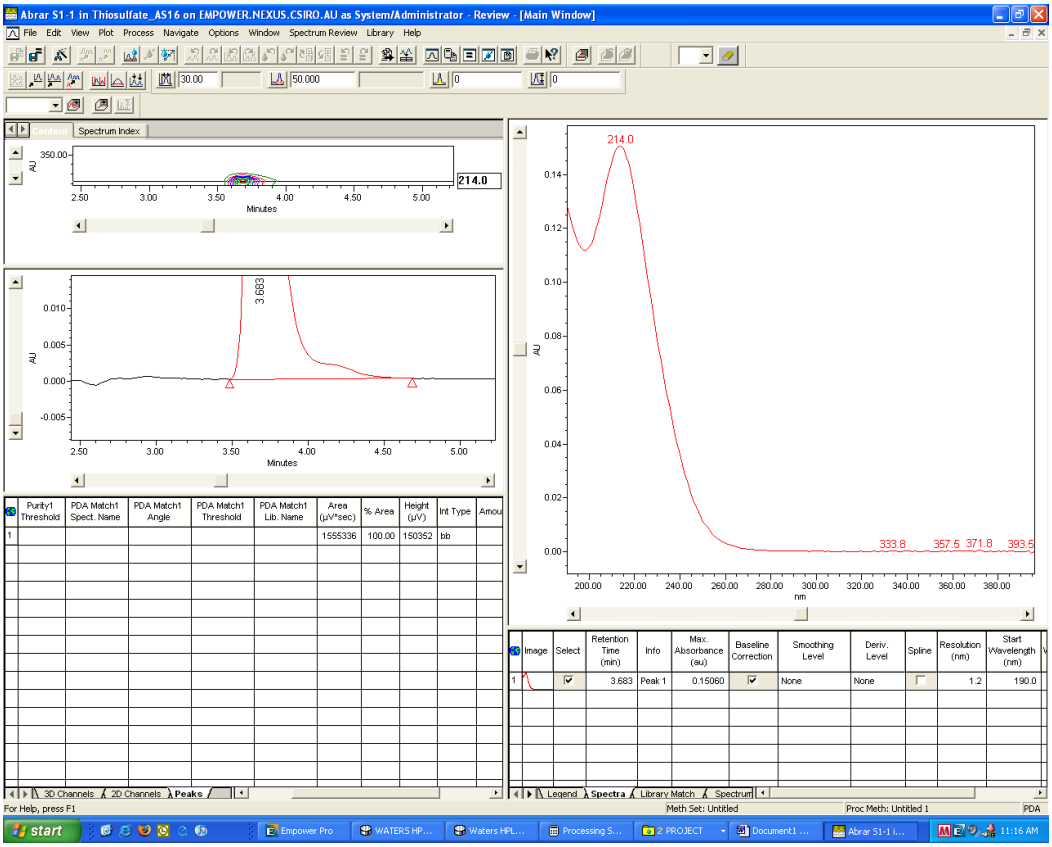

Figure A.3 An example of the HPLC chromatogram for the thiosulfate peak retention time and wavelength of UV adsorption

APPENDIX B

Appendix B contains additional information for the multiple components resin-solution systems (Chapter 4).

Table B.1 The equilibrium loading of thiosulfate, trithionate, tetrathionate and pentathionate on resin for the calculated equilibrium constant of pentathionate loading over tetrathionate

Experiment	1	2	3	4	5
Thiosulfate					
Init Concentration (mM)	1.579	1.577	1.541	1.549	1.531
Equil Concentration in Sol. (mM)	1.458	1.463	1.370	1.397	1.416
Equil Concentration on Resins (mM)	32.207	30.718	46.503	40.947	30.880
Trithionate					
Init Concentration (mM)	1.314	1.305	1.300	1.297	1.299
Equil Concentration in Sol. (mM)	0.765	0.768	0.763	0.758	0.755
Equil Concentration on Resins (mM)	146.264	145.632	146.051	145.269	145.859
Tetrathionate					
Init Concentration (mM)	2.519	2.518	2.542	2.547	2.541
Equil Concentration in Sol. (mM)	1.379	1.390	1.397	1.388	1.392
Equil Concentration on Resins (mM)	303.696	304.912	311.106	311.988	308.610
Pentathionate					
Init Concentration (mM)	0.959	0.957	0.881	0.882	0.878
Equil Concentration in Sol. (mM)	0.417	0.4200	0.382	0.381	0.381
Equil Concentration on Resins (mM)	144.208	145.519	135.665	134.960	133.397
K Tetrathionate-R + Pentathionate = Pentathionate-R + Tetrathionate	**1.569**	**1.580**	**1.597**	**1.578**	**1.580**

Note:

The concentration units for all the species in solution and on resin are taken as mmol/L of either solution or dry resin, which for simplicity is designed mM in both cases.

Table B.2 The concentration of gold thiosulfate based on ICP-OES analysis for the NARS system with 5 mM thiosulfate and trithionte, 0.2-10 mg/L gold thiosulfate and 5 g resin

Analytical Chemistry Unit				
Analyst:	SY	**Job No:**	8501	
Date:	29/10/2007	**File No:**	rep8501	
Job Code :	**LV44D**	**ICP-OES**		
			Concentration [mg/L]	
Sample ID	**LabID**	**Sample Info.**	**Analysis**	**Corrected**
G0 11	8291/1	0.2Au t=0	0.238	0.262
G0 12	8291/2	0.4Au t=0	0.436	0.480
G0 13	8291/3	0.6Au t=0	0.648	0.713
G014	8291/7	2Au t=0	1.841	2.025
G015	8291/8	5Au t=0	4.644	5.109
G016	8291/9	10Au t=0	9.524	10.476
G5 11	8291/4	0.2Au t=5	0.040	0.044
G5 12	8291/5	0.4Au t=5	0.058	0.064
G5 13	8291/6	0.6Au t=5	0.084	0.093
G5 14	8291/10	2Au t=5	0.234	0.258
G5 15	8291/11	5Au t=5	0.587	0.645
G5 16	8291/12	10Au t=5	1.238	1.362
G1 21	8291/13	0.2Au S1	0.666	0.733
G1 22	8291/14	0.4Au S1	1.349	1.484
G1 23	8291/15	0.6Au S1	2.125	2.337
G1 24	8291/19	2Au S1	6.252	6.877
G1 25	8291/20	5Au S1	15.2	16.715
G1 26	8291/21	10Au S1	31.5	34.683
G2 21	8291/16	0.2Au S2	0.037	0.041
G2 22	8291/17	0.4Au S2	0.021	0.023
G2 23	8291/18	0.6Au S2	0.036	0.039
G2 24	8291/22	2Au S2	0.245	0.269
G2 25	8291/23	5Au S2	0.215	0.237
G2 26	8291/24	10Au S2	0.384	0.422

Note:

The concentrations of gold thiosulfate based on ICP-OES analysis were corrected since the 10 mL samples were added with 1 mL NaCN (0.0176M) to convert the gold thiosulfate complex to the more stable gold cyanide complex.

Table B.3 The speciation of thiosulfate, polythionates and gold thiosulfate for the NARS system with the synthetic polythionates mixture solution, 0.2-10 mg/L gold thiosulfate and 5 g resin

Batch Num.	**Initial Concentrations**			
	Gold (mg/L)	$S_2O_3^{2-}$ (mM)	$S_3O_6^{2-}$ (mM)	$S_4O_6^{2-}$ (mM)
1	0.232	1.591	1.310	2.522
2	0.446	1.578	1.314	2.519
3	1.099	1.577	1.305	2.516
4	2.185	1.541	1.300	2.542
5	5.448	1.549	1.297	2.547
6	10.848	1.531	1.298	2.541
Batch Num.	**Equilibrium Concentrations**			
	Gold (mg/L)	$S_2O_3^{2-}$ (mM)	$S_3O_6^{2-}$ (mM)	$S_4O_6^{2-}$ (mM)
1	0.077	1.463	0.765	1.383
2	0.137	1.458	0.765	1.378
3	0.331	1.463	0.768	1.390
4	0.662	1.370	0.763	1.397
5	1.588	1.397	0.758	1.388
6	3.236	1.416	0.755	1.392
Batch Num.	**Loading-based Concentrations on Resin**			
	Gold (mg/L)	$S_2O_3^{2-}$ (mM)	$S_3O_6^{2-}$ (mM)	$S_4O_6^{2-}$ (mM)
1	0.154	26.742	140.030	302.014
2	0.309	25.318	141.681	304.594
3	0.768	25.271	142.668	305.554
4	1.523	24.698	146.066	299.818
5	3.860	22.692	139.639	302.578
6	7.611	21.626	140.663	301.124
Batch Num.	**Stripping-based Concentrations on Resin**			
	Gold (mg/L)	$S_2O_3^{2-}$ (mM)	$S_3O_6^{2-}$ (mM)	$S_4O_6^{2-}$ (mM)
1	37.091	34.255	145.766	304.304
2	76.095	32.207	146.264	303.696
3	189.612	30.718	145.632	304.912
4	388.692	46.503	146.051	311.106
5	963.999	40.947	145.269	311.988
6	1945.137	30.880	145.859	308.609

Table B.4 The concentration of gold thiosulfate based on ICP-OES analysis for the NARS system with the synthetic polythionates mixture solution with 0.2-10 mg/L gold thiosulfate and 5 g resin

Analytical Chemistry Unit				
Analyst:	SY	**Job No:**	8551	
Date:	20/03/2008	**File No:**	rep8551	
Job Code :	**LV44D**	**ICP-OES**		
			Concentration [mg/L]	
Sample ID	**LabID**	**Sample Info.**	**Analysis**	**Corrected**
P01	8551/1	0.2Au t=0	0.210	0.232
P02	8551/2	0.4Au t=0	0.405	0.446
P03	8551/3	1Au t=0	0.999	1.099
P1	8551/4	0.2Au t=5	0.070	0.077
P2	8551/5	0.4Au t=5	0.125	0.137
P3	8551/6	1Au t=5	0.301	0.331
P4	8551/7	0.2Au S1	0.472	0.519
P5	8551/8	0.4Au S1	1.014	1.115
P6	8551/9	1Au S1	2.515	2.766
P7	8551/10	0.2Au S2	0.033	0.036
P8	8551/11	0.4Au S2	0.025	0.028
P9	8551/12	1Au S2	0.030	0.034
P010	8551/13	2Au t=0	1.987	2.185
P011	8551/14	5Au t=0	4.953	5.448
P012	8551/15	10Au t=0	9.862	10.848
P10	8551/16	2Au t=5	0.602	0.662
P11	8551/17	5Au t=5	1.444	1.588
P12	8551/18	10Au t=5	2.942	3.236
P13	8551/19	2Au S1	5.094	5.603
P14	8551/20	5Au S1	12.854	14.139
P15	8551/21	10Au S1	26.086	28.694
P16	8551/22	2Au S2	0.106	0.117
P17	8551/23	5Au S2	0.163	0.180
P18	8551/24	10Au S2	0.249	0.274

Note:

The concentrations of gold thiosulfate based on ICP-OES analysis were corrected since the 10 mL samples were added with 1 mL NaCN (0.0176M) to convert the gold thiosulfate complex to the more stable gold cyanide complex.

Table B.5 The speciation of thiosulfate, polythionates and gold thiosulfate for the NARS system with 100 mM thiosulfate, 0.2-100 mg/L gold thiosulfate and 5 g resin

Batch Num.	**Initial Concentrations**			
	Gold (mg/L)	$S_2O_3^{2-}$ (mM)	$S_3O_6^{2-}$ (mM)	$S_4O_6^{2-}$ (mM)
1	0.218	100		
2	0.425	100		
3	0.958	100		
4	2.187	100		
5	5.358	100		
6	10.720	100		
Batch Num.	**Equilibrium Concentrations**			
	Gold (mg/L)	$S_2O_3^{2-}$ (mM)	$S_3O_6^{2-}$ (mM)	$S_4O_6^{2-}$ (mM)
1	0.023	97.807		
2	0.028	98.303		
3	0.040	98.008		
4	0.082	97.372		
5	0.156	97.223		
6	0.308	97.167		
Batch Num.	**Loading-based Concentrations on Resin**			
	Gold (mg/L)	$S_2O_3^{2-}$ (mM)	$S_3O_6^{2-}$ (mM)	$S_4O_6^{2-}$ (mM)
1	0.195	620.904		
2	0.396	618.294		
3	0.917	618.323		
4	2.105	620.143		
5	5.202	610.849		
6	10.412	617.544		
Batch Num.	**Stripping-based Concentrations on Resin**			
	Gold (mg/L)	$S_2O_3^{2-}$ (mM)	$S_3O_6^{2-}$ (mM)	$S_4O_6^{2-}$ (mM)
1	50.806	584.400		
2	95.983	462.621		
3	236.159	538.116		
4	474.480	703.696		
5	1189.735	746.863		
6	2418.255	765.206		

Table B.6 The concentration of gold thiosulfate based on ICP-OES analysis for the NARS system with 100 mM thiosulfate, 0.2-10 mg/L gold thiosulfate and 5 g resin

Analytical Chemistry Unit				
Analyst:	SY	**Job No:**	8524	
Date:	15/02/2008	**File No:**	rep8524	
Job Code :	**LV44D**	**ICP-OES**		
			Concentration [mg/L]	
Sample ID	**LabID**	**Sample Info.**	**Analysis**	**Corrected**
G 01	8524/1	0.2Au t=0	0.198	0.218
G 02	8524/2	0.4Au t=0	0.386	0.425
G 03	8524/3	1Au t=0	0.871	0.958
G 1	8524/4	0.2Au t=5	0.021	0.023
G 2	8524/5	0.4Au t=5	0.026	0.028
G 3	8524/6	1Au t=5	0.037	0.040
G 4	8524/7	0.2Au S1	0.671	0.738
G 5	8524/8	0.4Au S1	1.247	1.372
G 6	8524/9	1Au S1	3.126	3.439
G 7	8524/10	0.2Au S2	0.022	0.024
G 8	8524/11	0.4Au S2	0.033	0.036
G 9	8524/12	1Au S2	0.052	0.058
G 010	8524/13	2Au t=0	1.988	2.187
G 011	8524/14	5Au t=0	4.871	5.358
G 012	8524/15	10Au t=0	9.745	10.720
G 10	8524/16	2Au t=5	0.075	0.082
G 11	8524/17	5Au t=5	0.142	0.156
G 12	8524/18	10Au t=5	0.280	0.308
G 13	8524/19	2Au S1	6.357	6.993
G 14	8524/20	5Au S1	15.902	17.492
G 15	8524/21	10Au S1	32.289	35.517
G 16	8524/22	2Au S2	0.086	0.094
G 17	8524/23	5Au S2	0.184	0.203
G 18	8524/24	10Au S2	0.268	0.295

Note:

The concentrations of gold thiosulfate based on ICP-OES analysis were corrected since the 10 mL samples were added with 1 mL NaCN (0.0176M) to convert the gold thiosulfate complex to the more stable gold cyanide complex.

Table B.7 The concentration of gold thiosulfate based on ICP-OES analysis for the reaction of trithionate in the NARS system with 10 mg/L initial gold thiosulfate and 5 g resin

Analytical Chemistry Unit				
Analyst:	SY	**Job No:**	9439	
Date:	9/03/2009	**File No:**	Rep9439	
Job Code :	**R-580-3-4**	**ICP-OES**		
			Concentration [mg/L]	
Sample ID	**LabID**	**Sample Info.**	**Analysis**	**Corrected**
L01	9439/1	2.528Tri, t=0	9.070	9.977
L02	9439/2	2.830Tri, t=0	9.148	10.063
L03	9439/3	3.286Tri, t=0	9.146	10.061
L04	9439/4	4.132Tri, t=0	9.083	9.991
L05	9439/5	5.625Tri, t=0	9.203	10.123
L06	9439/6	7.390Tri, t=0	9.121	10.033
L07	9439/7	10.427Tri, t=0	9.107	10.018
L08	9439/8	14.508Tri, t=0	9.086	9.994
L51	9439/9	2.528Tri, t=5	0.198	0.218
L52	9439/10	2.830Tri, t=5	0.268	0.295
L53	9439/11	3.286Tri, t=5	0.447	0.492
L54	9439/12	4.132Tri, t=5	0.880	0.969
L55	9439/13	5.625Tri, t=5	1.771	1.948
L56	9439/14	7.390Tri, t=5	2.692	2.962
L57	9439/15	10.427Tri, t=5	3.931	4.324
L58	9439/16	14.508Tri, t=5	5.015	5.516
S1 1	9439/17	2.528Tri, t=S1	36.391	40.030
S1 2	9439/18	2.830Tri, t=S1	36.195	39.814
S1 3	9439/19	3.286Tri, t=S1	35.411	38.953
S1 4	9439/20	4.132Tri, t=S1	33.734	37.108
S1 5	9439/21	5.625Tri, t=S1	30.167	33.184
S1 6	9439/22	7.390Tri, t=S1	26.147	28.762
S1 7	9439/23	10.427Tri, t=S1	20.936	23.030
S1 8	9439/24	14.508Tri, t=S1	16.262	17.888
S2 1	9439/25	2.528Tri, t=S2	0.413	0.454
S2 2	9439/26	2.830Tri, t=S2	0.336	0.370
S2 3	9439/27	3.286Tri, t=S2	0.310	0.341
S2 4	9439/28	4.132Tri, t=S2	0.259	0.285
S2 5	9439/29	5.625Tri, t=S2	0.228	0.250
S2 6	9439/30	7.390Tri, t=S2	0.197	0.217
S2 7	9439/31	10.427Tri, t=S2	0.164	0.181
S2 8	9439/32	14.508Tri, t=S2	0.135	0.148

Table B.8 The speciation of trithionate and gold thiosulfate for the reaction of trithionate with gold thiosulfate in the NARS system with 10 mg/L initial gold thiosulfate and 5 g resin

	Initial Concentrations			
Batch Num.	Gold (mM)	$S_2O_3^{2-}$ (mM)	$S_3O_6^{2-}$ (mM)	$S_4O_6^{2-}$ (mM)
1	0.0506		2.528	
2	0.0511		2.830	
3	0.0511		3.286	
4	0.0507		4.132	
5	0.0514		5.625	
6	0.0509		7.390	
7	0.0509		10.427	
8	0.0507		14.508	
	Equilibrium Concentrations			
Batch Num.	Gold (mM)	$S_2O_3^{2-}$ (mM)	$S_3O_6^{2-}$ (mM)	$S_4O_6^{2-}$ (mM)
1	0.0011		0.681	
2	0.0015		0.936	
3	0.0025		1.357	
4	0.0049		2.169	
5	0.0099		3.781	
6	0.0150		5.493	
7	0.0220		8.710	
8	0.0280		12.021	
	Loading-based Concentrations on Resin			
Batch Num.	Gold (mM)	$S_2O_3^{2-}$ (mM)	$S_3O_6^{2-}$ (mM)	$S_4O_6^{2-}$ (mM)
1	11.2103		417.921	
2	11.9700		457.260	
3	10.6113		421.324	
4	10.1837		436.499	
5	10.5663		469.726	
6	9.6281		508.796	
7	6.9921		415.244	
8	5.8066		635.259	
	Stripping-based Concentrations on Resin			
Batch Num.	Gold (mM)	$S_2O_3^{2-}$ (mM)	$S_3O_6^{2-}$ (mM)	$S_4O_6^{2-}$ (mM)
1	11.6836		407.757	
2	12.3721		448.637	
3	10.9481		417.937	
4	10.6046		436.686	
5	10.8577		551.877	
6	9.9134		587.341	
7	7.1612		526.294	
8	5.8757		547.046	

APPENDIX C

Appendix C contains additional information for the multiple components resin-solution systems (Chapter 5).

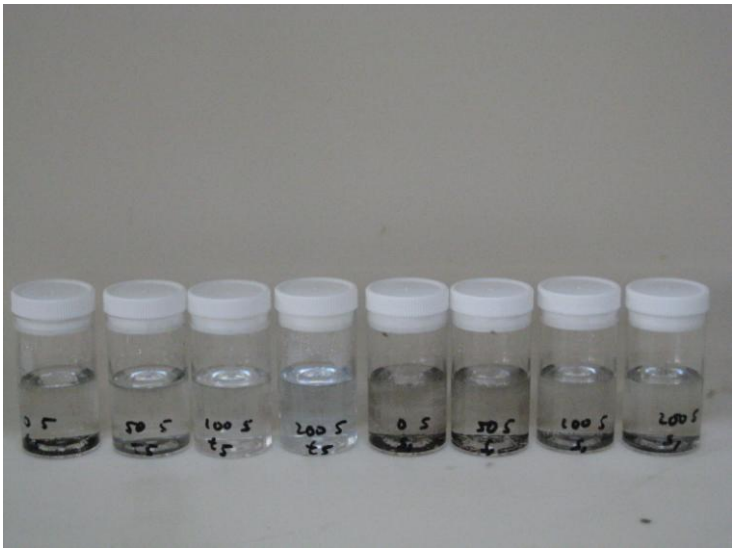

(a)

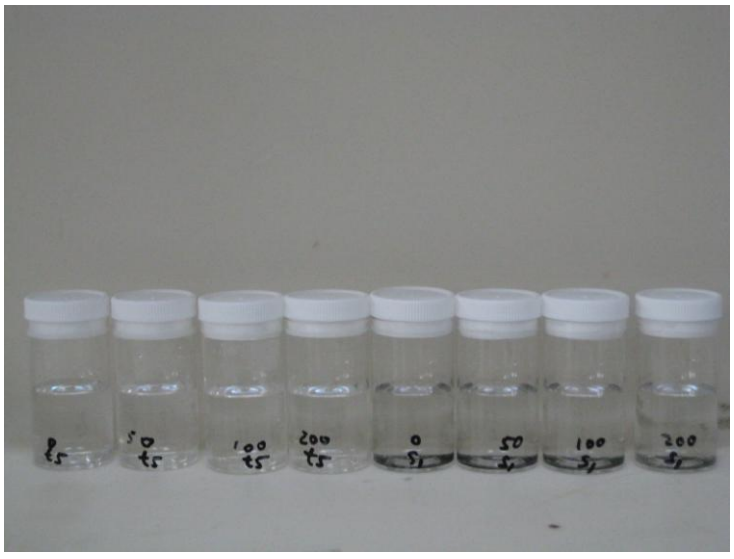

(b)

Figure C.1 Copper samples for ICP-OES analysis after 5 days with (a) 1 mL NaCN (0.0167 M) and (b) 2 mL NaCN (0.0167 M)

Table C.1 The concentration of gold thiosulfate based on ICP-OES analysis for the system with 25-100 mM thiosulfate, 5 mM trithionate, 2 mM copper (II), 5 g resin and the absence of ammonia

Analytical Chemistry Unit				
Analysts:	BL & MC	**Job No:**	9740 9783	
Date:	7/07/2009 22/07/2009	**File No:**	rep9740 rep9783	
Job Code :	**R-580-3-4**	**ICP-OES**		
			Concentration [mg/L]	
Sample ID	**LabID**	**Sample Info.**	**Analysis**	**Corrected**
1	9740/1	2Cu, 7.6T t=0	109.585	131.502
2	9783/1	2Cu, 9.5T t=0	114.771	137.725
3	9783/3	2Cu, 46.7T t=0	112.771	135.325
4	9740/3	2Cu,116.6T t=0	109.441	131.329
5	9783/5	2Cu, 143.1T t=0	109.242	131.090
6	9783/6	2Cu, 355.2T t=0	103.259	123.910
7	8291/4	2Cu, 7.6T t=2	73.342	88.010
8	9783/7	2Cu, 9.5T t=2	80.607	96.729
9	9783/9	2Cu, 46.7T t=2	92.977	111.573
10	9740/6	2Cu,116.6T t=2	94.958	113.950
11	9783/11	2Cu, 143.1T t=2	103.241	123.890
12	9783/12	2Cu, 355.2T t=2	100.700	120.840
13	9740/7	2Cu, 7.6T S1	97.774	117.329
14	9783/13	2Cu, 9.5T S1	79.159	94.991
15	9783/15	2Cu, 46.7T S1	49.417	59.300
16	9740/9	2Cu,116.6T S1	39.172	47.007
17	9783/17	2Cu, 143.1T S1	17.988	21.586
18	9783/18	2Cu, 355.2T S1	3.927	4.713
19	9740/10	2Cu, 7.6T S2	0.930	1.116
20	9783/19	2Cu, 9.5T S2	0.233	0.280
21	9783/21	2Cu, 46.7T S2	0.146	0.175
22	9740/12	2Cu,116.6T S2	1.000	1.200
23	9783/23	2Cu, 143.1T S2	0.059	0.071
24	9783/24	2Cu, 355.2T S2	0.029	0.034

Note:

The concentrations of copper based on ICP-OES analysis were corrected since the 10 mL samples were added with 2 mL NaCN (0.0176M)

Table C.2 The concentration of gold thiosulfate based on ICP-OES analysis for the system with 20 and 100 mM thiosulfate, 5 mM trithionate, 2 mM copper (II), 5 g resin and 0-400 mM ammonia

Analytical Chemistry Unit				
Analysts:	BL, MC % SY	**Job No:**	9740 9748 9783 9814 9945	
Date:	7/07/2009 9/09/2009 22/07/2009 31/07/2009 21/08/2009	**File No:**	rep9740 rep9748 rep9783 rep9814 rep9945	
Job Code :	**R-580-3-4**	**ICP-OES**		
			Concentration [mg/L]	
Sample ID	**LabID**	**Sample Info.**	**Analysis**	**Corrected**
1	9945/1	2Cu, 20T, 0A, t=0	103.433	124.120
2	9814/1	2Cu, 20T, 50A, t=0	105.021	126.025
3	9814/2	2Cu, 20T, 200A, t=0	103.873	124.648
4	9814/3	2Cu, 20T, 400A, t=0	103.853	124.624
5	9945/3	2Cu, 100T, 0A, t=0	105.054	126.064
6	9748/3	2Cu, 100T, 50A, t=0	102.561	123.073
7	9748/4	2Cu, 100T, 200A, t=0	101.851	122.222
8	9748/5	2Cu, 100T, 400A, t=0	102.759	123.311
9	9945/4	2Cu, 20T, 0A, t=2	71.547	85.857
10	9814/5	2Cu, 20T, 50A, t=2	86.359	103.631
11	9814/6	2Cu, 20T, 200A, t=2	90.740	108.888
12	9814/7	2Cu, 20T, 400A, t=2	93.906	112.687
13	9945/6	2Cu, 100T, 0A, t=2	87.933	105.520
14	9748/8	2Cu, 100T, 50A, t=2	89.287	107.145
15	9748/9	2Cu, 100T, 200A, t=2	91.840	110.208
16	9748/10	2Cu, 100T, 400A, t=2	94.651	113.581
17	9945/7	2Cu, 20T, 0A, S1	89.484	107.381
18	9814/9	2Cu, 20T, 50A, S1	47.118	56.541
19	9814/10	2Cu, 20T, 200A, S1	34.156	40.987
20	9814/11	2Cu, 20T, 400A, S1	28.604	34.325
21	9945/9	2Cu, 100T, 0A, S1	43.342	52.010
22	9748/13	2Cu, 100T, 50A, S1	33.714	40.456
23	9748/14	2Cu, 100T, 200A, S1	26.456	31.748
24	9748/15	2Cu, 100T, 400A, S1	21.983	26.380
25	9945/10	2Cu, 20T, 0A, S2	0.298	0.358

Sample ID	LabID	Sample Info.	Analysis	Corrected
26	9814/13	2Cu, 20T, 50A, S2	0.258	0.310
27	9814/14	2Cu, 20T, 200A, S2	0.315	0.378
28	9814/15	2Cu, 20T, 400A, S2	0.335	0.402
29	9945/12	2Cu, 100T, 0A, S2	0.117	0.141
30	9748/18	2Cu, 100T, 50A, S2	0.095	0.115
31	9748/19	2Cu, 100T, 200A, S2	0.078	0.093
32	9748/20	2Cu, 100T, 400A, S2	0.071	0.085

Note:

The concentrations of copper based on ICP-OES analysis were corrected since the 10 mL samples were added with 2 mL NaCN (0.0176M)

APPENDIX D

Appendix D contains additional information for the multiple components resin-solution system (Chapter 6).

$$
F = \left[
\begin{array}{c}
\ln \beta_1 + \ln\left[Cu^+\right] + \ln\left[S_2O_3^{2-}\right] - \ln\left[CuS_2O_3^-\right] \\
\ln \beta_2 + \ln\left[Cu^+\right] + 2\ln\left[S_2O_3^{2-}\right] - \ln\left[Cu(S_2O_3)_2^{3-}\right] \\
\ln \beta_3 + \ln\left[Cu^+\right] + 3\ln\left[S_2O_3^{2-}\right] - \ln\left[Cu(S_2O_3)_3^{5-}\right] \\
\ln \beta_4 + \ln\left[Cu^+\right] + \ln\ NH_3 - \ln\left[CuNH_3^+\right] \\
\ln \beta_5 + \ln\left[Cu^+\right] + 2\ln\left[NH_3\right] - \ln\left[Cu(NH_3)_2^+\right] \\
\ln \beta_6 + \ln\left[Cu^+\right] + 3\ln\left[NH_3\right] - \ln\left[Cu(NH_3)_3^+\right] \\
\ln \beta_7 + \ln\left[Cu^+\right] + \ln\left[NH_3^+\right] + \ln\left[S_2O_3^{2-}\right] - \ln\left[CuNH_3S_2O_3^-\right] \\
\ln \beta_8 + \ln\left[Cu^+\right] + \ln\left[NH_3^+\right] + 2\ln\left[S_2O_3^{2-}\right] - \ln\left[CuNH_3(S_2O_3)_2^{3-}\right] \\
VS^*\left(e^{\ln\left[Cu^+\right]} + e^{\ln\left[CuS_2O_3^-\right]} + e^{\ln\left[Cu(S_2O_3)_2^{3-}\right]} + e^{\ln\left[Cu(S_2O_3)_3^{5-}\right]} + e^{\ln\left[CuNH_3\right]} + e^{\ln\left[Cu(NH_3)_2^+\right]} + e^{\ln\left[Cu(NH_3)_3^+\right]} + e^{\ln\left[CuNH_3S_2O_3^-\right]} + e^{\ln\left[CuNH_3(S_2O_3)_2^{3-}\right]} - \left[Cu(I)\right]_{total}\right) + VR^*\left(e^{\ln\left[CuS_2O_3^-\right]} - R + e^{\ln\left[Cu(S_2O_3)_2^{3-}\right]} - R + e^{\ln\left[Cu(S_2O_3)_3^{5-}\right]} - R + e^{\ln\left[CuNH_3S_2O_3^-\right]} - R + e^{\ln\left[CuNH_3(S_2O_3)_2^{3-}\right]} - R\right) \\
VS^*\left(e^{\ln\left[CuS_2O_3^-\right]} + 2e^{\ln\left[Cu(S_2O_3)_2^{3-}\right]} + 3e^{\ln\left[Cu(S_2O_3)_3^{5-}\right]} + e^{\ln\left[CuNH_3S_2O_3^-\right]} + 2e^{\ln\left[CuNH_3(S_2O_3)_2^{3-}\right]} + e^{\ln\left[S_2O_3^{2-}\right]} - \left[S_2O_3^{2-}\right]_{total}\right) + VR^*\left(e^{\ln\left[CuS_2O_3^-\right]} - R + 2e^{\ln\left[Cu(S_2O_3)_2^{3-}\right]} - R + 3e^{\ln\left[Cu(S_2O_3)_3^{5-}\right]} - R + e^{\ln\left[CuNH_3S_2O_3^-\right]} - R + 2e^{\ln\left[CuNH_3(S_2O_3)_2^{3-}\right]} - R + e^{\ln\left[S_2O_3^{2-}\right]} - R\right) \\
VS^*\left(e^{\ln\left[CuNH_3\right]} + 2e^{\ln\left[Cu(NH_3)_2^+\right]} + 3e^{\ln\left[Cu(NH_3)_3^+\right]} + e^{\ln\left[CuNH_3S_2O_3^-\right]} + 2e^{\ln\left[CuNH_3(S_2O_3)_2^{3-}\right]} + e^{\ln\left[NH_3\right]} - \left[NH_3\right]_{total}\right) + VR^*\left(e^{\ln\left[CuNH_3S_2O_3^-\right]} - R + 2e^{\ln\left[CuNH_3(S_2O_3)_2^{3-}\right]} - R\right) \\
\ln K_1 + \ln\left[CuS_2O_3^-\right] + \frac{1}{2}\ln\left(\left[S_3O_6^{2-}\right] - R\right) - \ln\left(\left[CuS_2O_3^-\right] - R\right) - \frac{1}{2}\ln\left[S_3O_6^{2-}\right] \\
\ln K_2 + \ln\left[Cu(S_2O_3)_2^{3-}\right] + \frac{3}{2}\ln\left(\left[S_3O_6^{2-}\right] - R\right) - \ln\left(\left[Cu(S_2O_3)_2^{3-}\right] - R\right) - \frac{3}{2}\ln\left[S_3O_6^{2-}\right] \\
\ln K_3 + \ln\left[Cu(S_2O_3)_3^{5-}\right] + \frac{5}{2}\ln\left(\left[S_3O_6^{2-}\right] - R\right) - \ln\left(\left[Cu(S_2O_3)_3^{5-}\right] - R\right) - \frac{5}{2}\ln\left[S_3O_6^{2-}\right] \\
\ln K_4 + \ln\left[CuNH_3S_2O_3^-\right] + \frac{1}{2}\ln\left(\left[S_3O_6^{2-}\right] - R\right) - \ln\left(\left[CuNH_3S_2O_3^-\right] - R\right) - \frac{1}{2}\ln\left[S_3O_6^{2-}\right] \\
\ln K_5 + \ln\left[CuNH_3(S_2O_3)_2^{3-}\right] + \frac{3}{2}\ln\left(\left[S_3O_6^{2-}\right] - R\right) - \ln\left(\left[CuNH_3(S_2O_3)_2^{3-}\right] - R\right) - \frac{3}{2}\ln\left[S_3O_6^{2-}\right] \\
\ln K_6 + \ln\left(\left[S_2O_3^{2-}\right] - R\right) + \ln\left[S_3O_6^{2-}\right] - \ln\left(\left[S_3O_6^{2-}\right] - R\right) - \ln\left[S_2O_3^{2-}\right] \\
VS^*\left(e^{\ln\left[S_3O_6^{2-}\right]} - \left[S_3O_6^{2-}\right]_{total}\right) + VR^*e^{\ln\left[S_3O_6^{2-}\right] - R} \\
e^{\ln\left(\left[CuS_2O_3^-\right] - R\right)} + 3e^{\ln\left(\left[Cu(S_2O_3)_2^{3-}\right] - R\right)} + 5e^{\ln\left(\left[Cu(S_2O_3)_3^{5-}\right] - R\right)} + e^{\ln\left(\left[CuNH_3S_2O_3^-\right] - R\right)} + 3e^{\ln\left(\left[CuNH_3(S_2O_3)_2^{3-}\right] - R\right)} + 2e^{\ln\left(\left[S_2O_3^{2-}\right] - R\right)} + 2e^{\ln\left(\left[S_3O_6^{2-}\right] - R\right)} - 1300
\end{array}
\right]
$$

(D.1)

Table D.1 The Jacobian matrix of Newton-Raphson method for modelling copper complexes species in the system

					Column-i (1-19)				
1	**2**	**3**	**4**	**5**	**6**	**7**	**8**	**9**	**10**
1	-1	0	0	0	0	0	0	0	0
1	0	-1	0	0	0	0	0	0	0
1	0	0	-1	0	0	0	0	0	0
1	0	0	0	-1	0	0	0	0	1
1	0	0	0	0	-1	0	0	0	2
1	0	0	0	0	0	-1	0	0	3
1	0	0	0	0	0	0	-1	0	1
1	0	0	0	0	0	0	0	-1	1
$VS*e^{\ln\left[Cu^{+}\right]}$	$VS*e^{\ln\left[CuS_2O_3^{-}\right]}$	$VS*e^{\ln\left[Cu(S_2O_3)_2^{3-}\right]}$	$VS*e^{\ln\left[Cu(S_2O_3)_3^{5-}\right]}$	$VS*e^{\ln\left[CuNH_3^{+}\right]}$	$VS*e^{\ln\left[Cu(NH_3)_2^{+}\right]}$	$VS*e^{\ln\left[Cu(NH_3)_3^{+}\right]}$	$VS*e^{\ln\left[CuNH_3S_2O_3^{-}\right]}$	$VS*e^{\ln\left[CuNH_3\ S_2O_3\ _2^{3-}\right]}$	0
0	$VS*e^{\ln\left[CuS_2O_3^{-}\right]}$	$2VS*e^{\ln\left[Cu(S_2O_3)_2^{3-}\right]}$	$3VS*e^{\ln\left[Cu(S_2O_3)_3^{5-}\right]}$	0	0	0	$VS*e^{\ln\left[CuNH_3S_2O_3^{-}\right]}$	$2VS*e^{\ln\left[CuNH_3\ S_2O_3\ _2^{3-}\right]}$	0
0	0	0	0	$VS*e^{\ln\left[CuNH_3^{+}\right]}$	$2VS*e^{\ln\left[Cu(NH_3)_2^{+}\right]}$	$3VS*e^{\ln\left[Cu(NH_3)_3^{+}\right]}$	$VS*e^{\ln\left[CuNH_3S_2O_3^{-}\right]}$	$2VS*e^{\ln\left[CuNH_3\ S_2O_3\ _2^{3-}\right]}$	$e^{\ln\ NH_3}$
0	1	0	0	0	0	0	0	0	0
0	0	1	0	0	0	0	0	0	0
0	0	0	1	0	0	0	0	0	0
0	0	0	0	0	0	0	1	0	0
0	0	0	0	0	0	0	0	1	0
0	0	0	0	0	0	0	0	0	0
0	0	0	0	0	0	0	0	0	0
0	0	0	0	0	0	0	0	0	0

11	12	13	14	15	16	17	18	19	Row-i (1-19)
1	0	0	0	0	0	0	0	0	**1**
2	0	0	0	0	0	0	0	0	**2**
3	0	0	0	0	0	0	0	0	**3**
0	0	0	0	0	0	0	0	0	**4**
0	0	0	0	0	0	0	0	0	**5**
0	0	0	0	0	0	0	0	0	**6**
1	0	0	0	0	0	0	0	0	**7**
2	0	0	0	0	0	0	0	0	**8**
0	$VR*e^{\ln\left[CuS_2O_3^-\right]-R}$	$VR*e^{\ln\left[Cu(S_2O_3)_2^{3-}\right]-R}$	$VR*e^{\ln\left[Cu(S_2O_3)_3^{5-}\right]-R}$	$VR*e^{\ln\left[CuNH_3S_2O_3^-\right]-R}$	$VR*e^{\ln\left[CuNH_3\ S_2O_3\ _2^{3-}\right]-R}$	0	0	0	**9**
$VS*e^{\ln\left[S_2O_3^{2-}\right]}$	$VR*e^{\ln\left[CuS_2O_3^-\right]-R}$	$2VR*e^{\ln\left[Cu(S_2O_3)_2^{3-}\right]-R}$	$3VR*e^{\ln\left[Cu(S_2O_3)_3^{5-}\right]-R}$	$VR*e^{\ln\left[CuNH_3S_2O_3^-\right]-R}$	$2VR*e^{\ln\left[CuNH_3\ S_2O_3\ _2^{3-}\right]-R}$	$e^{\ln\left[S_2O_3^{2-}\right]-R}$	0	0	**10**
0	0	0	0	$VR*e^{\ln\left[CuNH_3S_2O_3^-\right]-R}$	$2VR*e^{\ln\left[CuNH_3\ S_2O_3\ _2^{3-}\right]-R}$	0	0	0	**11**
0	-1	0	0	0	0	0	0.5	0.5	**12**
0	0	-1	0	0	0	0	1.5	-1.5	**13**
0	0	0	-1	0	0	0	2.5	-2.5	**14**
0	0	0	0	-1	0	0	0.5	-0.5	**15**
0	0	0	0	0	-1	0	1.5	-1.5	**16**
-1	0	0	0	0	0	1	-1	1	**17**
0	0	0	0	0	0	0	$VR*e^{\ln\left[S_3O_6^{2-}\right]-R}$	$VS*e^{\ln\left[S_3O_6^{2-}\right]}$	**18**
0	$VR*e^{\ln\left[CuS_2O_3^-\right]-R}$	$3VR*e^{\ln\left[Cu(S_2O_3)_2^{3-}\right]-R}$	$5VR*e^{\ln\left[Cu(S_2O_3)_3^{5-}\right]-R}$	$VR*e^{\ln\left[CuNH_3S_2O_3^-\right]-R}$	$3VR*e^{\ln\left[CuNH_3\ S_2O_3\ _2^{3-}\right]-R}$	$2e^{\ln\left[S_2O_3^{2-}\right]-R}$	$2VR*e^{\ln\left[S_3O_6^{2-}\right]-R}$	0	**19**

Tables D.2 An example of Newton-Raphson application to obtain the D.2 plot in Figure 6.1 of Chapter 6

				Model Data								Exp. Data	
Note: B values as log(*B*)		**Check for solution**	**INPUTS**				**OUTPUTS**	**M**	**mM**		**mM**	**Thiosulfate**
Ref. *B* 1 for CuS2O3 -	1.95E+09	1.95E+09		**M**	**CHECK**	**Error (%)**	Cu+	4.18056E-12	4.18056E-09	5.4347E-13	10	Init Concentration (mM)
Ref. *B* 2 for Cu(S2O3)2 3-	1.48E+12	1.48E+12	Cu (I) total	0.002	2.00E-03	2.86E-05	CuS2O3 -	4.90493E-05	0.049049325	6.3764E-06	7.607171001	Equil Concentration (mM)
Ref. *B* 3 for Cu(S2O3)3 5-	3.02E+14	3.02E+14	S2O3 2- total	0.01	1.00E-02	2.11E-06	Cu(S2O3)2 3-	0.000223889	0.223888528	2.9106E-05	182.3698965	Measured Resin (mM)
Ref. *B* 4 for CuNH3 +	6.31E+05	6.31E+05	NH3 total	0	1.51E-09	1.00E+02	Cu(S2O3)3 5-	0.000275062	0.275062033	3.5758E-05		
Ref. *B* 5 for Cu(NH3)2 +	2.34E+10	2.34E+10	S3O6 2- total	0.005732203	5.73E-03	9.99E-13	CuNH3 +	3.48954E-15	3.48954E-12	4.5364E-16		
Ref. *B* 6 for Cu(NH3)3 +	8.51E+09	8.51E+09	Resin	1.3	1.300000002	1.69E-07	Cu(NH3)2 +	1.71515E-19	1.71515E-16	2.2297E-20		**Trithionate**
Ref. *B* 7 for CuNH3S2O3 -	4.68E+12	4.68E+12					Cu(NH3)3 +	8.2383E-29	8.2383E-26	1.0710E-29	5	Init Concentration (mM)
Ref. *B* 8 for Cu NH3(S2O3)2 3-	1.05E+14	1.05E+14					CuNH3S2O3 -	1.55657E-10	1.55657E-07	2.0235E-11	4.893192454	Equil Concentration (mM)
K1 for RCuS2O3	1.00E+02	99.99998985					CuNH3(S2O3)2 3-	2.09684E-11	2.09684E-08	2.7259E-12	381.2025771	Measured Resin (mM)
K2 for R3Cu(S2O3)2	1.06E+00	1.061					NH3	1.32292E-09	1.32292E-06	1.7198E-10		
K3 for R5Cu(S2O3)3	1.00E-08	1E-08					S2O3 2-	0.00601726	6.017260428	7.8224E-04		
K4 for RCuNH3S2O3	1.51E+00	1.51					CuS2O3 - R	0.045931105	45.93110486	3.5976E-05		**Copper**
K5 for R3CuNH3(S2O3)2	4.57E-05	4.56964E-05					Cu(S2O3)2 3- R	0.195060322	195.0603217	1.5278E-04	2.069273822	Init Concentration (mM)
K6 for R2S3O6	95	95					Cu(S2O3)3 5- R	1.98062E-07	0.000198062	1.5513E-10	1.384893254	Equil Concentration (mM))
							CuNH3S2O3 - R	2.20099E-09	2.20099E-06	1.7240E-12	242.2944497	Measured Resin (mM))
Vs	0.130	L					CuNH3(S2O3)2 3- R	7.8681E-13	7.8681E-10	6.1628E-16	113.5881055	Calculate Resin (mM)
Vr	0.001	L					S2O3 2- R	0.005554219	5.554219137	4.3504E-06	22.68290956	**Cu g/ kg dry resin**
Mr Cu	63.550	g/mol					S3O6 2- R	0.328889251	328.8892508	2.5761E-04		
m dry resin	0.261	g					S3O6 2-	0.00375061	3.750609696	2.9377E-06		
							Cu-R total		240.9916268		0.540609193	**Deviation (%)**
							Cu g/ kg dry resin		22.56094303		0.540609193	**Deviation (%)**

ITERATION			
Species	**ln(conc.)**	**Conc (M)**	**F**
Cu+	-20	2.06115E-09	8.891015514
CuS2O3 -	-10	4.53999E-05	11.02246058
Cu(S2O3)2 3-	-8	0.000335463	13.84143215
Cu(S2O3)3 5-	-8	0.000335463	14.85499354
CuNH3 +	-25	1.38879E-11	11.87780741
Cu(NH3)2 +	-15	3.05902E-07	2.364669973
Cu(NH3)3 +	-10	4.53999E-05	11.17375313
CuNH3S2O3 -	-8	0.000335463	11.782243
CuNH3(S2O3)2 3-	-8	0.000335463	-7.24E-05
NH3	-3.5	0.030197383	1.00E-02
S2O3 2-	-2.5	0.082084999	4.08E-03
CuS2O3 - R	-8	0.000335463	6.105170186
Cu(S2O3)2 3- R	-8	0.000335463	10.55921186
Cu(S2O3)3 5- R	-8	0.000335463	-0.920680744
CuNH3S2O3 - R	-8	0.000335463	3.912109651
CuNH3(S2O3)2 3- R	-8	0.000335463	0.506508962
S2O3 2- R	-1	0.367879441	-0.946123108
S3O6 2- R	-1	0.367879441	-4.13E-04
S3O6 2-	-8	0.000335463	0.175878779
Species	**1st Iter. (conc.)**	**Conc (M)**	**F**
Cu+	-28.88916867	2.8418E-13	0
CuS2O3 -	-10.93133821	1.78888E-05	0
Cu(S2O3)2 3-	-7.733078183	0.000438094	0
Cu(S2O3)3 5-	-5.847291664	0.002887709	0
CuNH3 +	-20.03385173	1.99255E-09	0
Cu(NH3)2 +	-14.01071445	8.22667E-07	0
Cu(NH3)3 +	-19.52352849	3.31924E-09	0
CuNH3S2O3 -	-7.648277188	0.000476865	-7.10543E-15
CuNH3(S2O3)2 3-	-7.972972358	0.000344653	2.35E-03
NH3	-4.499676597	0.01111259	8.22E-03
S2O3 2-	-3.433185045	0.032283951	1.61E-03
CuS2O3 - R	-1.088708365	0.336651043	-2.403963863
Cu(S2O3)2 3- R	0.82662105	2.285582808	0
Cu(S2O3)3 5- R	-10.10049345	4.10593E-05	0
CuNH3S2O3 - R	-4.402671746	0.012244582	0
CuNH3(S2O3)2 - R	-9.465976022	7.74424E-05	0
S2O3 2- R	-2.320070354	0.098266672	0
S3O6 2- R	0.070955446	1.073533394	5.78E-04
S3O6 2-	-5.596036137	0.003712551	8.249681805

Species	**2nd Iter. (conc.)**	**Conc (M)**	**F**
Cu+	-26.64623637	2.67724E-12	0
CuS2O3 -	-9.63461639	6.54243E-05	0
Cu(S2O3)2 3-	-7.382566859	0.000622002	0
Cu(S2O3)3 5-	-6.442990831	0.001591639	0
CuNH3 +	-18.86596164	6.40644E-09	0
Cu(NH3)2 +	-13.91786658	9.02708E-07	0
Cu(NH3)3 +	-20.50572283	1.24302E-09	0
CuNH3S2O3 -	-7.426597588	0.000595209	0
CuNH3(S2O3)2 3-	-8.697503249	0.000167002	9.69E-04
NH3	-5.574718813	0.003792542	2.85E-03
S2O3 2-	-4.379395537	0.012532932	6.22E-04
CuS2O3 - R	-2.524267399	0.080116985	-0.073048326
Cu(S2O3)2 3- R	-0.026963562	0.973396709	0
Cu(S2O3)3 5- R	-12.70301918	3.04193E-06	0
CuNH3S2O3 - R	-4.582357459	0.010230749	0
CuNH3(S2O3)2 - R	-11.39460285	1.12561E-05	0
S2O3 2- R	-4.06901147	0.017094278	0
S3O6 2- R	-0.658726852	0.517509782	1.79E-04
S3O6 2-	-5.52298781	0.003993897	2.779794959
Species	**3rd Iter. (conc.)**	**Conc (M)**	**F**
Cu+	-25.37847638	9.51191E-12	0
CuS2O3 -	-9.039349541	0.000118648	0
Cu(S2O3)2 3-	-7.459793146	0.000575775	0
Cu(S2O3)3 5-	-7.192710254	0.000752048	0
CuNH3 +	-18.67154576	7.78127E-09	0
Cu(NH3)2 +	-14.79679481	3.74829E-07	0
Cu(NH3)3 +	-22.45799517	1.76448E-10	0
CuNH3S2O3 -	-7.904674848	0.000369014	0
CuNH3(S2O3)2 3-	-9.848073645	5.28489E-05	4.20E-04
NH3	-6.648062921	0.001296531	8.42E-04
S2O3 2-	-5.051888673	0.00639724	2.34E-04
CuS2O3 - R	-2.224982224	0.10806934	-0.011976104
Cu(S2O3)2 3- R	-0.808918204	0.445339572	0
Cu(S2O3)3 5- R	-14.62728586	4.44069E-07	0
CuNH3S2O3 - R	-5.29534417	0.005014888	0
CuNH3(S2O3)2 - R	-13.2499016	1.76052E-06	0
S2O3 2- R	-5.21132351	0.00545445	0
S3O6 2- R	-1.116569652	0.32740097	3.67E-05
S3O6 2-	-5.511011707	0.004042016	0.814821286

Species	4th Iter. (conc.)	Conc (M)	F
Cu+	-25.3919887	9.38425E-12	0
CuS2O3 -	-9.234683616	9.75951E-05	0
Cu(S2O3)2 3-	-7.83694898	0.000394872	0
Cu(S2O3)3 5-	-7.751687847	0.000430016	0
CuNH3 +	-19.61843814	3.0187E-09	0
Cu(NH3)2 +	-16.67706725	5.71797E-08	0
Cu(NH3)3 +	-25.27164768	1.05843E-11	0
CuNH3S2O3 -	-9.033388985	0.000119357	0
CuNH3(S2O3)2 3-	-11.15860954	1.42521E-05	1.49E-04
NH3	-7.581442983	0.000509825	1.77E-04
S2O3 2-	-5.233710432	0.005333698	8.67E-05
CuS2O3 - R	-2.496276454	0.082391216	0.014499932
Cu(S2O3)2 3- R	-1.334526395	0.263282838	0
Cu(S2O3)3 5- R	-15.43368405	1.9826E-07	0
CuNH3S2O3 - R	-6.473542426	0.001543747	0
CuNH3(S2O3)2 - R	-14.70888985	4.0927E-07	0
S2O3 2- R	-5.492113506	0.004119129	0
S3O6 2- R	-1.230037822	0.292281523	1.65E-06
S3O6 2-	-5.525511639	0.00398383	0.166587

Species	5th Iter. (conc.)	Conc (M)	F
Cu+	-25.89551253	5.67181E-12	0
CuS2O3 -	-9.663284673	6.35754E-05	0
Cu(S2O3)2 3-	-8.190627258	0.00027724	0
Cu(S2O3)3 5-	-8.030443346	0.000325404	0
CuNH3 +	-21.02459182	7.39837E-10	0
Cu(NH3)2 +	-18.98585076	5.68264E-09	0
Cu(NH3)3 +	-28.48306103	4.26544E-13	0
CuNH3S2O3 -	-10.36461988	3.15285E-05	0
CuNH3(S2O3)2 3-	-12.41491766	4.05761E-06	4.13E-05
NH3	-8.484072822	0.000206735	4.00E-05
S2O3 2-	-5.158787653	0.005748665	3.24E-05
CuS2O3 - R	-2.894637884	0.055319053	0.030632848
Cu(S2O3)2 3- R	-1.549087047	0.212441835	0
Cu(S2O3)3 5- R	-15.48057684	1.89178E-07	0
CuNH3S2O3 - R	-7.758400779	0.000427139	0
CuNH3(S2O3)2 - R	-15.82608034	1.33912E-07	0
S2O3 2- R	-5.324445644	0.004871051	0
S3O6 2- R	-1.167925586	0.311011439	6.91E-07
S3O6 2-	-5.556144487	0.003863644	0.024838024

Species	6th Iter. (conc.)	Conc (M)	F
Cu+	-26.13169311	4.47868E-12	0
CuS2O3 -	-9.864688693	5.19781E-05	0
Cu(S2O3)2 3-	-8.357254727	0.000234688	0
Cu(S2O3)3 5-	-8.162294263	0.000285207	0
CuNH3 +	-22.22803722	2.22068E-10	0
Cu(NH3)2 +	-21.156561	6.48369E-10	0
Cu(NH3)3 +	-31.62103609	1.84994E-14	0
CuNH3S2O3 -	-11.53328873	9.79843E-06	0
CuNH3(S2O3)2 3-	-13.54880996	1.30565E-06	8.25E-06
NH3	-9.451337654	7.85844E-05	6.52E-06
S2O3 2-	-5.124011102	0.0059521	1.19E-05
CuS2O3 - R	-3.054946061	0.047125263	0.022380189
Cu(S2O3)2 3- R	-1.617184965	0.198456576	0
Cu(S2O3)3 5- R	-15.44821184	1.95401E-07	0
CuNH3S2O3 - R	-8.894226448	0.000137179	0
CuNH3(S2O3)2 - R	-16.86144309	4.75519E-08	0
S2O3 2- R	-5.223982725	0.005385836	0
S3O6 2- R	-1.124619407	0.324776051	3.57E-07
S3O6 2-	-5.578524675	0.003778135	0.002957063

Species	7th Iter. (conc.)	Conc (M)	F
Cu+	-26.18465575	4.24765E-12	0
CuS2O3 -	-9.909739957	4.96884E-05	0
Cu(S2O3)2 3-	-8.394394614	0.000226131	0
Cu(S2O3)3 5-	-8.191522773	0.000276992	0
CuNH3 +	-23.27478498	7.79631E-11	0
Cu(NH3)2 +	-23.19709388	8.42617E-11	0
Cu(NH3)3 +	-34.6553541	8.89961E-16	0
CuNH3S2O3 -	-12.57212512	3.46733E-06	0
CuNH3(S2O3)2 3-	-14.57973497	4.65695E-07	1.85E-06
NH3	-10.44512277	2.90898E-05	8.33E-07
S2O3 2-	-5.116099724	0.005999377	4.39E-06
CuS2O3 - R	-3.07565141	0.04615955	0.005730079
Cu(S2O3)2 3- R	-1.631237433	0.195687274	0
Cu(S2O3)3 5- R	-15.43896132	1.97217E-07	0
CuNH3S2O3 - R	-9.925367027	4.89179E-05	0
CuNH3(S2O3)2 - R	-17.86928068	1.73568E-08	0
S2O3 2- R	-5.200679735	0.005512816	0
S3O6 2- R	-1.114957873	0.327929093	2.00E-08
S3O6 2-	-5.584254754	0.003756548	0.000155147

Species	8th Iter. (conc.)	Conc (M)	F
Cu+	-26.19552161	4.20174E-12	0
CuS2O3 -	-9.918618753	4.92491E-05	0
Cu(S2O3)2 3-	-8.401286341	0.000224578	0
Cu(S2O3)3 5-	-8.196427432	0.000275637	0
CuNH3 +	-24.28448045	2.84043E-11	0
Cu(NH3)2 +	-25.20561896	1.13068E-11	0
Cu(NH3)3 +	-37.66270879	4.39839E-17	0
CuNH3S2O3 -	-13.57983352	1.26577E-06	0
CuNH3(S2O3)2 3-	-15.5854563	1.70342E-07	6.14E-07
NH3	-11.44395238	1.07141E-05	2.33E-07
S2O3 2-	-5.114112656	0.00601131	1.62E-06
CuS2O3 - R	-3.078349661	0.046035168	0.001085839
Cu(S2O3)2 3- R	-1.633520247	0.195241066	0
Cu(S2O3)3 5- R	-15.43618445	1.97765E-07	0
CuNH3S2O3 - R	-10.93153913	1.78852E-05	0
CuNH3(S2O3)2 - R	-18.87039311	6.37812E-09	0
S2O3 2- R	-5.195620058	0.00554078	0
S3O6 2- R	-1.112971104	0.32858126	7.95E-10
S3O6 2-	-5.585340593	0.003752471	2.13393E-05

Species	9th Iter. (conc.)	Conc (M)	F
Cu+	-26.19876715	4.18813E-12	0
CuS2O3 -	-9.921231399	4.91206E-05	0
Cu(S2O3)2 3-	-8.403266097	0.000224134	0
Cu(S2O3)3 5-	-8.197774298	0.000275266	0
CuNH3 +	-25.28738514	1.04191E-11	0
Cu(NH3)2 +	-27.20818279	1.52629E-12	0
Cu(NH3)3 +	-40.66493176	2.18497E-18	0
CuNH3S2O3 -	-14.58210531	4.64592E-07	0
CuNH3(S2O3)2 3-	-16.5870952	6.25628E-08	2.23E-07
NH3	-12.44361153	3.94283E-06	8.28E-08
S2O3 2-	-5.113479766	0.006015115	5.94E-07
CuS2O3 - R	-3.079735348	0.045971421	0.000318648
Cu(S2O3)2 3- R	-1.634120698	0.195123869	0
Cu(S2O3)3 5- R	-15.43523248	1.97954E-07	0
CuNH3S2O3 - R	-11.93335115	6.56767E-06	0
CuNH3(S2O3)2 - R	-19.8706527	2.34577E-09	0
S2O3 2- R	-5.194067632	0.005549388	0
S3O6 2- R	-1.112370215	0.32877876	7.12E-11
S3O6 2-	-5.585659241	0.003751276	6.88889E-06

Species	10th Iter. (conc.)	Conc (M)	F
Cu+	-26.19991519	4.18332E-12	0
CuS2O3 -	-9.922153368	4.90754E-05	0
Cu(S2O3)2 3-	-8.403961993	0.000223978	0
Cu(S2O3)3 5-	-8.198244121	0.000275136	0
CuNH3 +	-26.28841321	3.82902E-12	0
Cu(NH3)2 +	-29.20909089	2.06373E-13	0
Cu(NH3)3 +	-43.66571989	1.08697E-19	0
CuNH3S2O3 -	-15.58290731	1.70777E-07	0
CuNH3(S2O3)2 3-	-17.58767113	2.30023E-08	8.16E-08
NH3	-13.44349156	1.45066E-06	3.02E-08
S2O3 2-	-5.113253692	0.006016475	2.19E-07
CuS2O3 - R	-3.080288438	0.045946002	0.000112722
Cu(S2O3)2 3- R	-1.634327732	0.195083476	0
Cu(S2O3)3 5- R	-15.43488753	1.98022E-07	0
CuNH3S2O3 - R	-12.93399019	2.41457E-06	0
CuNH3(S2O3)2 - R	-20.87073977	8.62885E-10	0
S2O3 2- R	-5.19351565	0.005552452	0
S3O6 2- R	-1.112157029	0.328848859	8.95E-12
S3O6 2-	-5.585771963	0.003750853	2.45756E-06

Species	11th Iter. (conc.)	Conc (M)	F
Cu+	-26.20033401	4.18157E-12	0
CuS2O3 -	-9.922489563	4.90589E-05	0
Cu(S2O3)2 3-	-8.404215557	0.000223921	0
Cu(S2O3)3 5-	-8.198415055	0.000275089	0
CuNH3 +	-27.28878832	1.40809E-12	0
Cu(NH3)2 +	-31.2094223	2.79203E-14	0
Cu(NH3)3 +	-46.66600758	5.41016E-21	0
CuNH3S2O3 -	-16.5831998	6.2807E-08	0
CuNH3(S2O3)2 3-	-18.58788098	8.4603E-09	3.00E-08
NH3	-14.44344785	5.33692E-07	1.11E-08
S2O3 2-	-5.113171062	0.006016972	8.04E-08
CuS2O3 - R	-3.08049357	0.045936578	4.11111E-05
Cu(S2O3)2 3- R	-1.634402942	0.195068804	0
Cu(S2O3)3 5- R	-15.43476121	1.98047E-07	0
CuNH3S2O3 - R	-13.93422323	8.88063E-07	0
CuNH3(S2O3)2 - R	-21.87077127	3.17428E-10	0
S2O3 2- R	-5.193314117	0.005553571	0
S3O6 2- R	-1.112079238	0.328874442	1.19E-12
S3O6 2-	-5.585813075	0.003750699	8.94415E-07

Species	12th Iter. (conc.)	Conc (M)	F
Cu+	-26.2004877	4.18093E-12	0
CuS2O3 -	-9.922612913	4.90528E-05	0
Cu(S2O3)2 3-	-8.404308569	0.000223901	0
Cu(S2O3)3 5-	-8.198477729	0.000275072	0
CuNH3 +	-28.28892598	5.17935E-13	0
Cu(NH3)2 +	-33.20954392	3.77814E-15	0
Cu(NH3)3 +	-49.66611317	2.69328E-22	0
CuNH3S2O3 -	-17.58330711	2.31029E-08	0
CuNH3(S2O3)2 3-	-19.58795796	3.11213E-09	1.10E-08
NH3	-15.44343182	1.96337E-07	4.07E-09
S2O3 2-	-5.113140724	0.006017155	2.96E-08
CuS2O3 - R	-3.080569077	0.04593311	1.5083E-05
Cu(S2O3)2 3- R	-1.634430512	0.195063426	0
Cu(S2O3)3 5- R	-15.43471481	1.98056E-07	0
CuNH3S2O3 - R	-14.93430873	3.26672E-07	-3.9968E-15
CuNH3(S2O3)2 - R	-22.8707828	1.16774E-10	0
S2O3 2- R	-5.193240151	0.005553982	0
S3O6 2- R	-1.112050692	0.32888383	1.60E-13
S3O6 2-	-5.585828158	0.003750642	3.2775E-07

Species	13th Iter. (conc.)	Conc (M)	F
Cu+	-26.20054419	4.18069E-12	0
CuS2O3 -	-9.922658248	4.90506E-05	0
Cu(S2O3)2 3-	-8.404342752	0.000223893	0
Cu(S2O3)3 5-	-8.198500759	0.000275066	0
CuNH3 +	-29.28897657	1.90528E-13	0
Cu(NH3)2 +	-35.20958862	5.11293E-16	0
Cu(NH3)3 +	-52.66615199	1.34085E-23	0
CuNH3S2O3 -	-18.58334656	8.49875E-09	0
CuNH3(S2O3)2 3-	-20.58798625	1.14486E-09	4.06E-09
NH3	-16.44342592	7.22289E-08	1.50E-09
S2O3 2-	-5.113129572	0.006017222	1.09E-08
CuS2O3 - R	-3.080596856	0.045931834	5.54338E-06
Cu(S2O3)2 3- R	-1.634440642	0.19506145	0
Cu(S2O3)3 5- R	-15.43469775	1.9806E-07	0
CuNH3S2O3 - R	-15.93434016	1.20172E-07	0
CuNH3(S2O3)2 - R	-23.87078704	4.29585E-11	0
S2O3 2- R	-5.193212963	0.005554133	0
S3O6 2- R	-1.112040201	0.32888728	2.17E-14
S3O6 2-	-5.585833701	0.003750622	1.20399E-07

Species	14th Iter. (conc.)	Conc (M)	F
Cu+	-26.20056496	4.18061E-12	0
CuS2O3 -	-9.922674921	4.90498E-05	0
Cu(S2O3)2 3-	-8.404355323	0.00022389	0
Cu(S2O3)3 5-	-8.198509227	0.000275063	0
CuNH3 +	-30.28899518	7.00901E-14	0
Cu(NH3)2 +	-37.20960506	6.91949E-17	0
Cu(NH3)3 +	-55.66616626	6.67561E-25	0
CuNH3S2O3 -	-19.58336106	3.12647E-09	0
CuNH3(S2O3)2 3-	-21.58799666	4.21165E-10	1.49E-09
NH3	-17.44342376	2.65716E-08	5.51E-10
S2O3 2-	-5.11312547	0.006017247	4.00E-09
CuS2O3 - R	-3.080607075	0.045931364	2.03858E-06
Cu(S2O3)2 3- R	-1.634444367	0.195060723	0
Cu(S2O3)3 5- R	-15.43469148	1.98061E-07	0
CuNH3S2O3 - R	-16.93435171	4.42084E-08	0
CuNH3(S2O3)2 - R	-24.8707886	1.58035E-11	0
S2O3 2- R	-5.193202964	0.005554188	0
S3O6 2- R	-1.112036342	0.328888549	2.93E-15
S3O6 2-	-5.58583574	0.003750614	4.42691E-08

Species	15th Iter. (conc.)	Conc (M)	F
Cu+	-26.20057261	4.18057E-12	0
CuS2O3 -	-9.922681053	4.90495E-05	0
Cu(S2O3)2 3-	-8.404359946	0.000223889	0
Cu(S2O3)3 5-	-8.198512342	0.000275062	0
CuNH3 +	-31.28900203	2.57845E-14	0
Cu(NH3)2 +	-39.20961111	9.36445E-18	0
Cu(NH3)3 +	-58.66617151	3.32357E-26	0
CuNH3S2O3 -	-20.5833664	1.15016E-09	0
CuNH3(S2O3)2 3-	-22.58800048	1.54937E-10	5.49E-10
NH3	-18.44342296	9.77514E-09	2.03E-10
S2O3 2-	-5.113123961	0.006017256	1.47E-09
CuS2O3 - R	-3.080610834	0.045931192	7.49856E-07
Cu(S2O3)2 3- R	-1.634445737	0.195060456	0
Cu(S2O3)3 5- R	-15.43468917	1.98061E-07	0
CuNH3S2O3 - R	-17.93435596	1.62633E-08	0
CuNH3(S2O3)2 - R	-25.87078917	5.81379E-12	0
S2O3 2- R	-5.193199286	0.005554209	0
S3O6 2- R	-1.112034923	0.328889016	3.96E-16
S3O6 2-	-5.585836489	0.003750611	1.62825E-08

Species	16th Iter. (conc.)	Conc (M)	F
Cu+	-26.20057542	4.18056E-12	0
CuS2O3 -	-9.922683309	4.90494E-05	0
Cu(S2O3)2 3-	-8.404361647	0.000223889	0
Cu(S2O3)3 5-	-8.198513488	0.000275062	0
CuNH3 +	-32.28900454	9.48557E-15	0
Cu(NH3)2 +	-41.20961334	1.26734E-18	0
Cu(NH3)3 +	-61.66617344	1.65471E-27	0
CuNH3S2O3 -	-21.58336836	4.23119E-10	0
CuNH3(S2O3)2 3-	-23.58800189	5.69982E-11	2.02E-10
NH3	-19.44342267	3.59608E-09	7.45E-11
S2O3 2-	-5.113123406	0.006017259	5.42E-10
CuS2O3 - R	-3.080612217	0.045931128	2.75844E-07
Cu(S2O3)2 3- R	-1.634446241	0.195060358	0
Cu(S2O3)3 5- R	-15.43468832	1.98061E-07	0
CuNH3S2O3 - R	-18.93435753	5.98292E-09	0
CuNH3(S2O3)2 - R	-26.87078938	2.13877E-12	0
S2O3 2- R	-5.193197933	0.005554216	0
S3O6 2- R	-1.112034401	0.328889188	5.36E-17
S3O6 2-	-5.585836765	0.00375061	5.98958E-09
Species	**17th Iter. (conc.)**	**Conc (M)**	**F**
Cu+	-26.20057645	4.18056E-12	0
CuS2O3 -	-9.922684139	4.90493E-05	0
Cu(S2O3)2 3-	-8.404362273	0.000223889	0
Cu(S2O3)3 5-	-8.19851391	0.000275062	0
CuNH3 +	-33.28900547	3.48954E-15	0
Cu(NH3)2 +	-43.20961415	1.71515E-19	0
Cu(NH3)3 +	-64.66617415	8.2383E-29	0
CuNH3S2O3 -	-22.58336908	1.55657E-10	0
CuNH3(S2O3)2 3-	-24.58800241	2.09684E-11	7.43E-11
NH3	-20.44342256	1.32292E-09	2.74E-11
S2O3 2-	-5.113123202	0.00601726	1.99E-10
CuS2O3 - R	-3.080612726	0.045931105	1.01475E-07
Cu(S2O3)2 3- R	-1.634446426	0.195060322	0
Cu(S2O3)3 5- R	-15.43468801	1.98062E-07	0
CuNH3S2O3 - R	-19.9343581	2.20099E-09	0
CuNH3(S2O3)2 - R	-27.87078946	7.8681E-13	0
S2O3 2- R	-5.193197435	0.005554219	0
S3O6 2- R	-1.112034209	0.328889251	7.43E-18
S3O6 2-	-5.585836867	0.00375061	2.20338E-09

Table D.3 Model-based copper complexes species on resin for different equilibrium concentration of thiosulfate in solution in the multiple component resin-solution system without ammonia

Equilibrium Concentration Thiosulfate in Solution (mM)	7.607171001	9.513790386	35.92100079	116.1146572	141.3	353.25
Copper Complexes on Resin	**Concentration (% M)**					
$[CuS_2O_3^-]$-R	13.77933146	7.467067213	1.075203956	0.3263967	0.08876039	0.012785209
$[Cu(S_2O_3)_2^{3-}]$-R	58.5180965	57.4939147	43.11047085	28.7190535	13.93112803	3.539798174
$[Cu(S_2O_3)_3^{5-}]$-R	5.94185E-05	0.000105843	0.00041328	0.000604176	0.000522784	0.000234325
$[CuNH_3S_2O_3^-]$-R	6.60297E-07	3.67212E-07	5.37425E-08	1.63907E-08	4.54716E-09	7.0383E-10
$[CuNH_3(S_2O_3)_2^{3-}]$-R	2.36043E-10	2.38001E-10	1.81384E-10	1.21398E-10	6.00755E-11	1.64032E-11
Total	72.29748804	64.96108812	44.18608814	29.04605439	14.02041121	3.552817709
Copper Complexes in Solution	**Concentration (% M)**					
Cu^+	2.09028E-07	6.32229E-08	1.94807E-09	2.75251E-10	3.90894E-11	2.65662E-12
$CuS_2O_3^-$	2.452466236	1.31330848	0.169706394	0.05043715	0.014723997	0.002548168
$Cu(S_2O_3)_2^{3-}$	11.1944264	10.61350779	5.751642692	3.595601498	2.157709206	0.950881323
$Cu(S_2O_3)_3^{5-}$	13.75310167	23.08613003	50.46692252	67.99102053	84.10598885	95.50465908
$CuNH_3^+$	1.74477E-10	5.41582E-11	0.000906649	2.40771E-13	3.48821E-14	2.54749E-15
$Cu(NH_3)_2^+$	8.57577E-15	2.73183E-15	8.6957E-17	1.24017E-17	1.83294E-18	1.43845E-19
$Cu(NH_3)_3^+$	4.11915E-24	1.34661E-24	4.35667E-26	6.24245E-27	9.41221E-28	7.93742E-29
$CuNH_3S_2O_3^-$	7.78283E-06	4.27717E-06	5.61757E-07	1.67736E-07	4.9954E-08	9.2899E-09
$CuNH_3(S_2O_3)_2^{3-}$	1.04842E-06	1.02011E-06	5.61878E-07	3.52896E-07	2.16042E-07	1.02308E-07
Total	27.40000335	35.01295166	56.38917938	71.6370597	86.27842232	96.45808868

Table D.4 Model-based copper complexes species on resin for different initial concentration of ammonia in the multiple component resin-solution system

Initial Concentration	0	50	200	400
Copper Complexes on Resin	**Concentration (% M)**			
$[CuS_2O_3^-]$-R	4.986383956	1.920231154	0.779073079	0.440115814
$[Cu(S_2O_3)_2^{3-}]$-R	56.57264228	29.87760094	17.42023142	11.16362176
$[Cu(S_2O_3)_3^{5-}]$-R	0.00015346	0.000111149	9.31293E-05	6.77035E-05
$[CuNH_3S_2O_3^-]$-R	2.47188E-07	3.388144248	5.589501668	6.340941794
$[CuNH_3(S_2O_3)_2^{3-}]$-R	2.36068E-10	0.004437542	0.010520248	0.000270776
Total	61.55917994	35.19052503	23.79941954	17.94501784
Copper Complexes in Solution	**Concentration (% M)**			
Cu^+	2.89374E-08	9.20334E-09	3.06929E-09	1.61605E-09
$CuS_2O_3^-$	0.868367591	0.295247541	0.101412878	0.054182207
$Cu(S_2O_3)_2^{3-}$	10.13788015	3.6849125	1.303611927	0.706736658
$Cu(S_2O_3)_3^{5-}$	27.39612569	12.3785014	4.510280421	2.481181575
$CuNH_3^+$	2.49876E-11	0.000282863	0.000383569	0.000405569
$Cu(NH_3)_2^+$	1.27054E-15	0.511924133	2.822596634	5.993395615
$Cu(NH_3)_3^+$	6.31325E-25	0.0090539	0.202980485	0.865528831
$CuNH_3S_2O_3^-$	2.85081E-06	34.49978522	48.18352538	51.69699291
$CuNH_3(S_2O_3)_2^{3-}$	9.82226E-07	12.707417	18.27905718	19.90060187
Total	38.40237729	64.08712458	75.40384847	81.69902524

Table D.5 The concentration of gold thiosulfate based on ICP-OES analysis for the system with 25-100 mM thiosulfate, 5 mM trithionate, 2 mM copper (II), 5 g resin and the absence of ammonia

Analytical Chemistry Unit				
Analysts:	BL & MC	**Job No:**	9740 9783	
Date:	7/07/2009 22/07/2009	**File No:**	rep9740 rep9783	
Job Code :	**R-580-3-4**	**ICP-OES**		
			Concentration [mg/L]	
Sample ID	**LabID**	**Sample Info.**	**Analysis**	**Corrected**
1	9740/1	2Cu, 7.6T t=0	109.585	131.502
2	9783/1	2Cu, 9.5T t=0	114.771	137.725
3	9783/3	2Cu, 46.7T t=0	112.771	135.325
4	9740/3	2Cu,116.6T t=0	109.441	131.329
5	9783/5	2Cu, 143.1T t=0	109.242	131.090
6	9783/6	2Cu, 355.2T t=0	103.259	123.910
7	8291/4	2Cu, 7.6T t=2	73.342	88.010
8	9783/7	2Cu, 9.5T t=2	80.607	96.729
9	9783/9	2Cu, 46.7T t=2	92.977	111.573
10	9740/6	2Cu,116.6T t=2	94.958	113.950
11	9783/11	2Cu, 143.1T t=2	103.241	123.890
12	9783/12	2Cu, 355.2T t=2	100.700	120.840
13	9740/7	2Cu, 7.6T S1	97.774	117.329
14	9783/13	2Cu, 9.5T S1	79.159	94.991
15	9783/15	2Cu, 46.7T S1	49.417	59.300
16	9740/9	2Cu,116.6T S1	39.172	47.007
17	9783/17	2Cu, 143.1T S1	17.988	21.586
18	9783/18	2Cu, 355.2T S1	3.927	4.713
19	9740/10	2Cu, 7.6T S2	0.930	1.116
20	9783/19	2Cu, 9.5T S2	0.233	0.280
21	9783/21	2Cu, 46.7T S2	0.146	0.175
22	9740/12	2Cu,116.6T S2	1.000	1.200
23	9783/23	2Cu, 143.1T S2	0.059	0.071
24	9783/24	2Cu, 355.2T S2	0.029	0.034

Note:

The concentrations of gold thiosulfate based on ICP-OES analysis were corrected since the 10 mL samples were added with 2 mL NaCN (0.0176M) to convert the gold thiosulfate complex to the more stable gold cyanide complex.

APPENDIX E

Appendix E contains additional information for the non-ammoniacal resin-solution system in Chapter 7.

Table E.1 Kinetics isotherm adsorption of gold thiosulfate in solution based on ICP-OES analysis for the NARS system with the initial concentration of gold thiosulfate being 100 mg/L and 0.333 g resin

Analytical Chemistry Unit				
Analysts:	BL	**Job No:**	9782	
Date:	22/07/2009	**File No:**	rep9782	
Job Code :	**R-580-3-4**	**ICP-OES**		
			Concentration [mg/L]	
Sample ID	**LabID**	**Sample Info.**	**Analysis**	**Corrected**
1	9782/1	t=15 mins	5.419	59.611
2	9782/2	t=30 mins	3.446	37.909
3	9782/3	t=45 mins	2.091	23.005
4	9782/4	t=60 mins	1.298	14.281
5	9782/5	t=90 mins	0.374	4.119
6	9782/6	t=120 mins	0.172	1.890
7	9782/7	t=180 mins	0.030	0.330
8	9782/8	t=300 mins	0.029	0.319

Note:

The concentrations of gold thiosulfate based on ICP-OES analysis were corrected since the 10 mL samples were added with 1 mL NaCN (0.0176M) to convert the gold thiosulfate complex to the more stable gold cyanide complex.